U.PORTO

DOUTORAMENTO
CIÊNCIAS BIOMÉDICAS

Biogeochemical nutrient budgets in a temperate estuary (Lima, NW Portugal)

Élia Fernandes

D

2019

U.PORTO

Élia Fernandes. Biogeochemical nutrient budgets in a temperate estuary (Lima, NW Portugal)

Biogeochemical nutrient budgets in a temperate estuary (Lima, NW Portugal)

Élia Maria Raposo Fernandes

D.ICBAS 2019

SEDE ADINISTRATIVA INSTITUTO DE CIÊNCIAS BIOMÉDICAS ABEL SALAZAR

ÉLIA MARIA RAPOSO FERNANDES

BIOGEOCHEMICAL NUTRIENT BUDGETS IN A TEMPERATE ESTUARY (LIMA, NW PORTUGAL)

Tese de Candidatura ao grau de Doutor em Ciências Biomédicas submetida ao Instituto de Ciências Biomédicas Abel Salazar da Universidade do Porto.

Orientador

Professor Doutor Adriano A. Bordalo e Sá

Professor Associado com agregação do Instituto de Ciências Biomédicas Abel Salazar da Universidade do Porto.

Co-orientador

Doutora Catarina Teixeira

Investigadora do Centro Interdisciplinar de Investigação Marinha e Ambiental

The research reported in this thesis was conducted at:

Laboratório de Hidrobiologia e Ecologia do Instituto de Ciências Biomédicas Abel Salazar (ICBAS), Universidade do Porto

Unidade de Investigação & Desenvolvimento em Materiais (UIDM) – Escola Superior de Tecnologia e Gestão, Instituto Politécnico de Viana do Castelo

A drop of water, if it could write out its own history,
would explain the universe to us.

Lucy Larcom
(1824-1893)

AGRADECIMENTOS

Muitas pessoas contribuíram (direta ou indiretamente) para a realização desta tese, e por isso, gostaria de expressar os meus sinceros agradecimentos a todos aqueles, que de alguma forma, me apoiaram nesta etapa da minha vida.

Agradeço ao Professor Adriano Bordalo e Sá, pela reunião das condições necessárias à realização deste trabalho, pela orientação científica e crítica ao longo de todo o trabalho. Agradeço ainda pela disponibilidade, compreensão, entusiasmo e incentivo, em especial nas alturas mais complicadas e de baixa motivação.

Agradeço à Doutora Catarina Teixeira, pela orientação científica, disponibilidade ao longo do trabalho. Agradeço em especial os comentários críticos, a paciência, assim como o otimismo constante, em especial nas alturas de baixa motivação.

Agradeço ao Instituto Politécnico de Viana do Castelo, na pessoa do seu Presidente Professor Rui Teixeira e à Escola Superior de Tecnologia e Gestão, na pessoa da sua Diretora Professora Joana Guerreiro, pelo apoio e condições facultadas para a realização do estudo associado a esta tese.

Agradeço a todos os que tornaram possíveis as amostragens do Lima, ao Rui e ao Sr. Pinto. Um agradecimento muito especial ao Sr. José Manuel por nos aceitar como tripulantes, pela sua disponibilidade, boa disposição, ajuda preciosa e imenso conhecimento do rio Lima.

Agradeço a todos os elementos do Laboratório de Hidrobiologia e Ecologia por me terem proporcionado um ambiente de trabalho agradável e acolhedor, sentindo-me sempre muito bem-vinda, nomeadamente à Fernanda, Raquel, Sérgia, Paula e Hugo. Agradeço à Eva por me "apresentar" o estuário do Lima, pelos muitos conhecimentos transmitidos, pela disponibilidade e ajuda nas amostragens, assim como, pelos dias passados em cima de uma certa ponte, companhia nas viagens de e para "Viana city" e a sempre boa disposição. Agradeço à Cláudia pela ajuda nas amostragens e no laboratório, assim como a sua boa disposição e companhia nas viagens. Agradeço à Ana por me ter iniciado nas "bactérias", pela ajuda nas amostragens e no laboratório, pela constante disponibilidade, assim como, a preocupação, paciência e apoio nos momentos mais complicados.

Um obrigado muito especial à D. Lurdinhas, pelo imenso e árduo apoio laboratorial, pela disponibilidade, boa disposição e dedicação. Agradeço ainda o seu constante apoio, preocupação e a imensa paciência, principalmente nos momentos mais complicados, mas acima de tudo por criar um ambiente agradável e acolhedor, pela simpatia e a pela sua amizade.

Agradeço a todos os meus colegas da UIDM, pela disponibilidade constante para realizar as determinações aos meus sedimentos do Lima, nomeadamente, ao João Abrantes, Manuel Ribeiro, Vitorino, e Orlando.

Agradeço ainda aos meus colegas de trabalho pelo seu apoio durante o período de doutoramento. Em especial gostaria de agradecer, à Doutora Preciosa por permitir uma imensa flexibilidade no horário de trabalho; à Rosa, à Manuela e ao Doutor Cheng pela disponibilidade, apoio e amizade; à Luísa pela constante disponibilidade, boa disposição, paciência e amizade; e ao José Mário pela disponibilidade para ajudar, a imensa paciência, e acima de tudo pela sua amizade e preocupação constante com o meu bem-estar.

Por último quero agradecer à minha família, ao Fernando, ao David, ao Pedro e à Rita, pelo apoio incondicional, paciência e carinho; e em especial à minha irmã, pela sua disponibilidade e apoio constante, por me acompanhar sempre em todos os projetos, e nunca me deixar desistir dos meus sonhos.

A investigação desenvolvida no âmbito deste doutoramento foi parcialmente apoiada pelo projecto UNNOWN - *UNdiscovered Nitrogen micrOrganisms for Wastewater iNoculation: finding efficient microbial seed sludges for wastewater nitrogen removal* (referência PTDC/BTA-BTA/31098/2017), com cofinanciamento do COMPETE 2020, Portugal 2020 e União Europeia através do FEDER, e pela FCT através de Orçamento de Estado.

Cofinanciado por:

COMPETE 2020 PROGRAMA OPERACIONAL COMPETITIVIDADE E INTERNACIONALIZAÇÃO

PORTUGAL 2020

UNIÃO EUROPEIA
Fundo Europeu
de Desenvolvimento Regional

REPÚBLICA PORTUGUESA

FCT Fundação para a Ciência e a Tecnologia

ABSTRACT

Estuaries are among the most productive and dynamic aquatic ecosystems, playing an important role in global biogeochemical cycles, namely in the transport and processing of organic matter and nutrients, which occurs at different temporal and spatial scales. The high population density in coastal areas makes estuaries and coastal waters particularly vulnerable to anthropogenic impacts, with consequences on water quality, function, and structure of estuarine ecosystems, with nutrient enrichment being one of the impacts most important, due to its contribution to eutrophication and climate change.

The purpose of this study was to contribute to a comprehensive understanding of nutrient dynamics and key microbial descriptors in the Lima estuary (NW Portugal). By quantifying the fluxes between major compartments (water and sediments), the evaluation of the nutritional status of the Lima estuary was carried out for the first time, in order to ascertain its eventual role as a sink or source of nutrients to the coastal zone, aiming to contribute to an effective management of the estuary in terms of water quality.

The concentration gradients in the estuary water column were associated with variations in temperature, river flow and tidal action, with spatial and temporal patterns strongly linked to the hydrodynamic and climate setting, and the estuarine properties presenting greater temporal variability than spatial variability. The Lima river flow emerged as the driving force of most dynamic processes associated with the input of nitrate and silica, being the behavior of suspended solids and total dissolved carbon associated with the action of tidal cycles. Nitrate and silica recorded higher values during the ebb tides of the wet seasons (higher river flow), and chlorophyll *a* and bacteria during the dry seasons (higher availability of light and temperature). The tidal dynamics played a crucial role in the short-term variability of the water physical-chemical characteristics, with the distribution and dispersion patterns varying on an hourly scale due to the advection of freshwater, and the intrusion of seawater. Some parameters presented a behavior indicative of *in situ* processes (ammonium and phosphate, chlorophyll *a* and bacteria), despite the strong effect of tidal forcing.

Phytoplankton tended to burst within the oligohaline zone, while higher counts of bacterioplankton were found in the mesohaline zone. By applying a box model approach, similar tide-independent dynamics were observed for chlorophyll *a* and bacterial fluxes, with net growth in the upper less saline boxes, and consumption beneath the halocline. In the non-stratified upper estuary, phyto and bacterioplankton was controlled by nitrogen and carbon inputs. The Lima estuary presented a sediment grain size gradient due to energetic textural bipolarity, with the ebb currents reworking river sediments to the sea, and flood currents

introducing marine sediments into the estuary. Therefore, a selective sediment deposition, with the dominance of coarser to medium sand size sediments was found. Subtidal sediments were generally anoxic in the middle estuary and had higher amounts of mud than intertidal sediments. Oxygen, silicon, carbon, aluminum and potassium were the most abundant elements, with the amount of silicon and carbon associated with the mud contents of the sediments. The mineralogical composition of the sediments reflected the lithology of the watershed, being quartz, microcline, and albite the most representative minerals in line with the results obtained in the elementary characterization.

The present study showed a flux of nutrients from the water column to the sediments (sink). Although the seasonal supply of nutrients to the estuary was highly variable, nutrient concentrations in the sediments were strongly linked to grain size. The seawater input into the estuary was a relevant factor for observed spatial differences. Indeed, by means of a microcosm approach, benthic fluxes of dissolved inorganic nitrogen (NO_x and NH_4^+), and phosphorus (PO_4^{3-}), were measured. The overall decreasing trend recorded in the nutrients levels in the overlying water seemed to indicate their diffusion into the sediments and subsequent storage and/or turn-over by physical-chemical and biological processes.

The obtained results are a valuable contribution for the assessment of the ecological status of the Lima estuary, and serve as an important baseline for other studies concerned with the management of the estuarine environment, in the vein of the Water Framework Directive.

RESUMO

Os estuários estão entre os ecossistemas aquáticos mais produtivos e dinâmicos, desempenhando um papel importante nos ciclos biogeoquímicos globais, nomeadamente no transporte e processamento de matéria orgânica e nutrientes, que ocorre em diferentes escalas temporais e espaciais. A elevada densidade populacional nas áreas costeiras torna os estuários e as águas costeiras particularmente vulneráveis aos impactos antropogénicos, com reflexos na qualidade da água, e no funcionamento e estrutura dos ecossistemas estuarinos, sendo o enriquecimento de nutrientes um dos impactos mais importantes devido à sua contribuição para a eutrofização e as alterações climáticas.

O objetivo deste estudo foi contribuir para uma compreensão mais abrangente da dinâmica de nutrientes e dos principais descritores microbianos no estuário de Lima (NW Portugal). Ao quantificar os fluxos entre os principais compartimentos (água e sedimentos), a avaliação do estado nutricional do estuário de Lima foi realizada pela primeira vez, de modo a determinar o seu eventual papel como um sumidouro ou fonte de nutrientes para a zona costeira, visando contribuir para uma gestão eficaz do estuário em termos de qualidade da água.

Os gradientes de concentração na coluna de água do estuário foram associados a variações de temperatura, caudal do rio e ação das marés, com padrões espaciais e temporais fortemente ligados à hidrodinâmica e à climatologia. O caudal do rio Lima emergiu como a força motriz da maioria dos processos dinâmicos associados aos nitratos e à sílica, sendo o comportamento dos sólidos suspensos e carbono dissolvido total associado à ação dos ciclos de marés. Nitratos e sílica registraram valores mais altos durante a vazante das estações chuvosas (maior caudal fluvial), e a clorofila *a* e bactérias durante as estações secas (maior disponibilidade de luz e temperatura). A dinâmica das marés desempenhou um papel crucial na variabilidade de curto prazo das características físico-químicas da água, com os padrões de distribuição e dispersão variando numa escala de horas devido à advecção de água doce e à intrusão salina. Alguns parâmetros apresentaram comportamento indicativo de processos *in situ* (ião amónio e fosfato, clorofila *a* e bactérias), apesar do forte efeito da acção das marés.O fitoplâncton tendeu a florescer dentro da zona oligohalina, enquanto maiores contagens de bacterioplâncton foram encontradas na zona mesohalina. Aplicando uma abordagem de modelo de caixa, foram observadas dinâmicas similares independentes da maré para os fluxos de clorofila *a* e bactérias, com crescimento nas caixas superiores menos salinas e consumo abaixo da haloclina. No estuário superior não estratificado, o fito e o bacterioplâncton foram controlados por entradas de azoto e carbono. O estuário de Lima apresentou um gradiente de tamanho de grão dos sedimentos devido à bipolaridade textural energética, com as correntes de vazante retrabalhando os sedimentos do rio para o mar e as

correntes de enchente introduzindo sedimentos marinhos no estuário. Portanto, foi encontrada uma deposição seletiva de sedimentos, com dominância de sedimentos de areia de tamanho médio a grosseiro. Os sedimentos subtidais eram geralmente anóxicos no estuário intermédio e tinham maiores quantidades de finos do que os sedimentos intertidais. Oxigénio, silício, carbono, alumínio e potássio foram os elementos mais abundantes, com a quantidade de silício e carbono associada ao conteúdo de finos dos sedimentos. A composição mineralógica dos sedimentos refletiu a litologia da bacia hidrográfica, sendo quartzo, microclina e albite os minerais mais representativos em consonância com os resultados obtidos na caracterização elementar.

O presente estudo mostrou um fluxo de nutrientes da coluna de água para os sedimentos (sumidouro). Embora a descarga sazonal de nutrientes para o estuário fosse altamente variável, as concentrações de nutrientes nos sedimentos estavam fortemente ligadas ao tamanho do grão. A entrada de água do mar no estuário foi um fator relevante para as diferenças espaciais observadas. De facto, por meio de uma abordagem de microcosmo, fluxos bentónicos de azoto inorgânico dissolvido (NO_x e NH_4^+) e fósforo (PO_4^{3-}) foram medidos. A tendência geral de decréscimo registada nos níveis de nutrientes na água sobrejacente parece indicar a sua difusão nos sedimentos e subsequente armazenamento e/ou *turn-over* por processos físico-químicos e biológicos.

Os resultados obtidos são uma contribuição valiosa para a avaliação do estado ecológico do estuário de Lima, e servem como uma linha de base importante para outros estudos relacionados com a gestão do ambiente estuarino, na esteira do preconizado pela da Diretiva Quadro da Água.

TABLE OF CONTENTS

LIST OF FIGURES

LIST OF TABLES

LIST OF PAPERS

This thesis was based on the following papers:

Fernandes, E., Teixeira, C., Bordalo, A.A., 2019. Coupling between hydrodynamics and chlorophyll *a* and bacteria in a temperate estuary: a box model approach. Water 11 (3), 588. https://doi.org/10.3390/w11030588.

Fernandes, E., Teixeira, C., Bordalo, A.A., 2019. Spatial and seasonal dynamics of elemental composition and minerology of intertidal and subtidal sediments in the Lima estuary (NW Portugal). Arabian Journal of Geosciences 12 (13), 412. https://doi.org/10.1007/s12517-019-4569-8.

Fernandes, E., Teixeira, C., Bordalo, A.A., 2019. Seasonal and spatial characterization of the water column of Lima Estuary (Portugal): ebb and flood neap tides variability. In preparation for submission.

Fernandes, E., Teixeira, C., Bordalo, A.A., 2019. Water column characterization of Lima Estuary (Portugal) during ebb and flood tides: neap vs. spring tidal cycle variability. In preparation for submission.

Fernandes, E., Teixeira, C., Bordalo, A.A., 2019. Spatial patterns in Sediment and Water Column Nutrients in the mesotidal Lima Estuary (NW Portugal). In preparation for submission.

Fernandes, E., Teixeira, C., Bordalo, A.A., 2019. Sediment-water nutrient fluxes in intertidal and subtidal sediments from Lima estuary (NW Portugal). In preparation for submission.

CHAPTER 1

General Introduction

1.1 Estuaries - Definition of estuary

An estuary is a transition zone between the river and the sea, subject to forcing by tides, waves, freshwater influx and seawater intrusion. The mixing of seawater and freshwater provides the water column and sediments with high levels of nutrients, making estuaries among the most productive natural habitats in the world (McLusky and Elliott, 2004). The word "estuary" derives from the Latin word "*aestuarium*" which means tidal marsh, which in turn derives from the term "*aestus*", meaning tide. Several definitions have been proposed over the years to describe an "estuary", mainly according to the geomorphological, hydrographic and biological features of the system. Odum (1959) defined an estuary as the "*river mouth where tidal action brings about a mixing of salt and fresh water*", while Dionne (1963) described it as "*an inlet of the sea, reaching into the river valley as far as the upper limit of tidal rise, usually divisible into three sectors: a) a marine or lower estuary, in free connection with the open sea; b) a middle estuary, subject to strong salt and freshwater mixing, and c) an upper or fluvial estuary, characterized by freshwater but subject to daily tidal activity*". Pritchard (1967) described an estuary as "*a semi-enclosed body of water which has a free connection with the open sea and within which sea water is measurably diluted with fresh water derived from land drainage*". Although Pritchard further divided estuaries into four classes, based on geomorphological characteristics, the definition did not take into account the influence of the tide, excluding several coastal water bodies such as coastal lagoons and brackish seas. Later, Dyer (1997) expanded the definition by including the influence of tides: "*an estuary is a semi-enclosed coastal body of water which has a free connection to the open sea, extending into the river as far as the limit of the tidal influence, and within which sea water is measurably diluted with fresh water derived from land drainage*". A more comprehensive definition of an estuary was proposed by Potter et al. (2010), considering additional features such as periodic closure of mouths, and hypersaline conditions during dry periods: "*an estuary is a partially enclosed coastal body of water that is either permanently or periodically open to the sea and which receives at least periodic discharge from a river(s), and thus, while its salinity is typically less than that of natural sea water and varies temporally and along its length, it can become hypersaline in regions when evaporative water loss is high and freshwater and tidal inputs are negligible*". Defining the upper limits of an estuary is also not easy, as it is difficult to define where an estuary ends, given that the transition between river, estuary and coast is not always

easily identifiable in many estuaries due to the gradual change in its geomorphological forms (Wolanski and Elliott, 2016). For the definition, consideration has been given to the limit of saltwater intrusion (Pritchard, 1967), to the limit of tide influence (Day Jr., 1989; Perillo, 1995), or both (McLusky and Elliott, 2004). The definition of the estuary lower limits is also not consensual for coastal scientists and oceanographers, i.e., it can be a geographic feature or the seaward edge of a tidal plume in the open ocean (Wolanski et al., 2012).

Although each estuary is a unique system, some general characteristics prevail in all systems. The estuaries are subject to riverine influences (freshwater source, often a river flow), and marine influences (tidal and wave movements). A general and simplified schematic representation of an estuary is shown in Figure 1.1.

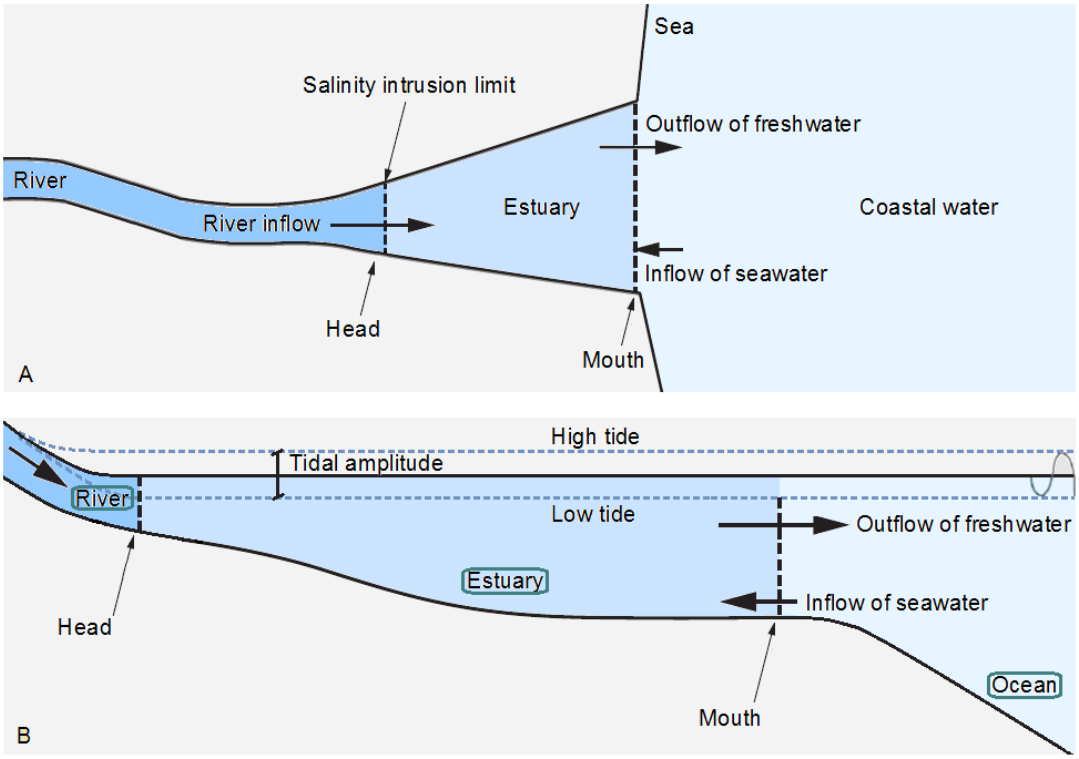

Figure 1.1 View of an idealized estuary. A – Top view; and B – Side view (adapted from Wolanski and Elliott (2016)).

Estuaries often comprise different segments, such as a section mostly dominated by tidal flow and tidal inlet that connects the estuary to the open sea (lower estuary), another where both tides and river flow are important (middle estuary), and a section mostly dominated by river flow (upper estuary).

The development of definitions allowed to produce environmental legislation and management strategies, namely the Water Framework Directive (EU, 2000), which defines the main legal criteria for water resources management in the European Union, identifies estuaries as "*transitional waters*" with the definition of " *bodies of surface water in the vicinity of river mouths*

which are partly saline in character as a result of their proximity to coastal waters but which are substantially influenced by freshwater flows". As a result of this definition, transitional waters include estuaries, fjords, lagoons and other intermediate water bodies (Elliott and McLusky, 2002).

1.2 The estuarine environment

Estuaries have unique characteristics resulting from their connectivity with both freshwater catchment and marine environments, with hydromorphology as the key to understanding their functioning (Wolanski and Elliott, 2016). Hydromorphology deals with problems related to the structure, evolution and dynamic morphology of hydrologic systems over time (Vogel, 2011), and determine the temporal and spatial variability in estuaries. The temporal and spatial estuarine variability is the combined result of several components, such as currents and mixing processes generated by the interaction between freshwater and seawater, tidal cycles, wind, rainfall and evaporation, oceanic events in coastal waters (e.g. upwelling, eddies, and storms), and the spatially and temporally varying bathymetry and geomorphology (Dyer, 1997; Wolanski and Elliott, 2016). Estuaries are characterized by a dominant hydrodynamic (and physicochemical) dimension, establishing environmental conditions. The estuarine hydrodynamic dimension shapes the ecosystems physiography and affects its properties due to the prevailing hydraulic forces (freshwater, tidal, and wave movements) that determine the sedimentation patterns (sediment balance and the erosion-deposition cycles), and condition of the system chemistry (e.g. salinity), and also the rate of system turnover (Basset et al., 2013). In systems with continuous links with rivers and/or sea (open estuaries), one of the main features is an accentuated gradient in salinity conditions (Elliott and McLusky, 2002), with selective influence on potential colonizers (Basset et al., 2013). In these systems, freshwater inflow along with tidal inputs determine the extent of saltwater intrusion, and the influence of the flushing rates and residence time of the estuary (Monsen et al., 2002), which in turn influence salinity (Azevedo et al., 2008), the ability to retain nutrients and the dispersion of plankton (Elliott and Whitfield, 2011). The riverine systems inputs and the tidal pulsing influence sediment dynamics, with erosion-deposition events occurring at different time scales, ranging from daily (ebb-flood) to millennia (the geomorphological time scales) (Wolanski and Elliott, 2016). Sediment dynamics, by establishing the estuarine bed habitats and influencing water column organisms, determine the estuarine biological structure and functioning (Wolanski and Elliott, 2016). Hydromorphology also affects the suspended matter in the water column, and consequently the estuaries turbidity. Suspended particles (inorganic sediments and biological matter) and turbidity influence the light conditions of the water column and, hence primary production (Elliott and Whitfield, 2011; Regnier et al., 2013), as well as the

nutrients retention, their uptake and use, and their export to coastal waters (de Jonge and Elliott, 2001; Regnier et al., 2013).

The organic matter amount of the estuaries result from autochthonous (e.g. reedbeds, seagrass meadows, mangroves and saltmarshes), as well as allochthonous (e.g. riverine primary producers, sea and upland runoff) sources (Day Jr. et al., 2013; Regnier et al., 2013). The ability of an estuary to remain a sink for allochthonous and autochthonous material or a material source for the coastal waters determines its trophic status (Wolanski and Elliott, 2016), as organic detritus are a food source for a variety of estuarine consumers (Day Jr. et al., 2013), with the residence time allowing or not, that the organic detritus remain in the estuary long enough for the nutrients (C, N and P) to be assimilated in the food chain.

Estuaries are important regions in the transport and transformation of materials from natural and anthropic sources, playing an important role in the nutrients processing exchanged between land and sea (Eyre and Twigg, 1997; Bruesewitz et al., 2013; Buzzelli et al., 2013). The chemistry of estuaries should be considered according to the physical processes of water circulation that occur there, since the distribution of dissolved and particulate substances is controlled by the circulation and mixing of their waters (Aston, 1978; Day Jr. et al., 2013; Regnier et al., 2013). Several studies on the import-export function of whole estuarine systems have reported the export of particulate organic material and nutrients (e.g., Dame et al., 1986; Baird and Winter, 1989), but studies carried out by Taylor and Allanson (1995) and Baird and Winter (1992), among others, have provided evidence that in many micro-tidal estuaries (e.g., South African coast) the material is imported from the coastal environment.

1.3 Salinity

Due to the salinity relevance in estuaries, the characterization of the estuarine collected samples with respect to the salinity is a standard procedure for chemical investigations, being known as the "'reactant method" (Morris, 1985). The correlation of the dissolved chemical species concentration with salinity for samples collected along the salinity range allows an assessment of the gain, loss or conservation of the constituent, as well as an indication of the relative species contributions of marine and freshwater sources, and deduce the salinity related to the reactivity location and the extent to which it has progressed.

1.4 Nutrients in estuaries

The role played by estuaries as a natural resource (Ketchum, 1969) results from the uninterrupted passage of nutrients and organic matter of continental origin (Bruesewitz et al., 2013), which undergo a variety of physical, geological, chemical, and biological processes during their stay inside the estuary (Joye and Paerl, 1993; Flynn, 2008; Regnier et al., 2013).

The availability of nutrients and organic matter in the estuaries is a function of their input rates into the system, and production and removal rates within the system (Seitzinger, 1990; Regnier et al., 2013). These inputs have natural sources, such as river and adjacent coastal zone, river drainage and rainfall, and anthropogenic sources, e.g., urban sewage, agricultural, and industrial activity (Ogilvie et al., 1997; Van Luijn et al., 1999; PincKney et al., 2001). The estuarine nutrients are also dependent on the estuary physical attributes, since residence time determines the time range that nutrients remain in the system and are available for biological processes (PincKney et al., 2001; Paerl, 2006; Buzzelli et al., 2013). Stratification also plays an important role in biological processing, as well as turbidity, affecting light availability (PincKney et al., 2001) for the growth of algal and seagrass. Variability and climate change also interact with these factors (Bruesewitz et al., 2013). The nutrient supply is tightly coupled with freshwater inflow, which, in turn, is driven by regional climate variability (Bruesewitz et al., 2013). Nutrients delivered with freshwater supply determine to a large extent the maximum of spring chlorophyll *a* in many estuaries (Kemp et al., 2005). Nutrients processes of decomposition and recycling are mainly ensured by microbial activity with an important function in the whole biological structure of an estuary (Day et al., 1989; PincKney et al., 2001).

Estuaries function as important sinks and nutrient transformers, by altering the quantity and quality of nutrients transported from land to sea (Jordan et al., 1991; Boonphakdee and Fujiwara, 2008; Flynn, 2008). On a real basis of any class of ecosystems, estuaries receive some of the highest nutrient inputs due to local influences from land drainage and often from pollution.

The 'nutrient' term usually refers to the dissolved inorganic forms of nitrogen, phosphorus, and silicon utilized by autotrophic organisms for organic matter production. Estuarine nutrient concentrations vary with land use, catchment and estuary characteristics, and climatic variability (Regnier et al., 2013). The chemical structure of estuaries is determined by four main factors: (1) the quality of inflowing river freshwater; (2) the oceanographic events (e.g., upwelling and coastal transport) which influence the tidal prism nutrient status; (3) the interactions which occur between these two primary sources of nutrients within the water column, and (4) their further modification over the tidally inundated saltmarshes (Allanson and Read, 1995).

River flow has been identified as a crucial factor influencing the estuaries due to its relevant role in sedimentary and hydrodynamic processes (Jordan et al., 1991; Whitfield, 1992; Mallin et al., 1993; Grange and Allanson, 1995; Bate et al., 2002; Regnier et al., 2013). Seasonal changes in river discharge cause regular and substantial changes in estuarine circulation and water column structure (Allanson and Winter, 1999; Regnier et al., 2013).

In a sedimentological context, estuaries are broadly regarded as sinks (net accumulation zones) (Cooper, 2001; Ji, 2017), and receive sediment from three main sources: inflowing

rivers, the sea, and material generated inside the estuary (mainly organic material) (Allanson and Winter, 1999; Ji, 2017). Sediments moving seaward from rivers pass through the estuaries and vice versa (Cooper, 2001; Regnier et al., 2013; Wolanski and Elliott, 2016), as a consequence, a progressive shallowing of the estuaries would be expected over time as tidal inflow and aeolian deposition combine with fluvial and anthropogenic inputs to fill estuarine channels (Wolanski and Elliott, 2016; Ji, 2017). In theory, this is not the case as floods periodically clean up the estuarine channels (Wolanski and Elliott, 2016), but the frequency of these floods has been decreasing due to impoundments, and the increase of freshwater abstraction for domestic, agricultural, and industrial use.

The interactions in the water column, which occur when the freshwater from rivers and the sea saltwater meet, involve complicated mixing processes. As a result, the estuarine zone presents strong gradients in chemical and physical properties (e.g., salts and temperature), emerging as important sites for biotic and abiotic transformations of inorganic and organic matter, with many of these changes occurring in saltmarshes (Morse et al., 2004). Saltmarshes perform important biogeochemical functions, such as, sediment stabilization and bank protection; removal, storage and release of nutrients; and inorganic nutrient transformations to organic forms (DeBusk, 1999; Day Jr. et al., 2013; Wolanski and Elliott, 2016). Saltmarshes are a nutrient sink in the growing season, reducing eutrophication by the absorption of nitrogen and phosphorus from the polluted water. In the remaining periods the nutrients are re-released during decomposition with potentially adverse effects (Adams et al., 1999).

The regeneration of organically bound nutrients to mineral nutrients takes place in sediments (Raimonet et al., 2013; Regnier et al., 2013; Serpetti et al., 2016). Transformations are mediated mostly by bacteria, resulting in gradients of nutrients that are released to the overlying water column (regeneration) (Day Jr. et al., 2013; Serpetti et al., 2016; Dunn et al., 2017; Parsons et al., 2017). Furthermore, the interaction between sediments and overlying water has been recognized as a relevant factor in the nutrient dynamics of estuarine and marine systems (Paerl, 2006; Corbett, 2010; Raimonet, et al., 2013; Dunn et al., 2017).

1.4.1 Nitrogen

Nitrogen is a key constituent of all living matter (Herbert, 1999), being essential for primary production, and generally considered an important limiting factor, and for eutrophication in estuarine and coastal waters (Herbert, 1999; Bruesewitz et al., 2013). The oxidation state of the nitrogen varies from +5 (nitrate) to -3 (ammonium), with the conversion through the oxidation states mediated by biologically controlled processes (Tett et al., 2003; Libes, 2009; Day Jr. et al., 2013) (Figure 1.2). In rivers and estuaries, dissolved inorganic nitrogen (DIN) is mainly found in the form of ammonium (NH_4^+), nitrite (NO_2^-), and nitrate (NO_3^-) ions.

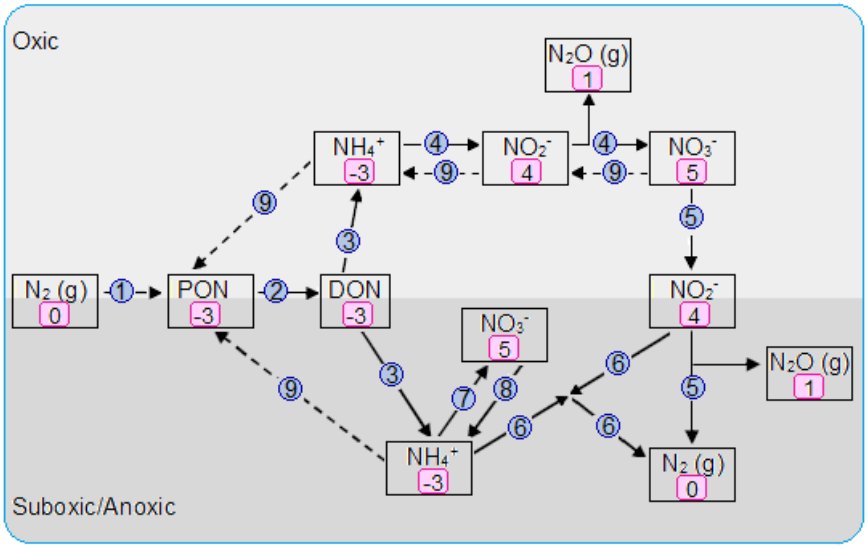

Figure 1.2 A simplified scheme of the aquatic nitrogen cycle illustrating redox and phase transitions mediated by microorganisms. PON: particulate organic nitrogen; DON: dissolved organic nitrogen. The boxes contain nitrogen species and oxidation number. The arrows represent transformation reactions: 1 – nitrogen fixation; 2 – solubilization; 3 – ammonification; 4 – nitrification; 5 – denitrification; 6 – anammox; 7 – anaerobic nitrification mediated by manganese reduction; 8 – dissimilatory nitrate reduction to ammonium (DNRA); 9 – assimilatory nitrogen reduction (adapted from Libes (2009)).

The nitrogen species concentration into an estuary is mainly determined by inputs from fluvial discharge (with terrestrial flow) (Bruesewitz et al., 2013), exchange across the sediment-water interface, biological production (particulate nitrogen) (Buzzelli et al., 2013), and the concentrations may be increased by anthropogenic inputs (Regnier et al., 2013), e.g. wastewater discharge, agricultural fertilizers, and organic industrial wastes (Pinckney at al., 2001).

The mineralized nitrogen amount by benthic flux, and the ratio of ammonium, nitrate, dissolved organic nitrogen, and nitrous oxide/dinitrogen released from the sediment to the overlying water column (Dunn et al., 2017), is determined by the quality (N:C ratio), quantity, spatial distribution of the degradable organic matter and the diffusibility of the decomposition products, which are, in turn, determined by the presence of rooted macrophytes, infauna and oxygen, ammonium, and nitrate concentrations already in the water column (Herbert, 1999). Phytoplankton is able of taking up a wide range of nitrogen chemical species from the solution, but generally requires a nitrogen form reduced, often being considered as preferring ammonium ion (NH_4^+) to nitrate (Paerl and Justic, 2011). Cyanobacteria, a specialized group of prokaryotes, with the nirogenase enzyme (Herbert, 1999), are able to fix gaseous nitrogen (N_2) dissolved in water to ammonia, (Day Jr. et al. 2013).

Nitrogen is removed from the euphotic zone by the downward movement of organic matter, (Regnier et al., 2013), and may occur from phytoplankton sinking, vertical mixing, or detritus

sinking of vertical migrator, resulting in the ammonium introduction at lower depths below the euphotic zone. The ammonium release from nitrogenous matter is known as ammonification (Herbert, 1999; Day Jr. et al., 2013). Not all of the ammonia produced from the organic nitrogen deamination in sediments is available to the primary producers, since a portion, which varies depending on the sediments physicochemical characteristics, can be oxidized to nitrate in the surface oxic zone (Pinckney at al., 2001), through nitrification. This process plays a key role in generating a source of nitrate for denitrifying bacteria (Herbert, 1999), carried out by ammonia-oxidizing bacteria (AOB) (Purkhold et al., 2000; Hatzenpichler, 2012), but also by ammonia-oxidizing *Archaea* (AOA) (Zehr and Kudela, 2011). On the other hand, denitrification is another key process in the sediment nitrogen cycle, which reduces the amount of nitrogen available to primary producers as the final products, nitrous oxide (N_2O), and dinitrogen (N_2) diffuse into the atmosphere (Herbert, 1999; Day Jr. et al., 2013).

1.4.2 Phosphorus

The major phosphorus reservoirs are sedimentary phosphate rocks, which is released into the ecosystems trough erosion (Ji, 2017). Phosphorus is a nutrient that controls the level of eutrophication in aquatic systems, together with nitrogen. Phosphorus transported in surface waters may be in dissolved or particulate forms, and may be organic or inorganic (mainly in solution as orthophosphate) (DeBusk, 1999; Ji, 2017). Besides natural sources (weathering of rocks, and organic matter decomposition), anthropogenic inputs are also major sources, and include discharges of domestic and industrial effluents, rainfall, urban and agricultural land drainage. Therefore, phosphorus concentrations in the estuarine and marine environments are controlled by biotic and abiotic factors, with sediments as active retention (Watson et al., 2018), cycling and release sites (Regnier et al., 2013; Dunn et al., 2017) (Figure 1.3).

Biological control of phosphorus concentrations occurs by assimilation of orthophosphate removed from the surface of organic detritus and suspended particles that are consumed by filter feeders (Regnier et al., 2013) and excreted as inorganic phosphorus, by bacteria and phytoplankton (under favorable light conditions) (Paytan and McLaughlin, 2007). Orthophosphate ions adsorption by clays and iron or aluminium oxides (chemisorption) in the soil, and phosphate precipitation with oxides of iron or aluminum or dissolved calcium in the soil or water column (Ji, 2017; Watson et al., 2018), may represent a relatively long term phosphorus storage, since the regeneration is very slow due to the stability of the formed complexes (DeBusk, 1999).

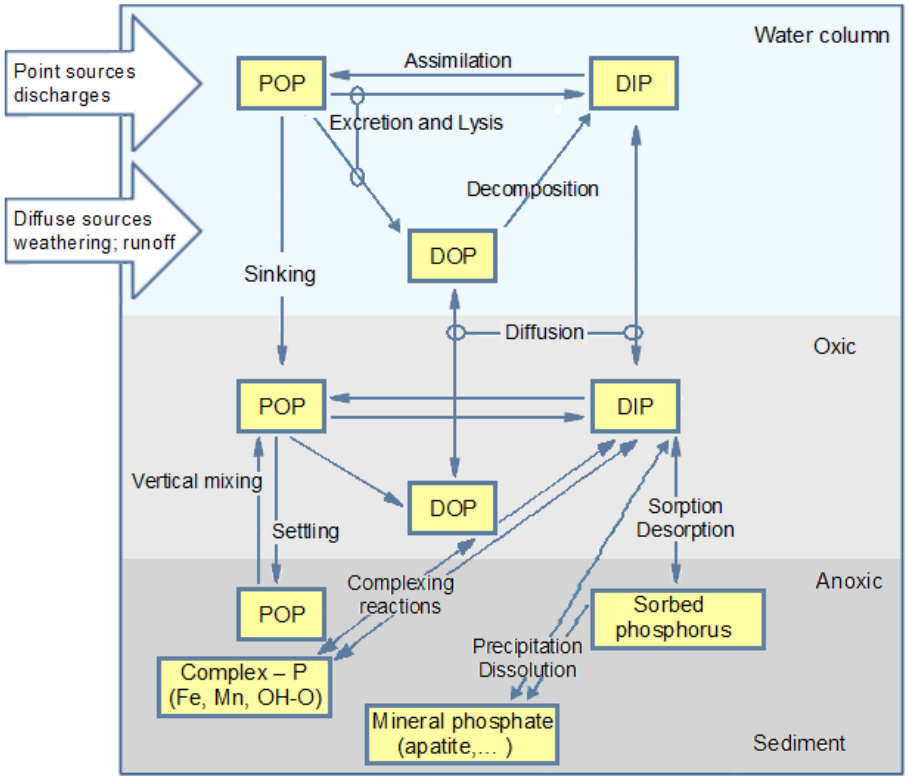

Figure 1.3 Transformations within the phosphorus cycle in estuarine systems. POP: particulate organic phosphorus; DIP: dissolved inorganic phosphorus; DOP: dissolved organic phosphorus (adapted from Day et al. (1989)).

1.4.3 Silicate

Silicon is mostly found as silica in the aquatic environment, as a dissolved compound (mostly silicic acid, called "dissolved silica", DSi), or as amorphous or crystalline particulate matter (Wollast, 1974; Canfield et al., 2005; Carbonnel et al., 2013) (Figure 1.4). DSi is a key nutrient for the aquatic ecosystem, as it is required by the diatoms to build its frustule made of particulate amorphous silica ("biogenic silica", BSi) (Martin-Jézéquel et al., 2000; Carbonnel et al., 2013). The diatoms are important constituents of the phytoplankton community (Sabater, 2009), supporting a short and efficient food chain (Ragueneau et al., 2006), playing an important role in sequestration of oceanic carbon (Ragueneau et al., 2000; Tréguer and Pondaven, 2000).

Riverine discharge of DSi from rock weathering (Ji, 2017) and the terrestrial silica cycle on land consist the main source of silica to the oceans (Wollast 1974; Tréguer et al., 1995; Derry et al., 2005; Tréguer and De La Rocha, 2013). Silica diagenesis is a dissolution reaction, not a bacteria-mediated respiratory process. Silica dissolution is a function of the undersaturation degree, pH, temperature, particulate silica concentration, salinity and nature of solid phase silica surfaces (Testa et al., 2013).

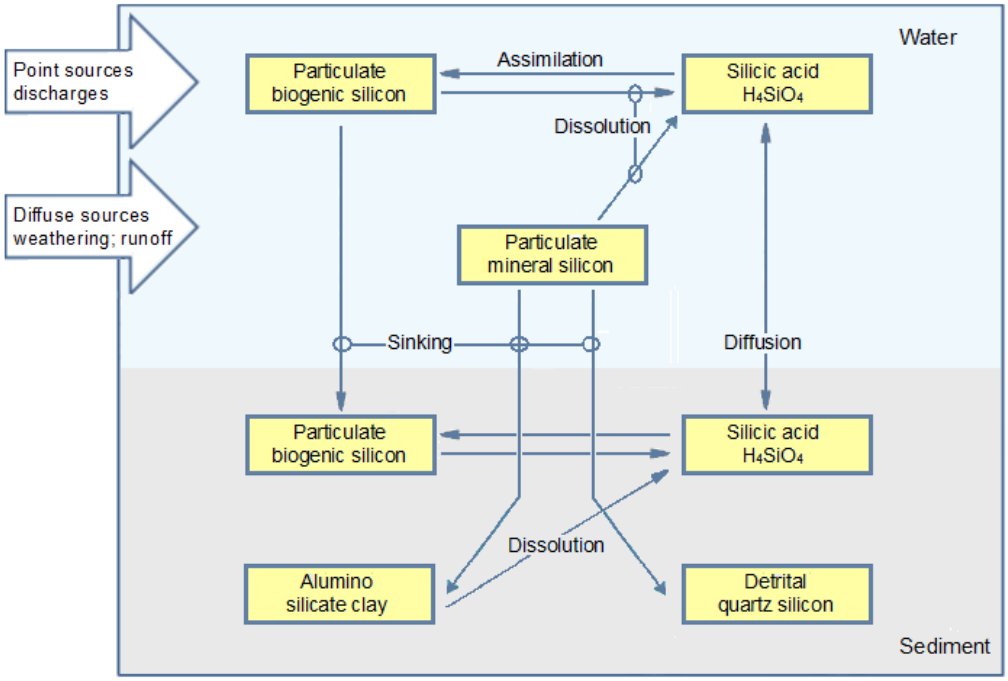

Figure 1.4 Transformations within the silicon cycle in estuarine systems (adapted from Day et al. (1989)).

1.5 Estuaries and anthropogenic pressure

Coastal and estuarine areas have been the most densely populated areas in the world, with approximately 60% of the world population in 2002 (Lindeboom, 2002). The choice of estuaries as settlement sites was a consequence of the advantages they provided (Edgar et al., 2000). Owing to its productivity (McLusky and Elliott, 2004; Day Jr. et al., 2013; Lebreton et al., 2016), estuaries are valuable to human society (Barbier et al., 2011), in terms of provisioning of fish and water, transportation, protection against floods and storms, water purification, primary production, and cultural and recreational services (Edgar et al., 2000; Beaumont et al., 2007; Russi et al., 2013). As a result, estuaries are exposed to many human-induced pressures, in addition to the set of natural processes that occur there (Wolanski and Elliott, 2016). The input of materials into estuaries comprises contaminants and pollutants (e.g., heavy metals, fertilizers, sewage, and synthetic compounds), which can accumulate in sediments by trapping, and later re-enter the water column by resuspension when sediments are disturbed (Roberts, 2012; Dunn et al., 2017). Other materials introduced into estuaries enclose sediments, energy (such as cold water from desalination plants, and hot water from power plants), and infrastructure (land claim, bridges, dams, etc.) (Wolanski and Elliott, 2016). Those infrastructures may affect water quality when they change the physicochemical water parameters (e.g. temperature, salinity, turbidity and dissolved oxygen), due to changes in terrestrial run-off, hydrodynamics, or the discharge of heated effluent (Clark et al., 2015). Materials taken out the estuaries include salt, water, fish, sediments, and ‘space’ (McLusky

and Elliott, 2004). Superimposed on these local anthropogenic activities and pressures are the consequences of climate changes,e.g., sea-level rise and changes in hydrology due to altered rainfall patterns, resulting in more pronounced seasonal variability in the salinity; surface saline incursion, and marine transgressions, which will affect the ecological functioning of the estuary (Little et al., 2017), but also bioinvasions, and estuarine acidification. The multitude of pressures affecting estuaries often result in a cumulative impact, leading to the degradation of these ecosystems and thus posing a risk to human and environmental health.

1.6 The study area

The Lima River is an international watershed, included in the Portuguese Hydrographic Region of Minho and Lima (RH1), covering 2,522 km^2, of which 1,199 km^2 (47.55%) are located in Portugal and 1,323 km^2 (52.43%) in Spain, and it is characterized by being mountainous, with pronounced slopes, and a maximum altitude at approximately 1,400 m (APA, 2016). This river, with an extension of about 108 km, has its source in Serra de S. Mamede, flowing along the province of Ourense (Spain) and draining into the Atlantic Ocean in the northwest coast of Portugal, at the vicinity of the city of Viana do Castelo (Figure 1.5). The geographic position of this region, framed by the Atlantic Ocean and mountainous areas, results in a wet climate, with an annual precipitation between 1,300 and 4,200 mm (APA, 2016).

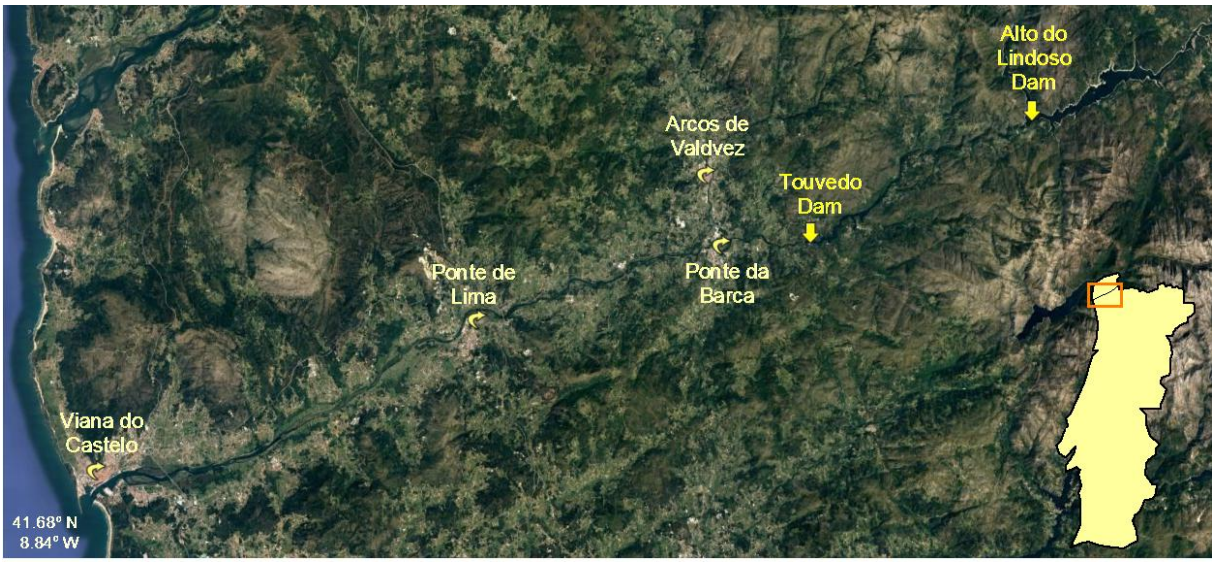

Figure 1.5 Aerial image of the Portuguese part of the Lima River, with its main urban areas (Viana do Castelo, Ponte de Lima, Ponte da Barca and Arcos de Valdevez) and dams (Touvedo and Alto Lindoso) (source: Google Earth).

The hydrogeology of this region is characterized by systems of fissured nature, supported by granitoid and metasedimentary rocks of the Hesperian Massif, and porous units (mainly alluviums and terraces), having a small spatial development (ARH Norte, 2012). The lithologies

with the highest representation belong to the metamorphic basements (mainly schists, greywackes, metapsamopelites, quartzites, metaconglomerates and micaschists), and magmatic basements (mainly granitoids). The Pleistocene and Holocene sedimentary units are represented by siliciclastic fluvial, colluvial, aeolian, estuarine and beach deposits (Carvalhido et al., 2014). The alluviums currently found are deposits consisting of mud (clay and silt), sands, and fluvial gravels (Martins et al., 2017). Thus, the Lima River presently runs on alluviums that occupy the latter valley, being the sands of feldspathic quartz and the gravels of granite, quartz, feldspar, and less frequently schist, quartzite and gneiss (Alves, 2004).

The Lima estuary is a small open estuary, tidally dominated (Falcão et al., 2013), extending up to about 24 km from its mouth, and covering an area of 10.4 km^2. The estuary is a temperate, with a semidiurnal and mesotidal regime (Vale and Dias, 2011). The average flushing rate is 0.40 m s^{-1}, the river flow is 70 m^3 s^{-1}, and the residence time 9 days, being partially mixed, with a seasonal vertical stratification of salinity during the winter period, in which salinity increases sharply with depth (Ramos et al., 2010). The semidiurnal tidal regime represents the main hydrodynamic forcing action, ranging from 1.1 m on neap tides to 3.7 m on spring tides, with the river regime controlled by the presence of two upstream hydroelectric power plants, which maintain an environmental flow throughout the year (Falcão et al., 2013). According to the morphology, bathymetry, salinity, and the presence/absence of saltmarshes, the estuary can be divided into three zones: lower, middle, and upper estuary. The lower estuary, located in the first 2.5 km, is adjacent to an urban area (Viana do Castelo), and consists of a narrow channel with walled banks, constantly dredged to a depth of 10 m to allow navigation (Amorim et al., 2016). The area is rather industrialized, with anthropogenic modifications such as the presence of a jetty at the river mouth deflecting the flow to the south, a large shipyard, a commercial sea-port, a marina and a fishing harbor (Azevedo et al., 2013). The middle estuary is predominantly a saltmarsh area, with several sand islands and intertidal channels, mainly colonized by sea rush *Juncus* spp. (Ramos et al., 2010). The most upstream section of the estuary, the upper estuary, is characterized by a narrow, shallow channel with some intertidal areas and undisturbed banks remaining almost in a natural state (Rebordão and Teixeira, 2009). In addition to the pressures caused by the constructed infrastructures and navigation activity, the estuarine system is impacted along its course by a cellulose factory in the upper stretches, agricultural runoff input, domestic and industrial wastewater discharges, leading to the introduction of nutrients and other substances, transported from urban, industrial and agricultural areas into the estuary (Almeida et al., 2011, Azevedo et al., 2013).

The Lima estuarine ecosystem comprises important and sensitive areas (e.g., saltmarsh, sand flats and mud flats), which still conserve an important biodiversity and represent an important wet natural space, both for the nesting of many species of birds, as well as for their food and shelter, reason why this space is classified as valuable for species and habitats conservation

(APA, 2016). Parts of the estuary are included in the Natura 2000 network. Several fish species of economical and/or conservational value occur in the Lima estuary (i.e. flounder - *Platichthys flesus*, sole - *Solea solea*, brill - *Scophthalmus rhombus*, sea bass - *Dicentrarchus labrax*, sea lamprey - *Petromyzon marinus*, European eel - *Anguilla anguilla*, allis shad - *Alosa alosa*, twaite shad - *Alosa fallax* and Atlantic salmon - *Salmo salar*), as well as important conservational species of birds (e.g. *Platea leucorodia*) and mammals such as *Lutra lutra*, (Costa-Dias et al,. 2010). As for riparian vegetation, the estuary shows high diversity of species, more specifically in the marginal and aquatic communities (APA, 2016).

1.7 Relevance and objectives of the thesis

The nutrient overenrichment of water is one of the oldest water quality problems created by humankind (Vollenweider, 1992). The nutrients N and P as the main overenrichment nutrients, and Si as a limiting nutrient for diatom production at sites with relatively high levels of N and P, have been reported in several review articles (Downing, 1997; Smith, 1998; Smith et al., 1999; Conley, 2000; NRC, 2000).

Nutrient overenrichment and eutrophication have resulted in the need for legislation to establish the current ecological status of aquatic ecosystems and to indicate measures for their monitoring and recovery. The Water Framework Directive (2000/60/EC), for example, is the European framework for protection of inland surface waters, transitional waters, coastal waters and groundwater (EU, 2000).

Hence, in order to ascertain possible nutrient overenrichment and deterioration of water quality, it is important to understand the nutrient loading relationships along the estuary and its compartments and ecological responses. In fact, the great concern raised by this problem has stimulated new research in the following areas: chemistry and biogeochemistry of nutrients in aquatic systems, quantification of the sources and sinks of nutrients, and dynamics of nutrient uptake and release.

The aim of this thesis was to evaluate the effects of changes in the magnitude of the freshwater inflow and variability of estuarine hydrodynamics, as well as in the water quality, allowing to a more comprehensive understanding of estuarine biochemistry, in order to guide effective management towards the preservation and improvement of the water quality. The study will attempt to establish the following key issues:

- Evaluate seasonal patterns of the physical, chemical, and biological parameters in the water column, along the estuarine gradient and during the tidal cycle (ebbing and flooding);
- Evaluate neap-spring tide patterns of physical, chemical, and biological parameters in the water column, along the estuarine gradient and during the tidal cycle (ebbing and flooding);

- Ascertain the seasonal dynamics, including the neap-spring tide dynamics, of phyto- and bacterioplankton during ebb tides, using a box model approach;
- Perform the seasonal inventory of intertidal and subtidal sedimentological components, including textural and geochemical descriptors, for the spatial and temporal characterization of the estuarine system;
- Characterize spatial and temporal variations of nutrient concentrations in the various estuary compartments (water column, pore water, and sediments) to investigate the interrelations of nutrients between the different compartments;
- Investigate the nutrients behavior in the subtidal and intertidal sediments;
- Estimate sediment-water fluxes of inorganic nitrogen and phosphorus along the Lima estuary in winter and summer seasons;
- Determine the behavior of the Lima estuary as a sink or source of nutrients.

The present thesis is organized in eight chapters. Chapter 1 provides a general introduction to the estuarine environment, the nutrient cycles included in the overall chemical structure of the estuary, and the adverse consequences of nutrients overenrichment. Chapter 2 addresses the spatial and temporal characteristics of key environmental variables, as well as relationships between them, with temporal data of seasonal and cycle tides surveys. Chapter 3 analyses the spatial and temporal characteristics of the main environmental variables, as well as the relationships between them, with temporal data taking into account the high-low tidal cycle and the neap-spring tidal cycle. Chapter 4 analyses the behavior of key planktonic descriptors, namely phyto and bacterioplankton at a spatial and temporal scale, to ascertain the dynamics of plankton during a spring and a neap tides, as well as an annual seasonal cycle, through the development and application of a box model, approach based on conservative salinity tracer property. Chapter 5 describes the spatial and seasonal dynamics of elemental composition and mineralogy of intertidal and subtidal sediments, relating their composition to the origin source and the transport processes. Chapter 6 investigates the pelagic-benthic coupling of nutrients through the spatial and temporal characterization of the different estuary compartments, i.e., water column, interstitial water, and sediments. Chapter 7 presents the estimation of inorganic nitrogen and phosphorus sediment-water fluxes along the Lima estuary in winter and summer seasons, by means of a microcosm approach. Chapter 8 includes the final conclusions and directions for future research.

CHAPTER 2

Seasonal and spatial characterization of the water column of Lima Estuary (Portugal): ebb and flood neap tides variability

Abstract

The spatial patterns of physico-chemical parameters, phytoplankton and bacteria were studied in seasonal surveys during ebb and flood neap tides in the mesotidal Lima estuary (NW Portugal). The Lima estuary (Portugal) was studied during an annual seasonal cycle (February to November 2014) with the water samples collected at eleven stations along the estuary (lower, middle and upper stretches). Lima river flow seems to be the driving force of most dynamic processes associated with nutrients (nitrates and silica), while the behavior of suspended solids and total dissolved carbon seems to be associated with the action of tidal cycles. The nutrients presented higher values during the wet seasons, while chlorophyll *a* and bacteria were elevated during the dry seasons. The behavior of some parameters within the estuary seems to indicate *in situ* processes (ammonium and phosphate, chlorophyll *a* and bacteria), despite the strong effect of the external and physical variables. The assessed parameters gradient structure in the estuary showed variations with temperature, river inflow and tidal action, with the spatial and temporal patterns of estuarine ecosystem strongly linked to the hydroclimatic setting. The patterns differences showed that some estuarine properties have greater seasonal (temporal) variability than spatial variability.

Keywords: nutrients; phytoplankton; bacteria; seasonal; ebb and flood tides; Lima Estuary.

2.1 Introduction

The geographic location of estuaries, situated between the river (freshwater) and ocean (saltwater) environments (Cloern et al., 2017), leads to both natural and anthropogenic pressures (Wolanski and Elliott, 2016). These areas are among the most densely populated in the world (Wolanski, 2007), with 60% of the world population located there in 2002 (Lindeboom, 2002). The estuaries form a transition zone being subjected to marine and riverine influences, with characteristics dependent on tidal pulses, river flow, hydrodynamic (Menéndez et al., 2012; Robins et al., 2016) and autochthonous biological processes (Saraiva et al., 2007; Wepener, 2007). The functioning of estuaries varies greatly, due to differences in estuary shapes and sizes, and external physical forcings such as river flow, sediments, tides,

wind and evaporation (Kappenberg et al., 2016). The hydrodynamic regime of the estuaries results from factors such as currents and mixing processes caused by the interaction between freshwater and seawater (Marcovecchio et al., 2009), the tides with their cycles (semidiurnal, diurnal, weekly, fortnightly, equinoctial and annual), wind, rain and evaporation, oceanic events in coastal waters, and bathymetry and geomorphology varying both spatially and temporally (Dyer, 1997; Prandle, 2009).

Estuaries are dynamic systems with large temporal and spatial gradients of biogeochemical compounds and processes (Chaudhuri et al., 2012; Robins et al., 2016). Temporal changes include diurnal cycling and event-based changes between high and low flow conditions, seasonal, decadal and longer time-scale (Robins et al., 2016). Spatial variations are a result of the continuous transporting and processing of the biogeochemical compounds in the freshwater and seawater along the estuary, with discontinuities due to the outputs and inputs from other sources (e.g., sediments). Therefore, estuaries play a decisive role in nutrients biogeochemical cycling, essential for the growth and resilience of plants and animals (Malham et al., 2014; Robins et al., 2016).

On a time scale of hours, the freshwater ebb advection and the salt water intrusion during the flood determine changes in several parameters of the water column, such as salinity, nutrients and suspended particulate matter (Montani et al., 1998), being the extent of such variations dependent on tidal amplitude (Montani et al., 1998). Moreover, the scenario may be greatly complicated by environmental variables, such as precipitation rate, affecting freshwater discharge (Page et al., 1995; Montani et al., 1998), temperature, solar irradiance, winds (Yin et al., 1995; Montani et al., 1998) and current velocity (Renshun 1992; Montani et al., 1998), being these variables driven by climate, which varies considerably within years (i.e., seasons) and among years. While the marine tidal cycles are predictable and reproducible, the freshwater discharge is variable because they reflect the seasons as well as the instability of the precipitation regime throughout the watershed (Lam-Hoai et al., 2006; Menéndez et al., 2012).

Estuaries are never in a steady state, and this is especially true in temperate regions with marked biological, physical, chemical and geological seasonal cycles (Morais et al., 2009). The influx of the river is another structural factor of the estuary's biotic and abiotic parameters, and may even be more determinant than the tides (Morais et al., 2009). River flow is decisive for setting nutrient concentration and its stoichiometry (Nixon, 2003), which affects primary and secondary production (Nixon, 2003), thus affecting estuarine dynamics and landings of coastal fisheries with economic impact inherent (Morais et al., 2009).

The aim of this study was to evaluate seasonal and spatial distribution of physical, chemical and biological parameters in the water column of Lima River estuary, during the tidal cycle

(ebbing and flooding), with the goal of understanding the variation of those parameters among seasons and within season between ebb and flood tides.

2.2 Material and methods

2.2.1 The study area

The Lima watershed has a total surface of approximately 2,450km^2 with 1,143 km^2 located in NW Portugal. The Lima estuary is a temperate estuary with a semidiurnal, mesotidal regime (Vale and Dias, 2011), with the geographical coordinates of 41.68º N; 8.84º W (WGS84) (Figure 2.1), having an extension of around 20 km, and an average river inflow of 70 m^3 s^{-1} (Ramos et al., 2006). The estuary can be divided into three stretches, lower, middle and upper estuary (Figure 2.1). The lower estuary consists of a narrow and deep navigation channel (9 m), with walled banks, being located in an area with anthropogenic modifications such a jetty, and constant dredging, comprising a large shipyard, a commercial seaport, a marina, and a fishing harbor (Ramos et al., 2010). The middle estuary, contains an area of salt marsh with several sand islands, and intertidal channels. The most upstream stretch of the estuary consists of a narrow and shallow channel, with some intertidal areas and undisturbed banks that remains in a natural state (Rebordão and Teixeira, 2009). This estuary suffers the impact of wastewaters discharges that input several substances, transported from urban, industrial and agricultural areas into the estuary (Almeida et al., 2011).

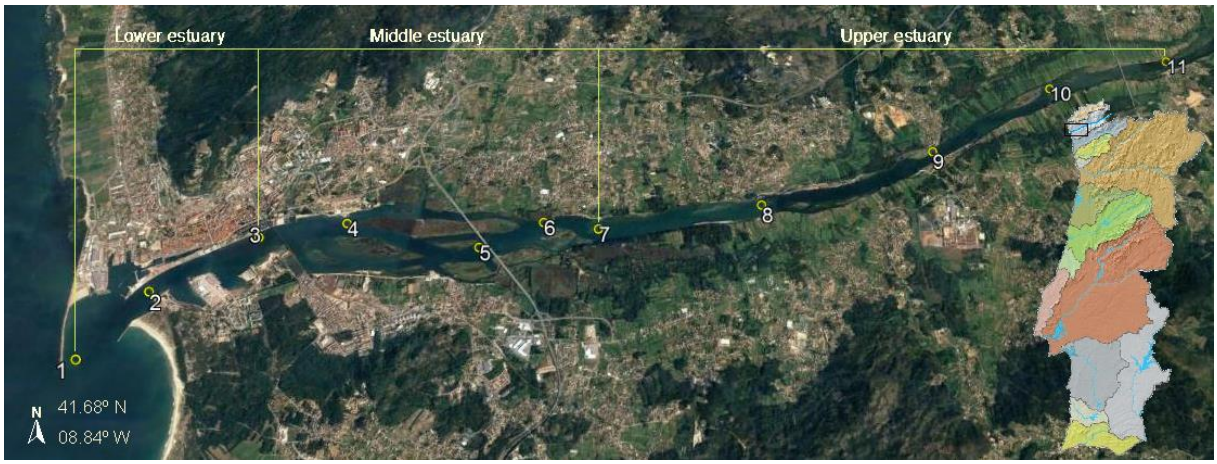

Figure 2.1 Satelite image of the Lima estuary sampling stations (source: Google earth).

2.2.2 Sampling

Sampling surveys were carried in the four seasons between February 2014 and November 2014, during the ebb and flood tides of the same day (25 February 2014; 2 June 2014; 1 September 2014; and 11 November 2014), and started 1:30 h before slack water. Samples

were collected from 11 locations along the estuary (Figure 2.1). At each sampling station, vertical profiles of salinity, temperature, turbidity, pH and dissolved oxygen (DO) were obtained with a YSI 6820 CTD multiprobe, calibrated according to the instructions from the manufacturer. The data presented for the remaining parameters resulted from the analytical determination of the samples collected in the water column with a Van Dorn bottle (surface, medium and bottom water), with the collected samples kept refrigerated in an ice chest until processing in the laboratory.

2.2.3 Analytical procedures

For the determination of total suspended solids (TSS) and volatile suspended solids (VSS), the water samples were filtered through pre-combusted glass fiber filters (GF/F Whatman), and dried at 105 °C (TSS), followed by combustion at 550 °C (VSS) (APHA, 1992). The dissolved orthophosphate, nitrite, ammonium and silicate determinations were performed by the methods of Koroleff (Grasshoff et al., 1983). The nitrate concentration was obtained by the method described by Jones (1984) and adapted by Joye and Chambers (1993), subtracting the nitrite from the total concentration of NO_x obtained. Determination of total dissolved carbon (TDC), dissolved organic carbon (DOC), and total dissolved nitrogen (TDN) was performed by high-temperature catalytic oxidation with a TOC-VCSN analyzer (Shimadzu Instruments). All analyzes were performed in triplicate. The analytical technique used for the chlorophyll *a* determination was molecular absorption spectrophotometry after extraction using 90% acetone (Parsons et al., 1984) and quantification using the SCOR-UNESCO equations (1966). Water samples were fixed with formaldehyde (4% v/v) for the determination of the total microbial cells (TCC). Subsamples (3 mL) were stained with 4',6'-diamidino-2-phenylindole (DAPI), and filtered onto black 0.2 μm Nucleopore polycarbonate membranes (Whatman, UK) (Porter and Feig, 1980). The microbial cells were counted with an epifluorescence microscope (Labphot, Nikon, Japan) equipped with a 100 W high-pressure Mercury lamp and a specific filter sets (UV-2B), at 1875x magnification. A total of 20 random microscope fields in different parts of the filter were counted in order to accumulate at least 300 cells per filter.

2.2.4 Data analysis

Bi-dimensional contour plots, generated by Surfer 8.01 software (Golden Software Inc.), were used to represent variations of measured variables with depth along the estuarine axis in the navigation channel. Data were interpolated using the Kriging gridding method (linear variogram model). STATISTICA 13.0® software package was used to perform the basic statistics, and statistical tests, being all statistical analyses considered at a significance level of 0.05. Principal component analysis was performed to investigate patterns of similarity between samples

based on environmental variables, in data previously log transformed to account for the non-normal distribution of variables and normalized to account for the different units in which variables expressed.

PRIMER 6 & PERMANOVA+ software package was used to investigate differences between results obtained at different times (seasons and tides) and in different spaces (depths and estuary areas). The permutational multivariate analysis of variance (Permanova), is a non-paramentric, based on dissimilarities, that uses permutation to calculate the *F* (pseudo-*F*) statistic. It allows the partitioning of variability, similar to ANOVA, allowing a complex design (multiple factors, nested design, interactions, covariables). It is meant to test differences between groups as an ANOVA test, but with a lot of variables, and with permutations to avoid possible biases. This tool was carried out for the similarity study of the obtained data, grouped by season, tide, estuary area and depth, using 9999 permutations. Permutational tests of homogeneity of multivariate dispersions (PERMDISP) were also performed.

2.3 Results

2.3.1 Key physical-chemical descriptors

The longitudinal salinity profiles for the seasonal surveys during ebb and flood tides are presented in Figure 2.2. The February and November ebb tide surveys did not present a salt wedge (salinity above 30). The remaining surveys contours showed that a salt wedge introduced during the flood tide, remained within estuary during low slack ebb tide.

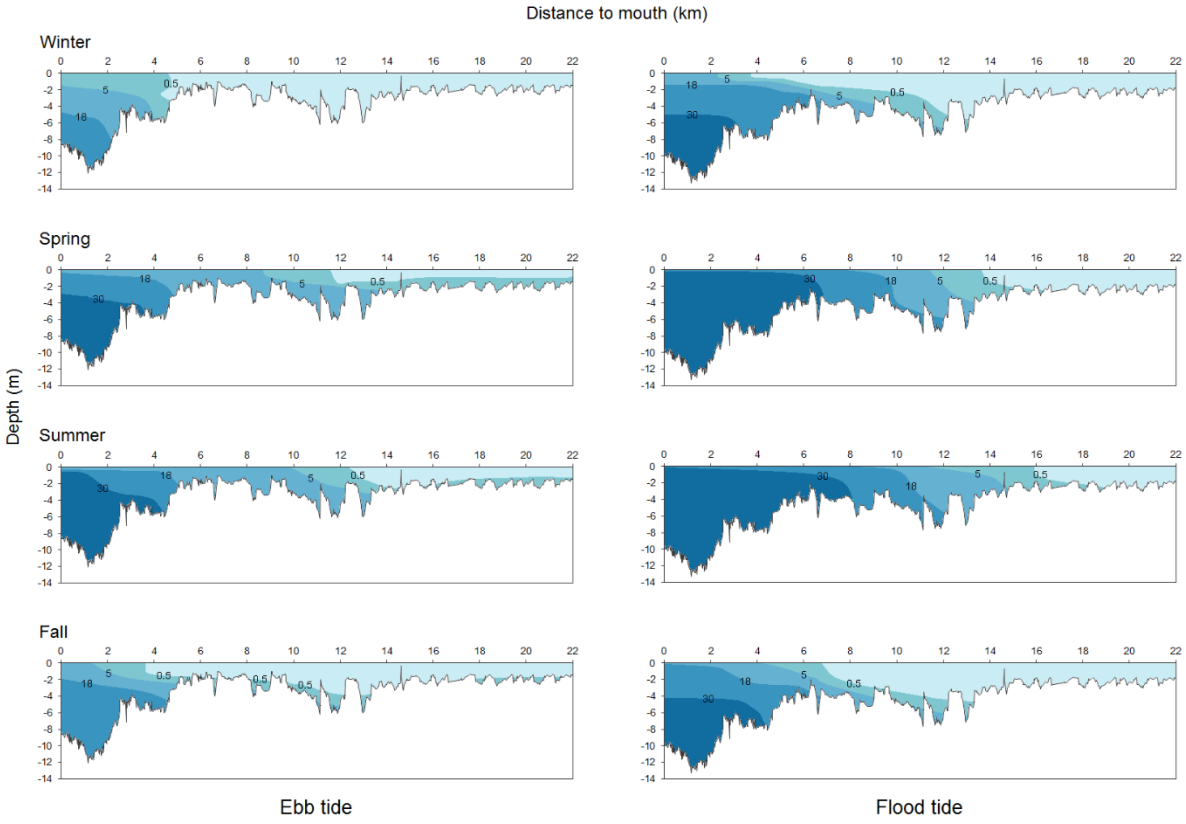

Figure 2.2 Longitudinal salinity profiles of the Lima Estuary during seasonal surveys.

Salinity profiles, for both ebb and flood tides, presented two distinct behaviors, one for the dry seasons (spring and summer) and another for the wet seasons (fall and winter), with seawater entering the dry seasons more extensively in the river (Figure 2.2 and Figure 2.3).

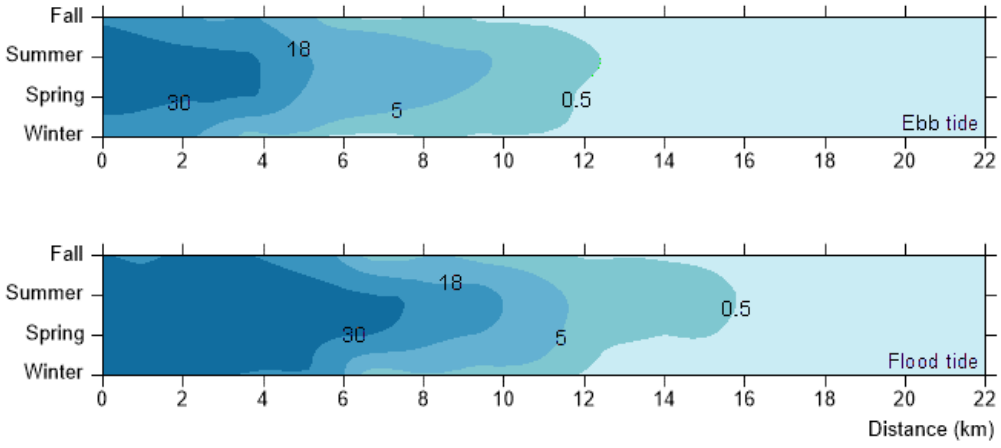

Figure 2.3 Diferences in the salinity boundaries within the Lima estuary during seasons and tides.

During high discharges periods and abundant rainfall, mostly in winter and fall (Figure 2.4), estuarine water almost flushed out at low tide. Comparing the ebb and flood tides, differences were observed in the location of salinity isolines into the estuary. The salinity isolines of 30 and

18, showed differences of 3 to 6 km between the two tides, for all seasons. The observed salinity values during the surveys were dependent on tidal conditions and river flow. The bottom salinity increased during the flood tides. The influence of the river flow on salinity was more evident at the surface, with values decreasing during the flood tide in all surveys, coincident with river flow increase.

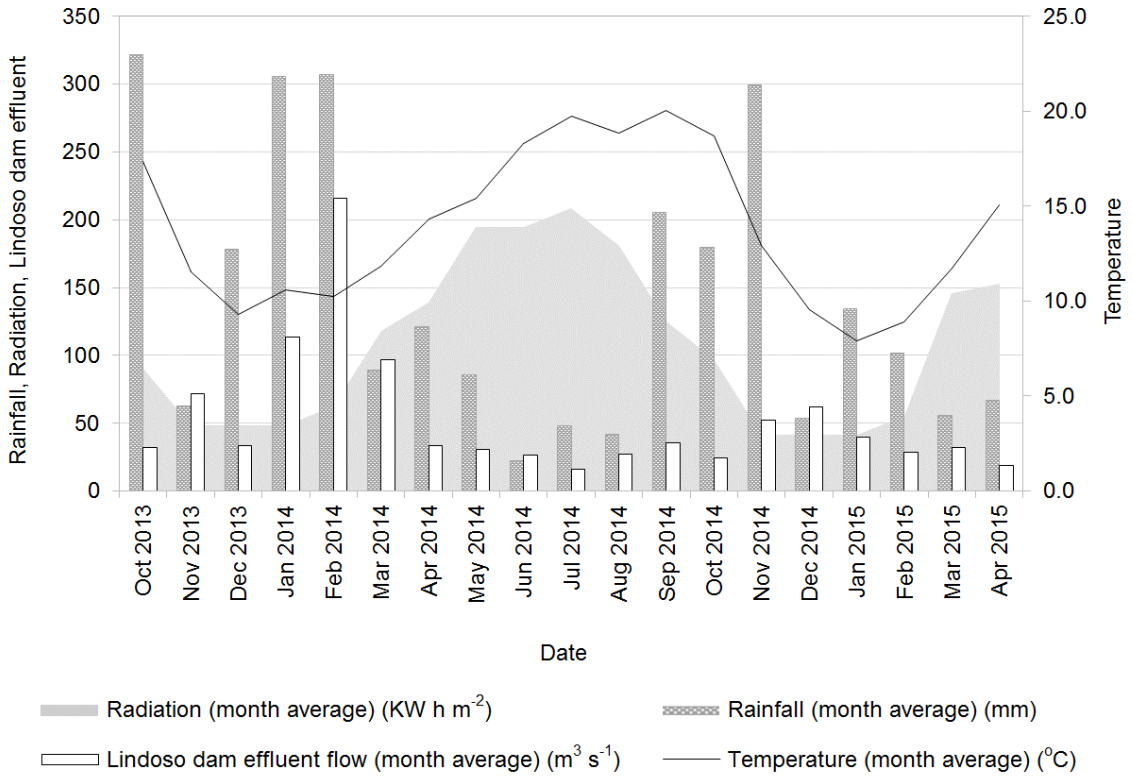

Figure 2.4 Meterological conditions in Viana do Castelo and effluent flow of the Lindoso dam (Data from: IPMA - Instituto Português do Mar e da Atmosfera and SNIRH - Sistema Nacional de Informação de Recursos Hídricos).

The salinity increase was accompanied by an increase in temperature and pH, of a decrease in dissolved oxygen, and within each season, the flood tide pH was higher than the ebb tide pH (Table S2.1).

Water temperature followed the seasonal trend, with the minimum values in the winter (11 ºC), and maximum values in summer (Ebb -19 ºC, and flood -18 ºC). The water temperature pattern was similar to seasonal trend, with a minimum of 10.1º (bottom sample) in winter, and a maximum of 23.49ºC (surface sample) in summer, both concentrations registered during flood tides in the upper estuary (Figure 2.5, Table S2.2). In the dry seasons, the temperature during the ebb tides was higher than during the flood tides, and the reverse behavior was observed in the wet seasons (Table S2.1).

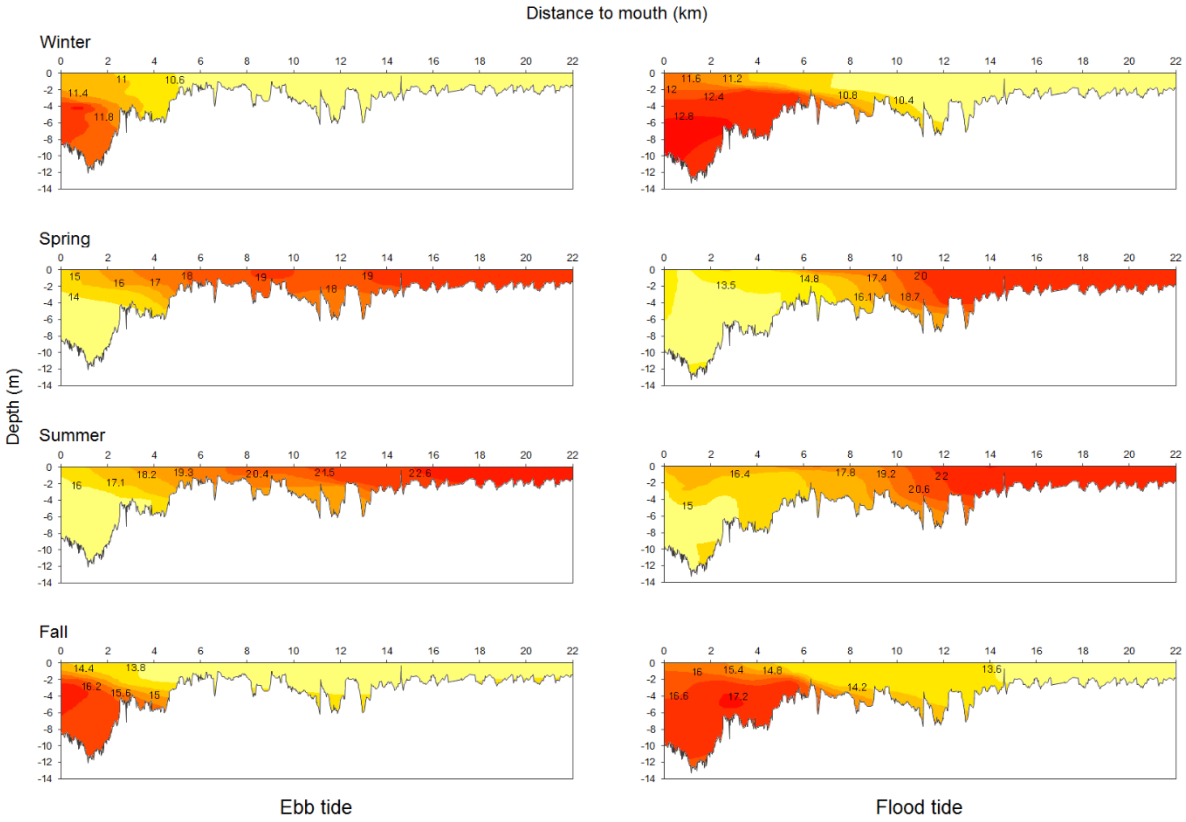

Figure 2.5 Longitudinal temperature profiles of the Lima Estuary during seasonal surveys.

Dissolved oxygen showed higher values in surface samples of the upstream estuary area (Figure 2.6). The maximum value recorded was 11.63 mg O_2 L^{-1} (surface sample) in winter, and the minimum value was 7.18 mg O_2 L^{-1} (bottom sample) in summer, both concentrations recorded during the ebb tide, in the upper and lower stretches of the estuary, respectively (Figure 2.6, Table S2.2). During the dry seasons, the flood tide always showed higher values than the ebb tide, but this tendency was not pronounced in the wet seasons, which showed similar high concentrations.

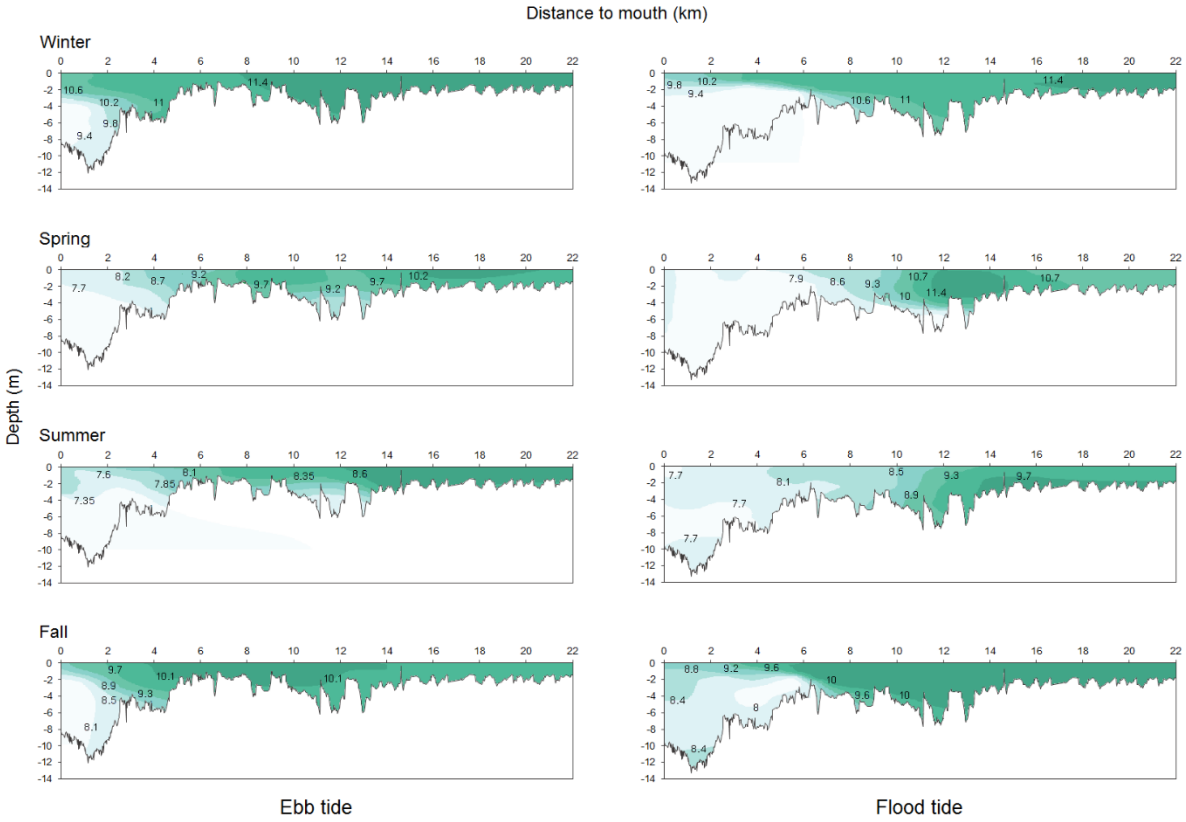

Figure 2.6 Longitudinal dissolved oxygen profiles of the Lima Estuary during seasonal surveys.

The turbidity showed higher concentration values in wet seasons and lower in dry seasons (Figure 2.7). The maximum concentration recorded was 16.4 NTU, in a bottom sample collected in the area most downstream of the estuary during the fall. The minimum concentration value of 0.20 NTU (surface sample) was recorded in the most upstream area of the estuary during the summer. Although in all seasons, the maximum concentration value was recorded during the flood tide, the average concentration did not follow the same pattern. In the wet seasons, the turbidity during the ebb tides was higher than during the flood tides, and the reverse behavior was observed in the dry seasons (Table S2.1).

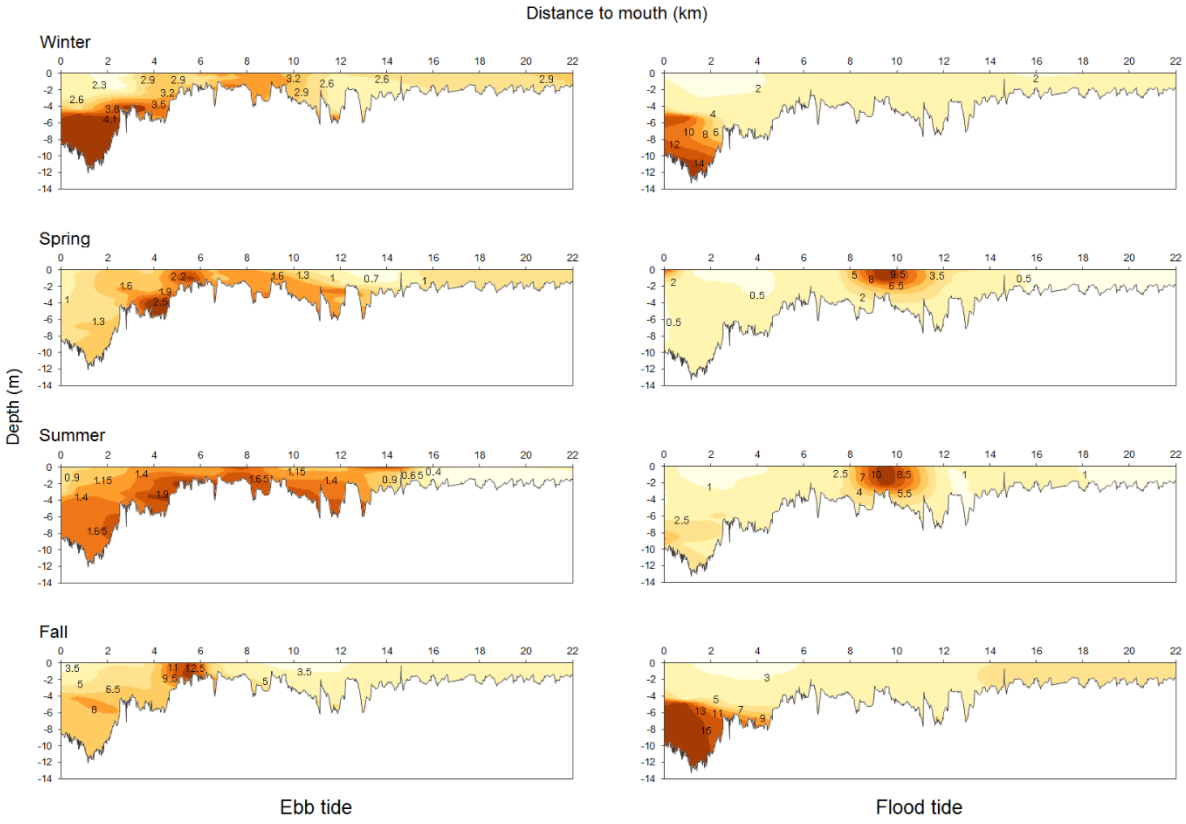

Figure 2.7 Longitudinal turbidity profiles of the Lima Estuary during seasonal surveys.

2.3.2 Seasonal variability of environmental variables

Seasonal variability of measured parameters is presented in Figure 2.8 and Table S2.1. Average nitrate and silicate concentrations throughout the estuary were higher during the winter (ebb-flood tides nitrate concentratios: 44–46 μM, and ebb-flood tides silica concentratios: 97–85 μM), being the lowest levels in summer (ebb-flood tides nitrate concentratios: 22–15 μM, and ebb-flood tides silica concentratios: 51–34 μM. For ammonium and phosphate no consistent pattern was observed, however with the higher ammonium concentration in summer ebb tide (2.52 μM).

Phosphate, nitrite, carbon (total and organic) and suspended solids (total and volatile) showed the higher values during flood tides. Nitrite, total carbon, and total and volatile suspended solids presented lower values in winter and fall (wet seasons), and higher in spring and summer (dry seasons). Chlorophyll *a* also presented lower values in winter, and higher in spring and summer when the temperature increased. TCC were lower in winter, followed by an increase in seasons with intermediate temperatures and finally the highest value was found in summer. Nitrate, silica and DO showed higher values at the surface corresponding to the lower water salinity values (Figure 2.8). Phosphate and nitrite generally showed the higher amounts at the bottom, where salinity was higher, presenting the higher values during the flood tides.

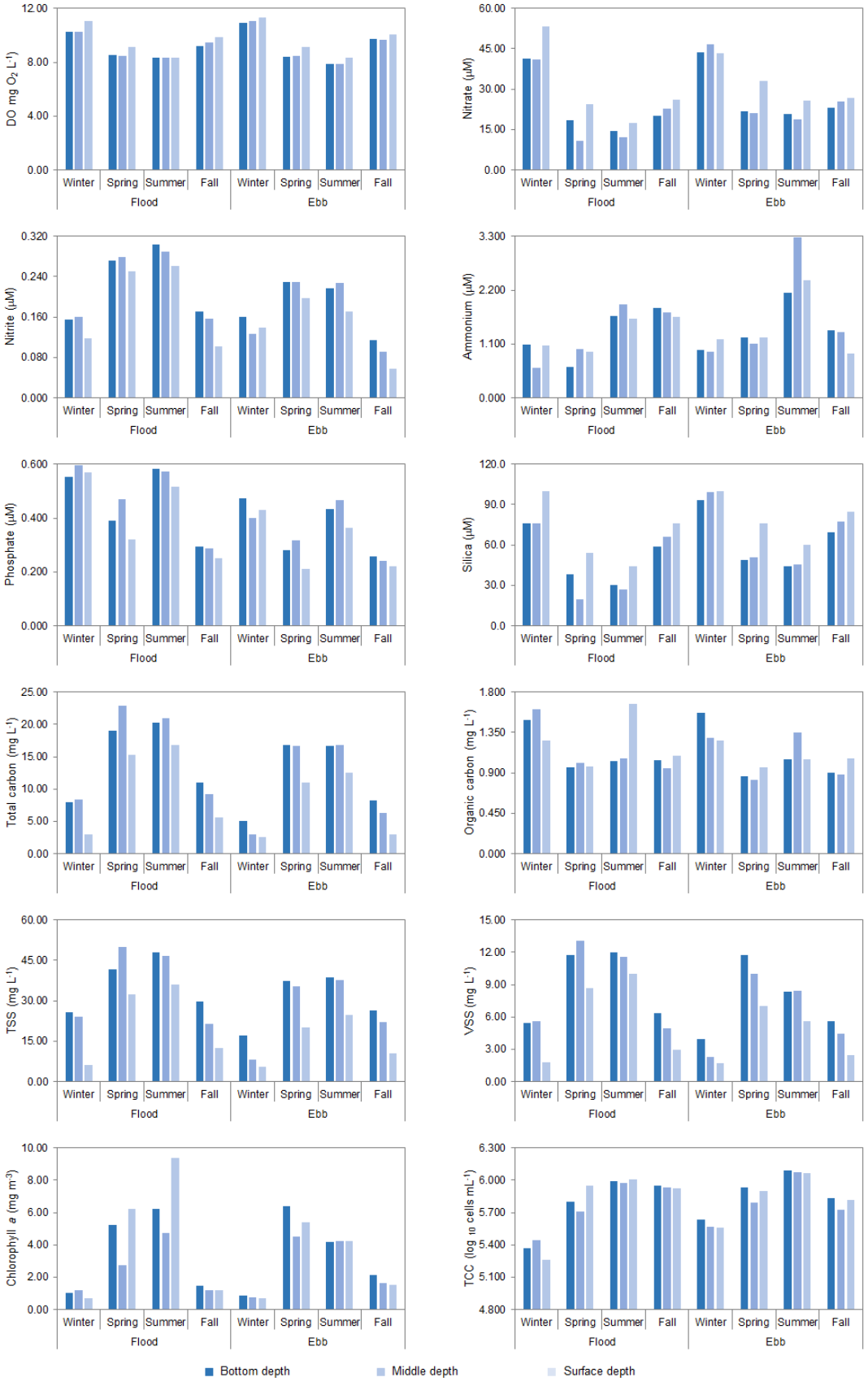

Figure 2.8 Seasonal variability of dissolved oxygen (DO), nutrients, total dissolved carbon, dissolved organic carbon, total suspended solids (TSS), volatile suspended solids (VSS), chlorophyll *a*, and total cell counts (TCC) in Lima River estuary water column (values represent the average of the 11 locations).

Ammonium did not show a clear pattern, although the highest concentration was at the middle depth (3.27 μM), followed by one at surface (2.40 μM) during the same summer ebb tide survey. Total carbon and suspended solids (total and volatile) presented lower values at surface, with higher values in dry seasons, mainly during flood tides. Organic carbon did not present a trend, having the highest value (1.672 μM) at surface at the summer flood tide, and the lowest (0.818 μM) at middle depth of the spring ebb tide. Concerning chlorophyll *a* and TCC, higher values were exhibited at bottom, except during the winter, spring and summer flood tides for both parameters, and summer ebb tide for chlorophyll *a* (Figure 2.8).

DO presented higher values in upper estuary surface water during winter ebb tide, and lower concentrations in the lower estuary bottom water during dry seasons. The averaged concentration values (Table S2.2) of temperature and DO increased along the estuary towards upstream (Figure 2.9), independently of the tide, with DO values recorded for ebb tides always higher than flood tides values.

2.3.3 Spatial variability of environmental variables

Nitrate and silica concentration values decreased from upstream to the estuary mouth independently on the tide (Figure 2.9; Table S2.2). During the study period, the nitrate concentration varied between 4.70 μM (summer) and 58.97 μM (winter), with the highest concentrations observed in the middle estuary during winter and in the upper estuary in the remaining seasons, for both tides. The silica concentration varied from 3,678 μM (lower estuary) to 121.7 μM (upper estuary), with the highest values recorded in the upper estuary. The averaged concentration values for both parameters showed an increasing trend along estuary, with greater values always during ebb tides. These observations, combined with that described above, that is, increased concentration with decreasing salinity, appear to indicate that river water plays the role of the main source of nitrate and silica.

Nitrite, total dissolved carbon and suspended solids (TSS and VSS) decreased from the estuary mouth to upstream. The higher values were found in the lower estuary, in the dry seasons (spring and summer) during the flood tides, and the lower in the upper estuary in the wet seasons (winter and fall) during ebb tides. Concerning ammonium, two distinct behaviors were recorded, according to the tides. During flood tides, the ammonium concentration decreased towards upstream along all estuary (except in winter). For ebb tides, ammonium amount decreased in the lower and middle estuary followed by an increase in the upper estuary, suggesting a sink of ammonium at around 7.2–9.5 km from the estuary mouth.

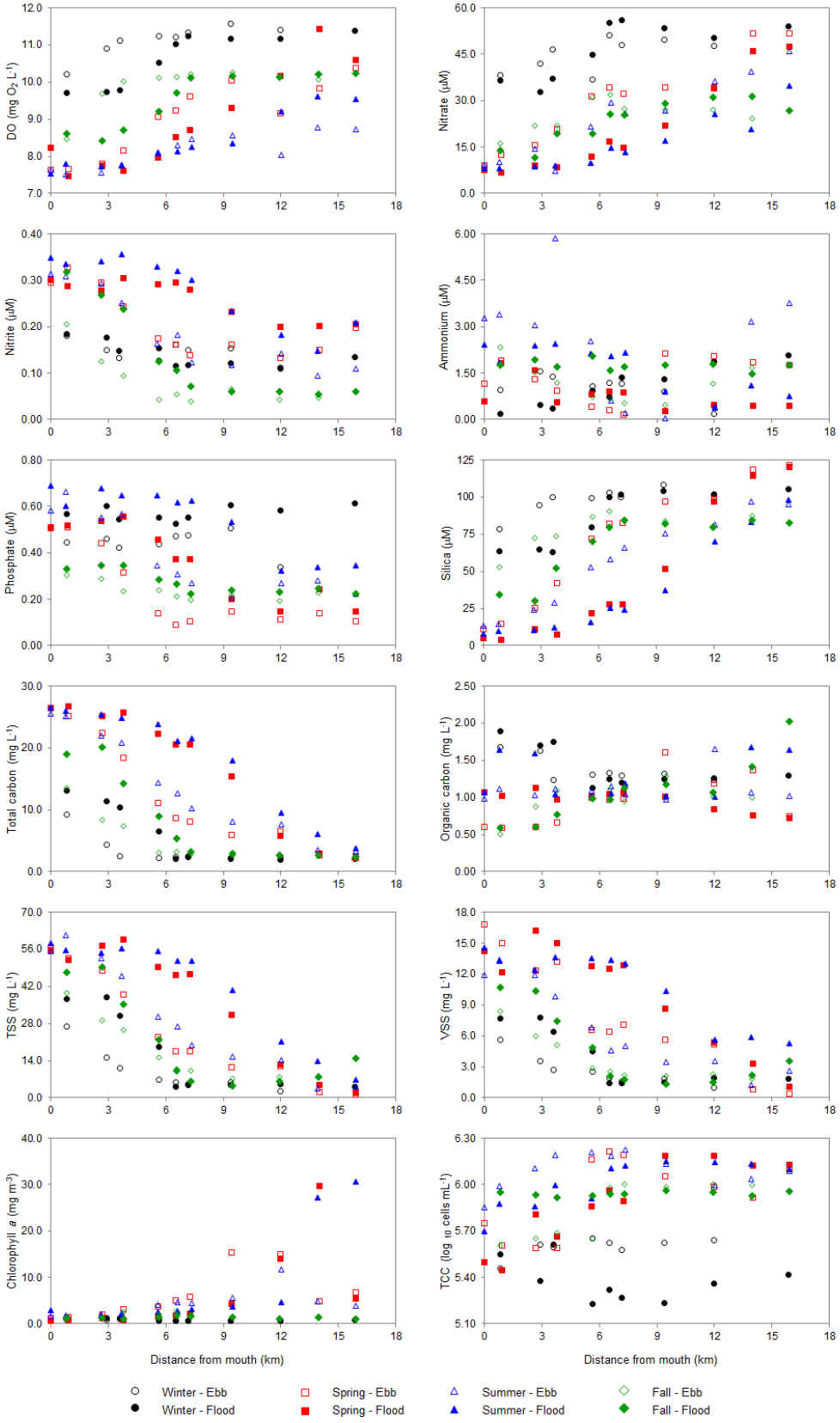

Figure 2.9 Spatial variability of dissolved oxygen (DO), nutrients, total dissolved carbon (TDC), dissolved organic carbon (DOC), total suspended solids (TSS), volatile suspended solids (VSS), chlorophyll *a* and total cell counts (TCC) in the Lima River estuary. Each value corresponds to depth-average data (surface, middle and bottom) of the samples collected at each sampling station.

Phosphate concentration ranged between 0.074 μM and 0.731 μM. The parameter did not showed an evident spatial trend, although higher values were found in the lower estuary, being the highest concentration found in summer flood tide. The phosphate averaged values decreased from estuary mouth to upstream river in both tides, with higher values during the flood tides. Although OC did not show a clear trend, the values were higher in the upper estuary (1.220 mg L^{-1}) during the ebb tide, and in lower estuary (1.23 mg L^{-1}) during the flood tide.
Regarding chlorophyll *a* values an increasing trend towards upstream was observed, with values that seem to indicate potential sources along the upper estuary during the dry seasons. A similar trend was showed by TCC with higher values during ebb tides, being the highest at the upper estuary (9.47 x 10^5 cells mL^{-1}). The pattern showed during dry seasons may suggest potential sources in the middle estuary.

2.3.4 Conservative environmental variables

The graphics presented in Figure 2.10 show the relationships of nutrients, carbon (TDC, DOC), suspended solids (TSS, VSS), chlorophyll *a* and TCC, and salinity, in order to investigate the existence of potential sources and sinks along the estuary. Dissolved oxygen presented a consistent decreasing trend with salinity. Nitrate and silicate showed a decrease trend close to a conservative behavior. Nitrite, TDC, TSS and VSS, increased consistently with salinity, except in the winter flood tide. Dissolved inorganic carbon (DIC) accounts for 80% of the total dissolved carbon (TDC), both having a similar relationship with salinity. Ammonium behavior was non-conservative, with levels decreasing in intermediate and high salinity water, but with the highest concentrations for each season tides in the higher salinity values. Phosphate presented the highest concentrations at the highest salinities, although it did not show a clear trend with salinity, but a behavior indicating possible dissipations along the estuary. The DOC did not showed a clear and consistent behavior with salinity, indicating potential sources (i.e., spring flood tide, and fall ebb tide), and sinks (i.e., spring ebb tide and fall flood tide) along the estuary. Chlorophyll *a* concentrations decreased with the salinity in the dry seasons (spring and summer), presenting however a non-conservative behavior, with increasing values along some salinity intervals, indicating potential sources in that areas. In both winter tides this parameter increased with salinity, but the behavior remained non-conservative. Bacteria behavior was clearly non-conservative, with increased numbers in the salinity range of 7–15.

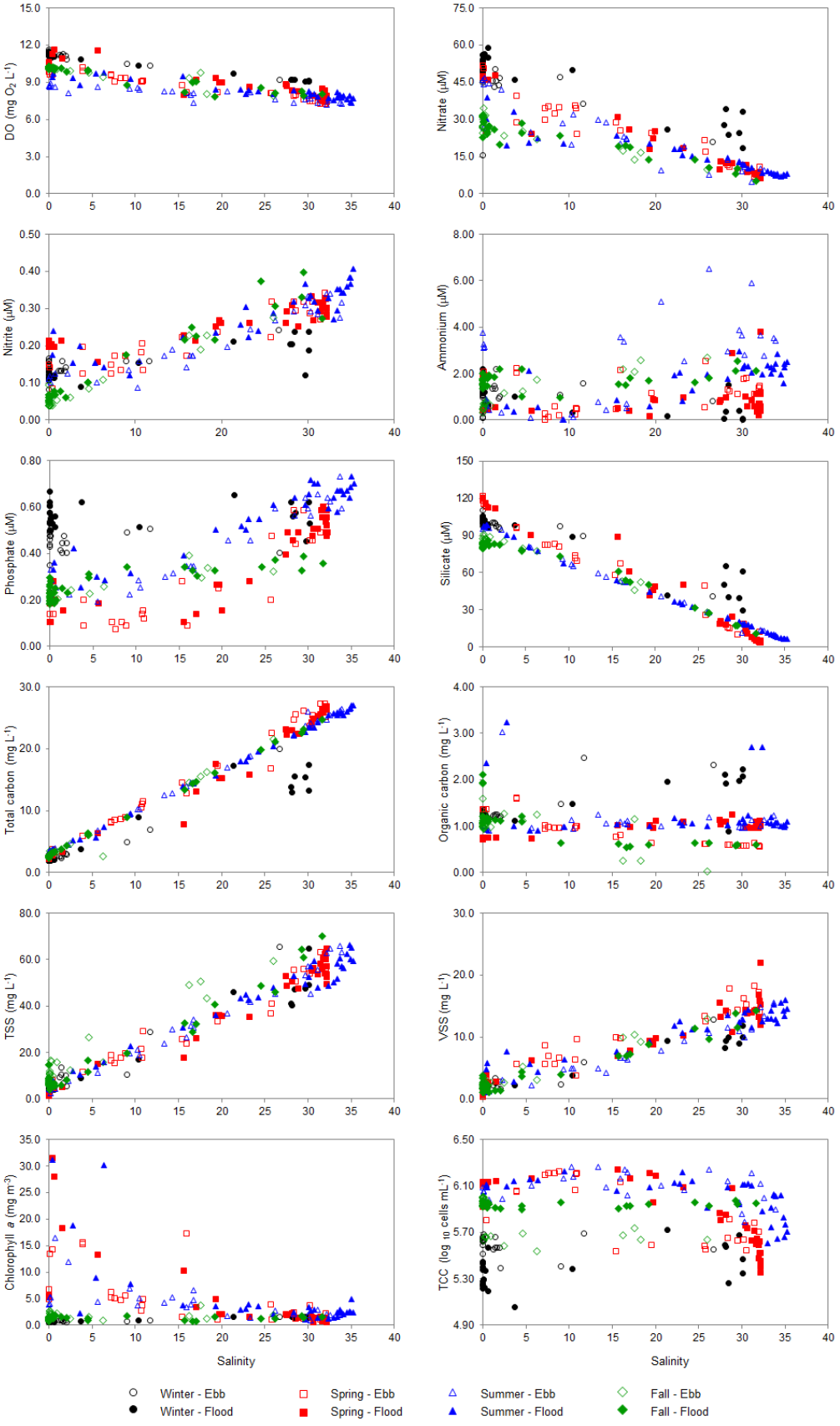

Figure 2.10 Relationships between dissolved oxygen (DO), nutrients, total dissolved carbon (TDC), dissolved organic carbon (DOC), total suspended solids (TSS), volatile suspended solids (VSS), chlorophyll *a*, total cells counts (TCC), and the salinity.

2.3.5 Redfield ratio

The N:P ratios show values generally above the Redfield ratio 16:1 (Figure 2.11), except for a few samples collected during summer and spring flood tides, in intermediate and high salinities, suggesting an overall excess of nitrogen availability and a potential limiting role for phosphate in the estuary. The presence of excess carbon in the estuary can be perceived by the values presented for the C:N ratios, although its availability may be limited during the both winter tides. Regarding Si:N indexes, silicon has a potential limiting role (12.7% of collected samples) only during dry seasons flood tides. In the Lima estuary it is clear that nitrogen concentrations are much lower than expected by the Redfield ratio (Figure 2.11A).

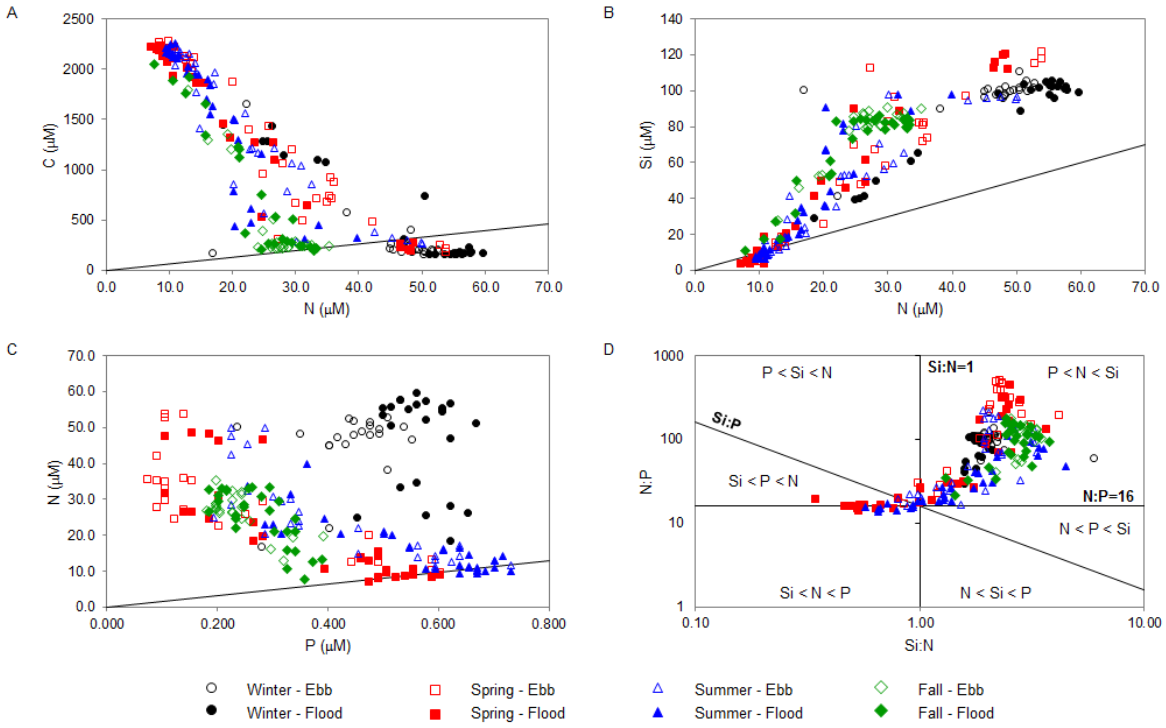

Figure 2.11 Scatter diagrams of the C:N (A), Si:N (B), N:P (C), and Si:N:P (D) atomic ratios in the water column. In the diagram D, molar quotients between the concentrations of potentially limiting nutrients are delimited in this logarithmic plot (log Si:N vs. log N:P) by the by the Si:N= 1:1, N:P= 16:1 and Si:P= 16:1 lines, which define six different areas within the plot, with each one characterized by the potentially limiting nutrients in order of priority.

2.3.6 Multivariate analysis

Principal component analysis (PCA) was performed in order to investigate patterns of similarities between samples based on the contribution of environmental variables and temporal and spatial parameters. The analysis gave four main factors (Eigenvalues > 1) explaining about 81.5% of the total variation of the data obtained in all samples (Table 2.1).

The first 2 components (PC1 and PC2) accounted for 67.7% of the total variation. The variables that contributed most to PC1 were OD, nitrate and silica (positively) and salinity, nitrite, total dissolved carbon and suspended solids (negatively), suggesting a dominant influence of salinity, i.e., seeming to reflect variables with a distribution pattern associated with salinity. For PC2, the variables that contributed most positively were temperature, chlorophyll *a* and TCC, and negatively the phosphate, suggesting a distribution profile related with temperature. PC3 was negatively participated by turbidity and positively by organic carbon. The variables that contributed mostly to PC4 were turbidity (positively) and ammonium (negatively).

Table 2.1 Eigenvectors of correlation matrix and principal component analysis factor loadings plot (factors 1 and 2).

	Factor 1	Factor 2	Factor 3	Factor 4
Temperature	-0.118	0.510	0.070	-0.045
Salinity	-0.340	-0.008	0.030	0.180
pH	-0.153	0.293	-0.165	-0.156
Turbidity	0.118	-0.102	-0.528	0.446
DO	0.331	-0.073	-0.004	0.024
NO_3^-	0.327	0.048	0.104	0.003
NO_2^-	-0.321	-0.046	0.081	-0.083
NH_4^+	-0.109	-0.070	-0.169	-0.740
PO_4^{3-}	-0.176	-0.376	0.252	-0.192
Si	0.323	0.154	-0.019	0.006
CHL *a*	-0.008	0.478	0.243	0.052
TDC	-0.353	-0.003	0.002	0.119
DOC	0.103	-0.105	0.718	0.186
TSS	-0.335	-0.063	-0.057	0.243
VSS	-0.340	-0.014	0.028	0.199
TCC	-0.059	0.470	-0.002	0.005
Expl.Var	7.744	3.095	1.137	1.055
% Total variance	48.40	19.35	7.109	6.595
Cumulative %	48.40	67.75	74.86	81.45

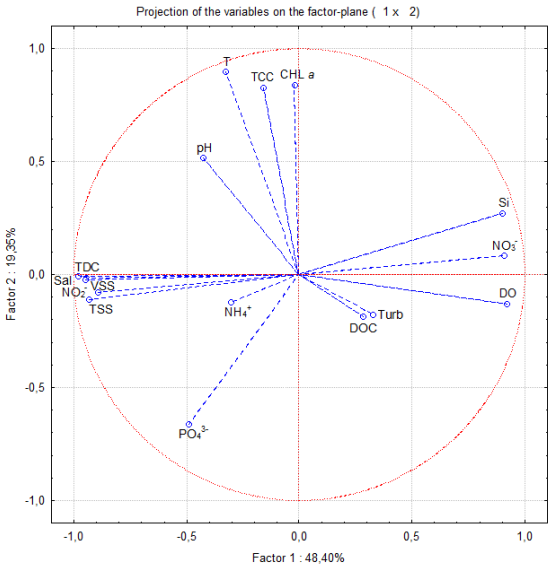

The representation of the projection of samples against the first 2 principal components is shown in Figure 2.12. When the samples were labeled by the season, the spring and summer samples presented a similar pattern, while fall and winter samples showed a distribution along the PC1 axis but with winter samples relating negatively with PC2 controlled by temperature. Thus, a clear seasonal pattern was observed. The separation of the samples of the wet seasons, fall and winter, can thus be explained by the difference in values presented by the variables influenced by salinity, such as DO, nitrate, silica, nitrite, total carbon and suspended solids (PC1). Summer and spring had lower concentration values for DO, nitrate and silica and

higher values of salinity, temperature, chlorophyll *a* and TCC. Regarding estuarine area, different spatial trends were found between the samples collected in the lower and upper estuary. Along the PC1 axis, samples from the upper estuary were projected to the same side of the positive contribution of nitrates, silica and DO, and the samples from the lower estuary to the opposite side, quadrant associated with positive salinity contributions, in agreement with the highest contribution of salinity to the lower estuary. In relation to PC2, samples from the upper estuary were spread on the positive side of the axis, being associated with the positive contributions of temperature, chlorophyll *a* and TCC. No clear association between samples based on tides and samples collected to different depths was observed.

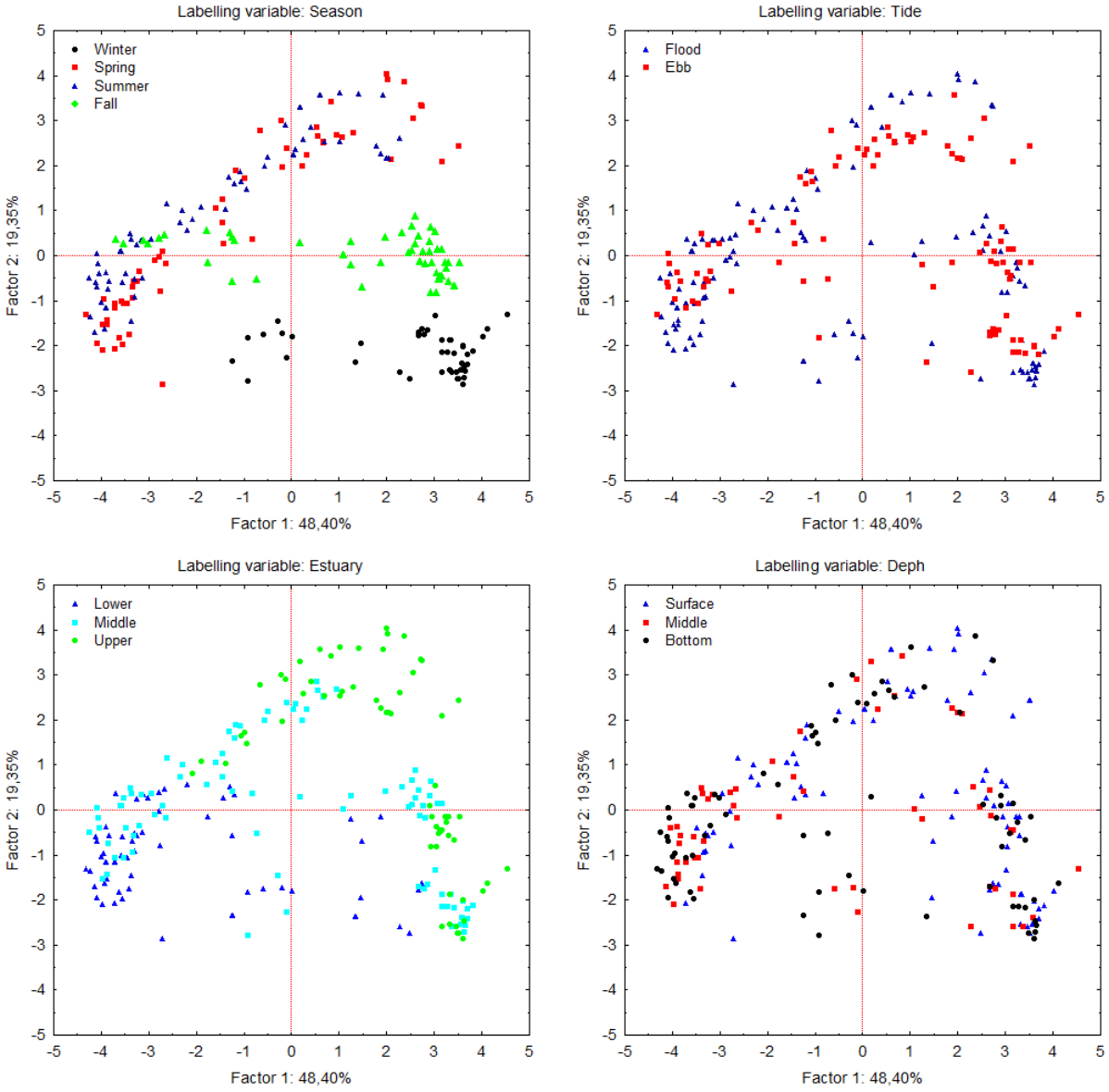

Figure 2.12 Projection of samples in the space defined by the first 2 principal components.

The Permanova similarity tests for the set of samples collected in the seasonal surveys showed differences between the various seasons of the year, the two tides, the three areas of the estuary and the three sampling depths.

For more information, the factors were crossed and hierarchized, and a nested design was created. The nested test design performed was the depths within the estuary areas, within the tides, within the seasons. The seasons were all different, and in each of them the tides were also different. The areas of the estuary were different for each of the tides of each season, except for the middle and upper estuary during the winter flood tide. Samples collected at of the bottom and surface in the middle estuary during the flood tide and in lower estuary during ebb tide were different for the seasons, except for winter. In the lower estuary, samples collected at different depths during the flood fall tide showed differences, that is, the surface samples were different from the bottom samples and the middle samples of the water column. The upper estuary showed no differences along the water column, in both tides and all seasons, the same in the middle estuary, but only at ebb tides. During winter, there were no differences in the water column samples collected in each area of the estuary and in each tide.

2.4 Discussion

2.4.1 Environmental parameters

Physicochemical parameters varied seasonally, especially in the lower estuary. The observed salinity variations, the localization of the salt wedge in the lower estuary during winter (flood tide), and the freshwater dominance during high flows were in accordance with those found in other estuarine systems, such as Guadiana estuary (Camacho et al., 2014; Garel et al., 2009). The Lima estuary is a dynamic system like most estuaries, being dependent on river inflow variability (Morais et al., 2009) associated to seasonal changes, which dominate water circulation (Vieira and Bordalo, 2000). Indeed, river flow resulting essentially from discharges of upstream dams, and rainfall, was an important driving force for water circulation in the Lima estuary, as described for other temperate estuaries (e.g., Hofmeister et al., 2017), that together with tidal conditions determined the extent of saltwater intrusion (Azevedo et al., 2010), residence time, and the concentration of various parameters (e.g., nutrients) in the estuary. The high flows of the river during winter and fall resulted in less seawater intrusion, even during flood tide, an increase of DO, nitrate and silica concentrations, and turbidity, and a decrease in the concentrations of the nitrite, total dissolved carbon, suspended solids, and chlorophyll *a* (Table S2.1). As in previous studies (Hitchcock and Mitrovic, 2015; Liu and Chan, 2016), freshwater was the main supplier of nitrogen in the estuary, particularly nitrates. Surface water generally presented characteristics closer to those observed in freshwater, and bottom water

closer to seawater, suggesting as main suppliers river water for the surface and coastal water for bottom. The estuary salinity gradient structure showed variations with river inflow, being spatial and temporal patterns of estuarine ecosystem variability strongly linked to the hydroclimatic setting (Morais et al., 2009; Cloern et al., 2017).

Salinity and water temperature revealed a marked seasonal variation typical of temperate estuaries (Gonçalves et al., 2015). Dissolved oxygen concentrations were higher in the winter and upstream (Figure 2.9), and temperature values in summer but with no significant relationship with the latitude. The inverse tendency observed between DO and temperature is in agreement with Garel and Ferreira (2011) data, which presented opposite trends in the same tidal phase during different seasons. In other words, during the ebb and flood phases, temperature and pH decreased and oxygen increased in wet seasons, whilst temperature and pH increased and oxygen decreased in dry seasons (Table S2.1). In winter, when the contribution of river water and rainwater is higher, low salinities, high oxygen values and low temperatures are characteristic (Camacho et al., 2014). In summer, when insolation and evaporation are the most important factors, salinity increases, oxygen decreases and temperature increases (Camacho et al., 2014).

Nitrates and silica showed an inverse linear relationship with salinity, with Lima river as the main source and with higher values in the surface of the water column during the wet seasons and ebb tides, in agreement with the tide–nutrient relationship reported by Pereira-Filho et al. (2001). The concentration of these parameters increased along the estuary towards upstream of the river, with the elevated values in the freshwater upper estuary (Figure 2.9, Table S2.2) probably attributed to agricultural activities and soil leaching (Caetano et al., 2016), being the chemical weathering of silicates on land (terrestrial input) the main process that supplies dissolved and particulate silicate to rivers (Domingues et al., 2005; Morais et al., 2009). Nitrite, total dissolved carbon and suspended solids (total and volatile) presented a linear relationship with salinity, with higher values at the bottom of the water column in the lower estuary during tidal floods of the dry seasons (Figure 2.8, Table S2.1), suggesting a source related to seawater. For this estuary, Ramos et al. (2017) reported a similar behavior of total suspended solids, volatile suspended solids, and dissolved carbon with salinity. The estuarine TSS concentrations depend on sediment transport from rivers and on locally derived suspended sediments associated with the resuspension of the estuarine bed sediment (Azevedo et al., 2008), and its relationship with salinity can also be influenced by winds and flood events (Azevedo et al., 2008). The predominance of estuarine suspensions (suspended solids) in the lower/middle estuary can be interpreted as a result of the water circulation (Oliveira et al., 2017) during tidal cycles with mixing of fluvial sediments and marine sediments in the lower estuarine channel (Caetano et al., 2016) and/or as the result of saltmarsh particles (Caetano et al., 2016), existent in the middle estuary. The TSS loads in the Lima estuary (8.0–12.6 mg

L^{-1}) were comparable to those found in the Douro estuary (10.9–11.1 mg L^{-1}) (Azevedo et al., 2006), but much lower than those presented by other estuarine systems such as Sado (Portugal), Gironde (France) and the Scheldt (Belgium and the Netherlands), with TSS concentrations in the upper estuarine region of 600 mg L^{-1}, higher than 200 mg L^{-1} and around 40 mg L^{-1}, respectively (Cabeçadas et al., 1999). The low particulate matter loads presented by the Lima and Douro estuarine systems can be justified by the fact that these rivers are dammed along the entire course (Azevedo et al., 2006). Beside that, these systems showed an increasing trend of TSS with salinity, in opposition of the trend of the other above-mentioned estuaries. The difference in behavior between TDC and DOC (Figure 2.10) seems to suggest that a significant portion of dissolved carbon comes from inorganic forms (DIC).

Ammonium and phosphate behaviors were non-conservative (Figure 2.10), did not show a clear trend with salinity, being the phosphate concentration higher during the flood tides, and ammonium higher during ebb tides and in the dry seasons. Although these parameters showed low correlation with salinity, their highest values were obtained for samples with high salinity values, collected at a bottom and middle depth in the lower estuary (Figure 2.8, Table S2.2), except during winter. The behavior described above for ammonium and phosphate seems to indicate potential sources and sinks along the estuary, being its concentration significantly affected by *in situ* processes (Cloern et al., 2017), despite the strong effect of external and physical variables, such as river flow, rainfall, and salinity (Magni and Montani, 2000). The ammonium and phosphate concentrations presented could be attributed to processes of nutrient regeneration within the estuary and the highest values recorded during the summer a result of the enhancement of the benthic decomposition processes (Magni and Montani, 2000). Higher concentrations of ammonia during ebb tides relative to flood tides (Table S2.1) appear to indicate release of ammonia from the sediment (Yin and Harrison, 2000), by remineralization process (Marcovecchio et al., 2009). The higher phosphate concentrations in the higher salinity values into lower and middle estuaries may be due to adsorption or desorption processes from the sediments during the period of high freshwater influence (Cabeçadas et al., 1999; Yin and Harrison, 2000). DOC averaged values were higher in the upper estuary during ebb tides and in the lower estuary during flood tides, suggesting that both freshwater and coastal water may be potential sources. Despite this, DOC did not show a clear tendency with salinity (Figure 2.10), apparently indicating potential sources and sinks along the estuary, being the concentration affected by *in situ* processes and dependent on the biological absorption and regeneration, and also of the equilibrium between the water column and the sediments, i.e., the nonlinear pattern observed along the salinity gradient, often implies estuarine processes of transformation and nonconservative behavior (Cloern et al., 2017).

Chlorophyll *a* presented a non-conservative behavior (Figure 2.10), with spring and summer showing higher concentrations than winter and fall. The higher values observed during the dry

seasons can be explained by the higher temperatures (Winder and Cloern, 2010; Buchan et al., 2014), higher light availability (Barrio et al., 2014; Lu and Gan, 2015) and hydrodynamic conditions favoring the existence of stratification/stabilization of the water column and longer residence times of water (Azevedo et al., 2008; Lu and Gan, 2015). In dry seasons, chlorophyll *a* presented the maximum concentrations at the surface of the water column (Figure 2.8) where salinity values were lower (Azevedo et al., 2008; Azhikodan and Yokoyama, 2016), while in winter the highest values were recorded in the higher salinity water (Fisher et al., 1888; Lu and Gan, 2015). The averaged values for each estuary area showed an increase in chlorophyll *a* from the lower estuary to the upper estuary during ebb and flood tides (Table S2.2, Figure 2.9). Chlorophyll *a* concentration tended to decrease with salinity, suggesting that river functioned as a source (Azevedo et al., 2008), except during winter. The occurrence of concentration peaks along estuary can be attributed to conditions that increase growth rates or decrease loss rates. The upper part of the estuary, surrounded by intensive agriculture (irrigated maize), seemed to behave as a source of chlorophyll *a*, suggesting an association with higher nitrogen content in the water column (Desmit et al., 2015), and lower concentration of total suspended solids. The range of chlorophyll *a* concentrations for Lima, Douro (Azevedo et al., 2006), Sado and Gironde (Cabeçadas et al., 1999) estuaries were similar, but much lower than the Scheldt estuary with maximum values above 200 mg m^{-3}. The maxima chlorophyll *a* for Sado and Gironde occurred in intermediate salinities, while for the Scheldt and the Douro was found in the most upstream part of the estuary, similarly to Lima estuary.

Bacterial counts maximum values were found in dry seasons, and minimum values in wet seasons (Bacelar-Nicolau et al., 2003) for both tides and higher values for ebb tides (except winter) (Table S2.1), with dynamic processes, such as growth, mortality, predation and physical dispersion, involved in the distribution of microorganisms within the estuary (Painchaud et al., 1996). The structure and activity of microbial community in stratified estuaries may depend on the variation of hydrodynamic conditions, with salinity being a property that can influence the control of the communities belonging to the inflow of river water, either in its abundance (Bunse et al., 2016), activity or in the structure of its community (Campbell and Kirchman, 2013; Xia et al., 2015). Previous studies indicated that salinity was determinant for bacterial communities and also for seasonal changes in bacterial communities in both marine and brackish environments (Herlemann et al., 2016). In the estuary of Lima, bacteria showed a different behavioral trend for dry and wet seasons (Figure 2.10). Along the estuary, the microbial amount did not always decrease downstream, as reported in other studies (e.g., Painchaud et al., 1996), with the highest values for winter and fall in areas with higher salinity. Despite this, the averaged values for each estuarine area showed an increase in bacteria from the lower estuary to the upper estuary in both tides, with higher values being recorded for the ebb tides (Table S2.2). During dry seasons, the highest bacterial cell counts

were found in mesohaline area, in the middle estuary (Ducklow et al., 1999), a stretch with saltmarsh islands and shallow channels. The presented pattern could be explained by the increment of the dissolved organic carbon and/or bacterial biomass from the terrestrial influx (Ducklow et al., 1999; Hitchcock and Mitrovic, 2015). The "bactericidal" activity of salinity (Hobbie, 1988; Munro et al., 1989) appeared to control the microbial abundance in high salinity range, and increase survival in intermediate salinity range (Bordalo, 2003). In addition, vertical stratification in the lower section of the Lima estuary may limit the advection and convection fluxes of microorganisms and substrate between the layers, and the reduction of substrate and unavailability of light to the bacteria may be determinant factors (Bordalo and Vieira, 2005).

Redfield molar ratios can be discussed as indicators of potential limitation in processes occurring in the estuary in terms of temporal and spatial scales (Gameiro et al., 2007). A N:P ratio < 16, which expresses a potential nitrogen deficiency, was recorded only in a few samples (5.7%) collected during summer and spring flood tides in areas of middle and lower estuary (Figure 2.11). During the dry seasons, Si:N < 1 was observed for some samples collected in the middle and lower estuary during flood tides, and in the lower estuary during ebb tides. This behavior may have resulted from the reduction of Si and DIN available in the estuary due to the reduction of river flow verified in the dry seasons (Morais et al., 2009). The concentrations of these parameters decreased towards the mouth of the estuary mainly in dry seasons (Figure 2.9), due to their origin being mainly the Lima river, (nitrate, dominant form of DIN and silica (Gameiro et al., 2004), showed negative correlation with salinity and increases with river discharge). The behavior presented by these parameters seems to show temporal and spatial heterogeneity conditions in the estuary (Gameiro et al., 2007).

The nutrients and suspended solids showed by Lima estuary water were low compared to other Portuguese estuaries, such as Douro (Azevedo et al., 2008) and Tagus (Gameiro et al., 2004; Gameiro et al., 2007; Gameiro and Brotas, 2010), considering to the annual averages ranges (Table 2.2).

The values presented by nitrates and ammonium were always below the limits established in Directive 75/440/EEC (EEC, 1975), with maximum values of 7.3% and 2.9% of limit values, respectively. Although the Lima estuary presented the maximum value of chlorophyll *a* concentration, the annual average value was lower, compared to the values presented by the other estuaries, which may be related to a shorter residence time (Azevedo et al., 2008).

Table 2.2 Concentration ranges of nutrients, total suspended solids and chlorophyll *a* in Douro, Tagus and Lima estuaries.

	Lima estuary[1]		Douro estuary[2]		Tagus estuary [3,4,5]	
Parameter	Range	Average	Range	Average	Range	Average
NO_3^- (μM)	4.70 – 58.97	27.39	1.3 – 498.9	81.3	0 – 125 [3]	41 [5]
NO_2^- (μM)	0.038 – 0.407	0.187	0.0 – 3.1	0.7	4 – 12 [3]	2.64 [5]
NH_4^+ (μM)	0.000 – 6.53	1.40	0.3 – 158.5	8.9	0 – 30 [3]	12 [5]
PO_4^{3-} (μM)	0.074 – 0.731	0.397	0.2 – 6.8	1.5	1.4 – 19.1 [4]	4.6 [4]
Si (μM)	3.68 – 121.7	63.42	0.9 – 257.2	56.3	3.7 – 258.4 [4]	59.6 [4]
CHL *a* (mg m^{-3})	0.538 – 54.04	3.30	0.3 – 15.8	3.8	0.2 – 32.3 [4]	5.4 [3]; 4.3 [4]
TSS (mg L^{-1})	1.20 – 70.00	27.16	2.2 – 100.8	17.2	3.9 – 113.3 [4]	29.6 [4]

[1] This study; [2] Azevedo et al., 2008; [3] Gameiro et al., 2004; [4] Gameiro and Brotas, 2010; [5] Gameiro et al., 2007.

2.4.2 Multivariate analysis

The results of the principal component analysis showed the factors that may have contributed most significantly to the control of the dynamic processes in the Lima estuarine system, with different factors being able to control those processes over time and space. The positive contributions given by the OD, nitrate and silica parameters, contrasting with the negatives of nitrite, TDC, suspended solids and salinity, show spatial and temporal differences throughout Factor 1. The parameters that contributed to factor 1 were exactly the same ones that presented conservative dispersion behavior (Figure 2.10), suggesting the freshwater inputs from the river (Pereira-Filho et al., 2001) and the tidal action (Oliveira et al., 2017) as the main factors responsible for the differences between samples in the estuary (Azevedo et al., 2010). Discharges from the Lima River seem to have been the driving force of most of the dynamic processes associated with the nutrients (nitrates and silica) that occurred in the estuary as observed in other temperate estuaries (e.g., Azevedo et al., 2008; Hofmeister et al. 2017). Suspended solids and TDC concentrations and its distribution in the estuary seem to result of the predominant action of the tide cycles. It seems clear that temporal differences emerged along FA 2, with the association of higher concentrations of chlorophyll *a* and TCC at higher temperatures (dry seasons), as opposed to that observed for phosphate concentrations, as reported in the Douro estuary (Azevedo et al., 2010). To determine the patterns of temporal and spatial similarities between samples, the first two factors were represented in two dimensions and the samples were labeled based on the seasons and tides to determine the temporal pattern (Robins et al., 2016), and estuarine areas and depth for the spatial pattern (Figure 2.12). In the PCA representation with samples labelled based on seasons, the spring and summer samples (dry seasons) were separated from those of fall and winter, and samples

from the latter seasons were also separated from each other, reflecting changes in the plotted variables concentrations. The differences showed by seasons suggest as an explanation the seasonal variations of the hydrodynamic conditions (Lima river flow and tidal cycles) and climatic conditions (rainfall and temperature). The high flow of the Lima river enhanced by rainfall seems to have a greater positive impact on wet seasons, as reported in other studies (Morais et al., 2009; Hofmeister et al., 2017) (PC1), while temperature and the tidal cycle appear to influence more dry seasons (PC2). Differences between dry and wet seasons were greater than between seasons within each group (wet and dry seasons). Comparing PCAs with samples labelled based on tides and seasons, it seems clear that seasonal variability was greater than tidal variability, similar to that showed by the Douro estuary (Azevedo et al., 2010), since samples of different tides do not appear to be represented in different positions in the graphic, suggesting that the influence of river flow was higher than that of the tidal cycle. Samples from the upper and lower estuaries were plotted in different quadrants of the PCA labelled based on the estuarine areas, both in relation to factor 1 and factor 2, suggesting differences between them, although there was no clear differentiation between those groups of samples and the samples collected in the middle estuary. Most samples from the upper estuary were projected for a positive factor 1 quadrant, associated with lower salinity and higher concentration of nitrates and silica (higher river flow) and also for a positive quadrant of factor 2, that is, associated with higher temperatures, higher amounts of chlorophyll *a*, as presented in other estuaries(Azevedo et al., 2010) and TCC. An inverse pattern was presented by the majority of samples from the lower estuary, i.e., they were projected in negative quadrants for both factors.

Similarity tests between the samples showed differences in all factors of the study, even when the samples appeared to be identical for some factors in the graphical representation of the PCAs. These differences observed between the samples seem to be related to the flow of the Lima river and the temperature that vary quite seasonally, as reported in Mondego estuary by Gonçalves et al. (2015), and also with the introduction and extension of coastal water in the estuary during the tidal cycle, as observed in the Guadiana estuary (Camacho et al., 2014), since in highly variable systems like the estuarine the photic and mixing conditions may vary on a hourly basis (Azevedo et al., 2010). These physical factors are precursors of the biogeochemical processes carried out in the estuary (Cloern et al., 2017), being related to the variables that contribute most to the existence of differences between the samples. When similarity tests were carried out, there were similarities between some groups. For high river flow periods (wet seasons), sometimes the upper and middle estuaries did not present vertical concentration gradients or differences between them, and did not even show differences between tides (e.g., fall in upper estuary). These behaviors suggest that high freshwater flows were the main property responsible for the concentrations of the variables that most contribute

to the differences (nitrates and silica) in the estuary, as well as the processes performed there (Camacho et al., 2014). The similarities between samples collected at bottom and the middle depth at each tide during wet seasons in the middle estuary, may result from the circulation of high flows freshwater, resuspension of estuarine bed sediments (Azevedo et al., 2008) and release of nutrients and suspended solids, adsorption or desorption of ions (Cabeçadas et al., 1999) and/or by processes *in situ* associated with the saltmarsh islands and shallow channels (Caetano et al., 2016) in the middle estuary. Low river flows and a more extensive saline intrusion observed in the dry seasons, as in other estuarine systems (Camacho et al., 2014; Morais et al., 2009), may explain the similarity between samples collected in the bottom at different tides, and the fact that samples collected at middle depth showed no differences for surface or bottom samples. In addition, the similarities obtained may also be due to water circulation (Oliveira et al., 2017) during tidal cycles in the estuary lower channel with resuspension of estuarine sediments (Azevedo et al., 2008) and release of nutrients trapped in sediments (Yin et al., 1995) and suspended solids, as well as the adsorption or desorption of ions (Cabeçadas et al., 1999) with sediments, and ions biological absorption and regeneration (Rahaman at al., 2014).

The nested design created to show the similarities between samples collected at various depths of each area of the estuary (spatial variables), for each tide of each season (temporal variables) resulted in similarities only in the spatial variables. Only one similarity was found relative to the estuary areas, i.e. in winter the upper and middle estuary during the winter flood tide, suggesting as a possible explanation the high river flows verified, resulting in an introduction of a very high volume of water along an extensive stretch of the estuary (Camacho et al., 2014). Similarities in the depth factor were found mainly in samples collected at the bottom and on the surface of the middle and lower estuary, which may have resulted from the tidal cycle, with a more extensive introduction of coastal water along the estuary, resuspension of solids and release of trapped nutrients in the sediments (Yin et al., 1995), ions adsorption or desorption (Cabeçadas et al., 1999) with sediments, and ions biological absorption and regeneration (Rahaman at al., 2014). The similarities patterns seems to show that some estuarine properties have greater seasonal (temporal) variability than spatial variability (Cloern et al., 2017).

2.5 Conclusions

This study provided information on the variability of chlorophyll *a*, bacteria and physico-chemical parameters of the Lima estuary water. The differences presented by the samples seem to be related to the flow of the Lima river and temperature that vary seasonally, and also with the tidal cycle. Data analysis seem to show that some estuarine properties have greater

seasonal (temporal) variability than spatial variability. Discharges from the Lima River seem to have been the driving force of most of the dynamic processes associated with nutrients (nitrates and silica), while the differences associated with suspended solids and total carbon seem to result from the predominant action of tidal cycles. The nutrients showed higher values during the ebb tides of the wet seasons (nitrates and silica), and the chlorophyll *a* and bacteria during dry seasons. The behavior patterns of some parameters, such as ammonium and phosphate, chlorophyll *a* and bacteria, seem to indicate *in situ* processes, despite the strong effect of external and physical variables. This study showed that seasonal patterns and tidal cycles can be recognized in the study area, the first being more evident. However, behavior patterns varied depending on the parameter, under the effect of physical variables (i.e., river runoff, rainfall, salinity, temperature) and *in situ* processes (i.e., biological processes - primary producer and consumer activity and metabolism, and physical processes - adsorption/desorption and sedimentation/resuspension). The data presented can serve as an important baseline for the management of the natural environment of the estuary, its ecosystems, and fisheries, flood protection, tourism and maintenance of issues relating to the navigation channel and its connections to a commercial seaport, a marina, a fishing harbour and a shipyard.

2.6 SUPPLEMENTARY INFORMATION

Table S2.1 Average and standard errors for selected variables during seasonal flood and ebb tides surveys.

Parameter[1]	Winter (Average ± SE)		Spring (Average ± SE)		Summer (Average ± SE)		Fall (Average ± SE)	
	Ebb	Flood	Ebb	Flood	Ebb	Flood	Ebb	Flood
Deph	1.56±0.35	2.00±0.42	1.71±0.39	2.24±0.48	1.65±0.32	2.09±0.40	1.23±0.28	1.75±0.35
T (ºC)	10.80±0.10	11.13±0.21	16.89±0.43	16.08±0.52	18.91±0.46	18.22±0.52	13.96±0.18	14.81±0.24
Salinity	2.7±1.4	8.8±2.6	15.7±2.3	22.6±2.2	17.3±2.3	24.1±2.1	4.3±1.6	8.4±2.1
pH	7.19±0.06	7.25±0.05	7.68±0.04	7.85±0.06	7.74±0.05	7.79±0.05	7.37±0.12	7.62±0.11
Turbidity	3.25±0.19	2.92±0.53	1.47±0.11	1.96±0.56	1.35±0.10	2.44±0.51	6.03±0.67	4.37±0.49
DO	11.09±0.11	10.56±0.18	8.73±0.19	8.73±0.24	8.05±0.10	8.33±0.13	9.84±0.14	9.50±0.17
NO_3^-	44.4±2.0	45.7±2.7	26.2±2.6	18.6±2.6	22.3±2.5	14.9±1.4	25.1±1.3	23.0±1.5
NO_2^-	0.144±0.007	0.142±0.009	0.216±0.015	0.266±0.008	0.202±0.017	0.285±0.014	0.086±0.016	0.142±0.021
NH_4^+	1.05±0.11	0.96±0.14	1.20±0.15	0.84±0.14	2.52±0.35	1.72±0.14	1.17±0.16	1.748±0.063
PO_4^{3-}	0.439±0.017	0.569±0.011	0.262±0.036	0.387±0.031	0.414±0.032	0.556±0.026	0.239±0.011	0.276±0.011
N:P	106.2±6.8	83.2±5.2	207±33	94±21	82±12	37.5±5.5	117.2±7.8	98.8±8.4
C:N	8.6±3.4	17.0.±4.6	75±15	144±19	76±12	125±14	23.6±7.2	46±12
Si	97.4±2.9	85.1±5.3	60.7±7.4	39.1±7.8	51.1±5.9	34.0±5.4	77.4±3.6	67.0±4.6
CHL *a*	0.783±0.048	0.952±0.085	5.50±0.97	4.9±1.4	4.21±0.63	6.8±2.0	1.77±0.15	1.322±0.061
TDC	3.63±0.85	6.2±1.2	14.4±1.7	18.7±1.7	15.1±1.6	19.3±1.4	5.7±1.2	8.6±1.5
DOC	1.385±0.075	1.434±0.077	0.892±0.062	0.980±0.025	1.128±0.073	1.26±0.10	0.964±0.076	1.035±0.080
TSS	10.6±3.0	18.0±4.1	29.9±3.9	40.5±3.8	32.8±4.0	43.5±3.3	19.0±3.4	21.1±3.8
VSS	2.70±0.56	4.11±0.76	9.4±1.0	10.97±0.92	7.31±0.85	11.16±0.64	4.05±0.71	4.73±0.78
TCC	5.589±0.018	5.348±0.035	5.883±0.051	5.831±0.053	6.076±0.023	5.993±0.032	5.801±0.039	5.935±0.004

[1] Units in which the parameters were expressed: deph – m; temperature (T) – ºC; pH – Sørensen scale; turbidity – NTU; dissolved oxygen (DO) – mg O_2 L^{-1}; NO_3^-, NO_2^-, NH_4^+, PO_4^{3-} and Si – μM; chlorophyll *a* (CHL *a*) – mg m^{-3}; total dissolved carbon (TDC), dissolved organic carbon (DOC), total suspended solids (TSS), and volatile suspended solids (VSS) – mg L^{-1}; and total cell counts (TCC) – $\log_{10}$ cells mL^{-1}.

Table S2.2 Average and standard errors for selected variables at estuary zones during the flood and ebb tides surveys.

Parameter[1]	Units	Lower (L1 – L3)		Middle (L4 – L7)		Upper (L8 – L11)	
		Ebb	Flood	Ebb	Flood	Ebb	Flood
Depth	m	2.34±0.38	3.20±0.53	1.18±0.20	1.69±0.26	1.19±0.27	1.44±0.26
Temperature	ºC	14.21±0.36	14.44±0.33	15.25±0.55	14.61±0.38	16.10±0.84	16.29±0.75
Salinity	-	20.1±2.1	27.6±1.4	8.2±1.4	18.2±2.0	1.84±0.89	4.2±1.2
pH	Sørensen scale	7.64±0.06	7.63±0.07	7.56±0.05	7.70±0.05	7.25±0.09	7.58±0.09
Turbidity	NTU	2.78±0.38	3.44±0.74	3.66±0.47	2.07±0.16	2.29±0.23	3.64±0.53
DO	mg O_2 L^{-1}	8.72±0.24	8.43±0.16	9.60±0.19	9.07±0.18	9.95±0.22	10.23±0.16
NO_3^-	µM	20.7±2.3	15.8±2.2	30.4±1.9	23.7±2.4	37.6±2.1	35.7±2.0
NO_2^-	µM	0.235±0.015	0.276±0.013	0.142±0.011	0.223±0.015	0.113±0.009	0.145±0.011
NH_4^+	µM	1.98±0.18	1.43±0.18	1.30±0.23	1.39±0.10	1.28±0.22	1.16±0.11
PO_4^{3-}	µ∴M	0.459±0.024	0.525±0.022	0.307±0.023	0.474±0.023	0.248±0.022	0.350±0.027
N:P	-	56.8±6.4	35.2±4.2	138±16	62.8±6.4	196±24	133±14
C:N	-	96±14	155±17	32.5±6.4	89±12	10.3±6.4	17.7±4.2
Si	µM	45.9±6.1	28.1±4.8	75.3±3.7	49.2±5.1	94.5±3.1	87.9±3.7
CHL *a*	mg m^{-3}	1.379±0.090	1.41±0.16	2.80±0.26	1.62±0.11	5.4±1.1	7.7±2.0
TDC	mg L^{-1}	16.6±1.7	21.0±1.1	8.4±1.0	14.7±1.4	4.02±0.61	5.27±0.86
DOC	mg L^{-1}	0.998±0.096	1.22±0.11	1.081±0.028	1.102±0.038	1.218±0.083	1.199±0.084
TSS	mg L^{-1}	41.1±3.6	49.3±2.6	20.3±2.1	34.6±3.3	7.6±1.3	11.8±1.9
VSS	mg L^{-1}	9.71±0.93	11.48±0.69	5.25±0.56	8.58±0.81	2.53±0.41	3.86±0.49
TCC	log_{10} cells mL^{-1}	5.689±0.038	5.668±0.048	5.903±0.044	5.775±0.043	5.914±0.032	5.883±0.052

[1] Parameters abreviations: Depth – water column depth; DO – dissolved oxygen; CHL *a* – chlorophyll *a*; TDC – total dissolved carbon; DOC – dissolved organic carbon; TSS – total suspended solids; VSS – volatile suspended solids; and TCC – total cell counts..

CHAPTER 3

Water column characterization of Lima Estuary (Portugal) during ebb and flood tides: neap vs. spring tidal cycle variability

Abstract

The spatial patterns and the variability of dissolved nutrient concentrations (nitrate, nitrite, ammonium, silica, and phosphate) along with salinity, dissolved carbon (total and organic), total suspended solids (TSS and VSS), chlorophyll *a* (CHL *a*), total cells count (TCC) and dissolved oxygen (DO) were investigated in the Lima estuary (NW Portugal). Sampling surveys were conducted during flood and ebb (daytime) of spring and neap phases in a tidal cycle (September 2014). These analyses were carried out to evaluate if tidal processes could regulate variability in short-term scale. Nitrate and silica concentrations were higher during the ebb tide conditions, especially of the spring phase, when the ebb advection of freshwater flow in the rivers was higher. Other parameters, such as ammonium and phosphate, chlorophyll *a* and bacteria, seem to be modulated by *in situ* processes, despite the strong effect of external and physical variables. The assessed parameters gradient structure in the estuary showed variations with tidal action, with the spatial and temporal patterns of estuarine ecosystem strongly linked to the hydrodynamic setting. The patterns differences seems to show that some estuarine properties have greater temporal variability than spatial variability.

Keywords: nutrients; phytoplankton; bacteria; ebb and flood tides; neap and spring tidal cycle; Lima Estuary.

3.1 Introduction

When natural waters such as freshwater and seawater meet, they create a unique environment, a distinct ecosystem where the freshwater from river mixes with the steadily intruding seawater, i.e. an estuary (Maznah et al., 2016; Das et al., 2017). The location of estuaries between river (freshwater) and ocean (saltwater) environments (Cloern et al., 2017) leads to natural and anthropogenic pressures (Wolanski and Elliott, 2016), since these areas are among the most densely populated areas of the world (Wolanski, 2007). The estuaries are transition zones between river and sea environments, subjected to marine and riverine influences, with characteristics dependent on tidal pulses, river flow, hydrodynamic (Menéndez et al., 2012, Robins et al., 2016), and autochthonous biological processes (Saraiva et al., 2007;

Wepener, 2007). Estuarine functioning varies as a result of differences in shape and size, and external physical forcings, by river flows, sediments, tides, wind and evaporation (Kappenberg et al., 2016).

The estuaries hydrodynamic regime is a result of factors such as currents and mixing processes caused by the interaction between freshwater and seawater (Marcovecchio et al., 2009), the tides with their cycles (semidiurnal, diurnal, weekly, fortnightly, equinoctial and annual), wind, rain and evaporation, oceanic events in coastal waters, and bathymetry and geomorphology varying spatially and temporally, so that an estuary is never in a steady state (Dyer, 1997; Prandle, 2009). Thus, an estuary is a buffer zone between river (freshwater) and the ocean (seawater) environments, that can be affected by factors such as asymmetries (Dias et al, 2013) and tides oscillations (tidal cycle - high and low tide), as well as spring-neap cycles. Seawater inflow is influenced by the tidal changes of spring tides and neap cycles while freshwater inflow is contributed by nearby rivers (Maznah et al., 2016). Temporal changes include diurnal cycling and event-based changes between high and low flow conditions, spring-neap cycle, seasonal, decadal and longer (Robins et al., 2016). A relevant aspect of the tidal estuaries high variability is associated to the short-time effects of a tidal cycle on the physicochemical characteristics of the water (Montani et al., 1998; Magni el al., 2002). On a time scale of hours, the freshwater ebb advection and the saltwater flood intrusion determine changes in several parameters of the water column, such as salinity, nutrients and suspended particulate matter (Montani et al., 1998; Magni el al., 2002), being the extent of such variations dependent on tidal amplitude (Montani et al., 1998). Moreover, the scenario can be greatly complicated by environmental variables, such as precipitation rate, affecting freshwater discharge (Page et al., 1995; Montani et al., 1998; Magni el al., 2002), temperature, solar irradiance, winds (Yin et al., 1995; Montani et al., 1998) and current velocity (Renshun, 1992; Montani et al., 1998), being these variables driven by climate, which varies considerably within years (i.e., seasons) and among years. Estuaries are highly dynamic ecosystems because they are subjected to the tide regime, which is especially noticeable in temperate regions with marked biological, physical, chemical, and geological seasonal cycles (Morais et al., 2009). The influence of the river is may even be more determinant than the tides (Morais et al., 2009), mainly for nutrient concentration and stoichiometry (Nixon, 2003), parameters affecting primary and secondary production (Nixon, 2003), and consequently influencing the estuarine dynamics (Morais et al., 2009).

Seasonal or annual monitoring of nutrients and associated biogeochemical parameters does not provide sufficient information for an adequate approach and assessment of all factors that control nutrient cycles in an estuary due to the inherent complexity of processes that vary significantly in time with several others phenomena (Yin and Harrison, 2000; Das et al., 2017), with the short-term variability of nutrients induced by the tide as an important example (Cabrita

et al., 1999; Yin and Harrison, 2000). Thus, for an adequate characterization of nutrient dynamics, it is necessary to consider the temporal changes in the environmental conditions resulting from the alternating replacement of underlying water with sea and river waters (Sakamaki et al., 2006), especially in meso-macro tidal estuaries (Das et al., 2017). In the estuaries, the seasonal variation of the biogeochemical parameters is frequently studied, with the water column chemistry, especially the solutes concentration, being able to be largely defined by the relative contribution of seawater and freshwater (Sakamaki et al., 2006; Das et al., 2017). In addition to conventional seasonal monitoring, it is important to examine short-term changes of various constituents during different tidal conditions to better understand their sources and cycling, particularly in coastal waters influenced by the tide (Das et al., 2017). The different tidal strength due to flood-ebb asymmetry and the spring-neap cycle may lead to variable effects on the interactions between freshwater and saltwater (Gao et al., 2009), so that tides play a key role in the functioning of many coastal systems, since they are responsible for midterm (spring-neap cycles) and short-term (low-high water cycles) variations in abiotic and biotic characteristics of these systems, with tidal flushing as one of the main bottom-up factors that control phytoplankton biomass in estuaries apart from nutrients (Davies and Ugwumba, 2013). Therefore, it is necessary to carry out studies that highlight the influence of tides on nutrient dynamics in this region.

The principal objective of the present study was to examine the impact of the neap-spring cycle and tides fluctuation on some parameters concentrations. The secondary objectives were: (1) to clarify how salinity and some selected parameters vary over a semidiurnal tidal cycle in the Lima estuary; (2) to compare the different effects of flood and ebb tides in the distribution isopleths of salinity and some selected parameters; (3) to elucidate how the spring and neap tides show their different influences on dynamics of salinity and some selected parameters. The sampling strategy and objectives were postulated to test if the tidal processes principally regulate the nutrient variability in short-term and midterm scale in the present study region.

3.2 Material and methods

3.2.1 The study area

The Lima estuary is located at the geographical coordinates of 41.68º N; 8.84º W (WGS84), NW Portugal (Figure 3.1), a temperate estuary with semi-diurnal and mesotidal regime (Vale and Dias, 2011), having an extension of about 20 km, and an average flow of 70 $m^3 s^{-1}$ (Ramos et al., 2006). The Lima estuary can be divided into three parts, lower, middle and upper estuaries (Figure 3.1). The lower estuary consists of a narrow and deep navigation channel (9 m) with walled benches, located in an area with anthropogenic modifications such as a jetty

and constant dredging, including a large shipyard, a commercial seaport, a marina and a fishing port (Ramos et al., 2010). The middle estuary comprises a saltmarsh area with several sand islands and intertidal channels. The upper estuary, i.e. the most upstream stretch of the estuary, consists of a narrow, shallow channel with some intertidal areas and undisturbed banks that remain almost in a natural state (Rebordão and Teixeira, 2009). Throughout its course, the estuary is impacted by discharges of wastewater that introduce various substances transported from urban, industrial and agricultural areas to the estuary (Almeida et al., 2011).

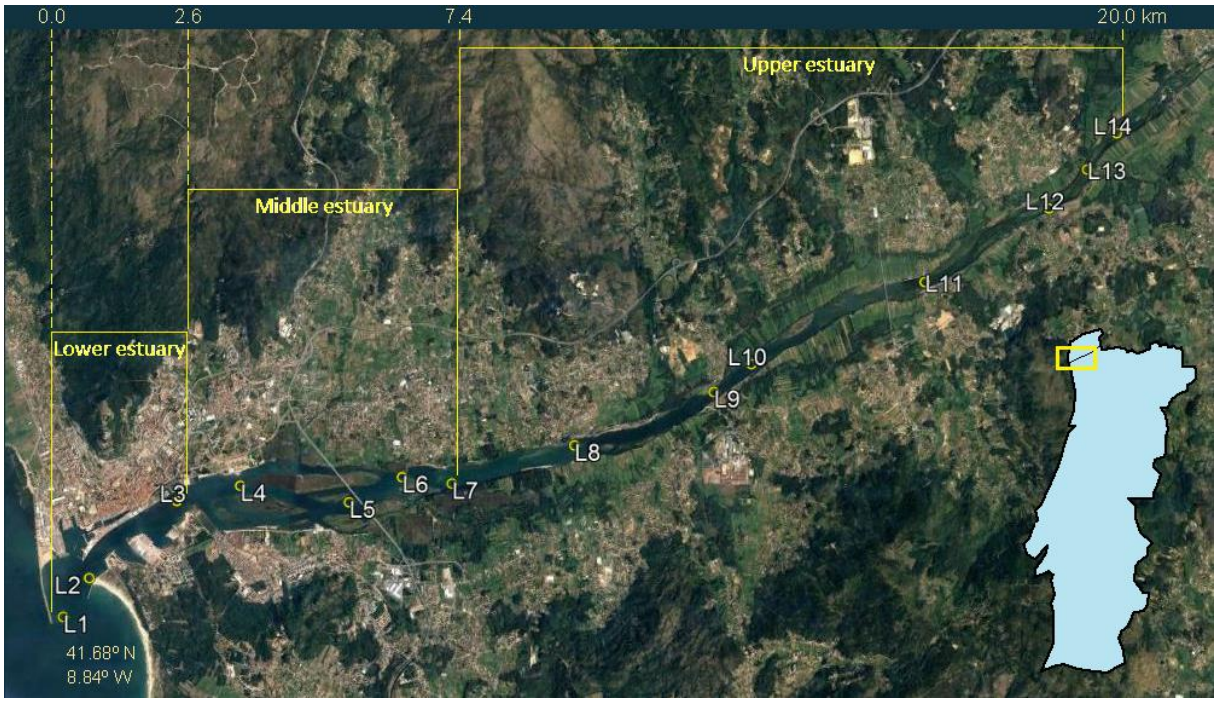

Figure 3.1 Satelite image of the Lima estuary sampling stations (source: Google earth).

3.2.2 Sampling

Sampling surveys were carried in the September 2014 at a neap (1 September 2014) and spring phase (10 September 2014), during the ebb and flood tides of the same day, and started 1:30 h before slack water. The neap and spring phases showed a tidal amplitude around 1.7 m and 3.7 m, respectively (IPMAR, 2017). Samples were collected from 11 locations along the estuary at neap tide and 14 at spring tide (Figure 3.1). At each sampling station, vertical profiles of salinity, temperature, turbidity, pH and dissolved oxygen (DO) were obtained with a YSI 6820 CTD multiprobe, calibrated according to the instructions from the manufacturer. The data presented for the remaining parameters resulted from the analytical determination of the samples collected in the water column with a Van Dorn bottle (surface, middle and bottom water), with the collected samples kept refrigerated in an ice chest until processing in the laboratory.

3.2.3 Analytical procedures

For the determination of total suspended solids (TSS) and volatile suspended solids (VSS), the water samples were filtered through pre-combusted glass fiber filters (GF/F Whatman), and dried at 105 °C (TSS), followed by combustion at 550 °C (VSS) (APHA, 1992). The dissolved orthophosphate, nitrite, ammonium and silicate determinations were performed by the methods of Koroleff (Grasshoff et al., 1983). The nitrate concentration was obtained by the method described by Jones (1984) and adapted by Joye and Chambers (1993), subtracting the nitrite from the total concentration of NO_x obtained. Determination of total dissolved carbon (TDC), dissolved organic carbon (DOC), and total dissolved nitrogen (TDN) was performed by high-temperature catalytic oxidation with a TOC-VCSN analyzer (Shimadzu Instruments). All analyzes were performed in triplicate. The analytical technique used for the Chlorophyll *a* determination was molecular absorption spectrophotometry after extraction using 90% acetone (Parsons et al., 1984) and quantification using the SCOR-UNESCO equations (1966). Water samples were fixed with formaldehyde (4% v/v) for the determination of the total microbial cells. Subsamples (3 mL) were stained with 4',6'-diamidino-2-phenylindole (DAPI), and filtered onto black 0.2 μm Nucleopore polycarbonate membranes (Whatman, UK) (Porter and Feig, 1980). The microbial cells were counted (TCC) with an epifluorescence microscope (Labphot, Nikon, Japan) equipped with a 100 W high-pressure Mercury lamp and a specific filter sets (UV-2B), at 1875x magnification. A total of 20 random microscope fields in different parts of the filter were counted in order to accumulate at least 300 cells per filter.

3.2.4 Data analysis

Bi-dimensional contour plots, generated by Surfer 8.01 software (Golden Software Inc.), were used to represent variations of measured variables with depth along the estuarine axis in the navigation channel. Data were interpolated using the Kriging gridding method (linear variogram model).

STATISTICA 13.0® software package was used to perform the basic statistics, and statistical tests, being all statistical analyses considered at a significance level of 0.05. Principal component analysis was performed to investigate patterns of similarity between samples based on environmental variables, in data previously log transformed to account for the non-normal distribution of variables and normalized to account for the different units in which variables expressed.

PRIMER 6 & PERMANOVA+ software package was used to investigate differences between results obtained at different times (neap-spring phase and tides) and in different spaces (depths and estuary areas). The permutational multivariate analysis of variance (Permanova),

is a non-paramentric, based on dissimilarities, that uses permutation to calculate the *F* (pseudo-*F*) statistic. It allows the partitioning of variability, similar to ANOVA, allowing a complex design (multiple factors, nested design, interactions, covariables). It is meant to test differences between groups as an ANOVA test, but with a large number of of variables, and with permutations to avoid possible biases. This tool was carried out for the similarity study of the obtained data, grouped by neap-spring phase, tide, estuary area and depth, using 9999 permutations. Permutational tests of homogeneity of multivariate dispersions (PERMDISP) were also performed.

3.3 Results

3.3.1 Key physical-chemical descriptors

The longitudinal salinity profiles for the neap and spring surveys during ebb and flood tides are presented in Figure 3.2. The salt wedge (water with salinity above 30) introduced during the flood tide remained within estuary during low slack ebb tide, being located about 4–4.5 km from the estuary mouth, in the middle estuary during the neap ebb tide, and moving 2 km downstream, to the lower estuary during the spring ebb tide. During the flood tide, the salt wedge was located in the upper estuary about 8 and 11 km from the river mouth, for the neap and spring phase surveys, respectively. Taking the neap tide survey as a starting point, it was found that during the spring tide survey the salt wedge moved downstream towards the river mouth during the ebb tide and upstream during the flood tide, resulting a greater distance of the salt wedge between ebb and flood tides during spring tide (8.5 km) than in the neap tide (3.5–4 km).

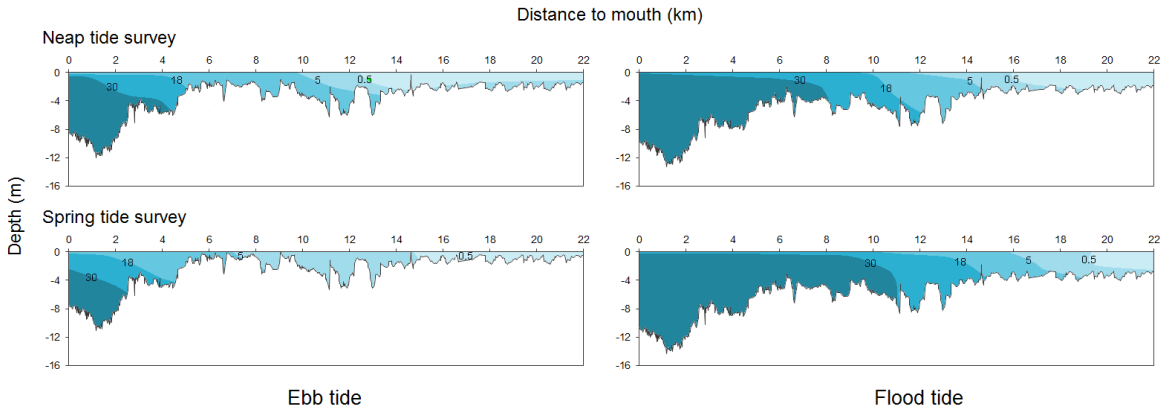

Figure 3.2 Longitudinal salinity profiles of the Lima Estuary during neap and spring tide surveys.

The estuary recorded a higher water temperature in the ebb tide than in the flood tide for the two spring and neap phases (Figure 3.3, Table S3.1). For both tidal phases, the minimum

value obtained was in bottom water of the lower estuary (13.8°C and 19.1°C for the neap and spring tides, respectively), and the maximum was in surface water of the upper estuary (23.5°C and 23.3°C for the neap and spring tides, respectively).

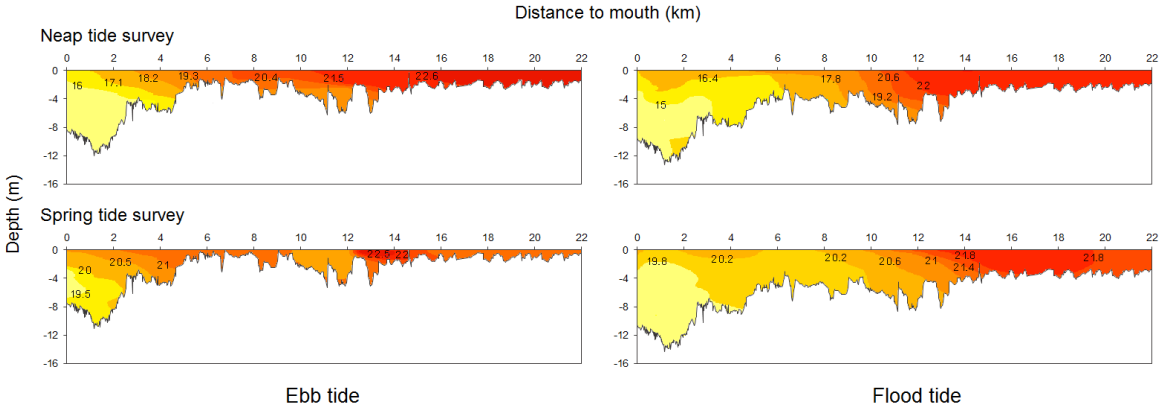

Figure 3.3 Longitudinal temperature profiles of the Lima Estuary during neap and spring tide surveys.

Dissolved oxygen was higher in the upper estuary, and the highest values were measured during the flood tide (Figure 3.4, Table S3.1). The values within the estuary ranged from 7.18–9.78 mg O_2 L^{-1} in the neap tide, and between 7.73–10.43 mg O_2 L^{-1} in the spring tide. All these maximum and minimum values were recorded on bottom samples. Samples collected during spring tide showed always higher values of dissolved oxygen in both tides.

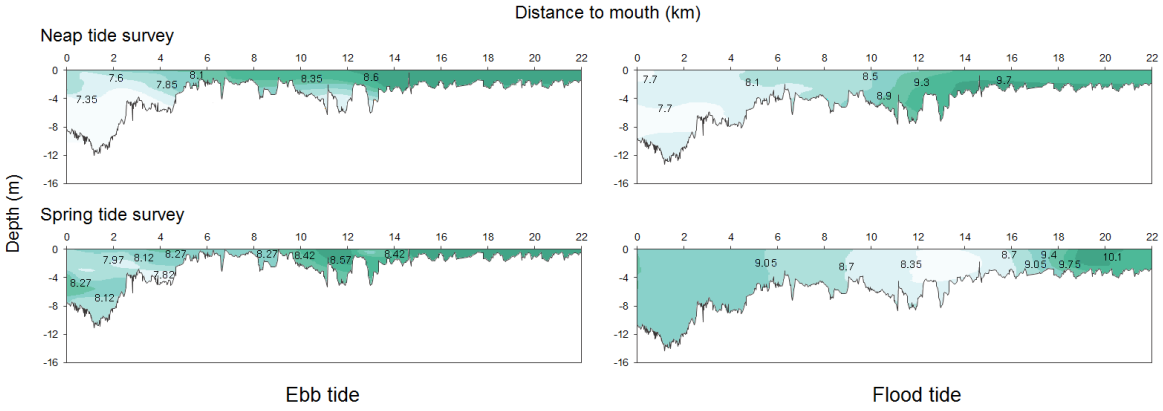

Figure 3.4 Longitudinal dissolved oxygen profiles of the Lima Estuary during neap and spring tide surveys.

During ebb tide, turbidity was elevated near the bottom (max. 11.1 NTU) in the lower estuary in the spring survey, and turbid bottom extended water further upstream the neap survey (Figure 3.5). During flood tide, a high turbidity zone emerged in the upper estuary (km 8–12) independently of the tidal phase (maximum values 10.9 NTU in neap tide).

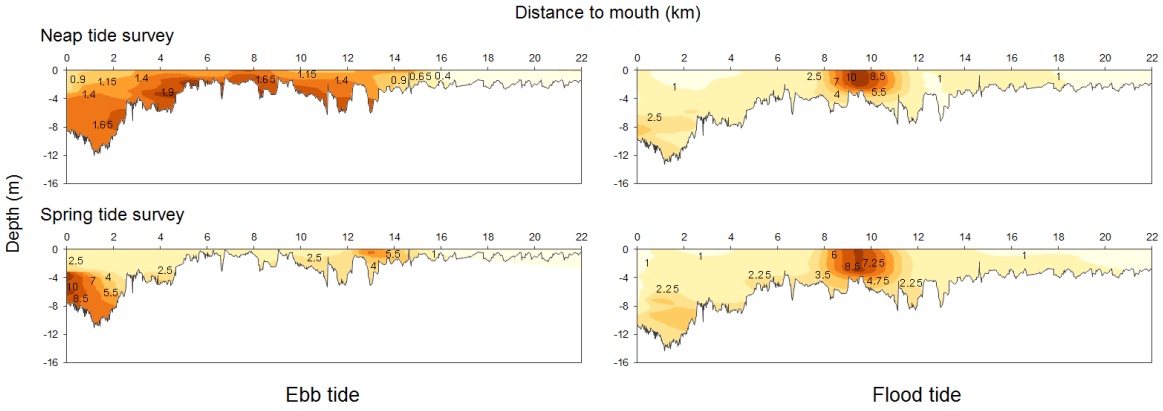

Figure 3.5 Longitudinal turbidity profiles of the Lima Estuary during a neap and spring tide surveys.

3.3.2 Spatial variability of environmental variables

Nitrate, silica and chlorophyll *a* averaged concentration values increased along the estuary towards upstream independently on the tide (Figure 3.6). Nitrate concentrations varied between 0.403 μM (L2, lower estuary bottom, spring tide) and 46.829 μM (L11, upper estuary surface, neap tide). The silica concentration ranged from 0.743 μM (lower estuary) to 99.17 μM (upper estuary). The average concentrations of both parameters showed an increasing tendency along the estuary, with higher values during the ebb tides. Regarding chlorophyll *a*, the concentrations varied between 0.958 mg m^{-3} (L1, lower estuary surface) and 54.04 mg m^{-3} (L10, upper estuary surface), suggesting potential sources along the upper estuary. Nitrites and ammonium showed the higher average concentrations in the lower estuary during the neap tides and in the upper estuary during spring tides (Table S3.2). For ebb tides, ammonium amount decreased in the lower and middle estuary followed by an increase in the upper estuary, suggesting a sink of ammonium at around 5.5–7.5 km (spring tide) and 7.2–9.5 km (neap tide) from the estuary mouth. Phosphate concentration range in the estuary was 0.076 μM (L1, flood spring tide) at 0.731 μM (L1, flood neap tide). The phosphate concentration during the ebb neap tide decreased along the lower and middle estuary, followed by an increase in the upper estuary indicating potential sinks of phosphorus, about 7.5–12 km from the mouth of the estuary. At flood tide, the behavior was reversed, with the amount of phosphate increasing along the estuary until the 12.5 km (upper estuary), then decreasing upstream of the estuary, appearing to indicate sources of phosphate in the upper estuary. Concerning to total dissolved carbon and suspended solids, average concentration values decreased from the lower estuary to the upper estuary. Despite this general pattern, during flood spring tide, the suspended solids recorded a concentration increase in the lower and middle estuary, resulting in the higher averaged values in the middle estuary, suggesting sources of suspended matter in this area.

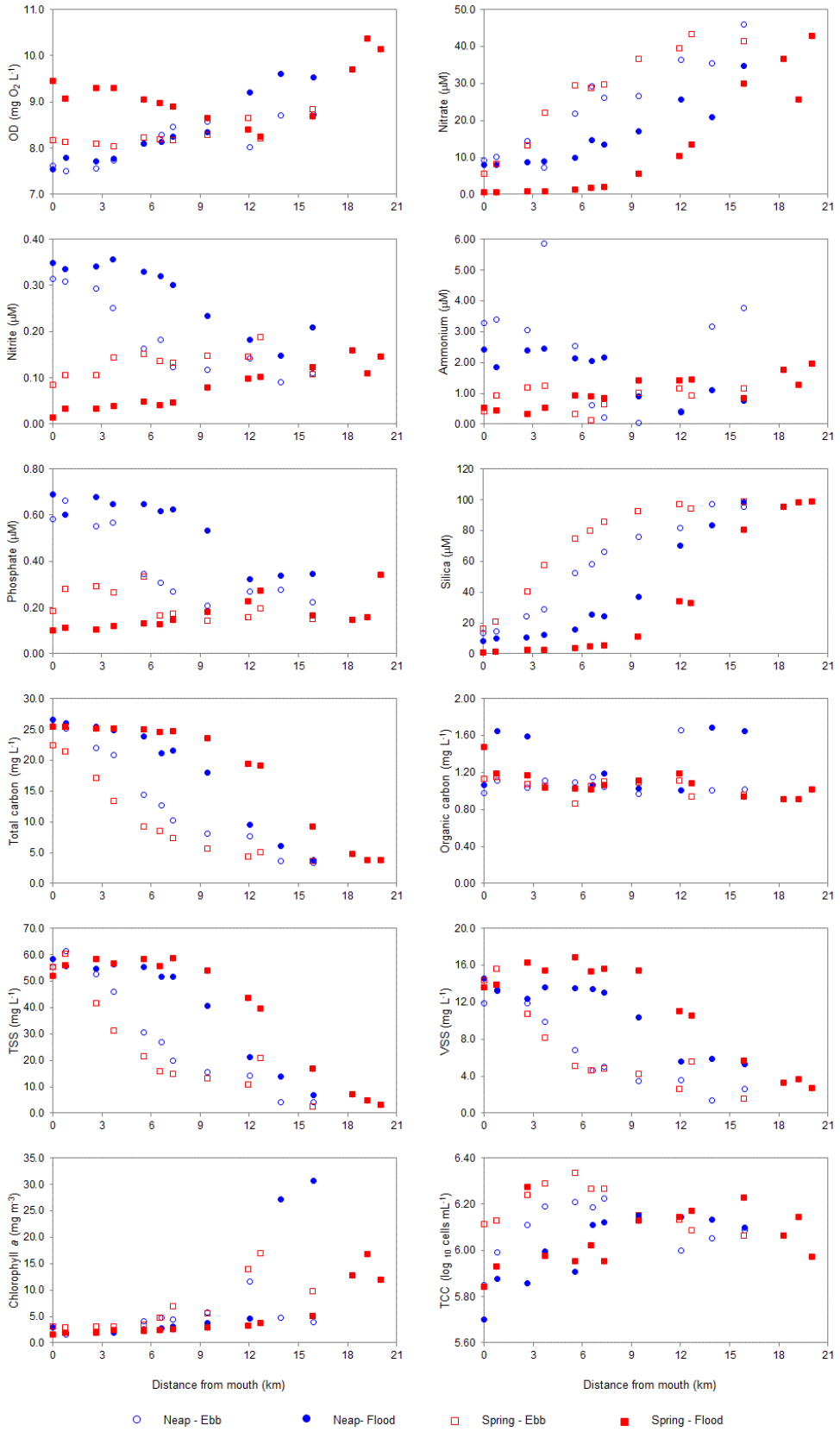

Figure 3.6 Spatial variability of dissolved oxygen (DO), nutrients, total dissolved carbon (TDC), dissolved organic carbon (DOC), total suspended solids (TSS), volatile suspended solids (VSS), chlorophyll *a* and total cell counts (TCC) in the Lima River estuary. Each point corresponds to depth-average value (surface, middle and bottom) of the samples collected at each sampling station.

Dissolved organic carbon amounts generally decreased upstream of the estuary during spring tides, being the higher averaged values found in the lower estuary (1.281 mgL^{-1} and 1.120 mgL^{-1} for flood and ebb tide, respectively). Although the neap tides did not show a clear trend, the lower estuary registered the higher average concentration during the flood tide (1.434 mgL^{-1}) and the upper estuary at ebb tide (1.238 mgL^{-1}). The behavior shown by bacteria along the estuary was similar in all surveys, with an increase from estuary mouth towards upstream in the lower estuary and part of the adjacent middle estuary, followed by a decrease in the upstream estuary strecthes, indicating possible bacteria sources. The difference between surveys consisted in the location of the peak area, that is, during the ebb tides the higher values were found in the middle estuary (6.6–9.5 km and 5.6–7.5 km for neap and spring tides, respectively), and in the flood tides in the upper estuary (9.4–12 km and 12.7–15.85 km for neap and spring tides, respectively), with highest values of 1.84 x 10^6 cells mL^{-1} and 2.22 x 10^6 cells mL^{-1} for ebb neap and spring tides, respectively, and 1.37 x 10^6 cells mL^{-1} and 1.94 x 10^6 cells mL^{-1} for flood neap and spring tides, respectively.

3.3.3 Conservative environmental variables

Dissolved oxygen had a relatively consistent decreasing trend with salinity during the ebb and flood neap tide (Figure 3.7). For the spring phase, the trend was not so evident, but lower values were found for both ebb and flood tides at the higher salinity values. Nitrate and silicate showed a decrease trend close to a conservative behavior, while TDC, TSS and VSS increased consistently with salinity. Nitrites and phosphates showed similar behavior, with concentration values responding positively to salinity changes during neap tides but not during spring tides. Ammonium behavior was non-conservative, as dissolved organic carbon that remained almost constant along the estuary. Chlorophyll *a* concentrations decreased with the salinity, presenting, however, a non-conservative behavior, with high values in low salinities, indicating potential sources in that areas. Bacteria behavior was clearly non-conservative, with lower values in the higher salinities.

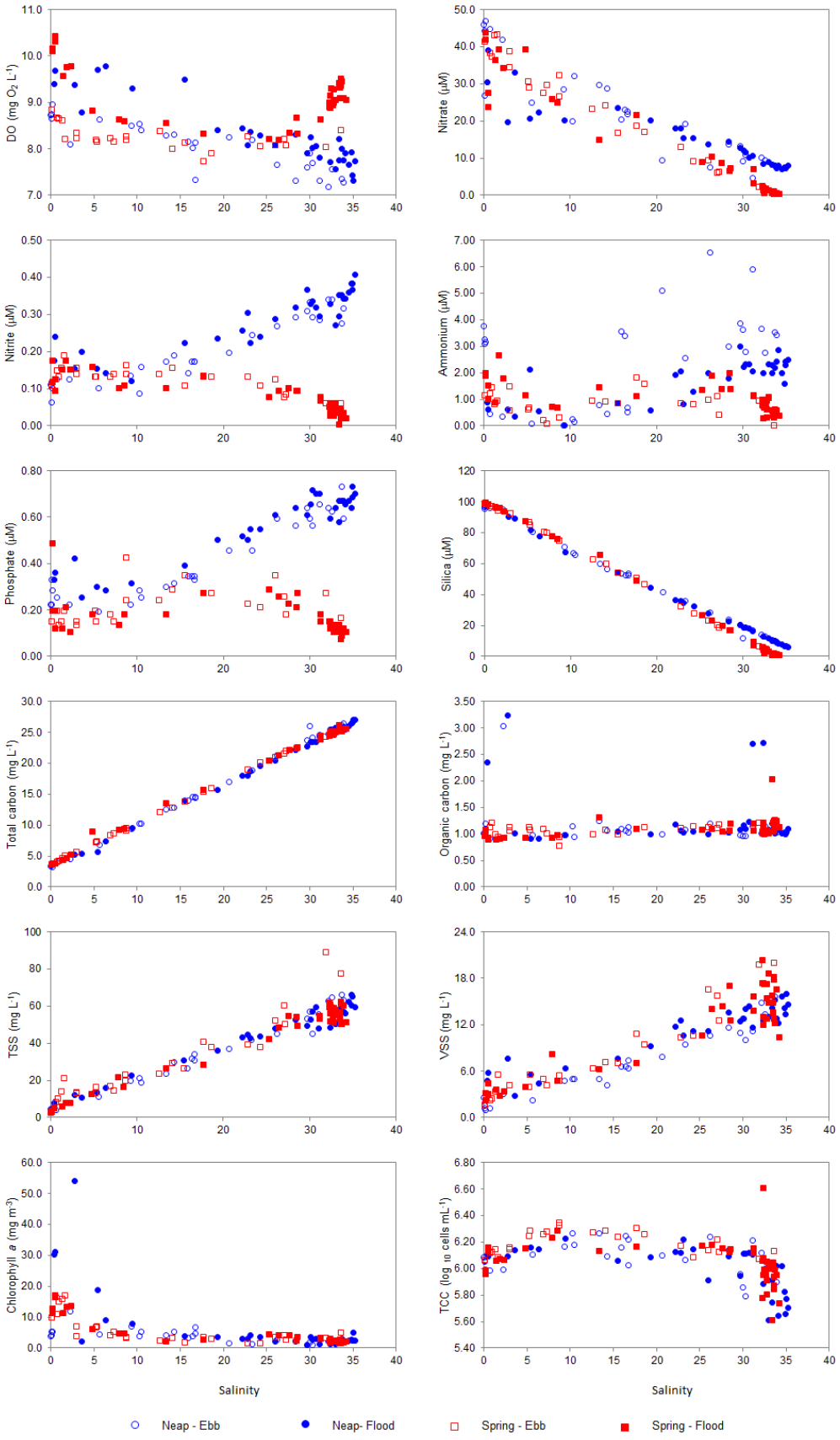

Figure 3.7 Relationships between dissolved oxygen (DO), nutrients, total dissolved carbon (TDC), dissolved organic carbon (DOC), total suspended solids (TSS), volatile suspended solids (VSS), chlorophyll *a* and total cells counts (TCC), and the salinity.

3.3.4 Tidal variability of environmental variables

The variability of measured parameters along the water column were presented in Figure 3.8. The DO showed higher averaged values at the surface during ebb tides, and there was almost no variation during the flood tides along the water column. Nitrate and silica presented higher values on the surface corresponding to the lower values of salinity in all tide surveys. Phosphate and nitrite presented a clear tidal variability with higher concentrations measured during neap tides. Ammonium usually showed higher values at the middle depth, except for the flood spring tide. The total and organic dissolved carbon, and the suspended solids showed the lower average values at the surface, with the higher amounts observed in the middle depth for the total dissolved carbon, and at the middle and bottom depths for the suspended solids. Dissolved organic carbon showed higher concentrations in surface during flood tides and at middle depth during ebb tides. Chlorophyll *a* presented higher values in the surface during the neap tides and in the bottom in the spring tides. Concerning the bacterial behavior, the higher values were recorded at the bottom of the water column, except for flood neap tide. Dissolved oxygen and bacteria registered higher values during the spring tide (*t*-test $p < 0.05$), and pH, nitrite, ammonium phosphate and DOC during the neap tide (*t*-test $p < 0.05$) (Table S3.1). The lower averaged concentrations, with respect to the tides, were presented during flood spring tide for nitrites (0.074 μM) and phosphates (0.164 μM), and ebb neap tide for turbidity (1.35 NTU) and chlorophyll *a* (4.21 mg m^{-3}). The ammonium with a reverse behavior, showed higher averaged values during ebb neap tide (2.52 μM) and flood spring tide (1.015 μM), and lower in the ebb spring tide (0.846 μM). Nitrates, silica and bacteria averaged concentrations presented higher values during ebb tides, i.e., 22.3 and 24.0 μM for nitrates, 51.1 and 62.2 μM for silica, and 1.252×10^6 and 1.600×10^6 cells mL^{-1}, for neap and spring tides, respectively. This behavior was the inverse of the recorded for the values of salinity. The total and organic dissolved carbon, and the suspended solids showed the higher averaged values during the flood tides and lower values in the ebb tides. Despite this, the maximum suspended solids concentration of 89.2 mg L^{-1} was shown in spring ebb tide.

The average concentrations of the parameters with respect to the flood and ebb tides showed differences for salinity, DO, nutrients, TDC, suspended solids and bacteria during neap and spring tide phases, turbidity and ammonium only during neap phase, and pH only for the spring phase (*t*-test $p < 0.05$).

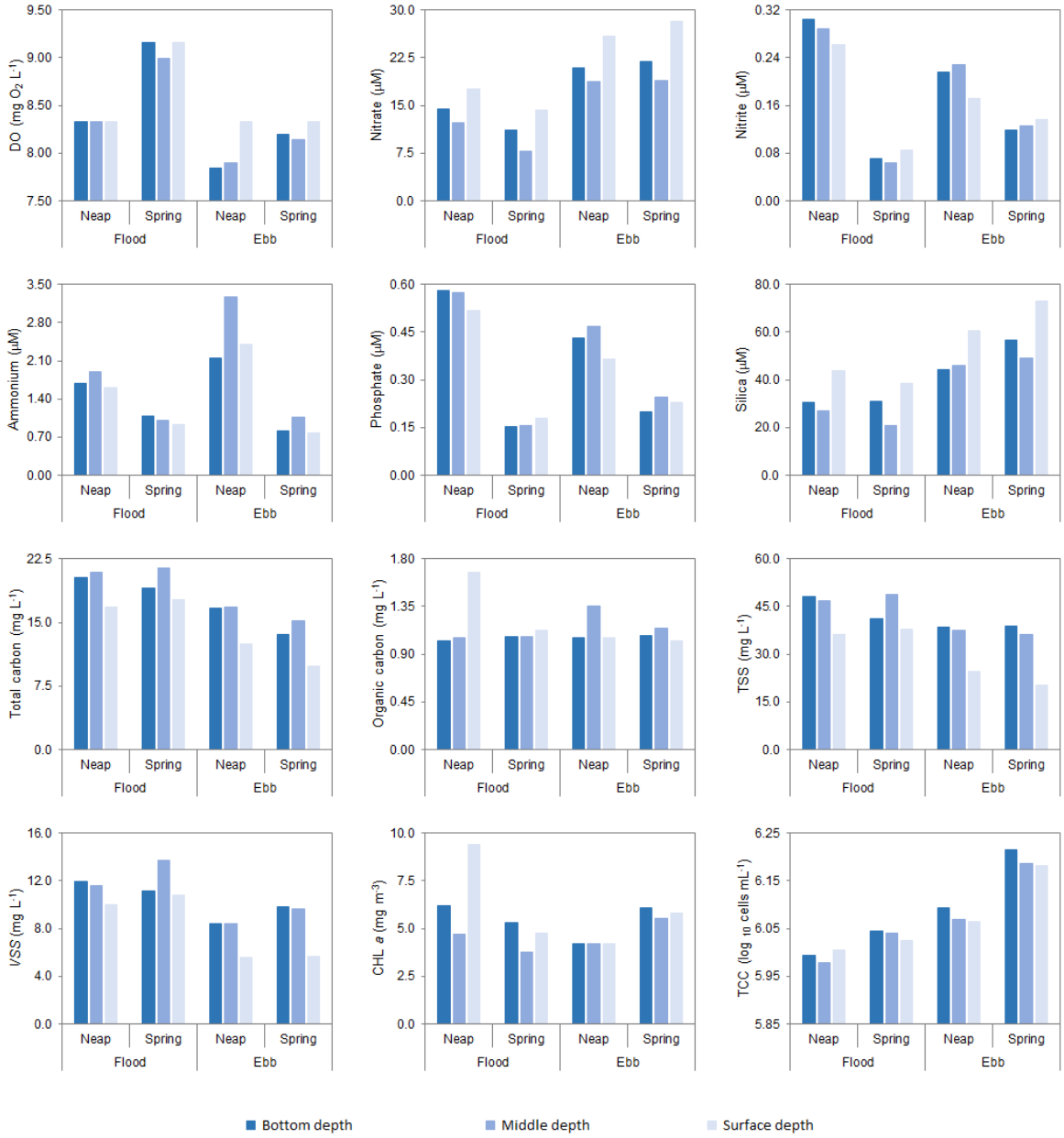

Figure 3.8 Neap and spring tides variability of dissolved oxygen (DO), nutrients, total dissolved carbon, dissolved organic carbon, total suspended solids (TSS), volatile suspended solids (VSS), chlorophyll *a*, and total cell counts (TCC) in Lima River estuary water column (values represent the average of all sampling locations).

3.3.5 Multivariate analysis

The factor analysis showed four main factors (Eigenvalues > 1) explaining about 80.9% (Table 3.1) of the total data variation in the collected samples. Principal component analysis (PCA) was performed to investigate similarities patterns between samples based on the contribution of environmental variables and temporal and spatial parameters (Figure 3.9). The first 2 components (PC1 and PC2) accounted for 65.5% of the total variation. Variables contributing

more to PC1 were silica, nitrate, chlorophyll *a* and temperature (positively), and salinity, total dissolved carbon and suspended solids (negatively), seeming to suggest variables with a distribution pattern associated with salinity and freshwater. For PC2 contributed most positively nitrite, ammonium and phosphates, and negatively dissolved oxygen, suggesting variables with an inverse distribution profile for neap and spring tides (salinity). PC3 was highly positively participated by turbidity and bacteria (TCC). The variable that contribute mostly to PC4 was organic carbon in a highly negative way.

Table 3.1 Factor loadings and Principal Component Analysis (PCA) factor loadings plot (factors 1 and 2).

	Factor 1	Factor 2	Factor 3	Factor 4
Temperature	0.772	-0.538	0.129	-0.070
Salinity	-0.952	-0.140	0.160	0.002
pH	-0.440	-0.308	0.156	-0.226
Turbidity	-0.145	-0.143	0.688	-0.133
DO	0.501	-0.620	-0.353	0.056
NO_3^-	0.748	0.586	0.205	-0.016
NO_2^-	-0.287	0.902	-0.002	-0.047
NH_4^+	-0.263	0.688	-0.172	0.104
PO_4^{3-}	-0.444	0.823	0.013	-0.140
Si	0.825	0.430	0.260	-0.041
CHL *a*	0.800	0.043	0.001	-0.235
TDC	-0.979	-0.127	0.074	0.020
DOC	-0.054	-0.014	-0.241	-0.936
TSS	-0.952	-0.132	0.188	-0.010
VSS	-0.915	-0.214	0.083	-0.078
TCC	0.425	-0.077	0.713	-0.042
Expl.Var	7.085	3.390	1.418	1.052
% Total variance	44.28	21.19	8.861	6.573
Cumulative %	44.28	65.47	74.33	80.90

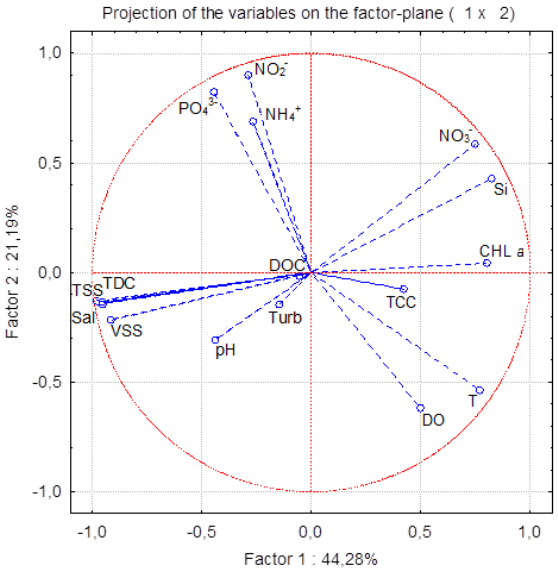

The representation of the projection of samples against the first 2 principal components is shown in Figure 3.9. When the samples were labeled by the neap-spring phases, part of the samples from each tidal phase presented a different distribution along the two PCs, being projected in different quadrants. The samples separation by neap and spring tides may result of the behavioral differences of some variables with salinity (Figure 3.7), such as ammonium, nitrite and phosphate (PC2), which increased with the salinity (PC1) in the neap tide and decreased in spring tide, and the dissolved oxygen with inverse behavior. The association between samples labeled on the basis of ebb and flood tides was not as clear, however, the ebb samples were mainly projected along the PC1 axis, in the quadrant with positive

contribution of silica, nitrate, chlorophyll *a* and temperature, and the flood samples projected in the opposite quadrant associated with positive contributions of salinity, total dissolved carbon (TDC) and suspended solids. Regarding PC2, the flood tides samples were represented in the quadrant with negative contribution of nutrients and positive of dissoved oxygen.

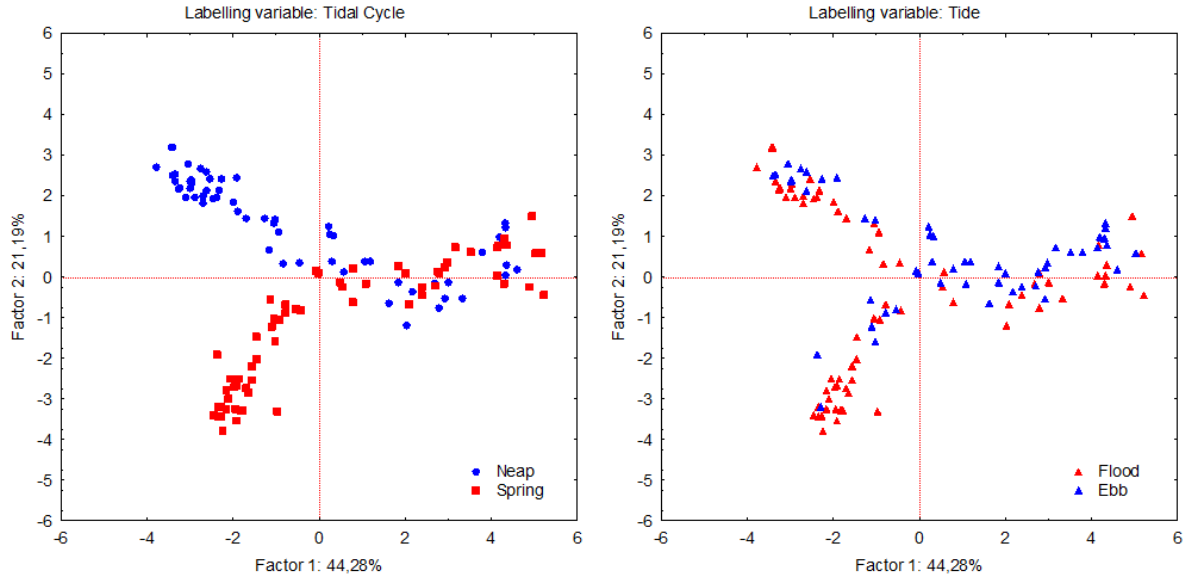

Figure 3.9 Projection of samples in the space defined by the first 2 principal components.

The Permanova similarity tests for the set of samples collected during the neap and spring tide surveys showed differences between the neap-spring cycle and flood-ebb tide. Similarity tests were performed by crossing the different groups. The tests showed differences between all crossed groups. Finally, the factors were hierarchized, and a nested design for similarity tests was created. The neap and spring phases were different, and in each of them the two ebb and flood tides were also different.

3.4 Discussion

3.4.1 Environmental parameters

Estuaries are dynamic ecosystems, subject to both marine influence, such as tides, waves and the influx of saline water, and riverine influences. During summer, river flows are normaly negligible and the estuaries become tidally dominated, causing strong saline intrusion, with an extension dependent on tidal phase (Morais et al., 2009; Camacho et al., 2014). The salinity data obtained for the neap and spring tides showed higher salinity during the flood tide compared to the ebb tide conditions, in accordance with most estuaries, since during the high tide the dominant highly saline seawater replaces river water with negligible salinity (Montani

et al., 1998; Das et al., 2017). In addition, the difference in salinity amplitude between high and low tide conditions was higher in the spring phase than in the neap phase. During spring tide, tidal amplitude in mesotidal estuaries generally remains very high, implying a higher seawater dominance during high tides, and a greater dominance of freshwater during low tides (Das et al., 2017). During the flood spring tide, the salt wedge was located further upstream, with maximum saltwater intrusion, and with the salt wedge moving to the estuary mouth in the same extension during the ebb spring tide, leading to highest ebb advection of river freshwater (Uncles and Stephens, 1996). On the contrary, during the neap tide, the tidal amplitude remained lower, so that the dominance of the seawater and freshwater was intermediate relatively to the spring tides (Das et al., 2017). The water column vertical salinity gradient, presented surface water generally with characteristics closer to those observed in freshwater (Azevedo et al., 2010) and bottom water closer to seawater, suggesting as main suppliers river water for the surface and coastal water for bottom, i.e., freshwater floating over saline water (Wolanski and Elliott, 2016). The data seem to indicate the salinity as a proxy for tidal influence in this region.

The river flow originated essentially from discharges of upstream dams and precipitation, as described for other temperate estuaries (e.g., Hofmeister et al., 2016) and the tidal fluctuation, are the main driving forces that determine the extent of saltwater intrusion (Azevedo et al., 2010), the residence time and the concentration of several parameters (e.g., nutrients) in the estuary. When the discharge decreases, as it happens during summer, vertical stratification of the water column takes place and the tidal influence dominates, being the tidal fluctuation may be the main driving force behind nutrient distribution throughout the estuary (Chaudhuri et al., 2012). In Lima estuary, the salinity increase corresponded to a decrease of DO and temperature (Figure 3.7, Table S3.1). Thus, the DO increased along estuary with higher values in the upper estuary. However, there was a decrease during the spring flood tide till 12 km from the estuary mouth (Figure 3.6, Table S3.2). A positive-landward sign of the temperature gradient during summer was found may have resulting from the temperature gradient between the cooler ocean and the warmer river waters (Cloern et al., 2017). The explanation seems to be supported by the fact that the temperature recorded in the ebb tide was higher than in the flood tide for the two neap and spring tides. The Lima river acts as a natural water, with an upstream influx fresh and oxygenated, which introduces dissolved oxygen into the estuary. Along the estuary, sediment resuspension may have occurred during spring flood tide due to flow turbulence, and may result in a decrease in O_2 in the water column due to the chemical oxidation of reduced compounds, or the increase in aerobic mineralization of organic matter accumulated in the sediment under anoxic conditions (Akomeah and Lindenschmidt, 2017). The higher DO recorded in flood tides may be due to upward movement of tidal surges which trap atmospheric oxygen, and/or influenced by generated wave action at high tide which

increased rate of oxygen saturation (Fatema et al., 2015). Usually, the pH recorded higher values during the flood, perhaps because of the higher pH downstream, since sea water has a slightly alkaline nature (Fatema et al., 2015). During the spring phase the river seems to have contributed to the turbidity, while in the neap phase the largest contribution seems to result from the coastal water, occurring the sediments resuspension within the middle estuary during the ebb tide. The predominant nitrogen form in the estuary was nitrate with an inverse relationship with salinity (Figure 3.7), suggesting that freshwater was the main source of nitrogen in the estuary, existing an effective dilution process during the mixing of river water with a seawater impoverished in nutrients (Cravo et al., 2014; Das et al., 2017). The higher nitrate concentration was showed in the water column surface of the upper estuary during the ebb tides, i.e., increasing concentrations with the decreasing in salinities, also by Azevedo et al. (2008). The same tendency was presented by silica, considered the best tracer of freshwater influence (Cravo et al., 2006), supporting the freshwater origin of these nutrients. The highest concentration values found in freshwater in the upper estuary were probably the result of agricultural activities and soil leaching (Caetano et al., 2016), with the chemical weathering of silicates on land, as the main input process of dissolved and particulate silicate into the rivers (Domingues et al., 2005; Morais et al., 2009). These parameters recorded maximum and minimum values during ebb and flood tides of spring phase respectively, probably due to the drag of saline water and freshwater in opposite directions for maximum distances in the estuary, resulting from the higher spring tidal amplitude (Das et al., 2017). Intra-tidal variations of salinity, nitrates and silica during spring tides were generally wider than those during neap tides (Figure 3.7), suggesting that, over a semidiurnal tidal cycle, neap tides tended to prevent Lima plume from extending seawards, i.e., flood currents during spring tides were more favorable to the intrusion of seawater (with high salinity and low nitrates and silica) than the flood currents in the neap tides, as reported by Gao et al. (2009).

Despite the non-conservative behavior presented by nitrites and phosphates, they showed an inverse tendency with salinity during the neap and spring phases, i.e., the concentration decreased during neap tides and increased during spring tides, towards upstream with higher values during the neap tides. The values recorded for both parameters in all surveys did not differ much in the most upstream estuary area, seeming to indicate the contribution of the river was not a differentiating factor for the exhibited behavior. The higher and lower concentrations were found in the lower estuary (higher salinity) during the neap flood tide and spring flood tide, respectively. Surficial water presented the lower concentrations during neap tides and the higher during spring tides. This behavior seems to suggest different origins for the tidal phase, i.e., during the spring phase, freshwater was the main source of these nutrients, while during the neap phase there was additional contribution of saltwater, since the water column surface generally shows characteristics closer to freshwater, as for the Douro estuary (Azevedo et al.,

2010). The lower nutrients concentration during the spring phase may be attributed not only to the relatively lower nutrients inflow but also to the reduction in residual outflow (Vinita et al., 2015). Ammonium showed lower concentrations in the salinity range of 5 to 10, in the middle estuary (spring and neap tides), and higher concentrations in the lower estuary during the ebb neap tide, and upper estuary during the flood spring tide. The minimum values presented in the range of 5–10 salinity seems to suggest the deposition/sinks of this nutrient in this area. The observed behavior for nitrites, ammonium and phosphates, showing non monotonic tendency with salinity, seems to indicate possible sources and sinks of those parameters along the estuary (Cloern et al., 2017). Concentrations appear to be significantly affected by *in situ* processes, in addition to external effects and physical variables, such as river flow, rainfall and salinity (Magni and Montani, 2000; Cloern et al., 2017). The concentrations recorded may be the result of nutrient regeneration processes within the estuary, with higher values during neap tide resulting from the improvement of benthic decomposition processes, due to more favorable conditions, i.e., less water turbulence (Magni and Montani, 2000) and prolonged tidal flushing time (Gao et al., 2009). The ammonia higher concentrations during the ebb neap tide seems to indicate the release of the ammonia from the sediments by remobilization processes (Marcovecchio et al., 2009). A possible explanation for higher phosphate concentrations in the higher salinities (lower estuary) during the neap tides may be its complicated adsorption or desorption from the sediments during the period of greatest influence of freshwater (Yin and Harrison, 2000).

The total dissolved carbon and suspended solids showed an increasing linear relationship with increased salinity (Figure 3.7), with higher values in the middle and bottom of the water column (Figure 3.8) in the lower estuary during the flood tides (Figure 3.6, Table S3.2), in agreement with the reported by Ramos et al. (2017) for this estuary, suggesting a source related to seawater. The higher values were recorded during the spring flood tide. Despite the decreasing pattern presented along the estuary toward the upstream river, suspended solids increased in the lower estuary and the adjacent middle estuary during the spring flood tide, suggesting suspended matter sources in this estuary area. The total suspended solids concentrations in an estuary depend on river sediment transport, sediments originating locally associated with resuspension of the estuarine sediment bed, and winds and flood events (Azevedo et al., 2008). The predominance of suspended solids in the lower/middle estuary can be interpreted as resulting from water circulation during tidal cycles with mixture of fluvial and marine sediments in the lower estuarine channel (Caetano et al., 2016; Oliveira et al., 2017) and/or resulting from saltmarsh particles (Caetano et al., 2016), existent in the middle estuary. The different behavior pattern between total dissolved carbon and dissolved organic carbon (Figure 3.7) seems to suggest that most of the total dissolved carbon came from dissolved inorganic forms. The increased values towards the estuary mouth were also recorded in other estuaries

(Oliveira et al., 2017). The estuary dissolved organic carbon averaged concentrations were higher during the flood tides, with higher values in the neap phase. A clear trend of concentration with salinity was not identified, suggesting potential sources and sinks along the estuary (Figure 3.7), and maybe the concentration could be affected by *in situ* processes, depending on the biological absorption, regeneration and equilibrium between the water column and the sediments. The nonlinear pattern of concentration with salinity may imply the existence of estuarine transformation processes and nonconservative behavior (Cloern et al., 2017).

Chlorophyll *a* decreased with salinity, but did not show a conservative behavior (Figure 3.7), with increased values along the estuary (Figure 3.6). The higher average values were found in upper estuary during the flood neap tide and ebb spring tide (Table S3.2), with the water column surface contributing with larger amounts during the neap phase and the bottom of the water column during the spring phase (Figure 3.8). The decrease in chlorophyll *a* concentration with salinity seems to indicate the river as a potential source (Azevedo et al., 2008), and the increased concentration values along the estuary may be attributed to conditions that increase the growth or decrease the loss rates. Independently of the tide, chlorophyll *a* peaked always in the estuary oligohaline area, unlike the reported for other estuaries where peaks of chlorophyll *a* were found in higher salinity areas (Fisher et al., 1988). However, Azhikodan and Yokoyam (2016) reported chlorophyll *a* maxima in the interface between freshwater and saltwater. The estuary upper part, surrounded by intensive agriculture (irrigated maize), seemed to behave as a source of chlorophyll *a*, suggesting association with higher nitrogen content in the water column (Desmit et al., 2015) and lower suspended solids amount.

The bacterial counts showed maximum values in the mesohaline area and minimum values in the higher salinity areas (Figure 3.7), being the highest values recorded during the ebb tides (Figure 3.8). Salinity is one of the estuarine properties that can influence the control of river water inflow communities (Xia et al., 2015; Bunse et al., 2016). Its "bactericidal" activity (Hobbie, 1988; Munro et al., 1989) appears to control the microbial abundance in high salinity range, being the increase survival in intermediate salinity range a consequence of dilution (Bordalo, 2003). Bacterial counts did not always increased towards upstream (Figure 3.6), however, the averaged values showed an increase from the lower estuary to the upper estuary (Table S3.2), with the higher values recorded in the middle estuary mesohaline area, as also reported by other studies (Ducklow et al., 1999). The increased values in an estuary stretch dominated by salty islands and shallow channels could be explained by the accretion of dissolved organic carbon and/or bacterial biomass from the terrestrial influx (Ducklow et al., 1999; Hitchcock and Mitrovic, 2015). In addition, the vertical stratification existing in the lower section of the Lima estuary can promote limited advection and convection fluxes of microorganisms and substrate between the layers, and the substrate supply for bacteria and

phytoplankton and light can be determinant factors due to their reduction and unavailability, respectively (Bordalo and Vieira, 2005).

3.4.2 Tidal variability

The principal component analysis results showed the factors that may have contributed most significantly to the control of the tidal and dynamic processes in the Lima estuarine system (Table 3.1). The positive contributions given by chlorophyll *a*, tempetature, nitrtates and silica parameters, contrasting with the negatives of TDC, suspended solids (TSS and VSS) and salinity, show spatial and temporal differences throughout Factor 1. The parameters contributing to factor 1 appear to be associated with the river freshwater inputs and the tidal action, as the main factors responsible for the differences between samples in the estuary (Azevedo et al., 2010). The discharge of the Lima River seems to have been the driving force of the dynamic processes associated with silica, nitrates and chlorophyll *a* that occurred in the estuary as observed in other temperate estuaries (e.g., Azevedo et al., 2008), while the concentrations of suspended solids, total dissolved carbon, and salinity and their distribution in the estuary seem to result from the predominant action of tidal cycles (Oliveira et al., 2017). Throughout Factor 2, a distribution associated to nitrites, ammonium and phosphates was observed, as opposed to that observed for DO concentrations. The similar distribution pattern presented by TCC and turbidity (Factor 3) seems to indicate the association of the bacteria with the suspended solids, as reported by Kara and Shade (2009) and Vallières et al. (2008).
To determine the patterns of similarities between samples, the first two factors were represented in two dimensions and the samples were labeled based on the tidal phase (neap and spring) and tides (ebb and flood tides) (Figure 3.9). The PCA representation showed a separation between the samples of the neap and spring phases, which were represented in opposite quadrants in relation to Factor 2, that is, during the neap phase, the increase of ammonia, nitrite and phosphate was associated to the increase of salinity, with an inverse trend during in the spring phase. The differences seem to suggest an explanation in the hydrodynamic variations (river flow and tidal phase) between neap and spring cycles, with the tidal phase appearing to be the main driving factor for the nutrient behavior in the estuary. The mixing of waters with different origins emerges as a primary factor for explaining the variance of results, according to the inverse relationships between nitrate and silicate with salinity (and tide height), as verified for other estuaries (Cravo et al., 2014). The mixing of the seawater and river water is promoted by tidal advection and dilution by diffusion processes since ocean water is poorer in nutrients than Lima river water, as reported for Ria Formosa (Cravo et al., 2014). The tide-labeled PCA showed a less evident separation of the sample distribution, leading to belief that estuary variability shown by the various parameters was higher between the neap

and spring phases, than between ebb and flood tides. Nevertheless, ebb tides samples were preferentially distributed in the quadrant with higher positive contribution of temperature, silica, nitrates and chlorophyll *a* and negative of salinity, suggesting the influence of the river flow, while flood tides samples were associated to the quadrant, with positive contributions of salinity, suspended solids and total dissolved carbon, seeming that saltwater contributed to this distribution. This analysis points as an explanatory factor for the results variance, the influence of the mixing of waters from different origins, as verified by the inverse relation between the nitrates, silicate and the salinity (and tide height), being the mixing promoted by tidal advection and dilution by diffusion processes (Cravo et al., 2014). The results were similar to other mesotidal systems, such as the Ria Formosa, since within the estuary the variability of the water chemical characteristics was also dependent on the tidal influence (Cravo et al., 2014).

Similarity tests between the samples showed differences for all study factors, even those that appeared to show no difference in the graphical representation of PCAs. The differences observed between the samples seem to be related to the extension of the freshwater and coastal water introduction into estuary, dependent on the tidal amplitude and promoted by semidiurnal and fortnightly tide cycles (Camacho et al., 2014), since in the estuarine systems highly variable, the mixing conditions may vary on an hourly basis (Azevedo et al., 2010). When similarity tests were performed crossing the factors, similarities between samples of different groups of factors arose. The comparison of samples from each fortnightly tidal cycle showed similarities between samples collected at different depths in the water column during the two tides (ebb and flood) considering the estuary as a whole or for the various estuary stretches. In the summer, due to low river flow and extensive saltwater intrusion (Morais et al., 2009; Camacho et al., 2014), tidal cycles may have promoted resuspension of estuarine sediments with release of nutrients (Yin et al. 1995) and solids, as well as adsorption or desorption of ions in sediments (Cabeçadas et al., 1999) and biological absorption and regeneration of ions (Rahaman et al., 2014), mainly in the lower and middle estuaries.

In addition, *in situ* processes associated with salty islands and surface channels in the middle estuary may have occurred (Caetano et al., 2016). In the semidiurnal tidal cycle, during the flood tide, saltwater is introduced into the lower estuary along the bottom layer of the water column, while in the ebb tide that saltwater mass goes out to the coastal zone, entering along the surface of the upper estuary, freshwater coming from the river, carrying both water bodies, constituents that contribute to the differences found between the samples (Wolanski and Elliott, 2016). Moreover, when the similarity tests did not take into account the tides, only samples from the lower estuary water column presented differences, that is, in the neap cycle, samples from middle and bottom depth were different to surface samples, whereas in the spring cycle, only surface and bottom samples were differents, suggesting circulation differences of the

saltwater and freshwater during the spring and neap cycles with varying mixing conditions in the estuary. This observation seems reinforced by results from water column samples collected during the ebb and flood tides of the two cycles with differences only in the lower estuary for both ebb and flood tides. The upper estuary water column, an area essentially influenced by the river flow with characteristics similar to the river freshwater (Wolanski and Elliott, 2016), presented a homogeneous water column.

3.5 Conclusions

Analyzing the global results, it can be inferred that tidal dynamics played a crucial role in regulating the short-term variability of the water physical-chemical characteristics in the tidal estuary of Lima. Concentrations of parameters such as salinity, suspended solids, carbon compounds, nutrients, chlorophyll *a* and bacteria showed substantial differences depending on neap-spring tidal phases and in its ebb-flood tides. The distribution pattern and dispersion of those parameters varied significantly on a time-scale of hours due to ebb advection of freshwater and flood intrusion of saltwater. The results point out as the main source to estuary of nitrate and silica to freshwater, and of TDC and suspended solids to seawater, with an effective dilution process during the mixing of river water with seawater. The differences between the samples seem to indicate as an explanation the hydrodynamic variations between neap-spring cycles and ebb-flood tides, with the tidal phase appearing to be the main driving factor for the behavior shown by the parameters under study, that is, the mixing of water of different sources promoted by tidal advection and dilution by diffusion processes, as factors to explain the variance of the results. The parameters concentrations variability was higher between the neap and spring phases, than between ebb and flood tides. Behavior patterns varied depending on the parameter, under the effect of physical variables and *in situ* processes (biological processes - primary producer and consumer activity and metabolism, and physical processes - adsorption/desorption and sedimentation/ resuspension). Similarity patterns seem to show that some estuarine properties have greater temporal variability than spatial variability. The data from this study can serve as a baseline for other studies concerning the management of the natural environment of the estuary and its ecosystems, as well as issues related to the navigation channel and its connections with existent structures.

3.6 SUPPLEMENTARY INFORMATION

Table S3.1 Average and standard errors for selected variables during neap and spring flood and ebb tides surveys.

Parameter[1]	Units	Neap (Average ±SE)		Spring (Average ±SE)	
		Ebb	Flodd	Ebb	Flodd
Deph	m	1.65±0.32	2.09±0.40	1.38±0.32	2.15±0.35
T (ºC)	ºC	18.91±0.46	18.22±0.52	20.88±0.15	20.65±0.14
Salinity	-	17.3±2.3	24.1±2.1	13.0±2.2	23.8±2.1
pH	Sørensen scale	7.74±0.05	7.79±0.05	7.50±0.08	7.76±0.05
Turbidity	NTU	1.35±0.10	2.44±0.51	2.94±0.50	2.00±0.33
DO	mg O_2 L^{-1}	8.05±0.10	8.33±0.13	8.24±0.05	9.11±0.09
NO_3^-	μM	22.3±2.5	14.9±1.4	24.0±2.7	11.2±2.3
NO_2^-	μM	0.202±0.017	0.285±0.014	0.128±0.006	0.074±0.007
NH_4^+	μM	2.52±0.35	1.72±0.14	0.846±0.094	1.015±0.089
PO_4^{3-}	μM	0.414±0.032	0.556±0.026	0.221±0.015	0.164±0.012
N:P	μM: μM	82±12	37.5±5.5	134±20	71±14
C:N	μM: μM	76±12	125±14	155±74	803±134
Si	μM	51.1±5.9	34.0±5.4	62.2±6.4	30.5±6.1
CHL *a*	mg m^{-3}	4.21±0.63	6.8±2.0	5.85±0.90	4.65±0.70
TDC	mg L^{-1}	15.1±1.6	19.3±1.4	12.3±1.4	19.3±1.3
DOC	mg L^{-1}	1.128±0.073	1.26±0.10	1.068±0.019	1.088±0.030
TSS	mg L^{-1}	32.8±4.0	43.5±3.3	30.1±4.4	42.2±3.3
VSS	mg L^{-1}	7.31±0.85	11.16±0.64	8.0±1.1	11.80±0.86
TCC	log_{10} cells mL^{-1}	6.076±0.023	5.993±0.032	6.194±0.017	6.037±0.027

[1] Parameters abreviations: Depth – water column depth; T – temperature; DO – dissolved oxygen; CHL *a* – chlorophyll *a*; TDC – total dissolved carbon; DOC – dissolved organic carbon; TSS – total suspended solids; VSS – volatile suspended solids; and TCC – total cell counts.

Table S3.2 Average and standard errors for selected variables at estuary zones during the flood and ebb tides surveys.

Parameter[1]	Tide	Estuary - Neap tide			Estuary - Spring tide		
		Lower	Middle	Upper	Lower	Middle	Upper
Deph (m)	Ebb	2.52±0.71	1.24±0.44	1.24±0.45	2.02±0.59	1.27±0.59	0.70±0.27
	Flood	3.34±0.85	1.74±0.57	1.45±0.44	3.6±1.0	2.26±0.63	1.38±0.30
T (ºC)	Ebb	16.24±0.29	19.08±0.47	21.38±0.44	20.26±0.18	21.19±0.12	21.26±0.35
	Flood	15.56±0.36	17.22±0.44	21.49±0.55	19.84±0.13	20.07±0.05	21.40±0.16
Salinity	Ebb	30.5±1.1	17.6±2.1	3.9±1.9	25.2±1.9	9.6±1.4	1.51±0.42
	Flood	33.78±0.41	29.6±1.2	10.1±2.7	33.54±0.16	32.71±0.10	13.6±2.9
pH	Ebb	7.80±0.01	7.76±0.03	7.66±0.14	7.88±0.02	7.45±0.08	7.06±0.08
	Flood	7.45±0.08	7.87±0.02	7.97±0.04	7.79±0.03	7.987±0.004	7.61±0.08
Turbidity (NTU)	Ebb	1.18±0.13	1.59±0.10	1.27±0.24	3.7±1.2	2.24±0.42	2.90±0.86
	Flood	1.92±0.49	1.392±0.081	4.0±1.3	1.41±0.41	1.76±0.18	2.43±0.66
DO (mg O_2 L^{-1})	Ebb	7.57±0.11	8.11±0.12	8.48±0.16	8.131±0.049	8.144±0.062	8.516±0.094
	Flood	7.687±0.060	8.064±0.065	9.14±0.17	9.279±0.060	9.058±0.047	9.06±0.18
NO_3^- (μM)	Ebb	11.2±1.2	19.8±3.0	36.3±3.4	9.0±1.9	26.9±1.4	39.6±1.2
	Flood	8.27±0.30	11.8±1.1	23.6±2.3	0.62±0.11	1.51±0.16	22.4±3.2
NO_2^- (μM)	Ebb	0.305±0.011	0.185±0.018	0.117±0.010	0.099±0.010	0.132±0.005	0.147±0.009
	Flood	0.342±0.014	0.327±0.009	0.192±0.013	0.026±0.005	0.044±0.003	0.116±0.008
NH_4^+ (μM)	Ebb	3.25±0.16	2.68±0.80	1.63±0.54	0.84±0.15	0.66±0.18	1.09±0.12
	Flood	2.23±0.11	2.204±0.090	0.79±0.17	0.433±0.040	0.793±0.067	1.43±0.12
PO_4^{3-} (μM)	Ebb	0.600±0.025	0.390±0.043	0.255±0.017	0.253±0.022	0.238±0.029	0.159±0.010
	Flood	0.658±0.015	0.635±0.019	0.388±0.031	0.107±0.007	0.132±0.005	0.211±0.020
N:P (μM:μM)	Ebb	25.6±3.2	68±11	155±18	38.3±7.1	131±17	262±13
	Flood	16.55±0.53	23.3±2.6	70.1±9.9	10.24±0.73	17.7±1.2	133±22
C:N (μM:μM)	Ebb	144±13	69±16	16.2±5.2	392±186	31.8±4.6	9.75±0.80
	Flood	201.7±6.8	146±15	39.9±9.6	2073±173	965±94	99±27
Si (μM)	Ebb	17.4±2.8	49.3±5.1	86.9±5.2	25.8±5.7	72.7±4.1	95.57±0.96
	Flood	9.5±1.1	19.5±2.9	69.8±7.5	1.53±0.36	4.07±0.42	60.9±8.4
CHL *a* (mg m^{-3})	Ebb	1.70±0.15	3.78±0.36	7.2±1.4	2.98±0.38	4.38±0.54	11.4±1.8
	Flood	2.23±0.33	2.57±0.17	15.3±5.0	1.820±0.075	2.422±0.069	7.4±1.2
TDC (mg L^{-1})	Ebb	24.18±0.81	15.2±1.5	5.9±1.3	20.4±1.2	10.06±0.92	4.74±0.31
	Flood	26.00±0.26	22.89±0.82	9.9±1.8	25.37±0.14	24.89±0.08	12.8±1.9
DOC (mg L^{-1})	Ebb	1.044±0.030	1.103±0.028	1.24±0.23	1.120±0.019	1.023±0.036	1.060±0.038
	Flood	1.43±0.21	1.081±0.021	1.31±0.23	1.281±0.097	1.036±0.012	1.029±0.027
TSS (mg L^{-1})	Ebb	56.4±2.9	32.3±3.6	9.9±3.2	52.4±6.8	22.1±2.9	11.8±2.1
	Flood	56.2±2.0	53.8±1.8	21.9±4.2	55.6±1.6	57.42±0.91	26.3±4.8
VSS (mg L^{-1})	Ebb	12.38±0.69	6.94±0.76	2.66±0.61	13.6±1.6	5.93±0.70	3.37±0.53
	Flood	13.40±0.39	13.38±0.39	6.91±0.79	14.62±0.90	15.80±0.76	7.9±1.2
TCC (log_{10} cells mL^{-1})	Ebb	5.977±0.040	6.192±0.021	6.046±0.020	6.157±0.022	6.289±0.011	6.120±0.013
	Flood	5.785±0.046	6.024±0.034	6.129±0.016	5.949±0.093	5.963±0.028	6.126±0.018

[1] Parameters abreviations: Depth – water column depth; T – temperature; pH – Sørensen scale; DO – dissolved oxygen; CHL *a* – chlorophyll *a*; TDC – total dissolved carbon; DOC – dissolved organic carbon; TSS – total suspended solids; VSS – volatile suspended solids; and TCC – total cell counts.

CHAPTER 4

Coupling between hydrodynamics and chlorophyll *a* and bacteria in a temperate estuary: a box model approach

Abstract

The spatial patterns of chlorophyll *a* and bacteria were assessed in a temperate Atlantic tidal estuary during seasonal surveys, as well as in consecutive summer spring and neap tides. A box model approach was used to better understand spatial and temporal dynamics of these key estuarine descriptors. The Lima estuary (NW Portugal) was divided into boxes controlled by salinity and freshwater discharge and balance equations were derived for each variable, enabling the calculation of horizontal and vertical fluxes of plankton, and therefore production or consumption rates. Chlorophyll *a* tended to burst within the oligohaline zone, whereas higher counts of bacteria were found in the mesohaline stretch. Whenever the water column was stratified, similar tide-independent trends were found for chlorophyll *a* and bacterial fluxes, with net growth in the upper less saline boxes, and consumption beneath the halocline. In the non-stratified upper estuary, other controls emerged for chlorophyll *a* and bacteria, such as nitrogen and carbon inputs, respectively. The presented results show that, while tidal hydrodynamics influenced plankton variability, production/consumption rates resulted from the interaction of additional factors, namely estuarine geomorphological characteristics and nutrient inputs. In complex estuarine systems, the rather simple box model approach remains a useful tool in the task of understanding the coupling between hydrodynamics and the behavior of plankton, emerging as a contribution toward the management of estuarine systems.

Keywords: nutrients; salinity; chlorophyll *a*; bacteria; hydrodynamics; box model; Lima Estuary.

4.1 Introduction

Estuaries all over the world are subject to increased pressure due the alterations in the land uses and increase of the population (Jickells et al., 2014). These alterations result in an accretion of inorganic and organic compounds, microbial loads, and changes in the discharge patterns of freshwater in the estuarine and marine coastal environments, resulting in complex ecosystem behaviors (Robson et al., 2008). Estuaries are influenced by both marine and riverine characteristics, and their features depend of tidal pulses, freshwater flow, hydrodynamic, and autochthonous biological processes (Saraiva et al., 2007). Mesotidal

temperate estuaries are characterized to have semi-diurnal tidal cycles in the range of 2–4 meters. Every fortnight, the influence of the moon generates another tidal event called spring tide, characterized by increased tidal amplitude. The complexity of estuarine circulation system may be described through a combination of several components, such as tidal forcing, depth and width, freshwater flow, as well as meteorological forcing (Bordalo and Vieira, 2005). The complex interaction between all the different processes and the need to quantify these interactions led to the development of models capable of evaluating various properties in space and time. In the case of a box model, the complex estuarine circulation system is simplified, being reduced to boxes (or reservoirs) linked by fluxes, and it is assumed that the boxes have homogeneous content. However, the concentration of a given descriptor in the box can vary as a function of time, due to input to (or loss of) the box, or due to production, consumption, or decrease of that descriptor within the box. Vertically-stratified estuaries add an important level of complexity to the modelling analysis. In an estuary, partially mixed or strongly stratified, the basic net circulation consists of an upper layer transporting a mass of fresh or brackish water toward the sea, and a lower layer moving in the opposite direction (Wolanski and Elliott, 2016). This movement of saltier water mass results in a net vertical flow, with upward direction and amplitude determined by the intensity of mixing in the river (Dyer, 1997). Pritchard (1969) developed a relatively simple model that can predict concentration distributions along the length of an estuary, in both upper and lower layer, based on various simplifying assumptions, such as, steady-state conditions, conservative pollutant behavior, and uniform constituent concentration within each layer or each segment. The model estimates the vertical non-advective exchange coefficients for each box, which are used to establish balance equations for the studied variable, allowing the calculation of horizontal and vertical fluxes, as well as the respective rates in order to ascertain its production or consumption (Bordalo and Vieira, 2005). The box model uses the property of salinity as a conservative tracer (Libes, 2009), in order to calculate the required transfer coefficients. Thus, as the water circulation controls the physical distribution of dissolved and particulate matter, the abundance in each box can be used to calculate the flux and, simultaneously, sources and sinks, i.e., a non-conservative fluxes (e.g. chlorophyll *a* and bacteria), along the salinity gradient. This way, some light can be shed on the behavior patterns of these quantities within the estuarine boundaries.

The metabolic balance of an estuarine system is dependent on the primary production and community respiration. The primary production depends on physical (light availability, temperature), chemical (nutrients), and biological (phytoplankton biomass, species composition, size and structure, grazing) factors (e.g., Cloern, 1991; Calbet and Landry, 2004; Cermeño et al., 2006). The freshwater inflow may have a tremendous effect since it controls residence time, and the susceptibility of the ecosystems to algal blooms, with effects on the food web (Kimmerer, 2002). Tides also influence phytoplankton dynamics leading to a biomass

increase during neap tides, and a decrease during spring tides (Cloern, 1991; Azhikodan and Yokoyama, 2016), and gradient variations in the ebb and flood tides (Roegner, 1998). As the phytoplankton rapidly responds to changes in the environmental conditions, the dynamic structure of phytoplankton communities reflects the health of the aquatic ecosystems (Valdes-Weaver et al., 2006; Chaudhuri et al., 2012).

Bacteria also have a key role on the functioning of estuaries, since the community is crucial for the biogeochemical cycle of nutrients (Hitchcock and Mitrovic, 2015; Anderson, 2016) and the turnover of organic matter (Attermeyer et al., 2015). In some estuaries, bacteria tend to reach a state of trophodynamic equilibrium (Painchaud et al., 1996), and therefore the normal behavior of those quantities differ from the conservative pattern, i.e., numbers do not decrease linearly with increase of salinity (Mallin et al., 2000).

The aim of this study was to understand the spatial dynamics of chlorophyll *a* and bacteria along a temperate estuary during the ebb tide at different flow/seasonal regimes by means of a box model approach. The different regimes were assessed through seasonal neap surveys, in order to cover different runoff conditions. Furthermore, an additional spring tide survey was carried out during the summer, thus covering two different tidal regimes (neap and spring). This approach led to a better understanding of the spatial and temporal dynamics of plankton through modeling, contributing to improve the knowledge of the dynamics and transformation processes within the estuary, emerging as a valuable tool for managers.

4.2 Material and methods

4.2.1 The study area

The Lima estuary is located in NW Portugal (41.68º N; 8.84º W) (WGS84), and belongs to the Portuguese hydrographic region of the Minho and Lima (RH 1), according to the Water Framework Directive (INAG, 2009) (Figure 4.1). The estuary extends over 20 km covering an area of 10.4 km^2, and has a semidiurnal, mesotidal regime (0.2–3.9 m) (Vale and Dias, 2011). According to the morphology, bathymetry, salinity, and the presence/absence of saltmarshes, the estuary can be divided into three geomorphological zones: lower, middle, and upper estuary (Figure 4.1).

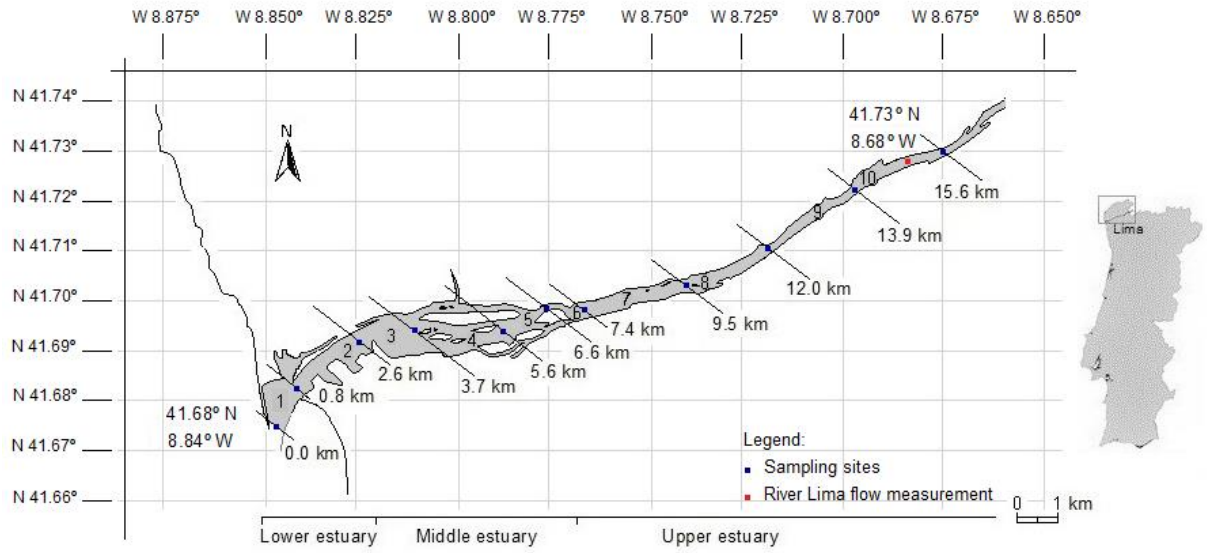

Figure 4.1 Map of the Lima estuary, sampling locations, and box boundaries used in the model.

The first zone, located within the first 2.5 km, is a navigation channel with walled banks, being narrow and deep (9 m), and characterized by the presence of seawater. The area is rather industrialized, with anthropogenic modifications such as the presence of a jetty at the river mouth deflecting the flow to the south, constant dredging operations, large shipyard, a commercial sea-port, a marina, and a fishing harbor (Azevedo et al., 2013). The middle estuary encompasses an area of saltmarshes with several sandy islands, and intertidal channels. Further upstream, the estuary continues as a narrow and shallow channel (0.5–1 m deep), remaining in a natural state with intertidal areas and undisturbed banks. This zone is characterized by low salinity water (oligohaline and freshwater), and is affected by agricultural run-off, domestic, and industrial wastewater discharges leading to the accretion of nutrients and other substances transported from urban, industrial, and agricultural areas into the estuary (Almeida et al., 2011).

4.2.2 Sampling

Seasonal surveys were carried out on the ebb of four neap tides (25 February 2014; 2 June 2014; 1 September 2014; and 11 November 2014), and on the ebb of a spring tide (10 September 2014). Each survey started 1:30 h before low tide slack water and lasted ca. 2:30 h to reduce the error due to the tide impact. In addition, sampling was performed from downstream (estuary mouth) to upstream (river), in order to follow the tide excursion, thus minimizing the hourly impact of the tide. Samples were collected from 11 locations along 15.6 km, corresponding to the navigable portions of the estuary, corresponding to 10 boxes (Figure 4.1). The boundaries for the boxes were chosen having into account geomorphological, geographic, and hydrological aspects of the Lima estuary. Particular attention was given to the

sediment type (lower and middle estuary), the presence of saltmarshes, sandy islands, and intertidal channels (middle estuary), and the presence of population clusters and/or constructed structures (lower, middle, and upper estuary). The smaller size of downstream boxes result from the presence of stronger vertical and longitudinal salinity gradient. Vertical profiles of salinity and temperature were obtained with a YSI 6920 CTD multiprobe, calibrated according to the instructions from the manufacturer. The data required for vertical profiles of chlorophyll *a* and bacteria, as well as for the physical-chemical characterization were achieved from the analytical determination in samples collected from the water column with a Van Dorn bottle (surface, middle water, and near bottom). The collected samples were kept refrigerated in an ice chest, transported to the laboratory, and processed within 8 hours.

4.2.3 Analytical procedures

For chlorophyll *a* determinations, 500 mL of water were filtered onto cellulose acetate 0.45 µm membranes (HA Millipore). Chlorophyll *a* was analytically determined by molecular absorption spectrophotometry after extraction using 90% acetone (Parsons et al., 1984) using the SCOR-UNESCO equations (1966). For total count of bacterial cells, water samples were fixed with formaldehyde (4% v/v). Subsamples (3 mL) were stained with 4',6'-diamidino-2-phenylindole (DAPI), and filtered onto black 0.2 µm Nucleopore polycarbonate membranes (Whatman, Little Chalfont, Buckinghamshire, UK) (Porter and Feig, 1980). The bacterial cells were counted directly with an epifluorescence microscope (Labphot, Nikon, Tokyo, Japan) equipped with a 100 W high-pressure mercury lamp and a specific filter sets (UV-2B), at 1,875x magnification. A total of 20 random microscope fields in different parts of the filter were counted in order to accumulate at least 300 cells per filter.

4.2.4 River flow

The river flow data were generated from weekly measurements carried out between January 2014 and February 2015, in the upper estuary (41.72º N; 8.68º W) (Figure 4.1). The velocity-area method was used (Herschy, 1995). The stream cross section was divided into numerous vertical subsections. In each subsection, the area was obtained by measuring its width and depth. The sum of areas yielded the cross-section of the river. The velocity was then measured using weighted floats (five to ten replicates), i.e., the velocity was equal to the distance between the cross-sections (bridge - 11.5 m) divided by the time taken by the float to cover this distance. The flow of the river was computed by multiplying the cross-section area of the river by the measured velocity.

4.2.5 The box model

From previous studies, it was found that, during summer, the Lima estuary tends to be vertically stratified to partially mixed in the lower and middle stretches, respectively (data not shown). Further upstream the estuary was found to be always vertically homogeneous in terms of salinity. A model with 10 boxes was adopted for this study, with two layered boxes in the first downstream sections, being the A-upper for the surface layer and B-lower for the deeper layer, and one-layer in the remaining boxes. The salinity used to define the stratification of the estuary water column, (i.e., the boundary between the upper and lower layers of the box) was 18 ppt corresponding to meso-polyhaline classification (see below). In the most upstream vertically stratified box, freshwater flowed downstream on the top layer, while in the bottom layer there was no movement of salt water to upstream. As such, it was assumed the existence of vertical advective and non-advective fluxes between the two layers, and that diffuse longitudinal (non-advective) processes between the boxes were insignificant, being therefore the contents of each box remains homogeneous longitudinally. The layout of the two layer boxes is presented in Figure 4.2B. Q_1 represents the flow rate ($m^3\ s^{-1}$) of the water with salinity S_1, out of the layer through the downstream boundary of the box; Q_2 is the flow rate ($m^3\ s^{-1}$) of water into the top layer with salinity S_2 through the upstream boundary; S_1 and S_2 are the mean salinities of the upper layer at the two box boundaries. Likewise, Q_3 represents the flow rate ($m^3\ s^{-1}$) of water with salinity S_3 into the box; Q_4 is the flow rate out ($m^3\ s^{-1}$) of the box of water with salinity S_4; S_3 and S_4 are the mean salinities of the lower layer at the two box boundaries. The non-advective (diffusive) vertical exchange coefficient between the two layers is represented by the letter E. S_U and S_L represent the mean salinities of the A-upper and B-lower layers, respectively. Q_V is the vertical flow rate ($m^3\ s^{-1}$) of water from the lower layer into the upper layer with salinity S_V, being S_V the average of the salinities S_U and S_L equation 4.1):

$$S_V = \frac{(S_U + S_L)}{2} \qquad (4.1)$$

Assuming the existence of steady state conditions and according to Figure 4.2B, the following salt equations conservation equations, could be obtained for the upper and lower layer, respectively, as described by Bordalo and Vieira (2005):

Upper layer $$Q_2S_2+Q_VS_V + E(S_L - S_U) = Q_1S_1 \qquad (4.2)$$

Lower layer $$Q_4S_4+Q_VS_V + E(S_L - S_U) = Q_3S_3 \qquad (4.3)$$

and, as result of the water mass balance:

$$Q_V = Q_1 - Q_2 = Q_3 - Q_4 \quad (4.4)$$

The calculation started at the most upstream box with two layers. In this box, the freshwater flux in the upper layer toward ocean (Q_2) equals the river discharge, with no flow toward upstream, resulting in a Q_4 equal to 0. Since river discharge and salinity data were known, it was possible to calculate Q_1 and Q_3 (Bordalo and Vieira, 2005). Then, the calculations were repeated (equations 4.2, 4.3 and 4.4) for the adjacent boxes consecutively toward the mouth of the estuary. Among the calculated values, those obtained for the exchange coefficients were essential to define the sources and sinks of both plankton parameters under study (chlorophyll *a* in mg m^{-3}; bacteria in cells mL^{-1}). To obtain the balance equations for each variable, salinity was replaced by the corresponding concentration values. The resulting balance equations for the A-upper and B-lower layers were, respectively:

Upper layer $$C_2Q_2 + Q_V\left(\frac{C_U + C_L}{2}\right) + E(C_L - C_U) - Q_1C_1 = P_U \quad (4.5)$$

Lower layer $$C_3Q_3 - Q_V\left(\frac{C_U + C_L}{2}\right) - E(C_L - C_U) - Q_4C_4 = P_L \quad (4.6)$$

P_U and P_L were the concentration fluxes into or out of the upper and lower layers of the box, respectively (in mg s^{-1}, cells s^{-1}). These values indicated the gain (+) or loss (-) of a quantity, therefore the presence of a net source or sink (i.e., non-conservative flux). The results obtained of P_U and P_L were divided by the respective layer volume, this procedure being necessary because the layers of each box had different volumes. The objective of this calculation was to obtain the rates of production or loss of chlorophyll *a* (mg m^{-3} s^{-1}), and bacteria (cells m^{-3} s^{-1}). For the remaining one-layer boxes, freshwater flow entering and leaving the box was represented by Q_B (m^3 s^{-1}) and Q_A (m^3 s^{-1}; Figure 4.2A), with salinity S_B and S_A, respectively. E corresponded to the non-advective (diffusive) horizontal exchange coefficient between adjacent boxes, and S_{in} and S_{out} the salinities inside and outside the box, being the equations for salt conservation and water mass balance:

$$Q_BS_B + E(S_{out} - S_{in}) = Q_AS_A \quad (4.7)$$

$$Q_B = Q_A \quad (4.8)$$

After the calculation of the exchange coefficients, the concentration flux of the studied variables into or out of the box (*P*; mg s^{-1} or cells s^{-1}) were obtained by replacing the salinity by its concentration (equation 4.9). The concentration flux was then divided by the box volume.

$$Q_B(C_B - C_A) + E(C_{out} - C_{in}) = P \qquad (4.9)$$

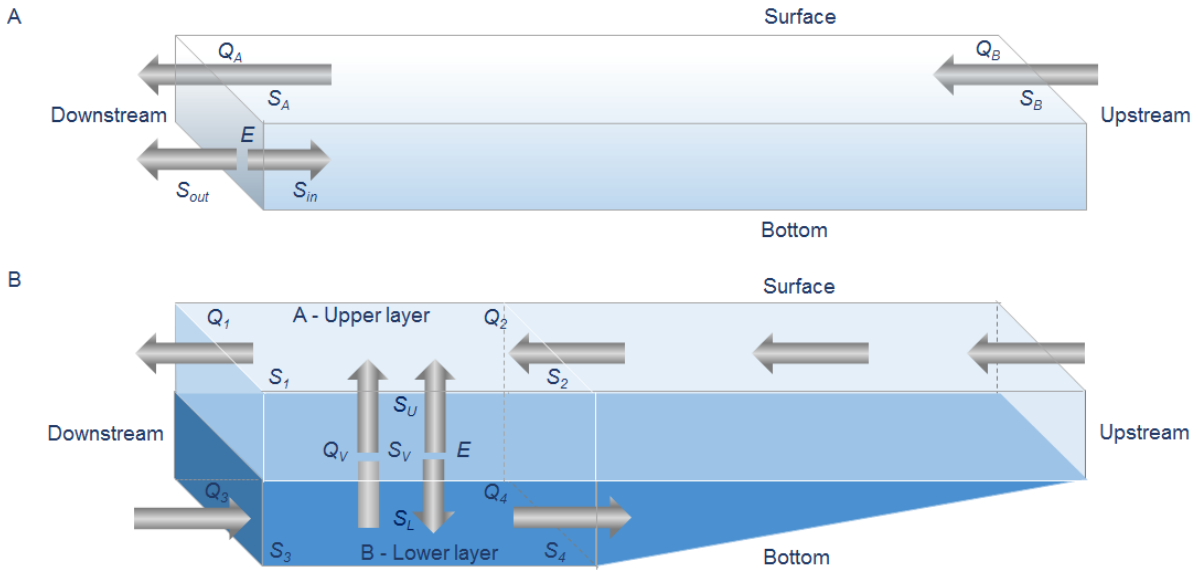

Figure 4.2 Layout of the box model used in this study: fluxes and exchange coefficients for the one layer box model (A), and two-layer box model (B). Q_x represents the flow rate ($m^3\ s^{-1}$) of the water with salinity S_x. S_U, S_L and S_V represents mean salinities. E corresponds to the non-advective exchange coefficient.

For the box model, the obtained salinity values at each sampling site were used to classify water masses according to the Venice System (1958) and the Water Framework Directive (EU, 2000), i.e., freshwater (salinity < 0.5), brackish water (0.5–30), and seawater or euhaline water (> 30), with brackish water subdivided into three groups, oligohaline (0.5–5), mesohaline (5–18) and polyhaline (18–30).

4.2.6 Data analysis

The generation time was calculated with the values obtained from the box model for the bacterial fluxes (cells $m^{-3}\ h^{-1}$), and the total cells counts (cells m^{-3}), whenever a positive bacterial flux was found, according to Robarts et al. (1996).

Vertical map profiles of salinity, chlorophyll *a* concentration and bacterial cells number along the main estuarine axis were created using Surfer 8.01 software (Golden Software Inc, Boulder, Colorado, USA), using kriging (linear variogram model) as the gridding method. *T*-tests were conducted to compare every two surveys, with a minimum $n = 21$ and a maximum $n = 28$. ANOVA was performed on the entire seasonal set, and also for the dataset from neap and spring summer tides. Statistical tests were performed using STATISTICA 13.0® software package.

4.3 Results

4.3.1 Bacteria and chlorophyll *a* profiles

The salinity profiles for the February and November surveys showed a well-mixed estuary in most of its extent, with polyhaline water confined to the first 2 km (Figure 4.3), owing to the inherent river discharge in winter and the fall (> 192 m^3 s^{-1}). The remaining surveys contours showed that a salt wedge (salinity above 30) introduced during the flood tide, remained within the estuary during low slack ebb tide. For June and September surveys, the salt wedge was located in the middle estuary around 3.5–4 km and 4–4.5 km, respectively. Nevertheless, the position of the boundary for 18 salinity was very similar for these surveys (4.5–5 km). The freshwater boundary reached km 3.5–4.5 during February and November, while not exceeding km 12 during June and September (Figure 4.3). Brackish water represented the largest water mass for winter and fall seasons and freshwater for the remaining ones.

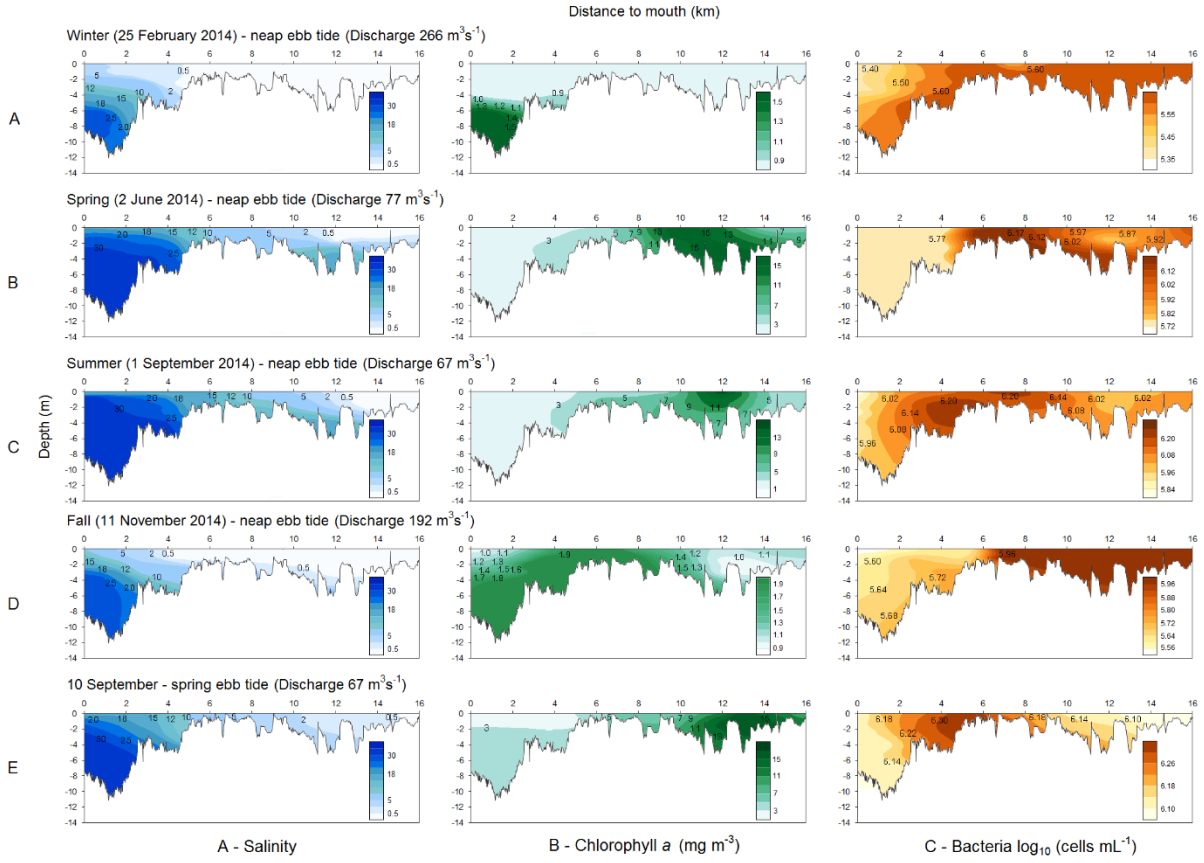

Figure 4.3 Longitudinal profile of salinity, chlorophyll *a* (mg m^{-3}), and bacteria (log_{10} cells mL^{-1}) during seasonal neap tide (A to D) and the spring tide (E) surveys.

Comparing neap and spring tides, the longitudinal salinity profiles showed that the salt wedge was located about 4–4.5 km from the river mouth during neap tide, while during the spring tide

survey it moved downstream to 2–2.5 km (Figure 4.3C and E). Inversely, the freshwater limit was found at 12–13 km upstream the river mouth in the neap survey, and pushed further upstream to 14.5–15.5 km during spring tide, being the discharge rate similar. The oligohaline water mass had an extension of ca. 7.5 km in the spring tide survey, but decreased to 2 km in the neap survey (Figure 4.3C and E).

The overall concentration of chlorophyll *a* in the estuary was significantly different for the different seasonal surveys (*t*-test $p < 0.05$), with the exception of summer and spring surveys (*t*-test $p > 0.05$). Chlorophyll *a* bloomed in spring and summer (15.69 and 16.50 mg m^{-3}, respectively) in the upper low salinity stretches of the estuary (Figure 4.3), being the lowest value recorded in the winter survey (0.57 mg m^{-3}) (Table 4.1).

For the summer neap and spring tidal surveys, the overall concentration of chlorophyll *a* in the estuary was not significantly different between the two tides (*t*-test $p > 0.05$). The spatial variation was also similar, with chlorophyll *a* increasing toward upstream, reaching the highest concentrations (~ 17.0 mg m^{-3}) within the upper estuary (Figure 4.3C and E). The lowest values were found during neap tide in seawater (0.96–2.92 mg m^{-3}), i.e. lower estuary (Table 4.1).

Table 4.1 Concentration ranges of chlorophyll *a* and bacteria in the Lima estuary.

		Salt water stretch				
Season	Concentration range	Freshwater	Oligohaline	Mesohaline	Polyhaline	Seawater
Winter	Chlorophyll *a* (mg m^{-3})	0.57 – 0.75	0.57 – 1.00	0.66 – 0.91	1.58	-
	Bacteria (log_{10} cells mL^{-1})	5.50 – 5.68	5.38 – 5.66	5.40 – 5.40	5.55	-
Spring	Chlorophyll *a* (mg m^{-3})	4.90 – 14.30	15.24 – 15.69	1.50 – 6.20	1.13 – 3.95	1.14 – 3.83
	Bacteria (log_{10} cells mL^{-1})	5.77 – 6.06	6.04 – 6.05	5.53 – 6.23	5.55 – 5.81	5.52 – 5.78
Summer	Chlorophyll *a* (mg m^{-3})	3.88 – 5.30	11.95 – 16.50	3.37 – 6.93	1.05 – 2.72	0.96 – 2.92
	Bacteria (log_{10} cells mL^{-1})	5.99 – 6.08	5.98	6.02 – 6.26	5.95 – 6.24	5.78 – 6.21
Fall	Chlorophyll *a* (mg m^{-3})	0.96 – 2.72	1.22 – 2.27	0.96 –1.67	1.30 – 1.92	-
	Bacteria (log_{10} cells mL^{-1})	5.63 – 6.00	5.57 – 5.69	5.53 – 5.73	5.62	-
Summer (spring tide)	Chlorophyll *a* (mg m^{-3})	9.78	7.13 – 17.04	1.86 – 7.02	1.50 – 4.16	3.37 – 4.87
	Bacteria (log_{10} cells mL^{-1})	6.06	6.09 – 6.16	6.23 – 6.35	6.08 – 6.26	6.07 – 6.13

Regardless of the tide and season, chlorophyll *a* biomass always peaked in the 0.5–5 oligohaline stretch of the estuary (Table 4.1 and Figure 4.4). During the summer neap tide survey, chlorophyll *a* decreased progressively from 6.96–0.96 mg m^{-3}, in the 5–35 salinity range, and salinity explained 61 % ($p < 0.0001$) of the chlorophyll *a* variability. In the summer spring tide survey, the concentration of chlorophyll *a* decreased in the salinity range 0–16, varying from 17.04–1.86 mg m^{-3}, increasing again (up to 4 mg m^{-3}) in higher salinities denoting the possible influence of the marine environment (Figure 4.4C). The observed patterns suggest

the presence of other processes besides dilution, with a chlorophyll *a* sink at the mesohaline range.

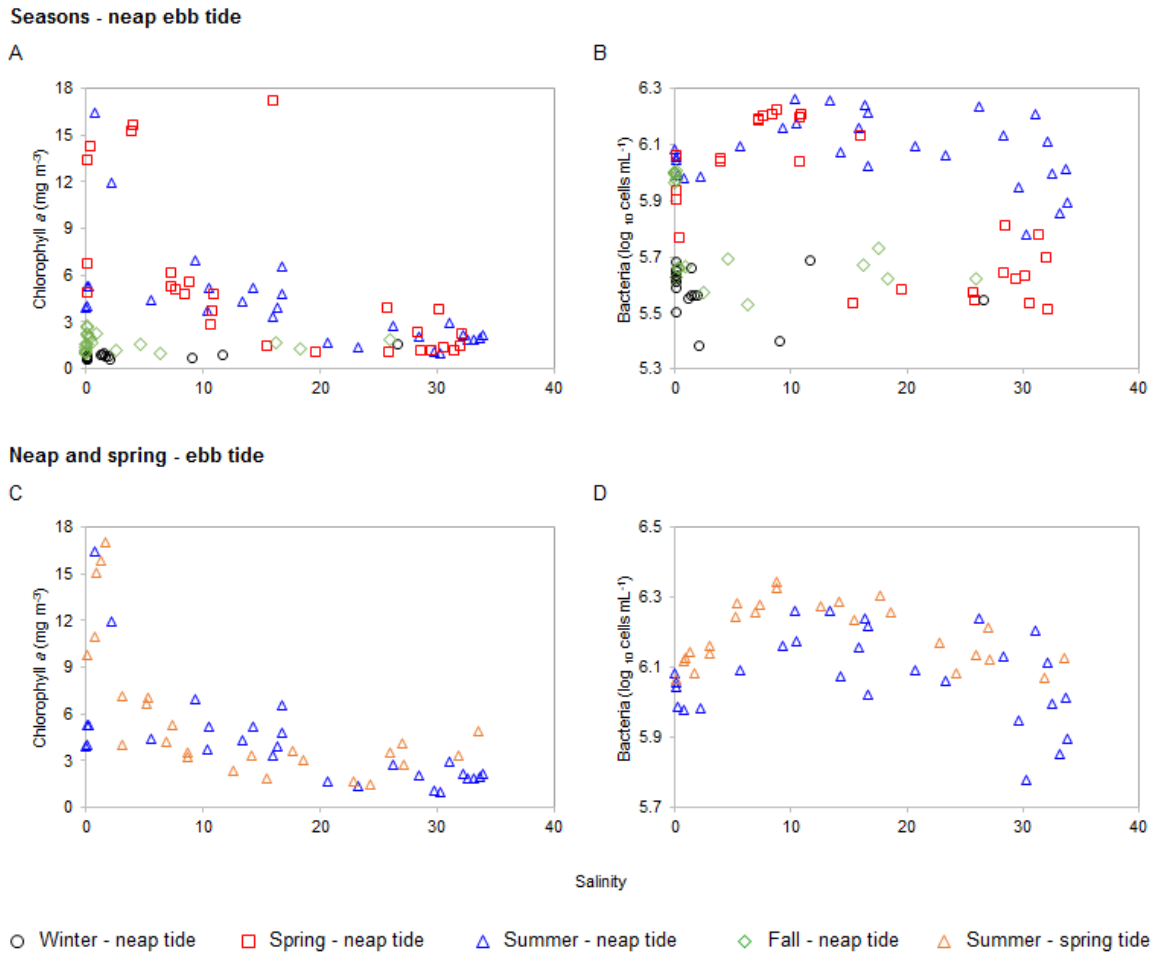

Figure 4.4 Relationship between chlorophyll *a*, and bacteria versus the conservative tracer salinity for seasonal neap tides (A and B), and a summer neap and spring tides (C and D) in the Lima estuary.

Bacteria presented a clear seasonal behavior. During the warmest period of the year, the highest concentrations were found in the middle estuary, within the mesohaline stretch, downstream the chlorophyll *a* maxima (1.7–1.8 × 10^6 cells mL^{-1}, respectively during spring and summer). In both surveys, bacteria tended to increase from freshwater to the mesohaline interval (salinity 18), then decreased toward seawater (Figure 4.4B), suggesting the existence of different bacterial communities for each stretch of the estuary. In the remaining surveys, higher bacterial numbers were found in freshwater (4.8 x 10^5 cells mL^{-1} for the winter survey, and 1.0 × 10^6 cells mL^{-1} for the fall survey) (Figure 4.4B). Winter survey presented decreased bacterial abundance (*t*-test $p < 0.0001$), independently of the salinity range, with the lowest value being found in seawater by the mouth of the estuary (0.25x 10^6 cells mL^{-1}).

Similar bacterial longitudinal distribution profiles were observed between neap and spring tides summer surveys (Figure 4.3 and 4.4). The highest concentrations were always found in the

middle estuary (2.2 x 10^6 cells mL^{-1} during the spring tide). At the seawater end-member, the values were always below 1.6 x 10^6 cells mL^{-1}, and in the freshwater end-member below 1.2 x 10^6 cells mL^{-1}. It was found that when tides were compared, the spring tide fostered higher bacterial abundance (*t*-test $p < 0.0005$) Regardless of the tide, bacteria tended to increase in the salinity range 8–15 (neap tide), and 9–12 (spring tide), further decreasing in a monotonically fashion toward seawater (Figure 4.4). Again, this behavior suggested the existence of different bacteria communities adapted to each stretch of estuary with salinity ca. 10 acting as a threshold.

Information on additional environmental variables measured during the seasonal surveys can be found as supplementary material (Table S4.1–S4.3, Figure S4.1).

4.3.2 Box model

The river flows measured for the Lima estuary were 266 $m^3 s^{-1}$ (winter), 77 $m^3 s^{-1}$ (spring), 67 $m^3 s^{-1}$ (summer), and 192 $m^3 s^{-1}$ (fall), and were used to feed the box model. Vertical salinity stratification, with an upper layer < 18 and a bottom layer within the polyhaline/seawater ranges, was found in the first four boxes (0 to 5.6 km) in spring and summer, whereas in fall and winter the vertical discontinuity was confined to the first two boxes within the lower estuary. As expected, vertical stratification was also observed during the spring tide survey.

In the stratified section of the estuary, the fluxes of chlorophyll *a* were always negative in the lower layer boxes (Figure 4.5), i.e., the consumption/loss of chlorophyll *a* surpassed production. On the other hand, chlorophyll *a* production was found in the upper boxes reaching 2.118 mg $m^{-3} h^{-1}$ (Figure 4.5E, box 2A) during spring tide survey performed during the summer. For the ebb tide surveys, chlorophyll *a* production was associated with the lower salinity upper layers, regardless of the seasons, reaching a maximum value of 2.750 mg $m^{-3} h^{-1}$ (Figure 4.5B, box 3A) during spring. In the winter and fall, the box 2A showed the higher chlorophyll *a* production within the estuary, with 0.109 mg $m^{-3} h^{-1}$ and 0.274 mg $m^{-3} h^{-1}$, respectively. In stratified conditions, upper layer fluxes were always positive showing a net biomass growth.

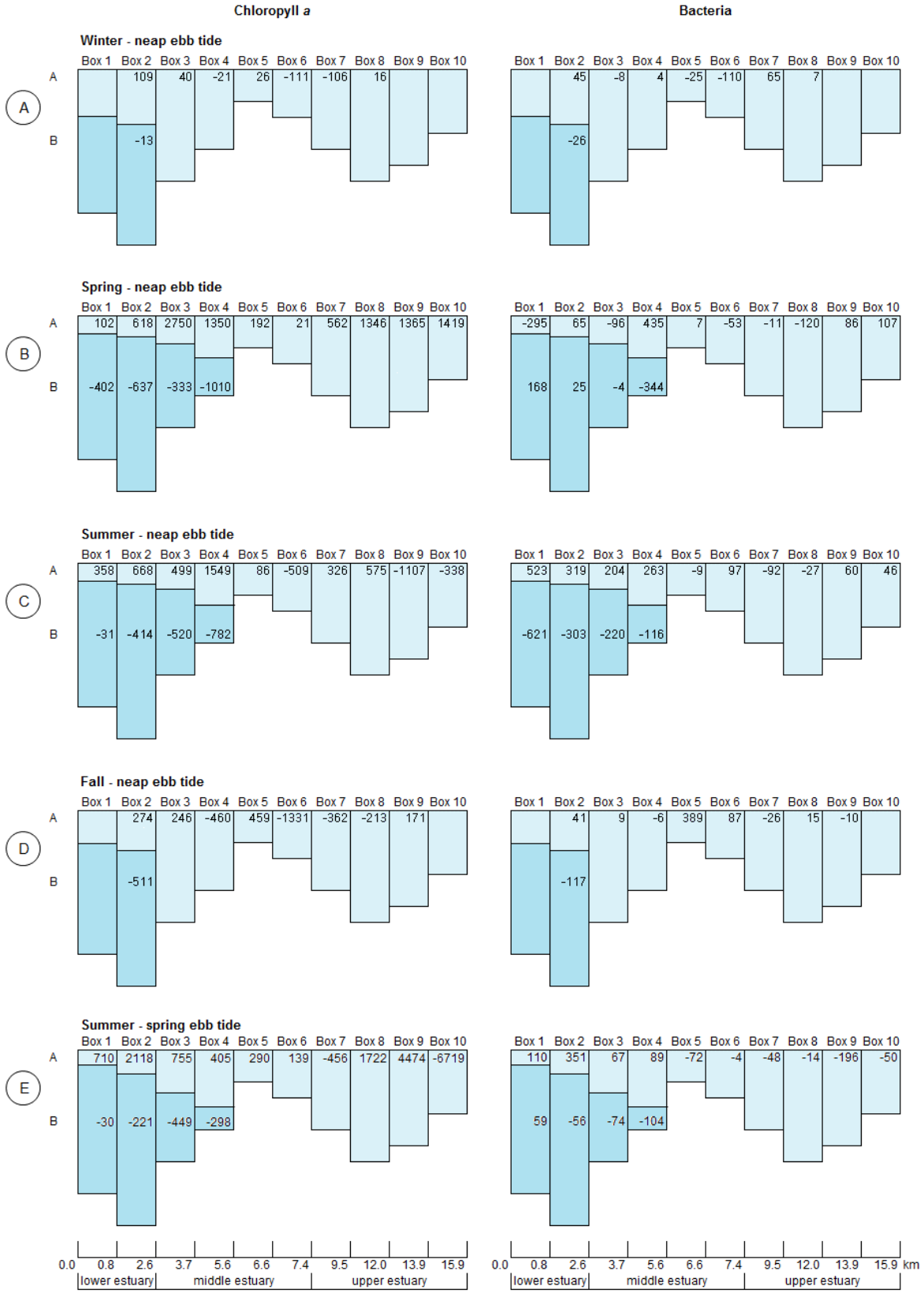

Figure 4.5 Model box results for chlorophyll *a* (10^{-3} mg m^{-3} h^{-1}) and bacteria (10^{9} cells m^{-3} h^{-1}), rates of production (positive values) and loss (negative values) for the seasonal neap tides (A – D), and the summer spring tide (E). A – upper layer corresponding to salinity lower than 18 and B – lower layer corresponding to salinity higher than 18. The vertical axis represents the relative depth of each box.

A similar behavior was observed for bacterial fluxes. Bacteria removal processes were usually dominant within polyhaline/seawater boxes. However, the positive fluxes in the box 1B during spring neap tide and summer spring tide, suggested a possible seawater input of bacteria into the estuary on these occasions. With the exception of winter, the lower layer of the stratified zone showed the highest bacteria removal, a process boosted in summer (6.21 x 10^{11} cells m^{-3} h^{-1}; Figure 4.5C, box 1B). Regarding the upper layer boxes, bacterial fluxes were positive, except in the box 1A and 3A (2.9 x 10^{11} cells m^{-3} h^{-1} and 9.6 x 10^{10} cells m^{-3} h^{-1}, respectively) during spring neap tide, indicating biomass growth or production downstream, in accordance with chlorophyll *a.*

In most of the middle and in the upper estuary, salinities were always lower than 18, translating into a single layer box model. At this section of the estuary, fluxes of chlorophyll *a* fluctuated between positive and negative, with exception of the seasonal spring survey when production was observed throughout (Figure 4.5B, boxes 3–10, and Figure S4.1). The highest chlorophyll *a* production occurred during the warmer months as expected. With the exception of the summer surveys, the river water seemed to be a source of chlorophyll *a* biomass, since the upstream boxes (corresponding to freshwater) had positive fluxes for chlorophyll *a*. Production of chlorophyll *a* was also present in the middle estuary. The comparison of the box models obtained for the two summer tidal surveys suggested a slight spatial dislocation of the boxes toward upstream, i.e., the box (n) in the neap tide seemed to be placed at the box (n + 1) of the spring tide, especially in the upper estuary. The higher chlorophyll *a* production reached 4.474 mg m^{-3} h^{-1} (box 9, Figure 4.5E) during the spring tide. In regards to consumption, the higher values were 1.107 mg m^{-3} h^{-1} (box 9, Figure 4.5C), and 6.719 mg m^{-3} h^{-1} (box 10, Figure 4.5E), for neap and spring tides, respectively.

The bacterial behavior within the non-stratified stretch of estuary was also irregular, although freshwater appeared to introduce bacteria into the estuary as in the case of chlorophyll *a*, with exception of the fall. The highest bacterial removal was found in winter (Figure 4.5A, box 6, 1.10 x 10^{11} cells m^{-3} h^{-1}), and highest bacterial growth in the fall (Figure 4.5D, box 5, 3.89 x 10^{11} cells m^{-3} h^{-1}), within the middle estuary. Surprisingly, during the summer spring tide, all bacterial fluxes were negative, denoting the dominance of removal processes.

During the warmest months of the year, bacteria grew faster (Table 4.2), with higher values within the lower and middle estuarine stretches, during the neap tide surveys, meaning that the population had the ability to potentially double several times over a single tidal cycle (12 h). On the other hand, the higher generation times were found during the coldest months.

Table 4.2 Bacteria generation times, calculated for boxes with growth, assuming the linearity of growth over 24 h.

		Generation time (h)				
		Winter	Spring	Summer		Fall
Estuary stretch	Box	Neap tide	Neap tide	Neap tide	Spring tide	Neap tide
Lower estuary	box 1A	-	-	1.55	12.32	-
	box 1B	-	2.82	-	22.13	-
	box 2A	6.95	5.97	3.48	4.56	10.16
	box 2B	-	16.52	-		-
Middle estuary	box 3	-	-	-	-	53.56
	box 3A	-	-	6.81	27.43	-
	Box 4	101	-	-		-
	box 4A	-	2.01	5.90	22.40	-
	box 5	-	211	-	-	1.80
	box 6	-	-	16.47	-	11.23
Upper estuary	box 7	6.19	-	-	-	-
	Box 8	64.55	-	-	-	64.29
	box 9	-	10.40	17.41	-	-
	box 10	-	10.80	24.86	-	-

4.4 Discussion

4.4.1 Freshwater inflow

The freshwater inflow was a major driving force for water circulation in the Lima estuary, coming essentially from the discharges of upstream dams, as reported for other temperate estuaries (e.g., Hofmeister et al., 2017). Therefore, the inflow together with salinity was used to calculate the required coefficients for the box model. A remarked seasonality occurred with the highest values occurring in winter and the lowest in summer. When the discharge decreased, vertical stratification of the water column was established and the tidal influence dominated. This phenomenon occurred due to two major factors: the tidal forces were insufficient to overcome stratification, and the runoff did not eliminate the salt wedge resulting from the previous flood tide.

4.4.2 Chlorophyll *a* and bacteria dynamics

Chlorophyll *a* values measured in the Lima estuary (0.96–17.04 mg m^{-3}) were within the range found in other temperate systems (Gonçalves et al., 2015; Iriarte et al., 2015; Carbone et al., 2016). During the spring and summer seasons, chlorophyll *a* concentrations were substantially

higher than during the winter and fall (Table 4.1). Several factors may explain the seasonal increasing of values, namely higher temperatures (Winder and Cloern, 2010; Buchan et al., 2014), greater light availability (Winder and Cloern, 2010; Barrio et al., 2014; Buchan et al., 2014; Lu and Gan, 2015), and hydrodynamic conditions favorable to the existence of stratification/stabilization of water column, and longer water residence times (Lu and Gan, 2015). In the spring and summer seasons, independently of the tide, chlorophyll *a* peaked in the upstream oligohaline area of the estuary (salinity 0.5–5), whereas in the fall it peaked in freshwater, and during winter in the downstream polyhaline area. The observed patterns during the warmest period of the year at the interface between freshwater and saltwater, were also reported previously (Azhikodan and Yokoyama, 2016), as well as for the fall (Bukaveckas et al., 2011). Moreover, chlorophyll *a* peaks may also occur in higher salinity areas (Lu and Gan, 2015; Fisher et al., 1988). Chlorophyll *a* peaks spatially when growth rates increase and/or loss rates decrease. The latter include retention mechanisms, since the entrainment of exogenous chlorophyll *a* foment their accumulation, even in low growth rates (Bukaveckas et al. 2011). With the exception of winter, the upper part of the estuary, surrounded by intensive agriculture (irrigated maize), seemed to behave as a source of chlorophyll *a*, as well as of nitrogen in the water column (Tables S4.1–S4.3). The same pattern was found in other estuaries (Desmit et al., 2015; Wolanski and Elliott, 2016). During winter, chlorophyll *a* showed its maximum within the estuarine area with the highest suspended solids (Figure S4.1), and retention has been suggested as a mechanism to explain the abundance in less light availability locations (Bukaveckas et al. 2011).

Bacterial concentrations (5.38–6.26 $\log_{10}$ cells mL^{-1}) were also similar to levels found in other temperate estuaries (Selje and Simon, 2003; Bordalo and Vieira, 2005). Bacterial abundance followed the expected seasonal pattern, with higher values in summer and spring, and minima in winter and fall (Bacelar-Nicolau et al, 2003). The distribution of microorganisms within an estuary depends of the interaction of various dynamic processes, namely, growth, mortality, predation, and physical dispersion (Painchaud et al., 1996). For estuaries with stratified waters, the variation in the hydrodynamic conditions can lead to important consequences in the control of the structure of microbial community and its activity. Salinity is one of the estuarine properties that can have relevance in the control of the communities arriving with the inflow of river water. This evidence appears to control the microbial abundance as a consequence of the dilution and "bactericidal" activity of salinity (Hobbie, 1988; Munro et al., 1989) in the polyhaline/euhaline range, and in the increased survival in the mesohaline salinity range (Bordalo, 2003). Moreover, salinity not only controls the abundance (Bunse et al., 2016) and activity of microorganisms, but also its community structure (Campbell and Kirchman, 2013; Xia et al., 2015). Previous studies suggested that salinity was determinant for bacterial communities, and seasonal changes in bacterial communities in both marine and brackish

environments (Herlemann et al., 2016). In this study, the behavioral trend presented by the chlorophyll *a* and bacteria within the estuarine salinity range and seasons was variable (Figure 4.4). Therefore, in this partially stratified system, the knowledge of the relationship between these variables and the salinity is insufficient to understand their behavior per se.

Along the estuary, bacteria presented two different behavioral trends, one for the warmest period of the year (spring and summer) and another for the coldest seasons (Figure 4.4). Although, the microbial amount did not always decrease toward downstream, as reported in previous studies (e.g., Painchaud et al., 1996), during fall and winter the highest values were indeed found in the freshwater stretch. During spring and summer, increased bacterial cell counts were observed in the middle estuary, a mesohaline area in agreement with Ducklow et al. (1999), in an intermediate zone of the estuary dominated by saltmarsh islands and shallow channels. The accretion of dissolved organic carbon and/or bacterial biomass from terrestrial inflow might help to explain the observed pattern (Hitchcock and Mitrovic, 2015). Since in the Lima estuary a vertical stratification is always present (although varying in extent) in the downstream stretch, limited fluxes of advection and convection of microorganisms and substrate between the upper and lower layers may occur. Therefore, the substrate supply for bacteria and chlorophyll *a*, including light, can become priority factors in the stratified waters, due to nutrient reduction and light unavailability (Bordalo and Vieira, 2005).

4.4.3 Box model approach

Here, we constructed a box model based on the conservative properties of salinity and river flow to better understand the processes controlling the chlorophyll *a* and bacteria distribution in the estuary. This model is a simple and straightforward tool (does not require complex calculations and computer power), it is easy to apply and interpret, being therefore accessible for non-scientific end-users (e.g., managers). Moreover, since its development by Pritchard (1969), it has been successfully applied to other estuaries (e.g., Painchaud et al., 1996; Bordalo and Vieira, 2005; Testa and Kemp, 2008). However, the simplification of a complex system implies some compromises in processes related with phytoplankton (e.g., primary production, predation, mortality), and bacteria (e.g., lateral inputs due to wastewater, death or predation). Therefore, it must be applied with caution.

For all surveys, according to the model (Figure 4.5), the sea end-member did not act as a source of chlorophyll *a*, given that the fluxes were always negative for salinities higher than 18. Indeed, chlorophyll *a* values were overall lower in higher salinities (Figure 4.4). In general, the bacterial fluxes for salinity above 18 were also negative, probably due to the dominance of some physical control, such as sedimentation, in the lower end of the estuary. In the summer neap tide, the loss of bacteria in the lower boxes was more pronounced in the lower estuary,

while in the following spring tide, the trend was inverse, with a positive flux in box 1B. This trend was mimicked during the neap tide of the spring season when net bacterial growth occurred. Therefore, with the exception of the spring neap and summer spring tidal surveys, coastal waters did not appear to be a source of bacteria to the Lima estuary.

As a general picture, the upper limit of polyhaline/seawater appeared to regulate the coupling of chlorophyll *a* and bacteria regardless of the tide. Indeed, similar trends were found for chlorophyll *a* and bacterial fluxes in the lower, and part of the middle, estuary; with net growth (positive values) in the upper boxes and consumption (negative values) in the bottom boxes found.

Neap tide chlorophyll *a* production fluxes presented in both mesohaline and freshwater zones were higher in spring compared to summer, as reported for other estuaries (Martinez et al., 2011; Lyngsgaard et al., 2017). In the middle estuary, the spring higher chlorophyll *a* production, despite higher solar radiation in the summer, can be explained by the greater availability of nutrients brought by winter mixing (Martinez et al., 2011). Comparing the summer spring/neap tides chlorophyll *a* behavior, a similar spatial trend was found, peaking in the mesohaline as well as in the low salinity uppermost stretch. The larger tidal amplitude during the spring tide event favored the availability of nutrients due to the potential increase of mixing, flooding, and further washout of tidal flats and saltmarshes within the estuary. Some authors (e.g., Van Alstyne et al., 2015) also noted a dichotomy between neap-spring tides.

During fall and winter, the chlorophyll *a* production peaked in the upper boxes of the lower estuary, corresponding to a higher temperature stretch (Figure S4.1), and higher river flow pushing the bloom toward sea end-member (Lu and Gan, 2015). Nevertheless, the positive fluxes were rather modest when compared to the warmest period of the year.

The seasonal bacteria production during neap tides occurred usually in the upper layer boxes when stratification was present (positive fluxes), except for the two down-most boxes during spring. Stratification, both vertical and horizontal, appeared to foster the co-existence of two bacterial populations during the warmest months, one associated to higher salinity, and another adapted to salinity below 10. Freshwater seemed to be a source of bacteria except in the fall, since bacterial growth was noticed in the uppermost boxes. Indeed, freshwater inflow plays a key role in the delivery of organic matter and nutrients to estuaries (Hitchcock and Mitrovic, 2015; Liu and Chan, 2016), acting as a carrier for chlorophyll *a* and bacteria. For salinities higher than 18, bacterial fluxes were negative. The resuspension of particles with the saline intrusion, followed by sedimentation in the slack tide period, could trap bacteria in sediments (Kara and Shade, 2009).

During the summer neap tide, bacteria growth was higher in the lower stretches, with fast generation times, increasing monotonically toward the upper part of the estuary (Table 4.2). A similar trend was found during the following spring tide, but generation times were higher,

probably as a result of the synergistic interaction between freshwater and tidal flushing (Wan et al., 2013). During the neap tide, the utilization of terrestrial dissolved organic carbon in the upper reaches of the estuary (Ducklow et al., 1999) may have played a pivotal role, as well as the higher values of total suspended solids (Figure S4.1), resulting in a larger amount of available, particle-attached bacteria (Vallières et al., 2008) that grow faster than free-living bacteria (Campbell and Kirchman, 2013). Given that generation times are much lower than residence time of ca. 7 days for the Lima estuary (Saraiva et al., 2007), an estuarine community can develop in intermediate salinities in addition to the presence of freshwater and marine populations (Crump et al., 2004).

Except for winter, bacteria growth peaked into estuary mid-stretch, as observed in Chesapeake Bay and in the Delaware estuary (Ducklow et al., 1999), in an area of the estuary with saltmarsh islands and shallow channels containing high concentrations of particulate matter, which can provide substrates for microbial colonization and growth (Vallières et al., 2008). The maximum growth of bacteria in the freshwater verified during the winter, may be related to a greater riverine nutrients input due to the increase of the river flow. In agreement with other studies (e.g., Crump et al., 2004), the bacterial production presented a clear seasonal pattern, being higher in summer, lower in winter, and intermediate in spring and fall.

Positive values of chlorophyll *a* production were followed by bacterial growth (Figure 4.5) within the lower estuary, except during spring. Bacterial biomass and production often presented covariance with phytoplankton (primary production or chlorophyll *a*), as reported by Hoch and Kirchman (1993). However, the uncoupling of bacterial production to primary chlorophyll *a* production is not uncommon in estuaries, especially when allochthonous carbon inputs are high (Hitchcock and Mitrovic, 2015). The organic nutrition improvement factor due to the phytoplankton could be annulled, either by the release of compounds with anti-bacterial activity (Hulot et al., 2001; Bordalo and Vieira, 2005), or by the competition for the same substrate resulting in an effective control of bacterial dynamics (Martinussen and Thingstad, 1987; Buchan et al., 2014; Bunse et al., 2016).

4.5 Conclusions

The maximum concentrations of chlorophyll *a* were found in the upper oligohaline area regardless of the tide for all seasons, except during the winter, when the peak moved to the downstream polyhaline area. A net loss of chlorophyll *a* was always found at salinities above 18. For all surveys, the higher bacterial amount was found in the middle estuary, an area with saltmarsh islands, but also in the upper estuary during the coldest period of the year. Freshwater appeared to be the main source of bacteria during neap tides, with the exception of fall, whereas coastal waters have assumed this role during the summer spring tide and for

the fall neap tide. Bacterial growth was higher during the warmest months of the year, with faster generation times in the lower stretches, increasing monotonically toward the upper estuary, being the highest at the spring tide. The coupling between chlorophyll *a* and bacteria was spatially limited by water column stratification, while upstream, the plankton responded differently to environmental conditions. The results showed the coupling between estuarine hydrodynamics and bacterial dynamics, thus explaining the differences between chlorophyll *a* and bacteria behavior in estuaries with seasonal variability and noticeable neap and spring tides. A future approach should aim at understanding the spatial and temporal salt wedge structure as a result of tidal dynamics (flood and ebb tides), coupled with the influence of different inflow regimes (seasonality), toward the evaluation of the response of the entire estuarine system to the geomorphologic and river discharge variations imposed by human activity.

4.6 SUPPLEMENTARY INFORMATION

Additional physical-chemical analyses were performed for the water samples collected in the Lima estuary. For the determination of total suspended solids (TSS), the water samples were filtered through pre-combusted glass fiber filters (GF/F Whatman), and dried at 105 °C (APHA, 1992). The dissolved orthophosphate, nitrite, ammonium and silicate determinations were performed according the methods described by Koroleff (Grasshoff et al., 1983). Orthophosphate ions react with an acid solution containing molybdate and antimony ions to form a phosphomolybdate antimony complex, followed by reduction of the latter with ascorbic acid to form a blue molybdenum complex. For dissolved silica quantification, an acidic solution of ammonium molybdate was added to the sample to produce silicomolybdic acid which is then reduced to silicomolybdous acid (a blue compound) using ascorbic acid. Ammonia, in moderately alkaline solutions, reacts with the hypochlorite to form monochloramine, which in the presence of a catalyst (nitroprusside), phenol, and excess hypochlorite gives rise to an intense blue complex (indophenol blue). The nitrite was determined by diazotizing nitrite with sulfanilamide and coupling it with N-(1-napthyl)-ethylenediamine hydrochloride to form a highly coloured azo dye. The concentration of nitrate was obtained by the method described by Jones (1984), and adapted by Joye and Chambers (1993), which consists of the nitrite determination procedure, after the reduction of nitrate to nitrite using spongy cadmium (total concentration of NO_x). The nitrate concentration was obtained subtracting the nitrite from the total concentration of NO_x obtained. After color development, all nutrients were determined by molecular absorption spectrophotometry. Determination of total dissolved carbon (TDC), dissolved organic carbon (DOC), and total dissolved nitrogen (TDN) was performed by high-temperature catalytic oxidation with a TOC-VCSN analyzer (Shimadzu Instruments), according to

Magalhães et al. (2008). Briefly, TDC was measured by high temperature catalytic oxidation followed by nondispersive infrared detection of CO_2. For DIC determination, samples were automatically acidified (1.5% HCl 2 M), and sparged with carrier gas (purified air) to convert only the inorganic carbon to CO_2. DOC was determined by the difference between TDC and DIC. TDN was thermally decomposed in a combustion tube and the resulting nitric oxide detected by chemiluminescence. All analyzes were performed in triplicate.

Table S4.1 Mean concentrations ± SE for key environmental parameters measured at the surface of the sampling sites: Secchi disc (SD) – m (in bold – bottom depth); temperature – ^{o}C; salinity; dissolved oxygen (DO) – mg O_2 L^{-1}; pH – Sørensen scale; NO_3^-, NO_2^-, NH_4^+, PO_4^{3-}, N:P, and Si – μM; chlorophyll *a* (CHL *a*) – mg m^{-3}; total cell counts (TCC) – $\log_{10}$ cells mL^{-1}. In brackets – minimum and maximum values.

Site	SD	T	Salinity	DO	pH	NO_3^-	NO_2^-	NH_4^+	PO_4^{3-}	N:P	Si	CHL *a*	TCC
1	2.48 ± 0.33 (1.30–3.30)	15.47 ± 1.58 (11.06–20.56)	18.29 ± 5.89 (1.99–30.30)	8.80 ± 0.60 (7.69–10.89)	7.75 ± 0.09 (7.51–7.96)	19.97 ± 7.09 (9.12–46.75)	0.189 ± 0.043 (0.108–0.295)	1.517 ± 0.355 (0.818–2.800)	0.384 ± 0.065 (0.211–0.562)	60 ± 17 (25–107)	47.01 ± 16.59 (15.29–95.67)	1.04 ± 0.16 (0.57–1.50)	5.72 ± 0.12 (5.38–6.08)
2	2.46 ± 0.39 (1.30–3.30)	15.65 ± 1.57 (11.06–20.64)	17.32 ± 5.53 (1.99–29.70)	8.87 ± 0.58 (7.61–10.89)	7.81 ± 0.07 (7.57–7.96)	22.42 ± 6.31 (13.00–46.75)	0.202 ± 0.046 (0.110–0.319)	2.000 ± 0.557 (0.850–3.877)	0.409 ± 0.076 (0.226–0.639)	66 ± 15 (27–107)	50.49 ± 15.19 (20.41–95.67)	1.08 ± 0.18 (0.57–1.69)	5.71 ± 0.15 (5.38–6.17)
3	2.32 ± 0.46 (1.10–3.80)	16.13 ± 1.74 (10.93–21.09)	12.49 ± 4.44 (1.59–23.30)	9.14 ± 0.63 (8.14–11.26)	7.84 ± 0.11 (7.44–8.12)	25.91 ± 5.15 (16.75–45.71)	0.162 ± 0.036 (0.062–0.245)	1.576 ± 0.335 (0.839–2.554)	0.355 ± 0.049 (0.243–0.477)	81 ± 13 (48–103)	64.19 ± 11.75 (35.71–97.58)	1.29 ± 0.17 (0.81–1.86)	5.80 ± 0.14 (5.56–6.23)
4	2.12 ± 0.40 (1.10–3.10)	16.41 ± 1.88 (10.76–21.28)	10.05 ± 4.00 (0.40–20.70)	9.37 ± 0.57 (8.25–11.18)	7.85 ± 0.12 (7.45–8.21)	26.56 ± 5.82 (9.46–45.78)	0.146 ± 0.032 (0.038–0.222)	1.746 ± 0.854 (0.472–5.115)	0.320 ± 0.049 (0.205–0.455)	96 ± 17 (32–128)	69.79 ± 10.52 (41.35–100.22)	1.63 ± 0.23 (0.92–2.38)	5.82 ± 0.15 (5.53–6.27)
5	1.58 ± 0.34 (**1.00**–2.90)	16.63 ± 2.00 (10.52–21.33)	7.08 ± 3.09 (0.05–15.90)	9.38 ± 0.60 (8.15–11.31)	7.79 ± 0.12 (7.46–8.12)	25.81 ± 3.56 (15.71–35.61)	0.118 ± 0.024 (0.046–0.182)	1.176 ± 0.614 (0.248–3.563)	0.287 ± 0.048 (0.138–0.425)	117 ± 38 (60–262)	78.01 ± 7.84 (53.31–100.59)	2.52 ± 0.52 (0.66–3.54)	5.96 ± 0.14 (5.63–6.33)
6	1.60 ± 0.39 (**0.80**–3.10)	16.79 ± 2.05 (10.50–21.42)	5.60 ± 2.53 (0.03–13.40)	9.39 ± 0.58 (8.23–11.23)	7.52 ± 0.14 (7.09–7.90)	35.72 ± 4.16 (27.63–51.37)	0.139 ± 0.024 (0.046–0.174)	0.565 ± 0.167 (0.141–0.968)	0.238 ± 0.062 (0.074–0.439)	208 ± 70 (102–483)	82.90 ± 6.91 (59.60–101.79)	3.39 ± 0.77 (0.75–5.06)	6.06 ± 0.12 (5.61–6.26)
7	1.30 ± 0.08 (**1.10**–**1.50**)	16.99 ± 2.11 (10.54–21.41)	4.56 ± 2.01 (0.02–10.30)	9.58 ± 0.57 (8.19–11.34)	7.30 ± 0.14 (6.97–7.67)	30.98 ± 4.55 (19.93–47.56)	0.108 ± 0.021 (0.038–0.158)	0.536 ± 0.206 (0.018–1.243)	0.249 ± 0.060 (0.106–0.462)	152 ± 36 (71–283)	83.76 ± 5.23 (66.80–99.55)	3.79 ± 1.19 (0.74–6.67)	6.04 ± 0.14 (5.50–6.26)
8	1.18 ± 0.17 (**0.60**–**1.60**)	17.08 ± 2.15 (10.50–21.10)	2.50 ± 1.10 (0.00–5.60)	9.76 ± 0.59 (8.35–11.63)	7.39 ± 0.15 (6.90–7.71)	33.98 ± 4.64 (24.87–49.91)	0.126 ± 0.012 (0.094–0.157)	0.916 ± 0.355 (0.077–2.047)	0.253 ± 0.058 (0.150–0.477)	154 ± 29 (108–265)	91.67 ± 4.48 (80.57–105.41)	5.13 ± 2.63 (0.59–15.24)	5.97 ± 0.10 (5.59–6.14)
9	2.02 ± 0.25 (**1.30**–2.70)	17.13 ± 2.19 (10.58–22.20)	0.30 ± 0.16 (0.00–0.70)	9.72 ± 0.52 (8.65–11.63)	7.29 ± 0.24 (6.68–8.05)	41.05 ± 4.11 (26.51–50.60)	0.116 ± 0.020 (0.038–0.149)	0.867 ± 0.343 (0.306–2.068)	0.234 ± 0.055 (0.106–0.431)	227 ± 70 (105–499)	97.89 ± 5.73 (79.68–115.55)	8.53 ± 3.25 (0.66–16.50	5.93 ± 0.08 (5.63–6.12)
10	1.11 ± 0.348 (**0.35**–**2.50**)	19.60 ± 2.11 (13.74–23.30)	0.46 ± 0.38 (0.00–1.60)	9.27 ± 0.43 (8.21–10.07)	7.17 ± 0.21 (6.66–7.51)	41.61 ± 6.01 (24.35–51.83)	0.122 ± 0.031 (0.046–0.189)	1.912 ± 0.462 (0.940–3.164)	0.212 ± 0.031 (0.138–0.286)	227 ± 59 (114–391)	99.36 ± 6.63 (87.64–118.35)	7.11 ± 3.43 (1.22–17.04)	5.99 ± 0.04 (5.90–6.09)
11	0.38 ± 0.02 (**0.35**–**0.40)**	21.44 ± 0.89 (20.02–23.08)	0.04 ± 0.03 (0.00–0.10)	9.32 ± 0.53 (8.72–10.38)	7.24 ± 0.14 (6.98–7.45)	46.44 ± 2.97 (41.54–51.81)	0.139 ± 0.030 (0.108–0.198)	2.225 ± 0.786 (1.160–3.758)	0.160 ± 0.035 (0.106–0.224)	339 ± 87 (222–508)	105.35 ± 8.23 (95.45–121.69)	6.80 ± 1.70 (3.88–9.78)	6.07 ± 0.01 (6.06–6.08)

Table S4.2 Mean concentrations ± SE for key environmental parameters measured at middle depth of the sampling sites: temperature – ^{o}C; salinity; dissolved oxygen (DO) – mg O_2 L^{-1}; pH – Sørensen scale; NO_3^-, NO_2^-, NH_4^+, PO_4^{3-}, N:P, and Si – μM; chlorophyll *a* (CHL *a*) – mg m^{-3}; total cell counts (TCC) – log_{10} cells mL^{-1}. In brackets – minimum and maximum values.

Site	T	Salinity	DO	pH	NO_3^-	NO_2^-	NH_4^+	PO_4^{3-}	N:P	Si	CHL *a*	TCC
1	15.48 ± 1.47 (11.24–20.32)	23.43 ± 4.36 (8.99–33.20)	8.44 ± 0.52 (7.65–10.51)	7.59 ± 0.22 (6.73–7.90)	17.62 ± 7.54 (6.32–47.02)	0.224 ± 0.047 (0.084–0.333)	1.768 ± 0.587 (0.425–3.639)	0.438 ± 0.079 (0.180–0.593)	47 ± 15 (18–98)	38.21 ± 16.74 (10.35–97.65)	1.56 ± 0.35 (0.66–2.75)	5.72 ± 0.12 (5.40–6.12)
2	15.45 ± 1.49 (11.24–20.28)	23.29 ± 4.34 (8.99–32.60)	8.35 ± 0.55 (7.52–10.51)	7.59 ± 0.22 (6.73–7.89)	18.84 ± 7.16 (9.44–47.02)	0.234 ± 0.043 (0.124–0.340)	1.842 ± 0.369 (0.979–2.758)	0.452 ± 0.052 (0.336–0.624)	47 ± 14 (20–98)	39.99 ± 16.14 (12.69–97.65)	1.75 ± 0.49 (0.66–3.54)	5.74 ± 0.14 (5.40–6.14)
3	15.30 ± 1.53 (11.00–20.35)	16.37 ± 5.66 (1.91–28.40)	8.80 ± 0.71 (7.31–11.11)	7.68 ± 0.12 (7.21–7.89)	22.37 ± 5.87 (11.75–43.98)	0.192 ± 0.047 (0.086–0.319)	1.609 ± 0.357 (0.944–2.975)	0.410 ± 0.073 (0.228–0.587)	70 ± 20 (23–116)	52.54 ± 15.62 (15.97–96.75)	1.97 ± 0.38 (0.83–3.09)	5.86 ± 0.14 (5.56–6.26)
4	15.62 ± 1.67 (10.83–20.70)	13.65 ± 5.55 (0.90–26.20)	9.00 ± 0.68 (7.66–11.13)	7.65 ± 0.10 (7.26–7.87)	24.63 ± 5.71 (7.57–43.32)	0.167 ± 0.037 (0.054–0.269)	2.024 ± 1.139 (0.551–6.533)	0.338 ± 0.073 (0.202–0.593)	94 ± 19 (24–132)	65.37 ± 13.10 (28.21–100.15)	2.64 ± 0.52 (0.91–3.95)	5.87 ± 0.16 (5.56–6.29)
5	16.57 ± 1.97 (10.54–21.33)	7.22 ± 3.16 (0.05–16.40)	9.32 ± 0.60 (8.02–11.22)	7.61 ± 0.14 (7.18–7.87)	34.09 ± 4.23 (23.11–49.13)	0.146 ± 0.029 (0.038–0.206)	1.220 ± 0.560 (0.321–3.390)	0.293 ± 0.055 (0.154–0.477)	136 ± 26 (77–230)	76.98 ± 7.93 (52.27–100.25)	2.73 ± 0.59 (0.74–3.90)	6.02 ± 0.15 (5.66–6.35)
6	16.81 ± 2.05 (10.50–21.41)	5.89 ± 2.63 (0.04–13.85)	9.44 ± 0.57 (8.19–11.23)	7.43 ± 0.12 (7.06–7.73)	34.71 ± 4.19 (28.71–51.24)	0.134 ± 0.022 (0.054–0.182)	0.639 ± 0.168 (0.139–1.198)	0.253 ± 0.064 (0.106–0.473)	171 ± 38 (98–314)	83.02 ± 7.40 (58.04–103.23)	3.55 ± 0.81 (0.75–4.79)	6.05 ± 0.12 (5.61–6.27)
7	16.98 ± 2.11 (10.54–21.41)	4.59 ± 2.02 (0.02–10.40)	9.56 ± 0.58 (8.18–11.33)	7.27 ± 0.15 (6.91–7.64)	32.64 ± 3.96 (26.05–47.92)	0.116 ± 0.020 (0.038–0.149)	0.535 ± 0.182 (0.156–1.161)	0.244 ± 0.064 (0.106–0.477)	166 ± 38 (99–306)	83.61 ± 5.36 (66.18–99.87)	3.93 ± 1.15 (0.70–6.85)	6.05 ± 0.12 (5.56–6.26)
8	17.00 ± 2.12 (10.50–21.11)	2.88 ± 1.39 (0.00–7.45)	9.75 ± 0.60 (8.30–11.58)	7.30 ± 0.15 (6.84–7.64)	34.89 ± 4.22 (26.67–49.85)	0.130 ± 0.018 (0.066–0.162)	0.915 ± 0.350 (0.048–2.137)	0.245 ± 0.067 (0.142–0.507)	187 ± 43 (101–311)	91.36 ± 5.54 (75.67–108.11)	5.76 ± 2.64 (0.62–15.47)	5.99 ± 0.10 (5.62–6.15)
9	16.98 ± 2.11 (13.74–23.30)	0.70 ± 0.41 (0.00–2.20)	9.58 ± 0.58 (8.10–11.41)	7.07 ± 0.16 (6.58–7.52)	36.39 ± 4.63 (25.25–50.16)	0.092 ± 0.016 (0.054–0.133)	1.066 ± 0.358 (0.105–1.937)	0.186 ± 0.021 (0.135–0.235)	207 ± 23 (146–289)	97.51 ± 5.23 (80.80–113.07)	8.57 ± 3.23 (0.57–15.07)	5.91 ± 0.09 (5.65–6.13)
10	19.60 ± 2.11 (13.74–23.30)	0.436 ± 0.39 (0.00–1.60)	9.22 ± 0.44 (8.21–10.07)	7.15 ± 0.20 (6.66–7.51)	36.60 ± 6.62 (24.35–51.83)	0.112 ± 0.034 (0.046–0.189)	1.933 ± 0.482 (0.940–3.249)	0.223 ± 0.041 (0.138–0.332)	206 ± 68 (91–391)	99.54 ± 6.61 (87.64–118.35)	7.11 ± 3.43 (1.22–17.04)	6.01 ± 0.04 (5.90–6.09)
11	21.44 ± 0.89 (20.02–23.08)	0.04 ± 0.03 (0.00–0.10)	9.32 ± 0.53 (8.72–10.38)	7.24 ± 0.14 (6.98–7.45)	46.44 ± 2.97 (41.54–51.81)	0.139 ± 0.030 (0.108–0.198)	2.225 ± 0.786 (1.160–3.758)	0.160 ± 0.035 (0.106–0.224)	339 ± 87 (222–508)	105.35 ± 8.23 (95.45–121.69)	6.80 ± 1.70 (3.88–9.78)	6.07 ± 0.01 (6.06–6.08)

Table S4.3 Mean concentrations ± SE for key environmental parameters measured near bottom of the sampling sites: temperature – ^{o}C; salinity; dissolved oxygen (DO) – mg O_2 L^{-1}; pH – Sørensen scale; NO_3^-, NO_2^-, NH_4^+, PO_4^{3-}, N:P, and Si – μM; chlorophyll *a* (CHL *a*) – mg m^{-3}; total cell counts (TCC) – log_{10} cells mL^{-1}. In brackets – minimum and maximum values.

Site	T	Salinity	DO	pH	NO_3^-	NO_2^-	NH_4^+	PO_4^{3-}	N:P	Si	CHL *a*	TCC
1	15.48 ± 1.19	30.32 ± 1.69	8.02 ± 0.37	7.76 ± 0.16	9.37 ± 3.27	0.233 ± 0.045	1.613 ± 0.629	0.394 ± 0.073	28 ± 9	17.57 ± 7.38	2.33 ± 0.66	5.79 ± 0.10
	(12.56–19.13)	(26.00–30.90)	(7.28–9.24)	(7.20–8.14)	(1.10–21.07)	(0.060–0.317)	(0.000–3.428)	(0.165–0.593)	(7–55)	(2.25–41.33)	(1.14–4.87)	(5.55–6.13)
2	15.61 ± 1.33	30.06 ± 1.56	7.95 ± 0.35	7.76 ± 0.16	9.86 ± 3.09	0.240 ± 0.048	1.881 ± 0.528	0.466 ± 0.087	28 ± 8	18.18 ± 7.12	2.05 ± 0.34	5.79 ± 0.11
	(12.56–19.87)	(26.00–33.70)	(7.25–9.24)	(7.20–8.14)	(2.23–21.07)	(0.060–0.343)	(0.830–3.536)	(0.272–0.731)	(12–55)	(4.82–41.33)	(1.47–3.37)	(5.55–6.07)
3	14.89 ± 1.49	23.83 ± 4.21	8.49 ± 0.61	7.61 ± 0.20	16.14 ± 5.38	0.226 ± 0.050	2.005 ± 0.446	0.457 ± 0.064	40 ± 10	37.91 ± 14.90	2.22 ± 0.54	5.84 ± 0.14
	(11.20–20.06)	(11.66–32.20)	(7.18–10.36)	(6.88–7.93)	(5.96–36.39)	(0.076–0.340)	(1.124–3.652)	(0.257–0.639)	(22–75)	(12.61–89.83)	(0.91–4.16)	(5.52–6.21)
4	15.02 ± 1.58	19.61 ± 5.39	8.69 ± 0.74	7.57 ± 0.15	19.81 ± 7.94	0.205 ± 0.035	2.592 ± 0.834	0.426 ± 0.068	58 ± 18	46.35 ± 15.02	3.04 ± 0.53	5.91 ± 0.14
	(10.89–20.48)	(1.45–31.10)	(7.32–11.08)	(7.17–7.88)	(4.70–50.22)	(0.132–0.287)	(1.368–5.895)	(0.272–0.654)	(17–116)	(16.63–99.82)	(1.00–3.83)	(5.63–6.30)
5	16.44 ± 1.93	7.33 ± 3.20	9.35 ± 0.59	7.55 ± 0.14	31.12 ± 4.16	0.133 ± 0.023	0.655 ± 0.122	0.298 ± 0.073	126 ± 24	76.32 ± 7.75	3.14 ± 0.79	6.01 ± 0.15
	(10.54–21.33)	(0.056–16.70)	(8.154–11.19)	(7.10–7.81)	(21.86–45.60)	(0.046–0.174)	(0.321–1.042)	(0.122–0.552)	(65–203)	(52.31–97.73)	(0.75–4.86)	(5.63–6.35)
6	16.77 ± 2.04	6.11 ± 2.73	9.43 ± 0.58	7.37 ± 0.13	34.77 ± 4.24	0.145 ± 0.022	0.558 ± 0.236	0.258 ± 0.073	185 ± 56	82.64 ± 7.91	3.92 ± 0.95	6.04 ± 0.12
	(10.50–21.40)	(0.04–14.30)	(8.15–11.22)	(7.03–7.72)	(28.74–51.11)	(0.062–0.190)	(0.080–1.427)	(0.090–0.507)	(93–394)	(56.49–104.67)	(0.74–5.57)	(5.62–6.28)
7	16.97 ± 2.11	4.62 ± 2.04	9.54 ± 0.58	7.23 ± 0.15	34.30 ± 3.69	0.124 ± 0.022	0.534 ± 0.163	0.240 ± 0.068	180 ± 41	83.46 ± 5.50	4.08 ± 1.15	6.05 ± 0.12
	(10.54–21.40)	(0.02–10.50)	(8.16–11.31)	(6.85–7.61)	(27.60–48.27)	(0.038–0.158)	(0.139–1.078)	(0.106–0.492)	(101–330)	(65.57–100.19)	(0.66 –7.02)	(5.62–6.28)
8	16.93 ± 2.09	3.25 ± 1.70	9.74 ± 0.61	7.21 ± 0.15	35.80 ± 4.18	0.134 ± 0.026	0.915 ± 0.407	0.236 ± 0.079	219 ± 69	91.04 ± 6.66	6.40 ± 2.68	6.00 ± 0.09
	(10.50–21.12)	(0.00–9.30)	(8.24–11.52)	(6.77–7.56)	(26.71–49.79)	(0.038–0.198)	(0.018–2.227)	(0.090–0.537)	(94–469)	(70.77–110.81)	(0.66–15.69)	(5.65–6.16)
9	16.09 ± 1.80	6.79 ± 3.90	9.13 ± 0.72	7.07 ± 0.21	33.28 ± 5.12	0.138 ± 0.026	1.065 ± 0.375	0.223 ± 0.051	192 ± 47	80.00 ± 9.07	8.28 ± 3.54	5.98 ± 0.09
	(10.54–20.68)	(0.00–16.70)	(7.33–11.40)	(6.50–7.65)	(22.53–48.03)	(0.038–0.174)	(0.141–2.161)	(0.090–0.348)	(70–312)	(53.43–102.31)	(0.74–17.24)	(5.63–6.14)
10	19.62 ± 2.11	0.43 ± 0.39	9.20 ± 0.435	7.12 ± 0.19	40.99 ± 5.86	0.126 ± 0.030	1.895 ± 0.448	0.196 ± 0.021	236 ± 57	99.31 ± 6.63	6.81 ± 3.50	6.01 ± 0.04
	(13.74–23.30)	(0.00–1.60)	(8.21–10.07)	(6.66–7.51)	(24.35–51.83)	(0.046–0.189)	(0.940–3.098)	(0.138–0.228)	(114–391)	(87.64–118.35)	(1.22–17.04)	(5.90–6.09)
11	21.44 ± 0.89	0.04 ± 0.03	9.32 ± 0.53	7.24 ± 0.14	46.44 ± 2.97	0.139 ± 0.030	2.225 ± 0.786	0.160 ± 0.035	339 ± 87	105.35 ± 8.23	6.80 ± 1.70	6.07 ± 0.01
	(20.02–23.08)	(0.00–0.10)	(8.72–10.38)	(6.98–7.45)	(41.54–51.81)	(0.108–0.198)	(1.160–3.758)	(0.106–0.224)	(222–508)	(95.45–121.69)	(3.88–9.78)	(6.06–6.08)

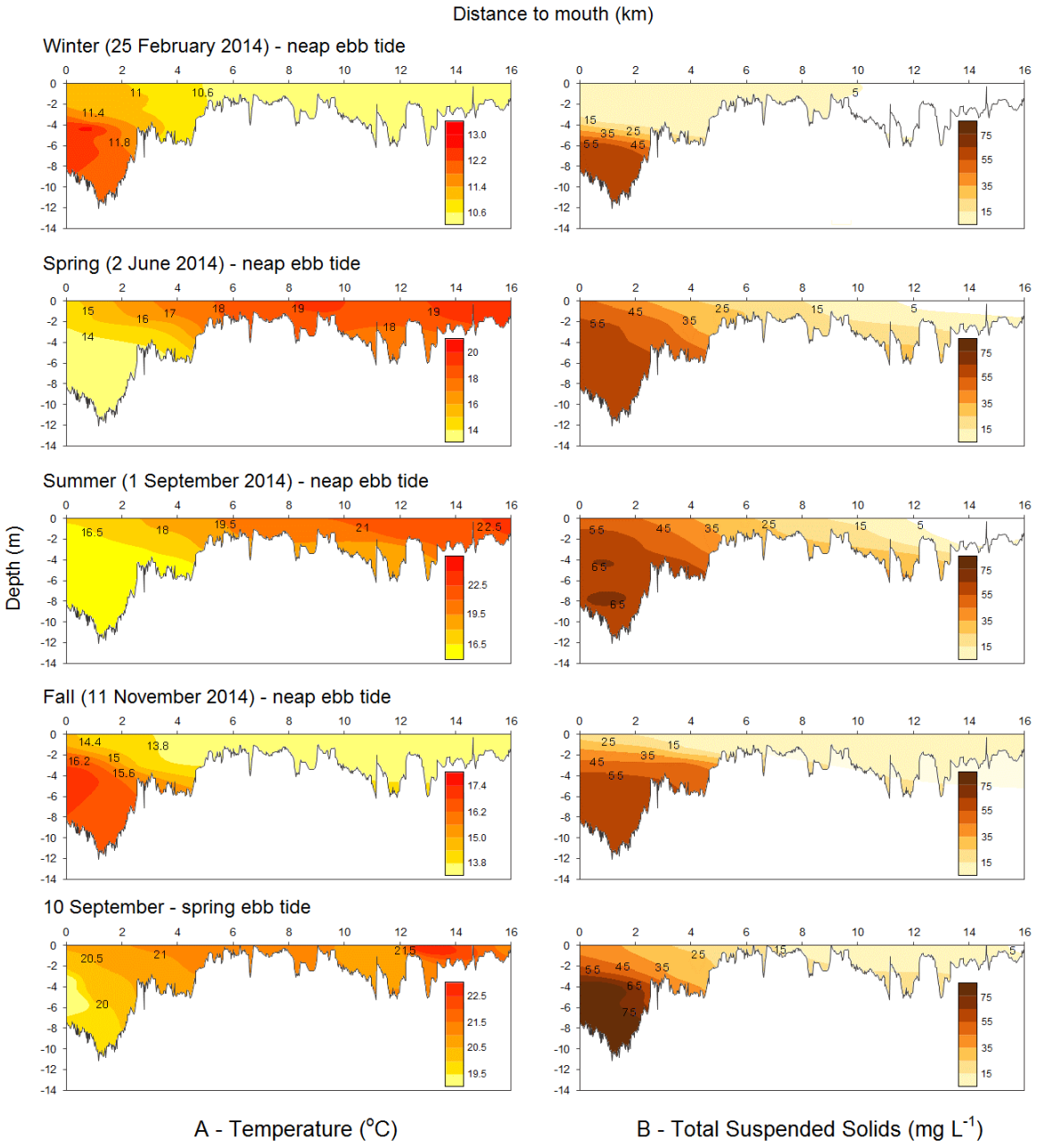

Figure S4.1 Longitudinal profiles of temperature and total suspended solids in the temperate Lima estuary.

CHAPTER 5

Spatial and seasonal dynamics of elemental composition and minerology of intertidal and subtidal sediments in the Lima estuary (NW Portugal)

Abstract

In estuaries, the mineral distribution in the top sediment layer results from the combined effect of fluvial and coastal inputs, and may present seasonal patterns owing to forcing e.g., floods, storms, waves, and tides. Our main goal was to study the estuarine sedimentological components, including textural and geochemical parameters, in order to characterize the seasonal and spatial dynamics of subtidal and intertidal sediments in a highly energetic temperate estuary (River Lima, NW Portugal). Subtidal sediments were usually anoxic within the middle estuary, and presented higher amounts of clay and silt than intertidal sediments. Oxygen, silicon, carbon, aluminium and potassium were the most abundant elements. The amount of silicon and carbon was related to the clay and silt content of the sediments. The mineralogical composition of sediments reflected the lithology of the watershed, with the most representative minerals being quartz, microcline (k alkaloid feldspar), and albite (plagioclase), in line with the results obtained in the elementary characterization. The lower stretches were particularly rich in iron silicates and anatase. No clear seasonal variation was found for sediment elemental and mineralogical compositions. Factor analysis explained 80% of the elemental origin, being 33% related to terrigenous origin, 24% to marine sediments, and 15% to anthropogenic inputs.

Keywords: Elemental composition; mineralogy; intertidal and subtidal sediments; seasons; Lima Estuary.

5.1 Introduction

River inputs reach the coastal seas via estuaries which are important sites in the global biogeochemical system, where riverine fluxes of dissolved and particulate matter can be modified (Jickells et al., 2016). Riverine sediments are derived and composed of natural physical, chemical and biological components generally related to their watersheds (Brils, 2008). Sediment particles result from weathering and erosion processes (Guagliardi et al., 2013; Anaya-Gregorio et al., 2018), being transported by agents such as wind, water or ice

and/or by the force of gravity (Libes, 2009). When the energy of the transporting current is not strong enough to transport the particles, its deposition occurs in the river bed (Négrel et al., 2014). According to the deposition type, the sediments can be grouped as clastic, chemical, and biochemical sediments. Clastic sediments are generated by the fragmentation of rocks pre-existing on the surface, followed by weathering. As these sediments are generated from rocks composed predominantly by silicates, they are denominated as siliciclastic (Libes, 2009). Its mineral composition is varied, but the presence of unaltered quartz, which is a weather-resistant mineral, is common in clastic sediments (Marathe, 2012). Examples of other minerals present are feldspar and clays. Weathering, in addition to generating mineral particles (Azam and Tripathi, 2016; Tapia-Fernandez et al., 2017), also generates dissolved material such as ions in solution (Anaya-Gregorio et al., 2018). The sediments resulting from the chemical precipitation of the material dissolved in water, and from the biochemical reactions, are called chemical and biochemical sediments, respectively. Chemical sediments are formed at or near the deposition site. Biochemical sediments are undissolved minerals from the remains of organisms or minerals precipitated by biological processes, such as calcite, aragonite, opal, barite, and celestite (Libes, 2009). In shallow coastal environments, biochemical sediments are mainly composed of two calcium carbonate minerals - calcite and aragonite ($CaCO_3$) originated from shells (Lalli and Parsons, 2006). Inorganic processes also lead to the precipitation of chemical sediments. For example, the evaporation of sea water can precipitate gypsum ($CaSO_4 \cdot 2H_2O$) or halite (NaCl). The characteristics of the sediments depend on the composition of the eroded rock (modal composition), transport agent, transport duration, biological activity, the chemical environment, and the physical conditions of the sedimentation basin (Guagliardi et al., 2013; Pastor-Galán et al., 2013; Ramos-Vázquez et al., 2018).

Estuarine sediments, in particular, result from a continuous process of sedimentation, receiving inputs of both marine and fluvial areas. The mineral and geochemical composition of sediments can thus be used to infer the provenance, weathering history, and depositional processes (Anaya-Gregorio et al., 2018; Hernández-Hinojosa et al., 2018). Additionally, the sedimentation record has been previously used to evaluate the coastal contamination by anthropogenic activities (Sundararajan and Natesan, 2010).

The Lima estuary is located in NW Portugal and belongs to the hydrographic region of the Minho and Lima, with the watersheds of the Minho, Lima, Âncora, and Neiva rivers as the main contributors (INAG, 2009; ARH Norte, 2012). This hydrographic region is part of the Central Iberian Zone (Figure S5.1), being composed by geologic units of the Hesperic Massif, consisting essentially of a rocky substrate of Paleozoic and of late Proterozoic age (Armendáriz et al., 2008; Solá et al., 2011; Viveen et al., 2013).

In geological terms, the hydrographic region can be divided into three main domains: i) Western (coastal strip), consisting of granitoids, highly fractured metasedimentary rocks of the

schist-greywacke complex, quartzite rocks and schist rocks of the early Paleozoic; ii) Central, formed by a strip of metasedimentary rocks (Central and West Minho Unit), of early Paleozoic; and iii) Eastern, characterized by the great granite area of the Minho, with granitoids of varied nature covering a much larger area than metasediments (ARH Norte, 2012; CGP, 2010). Moreover, the NW Portugal region has an abundance of Hercynian granitoids that intruded and metamorphosed the Paleozoic sediments (Alves, 2004; Cardoso et al., 2008), being partially covered by vestiges of sedimentation occurring during late Cenozoic, attributed to Pliocene and Quaternary (Carvalhido et al., 2014). In the coastal strip, deposits of ancient beaches and dunes can be found, while in the inner region, continental formations arise generated by fluvial systems, represented by terrace deposits occurring in the river basins (Alves, 2004). The most representative soils are the Cambisols (Inácio et al., 2008).

Few geological studies are available, dealing with the geomorphological and sedimentological characteristics for the characterization and dating of Minho-Neiva area deposits (Carvalhido et al., 2014), the sedimentary dynamics (Oliveira et al., 2000; 2002), and sediment composition in the river deposits (Alves, 2004). Moreover, the spatial and temporal characterization of the estuary, from the point of view of mineralogy and geochemical composition, has not been addressed.

The aim of this study was to perform the inventory of intertidal and subtidal sedimentological components, including textural and geochemical descriptors, to investigate the spatial and temporal characterization of the Lima temperate estuarine system. These tools were also used to infer the origins and processes by which the sediments are transported, as well as to evaluate the pathways whereby the materials transported by the river are deposited in the estuary.

5.2 Material and methods

5.2.1 Sampling

The Lima estuary is located in NW Portugal [41.68º N; 08.84º W (WGS84)]. According to the morphology, bathymetry, salinity, and the presence/absence of saltmarshes, the estuary can be divided into three geomorphological zones: lower, middle, and upper estuary. Along the 12.6 km estuarine stretch, 7 samples of subtidal sediments and 7 samples of intertidal sediments were collected, in the three estuarine zones (Figure 5.1). Sampling surveys were carried out on May (spring), July (summer), and November (fall) of 2015, and January (winter) 2016, during the ebb tide, starting 1:30 h before slack water. Samples of subtidal sediments were collected with a Petite-Ponar grab with a sediment penetration of ca. 10 cm, and with plastic cores in the case of intertidal samples. The oxidation–reduction potential (ORP) was

measured directly on wet sediments with a HI 9023 meter, equipped with a HI 3130 electrode (Hanna Instruments).

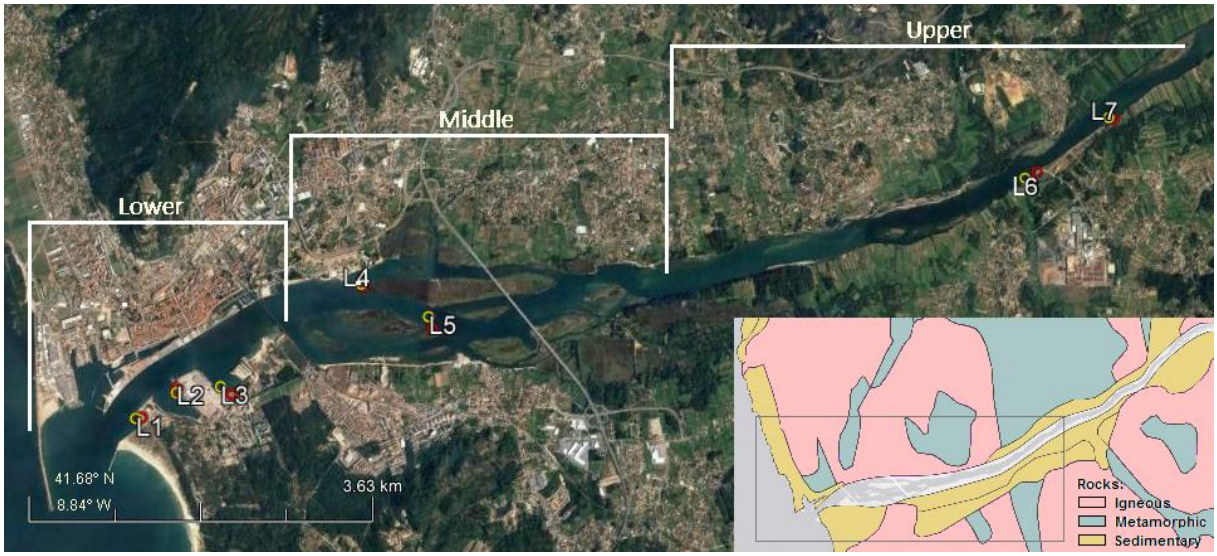

Figure 5.1 Map of the Lima estuary and sediment sample locations (base map: Google Earth and maps of LNEG - Laboratório Nacional de Energia e Geologia, 2017).

5.2.2 Analytical procedures

Salinity and temperature of sediments interstitial water were measured with a YSI30 probe (Xylem). Organic matter (OM) was estimated by the loss on ignition method, sediment samples were dried at 105 ^{o}C (24 h), and ignited at 500 ^{o}C (4 h) (APHA, 2005). Grain size analysis was performed by dry sieving (ISO 3301.1 sieves, CISA Sieve Shaker Mod. RP.08). Sediment fractions were separated according to the classification proposed by Folk (1954) in the following three major groups: mud (silt and clay) (< 0.063 mm), sand (0.063–2 mm), and gravel (> 2 mm). The sand group was further divided into the following five groups - very fine sand (0.063–0.125 mm), fine sand (0.125–0.250 mm), medium sand (0.250–0.5 mm), coarse sand (0.5–1 mm), and very coarse sand (1–2 mm). Each fraction was weighed and expressed as a percentage of the total weight.

For sediments composition analysis, the bulk sample was grounded to fine powder (0.063 mm). A mechanical wet milling (in deionized water) was performed using a nylon vessel with zirconia beads of varying diameter (0.5 to 2.5 cm), for 30 minutes at a speed of 30 Hz (1800 rpm). The milled samples were dried in an oven at a temperature below 40 ^{o}C, and disaggregated in a mortar.

Elemental chemical characterization was performed by scanning electron microscopy (SEM-EDS), using a Hitachi S4100 microscope equipped with a detector for energy dispersion

spectroscopy, with elemental distribution being partially quantified using semi-quantitative methods for spectrum analysis (EDS–EDAX with detector Bruker AXS; software: Quantax).
The mineral composition of the samples was carried out by a high-resolution Bruker D8 Advance DaVinci diffractometer (XRD), with a cooper radiation (CuKα1 = 1.5406 Å), and 2θ range of 5–50° at 0.1° intervals and a counting speed of 0.02°s^{-1}. The mineralogical determination was performed by simple adjustment of the diffractograms using the software code EVA® 2.2, since the structure of these minerals is well-documented in the literature. For mineral quantification, the software TOPAS version 4.2 (Bruker AXS, Karlsruhe, Germany) was used.

5.2.3 Data analysis

Basic statistics, statistical tests, correlation coefficients, and Factor Analysis (FA) were performed using STATISTICA 13.0® (version 7.0) software package. Factor analysis was performed on the entire data set used in the correlation matrices of the chemical elements, in order to determine potential inter-data relationships and the common origin of the data. The statistical techniques of factor analysis were used in the data provided by SEM-EDS and XRD analysis, applying the Varimax normalization technique. All statistical analyses were considered at a significance level of 0.05.

5.3 Results

5.3.1 Grain size distribution and environmental characteristics

Intertidal sediments showed positive ORP values, while the subtidal sediments collected at locations L2, L3 (lower estuary), and L4 (middle estuary) presented mostly negative values (reduction conditions) (Table 5.1). The amount of OM obtained for sediments with negative ORP values was higher when compared to the ones obtained for the remaining sediments. The maximum amount of OM was detected during the winter in the middle estuary, both for the subtidal sediment (L4, 14.51%), and for intertidal sediments (9.07%, L3). The sediments with higher percentage of fine size (2SS and 3SS) presented the highest values of OM (Figure 5.2), as expected. Except for summer, the subtidal sediment with the highest amount of clay and silt (mud) was the 4SS, with values from 13.2% to 53.4% (spring and winter, respectively). For the intertidal sediment, the higher contents were found in the 3SS (spring and fall) and 4SS (summer and winter), with values in the range 5.5% (summer) to 12.9% (spring).

Table 5.1 Characterization of the sediments in the Lima estuary.

		Sediments: Subtidal					Sediments: Intertidal				
Season	Location	Ref.	ORP (mV)	Temp. (ºC)	Sal.	OM (%)	Ref.	ORP (mV)	Temp. (ºC)	Sal.	OM (%)
Spring	L1	1SS	220.6	21.0	27.2	1.17	1SI	230.2	22.6	19.6	0.89
	L2	2SS	-138.3	17.1	31.3	10.29	2SI	133.2	20.5	25.3	1.13
	L3	3SS	-62.9	20.3	26.1	2.39	3SI	63.2	20.0	25.9	9.07
	L4	4SS	-144.2	18.5	20.3	4.89	4SI	203.5	22.1	23.3	1.01
	L5	5SS	176.2	19.6	8.8	0.61	5SI	245.2	20.5	6.0	0.66
	L6	6SS	318.9	17.2	1.2	0.66	6SI	279.5	21.2	0.5	0.44
	L7	7SS	359.5	19.4	0.0	1.09	7SI	352.6	19.1	0.2	0.80
Summer	L1	1SS	139.6	26.8	33.6	1.43	1SI	163.0	24.9	30.7	0.91
	L2	2SS	-221.0	16.8	29.6	8.94	2SI	152.0	21.7	30.8	1.52
	L3	3SS	-310.0	16.9	28.4	10.82	3SI	146.0	22.5	7.7	0.75
	L4	4SS	-347.0	19.4	23.1	9.84	4SI	168.0	21.6	21.8	2.08
	L5	5SS	202.1	23.2	21.6	0.86	5SI	202.1	22.8	23.4	0.73
	L6	6SS	240.1	24.9	7.0	0.72	6SI	269.5	26.5	9.0	0.55
	L7	7SS	-112.5	25.3	4.6	1.75	7SI	237.5	26.5	3.6	0.63
Fall	L1	1SS	162.7	16.8	27.3	1.69	1SI	189.5	16.4	13.4	0.82
	L2	2SS	-44.4	16.2	24.9	1.01	2SI	194.3	16.9	24.4	1.06
	L3	3SS	-189.7	16.8	32.8	9.94	3SI	61.8	16.6	20.0	4.47
	L4	4SS	-363.1	15.5	27.3	12.29	4SI	-82.1	16.4	22.2	1.12
	L5	5SS	-83.7	16.0	17.6	1.35	5SI	160.3	16.1	10.9	0.56
	L6	6SS	230.1	15.9	3.9	3.03	6SI	235.4	15.9	0.4	0.57
	L7	7SS	111.2	15.6	0.2	1.98	7SI	268.7	16.1	0.3	0.94
Winter	L1	1SS	136.2	12.3	21.5	1.62	1SI	222.2	11.8	8.6	0.64
	L2	2SS	-146.4	12.1	15.8	2.11	2SI	162.7	12.2	21.4	1.32
	L3	3SS	-178.6	12.0	21.7	10.64	3SI	120.2	11.8	13.1	2.43
	L4	4SS	-241.7	11.8	17.9	14.51	4SI	206.7	11.7	13.8	2.29
	L5	5SS	160.7	11.7	4.6	1.10	5SI	184.8	11.7	0.5	0.57
	L6	6SS	248.1	12.0	3.2	0.62	6SI	244.9	12.0	1.5	0.60
	L7	7SS	265.9	11.9	0.1	0.45	7SI	268.2	11.8	1.0	1.06

Parameters information: ORP – Oxidation–reduction potential of the sediment; Temp. – Temperature of the sediment; Sal. – Salinity of the interstitial water; OM – Organic matter content in the in dry matter.

A statistically significant correlation ($p < 0.05$) between the amount of mud, OM, and ORP was found (Figure S5.2). When the amount of mud increased, the OM increased linearly, and the ORP tended to decrease monotonically. The amount of mud in the sediments explained between 75% (summer, $p < 6x10^{-05}$) and 97% (fall, $p < 3x10^{-10}$) of the OM variability, and 57% (summer, $p < 2x10^{-03}$) at 67% (spring, $p < 4x10^{-04}$) of the ORP variability. The sediments that presented negative values of ORP, contained greater percentage of mud, and belonged to the subtidal areas.

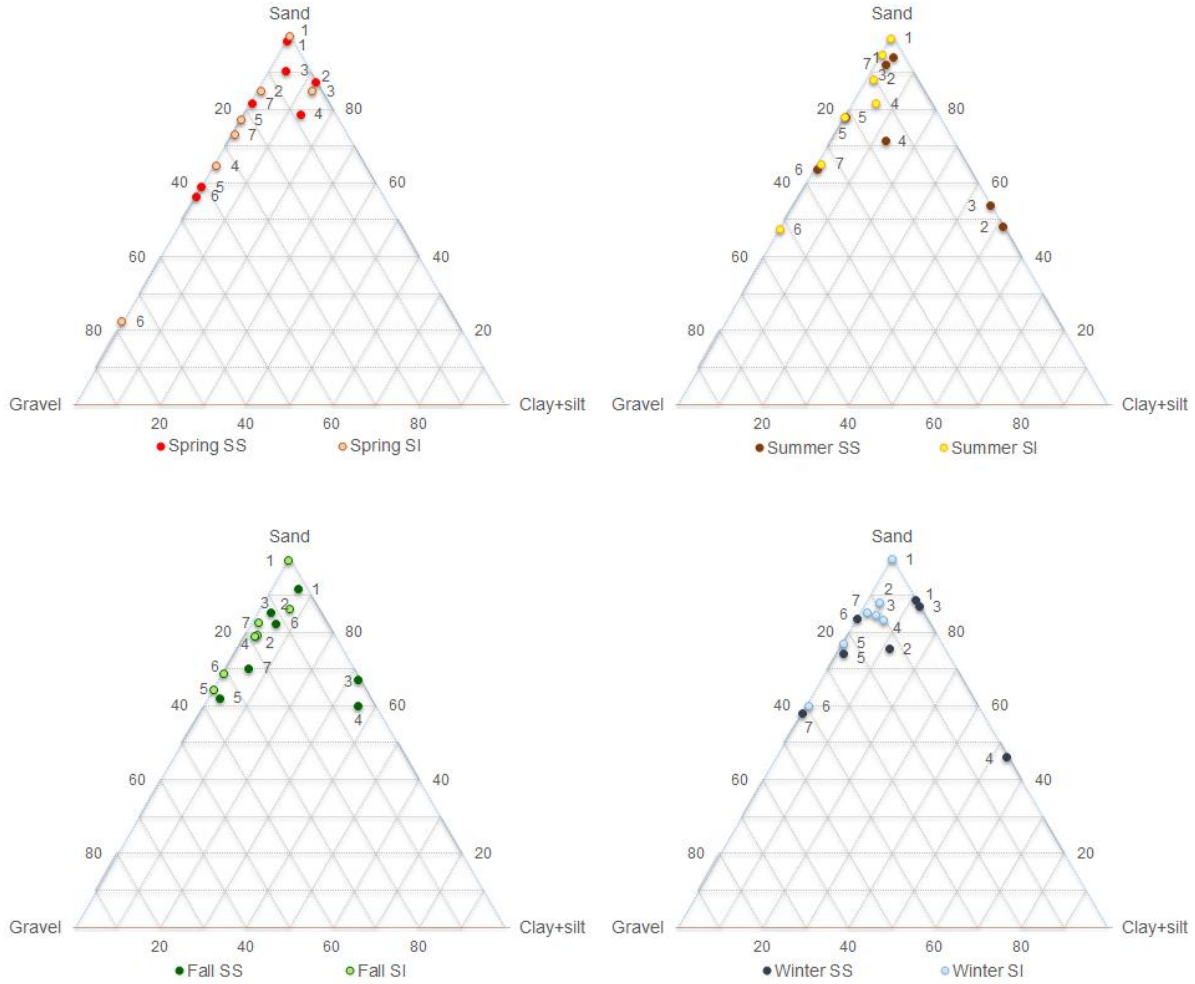

Figure 5.2 Seasonal sediments size distribution along the Lima estuary.

5.3.2 Mineralogical property

In the mineralogical analysis of the XRD, over 90% of the minerals present in sediments were identified (Figure 5.3). In 61% of the sediments, an almost complete mineral composition was achieved (less than 1% of the unidentified mineral composition).

The most representative minerals recorded in the composition of all sediments were quartz (22–52%), microcline (11–41%), and albite (10–33%). Generally, quartz and microcline were found in higher quantities in intertidal sediments, and albite in the subtidal sediments. The percental contribution of quartz and microcline to the composition of the sediments decreased with the increase of the mud percentage, being these minerals found in higher concentrations in the upper estuary. Two micas were found, muscovite and biotite, being the first one present in greater quantity. Calcite, halite, and zeolite were present in higher amounts in the lower estuary. The maximum values in the subtidal sediments were 8.05% (L3, winter), 2.68% (L2, summer), and 5.16% (L2, summer), for calcite, halite, and zeolite, respectively. In intertidal sediments, the maximum concentration of these minerals was found in L1, with values of

4.28% (summer), 2.20% (fall), and 5.29% (spring) for calcite, halite, and zeolite, respectively. Halite and zeolite appeared to be associated with finer sediments, i.e., sediments with the highest amount of mud.

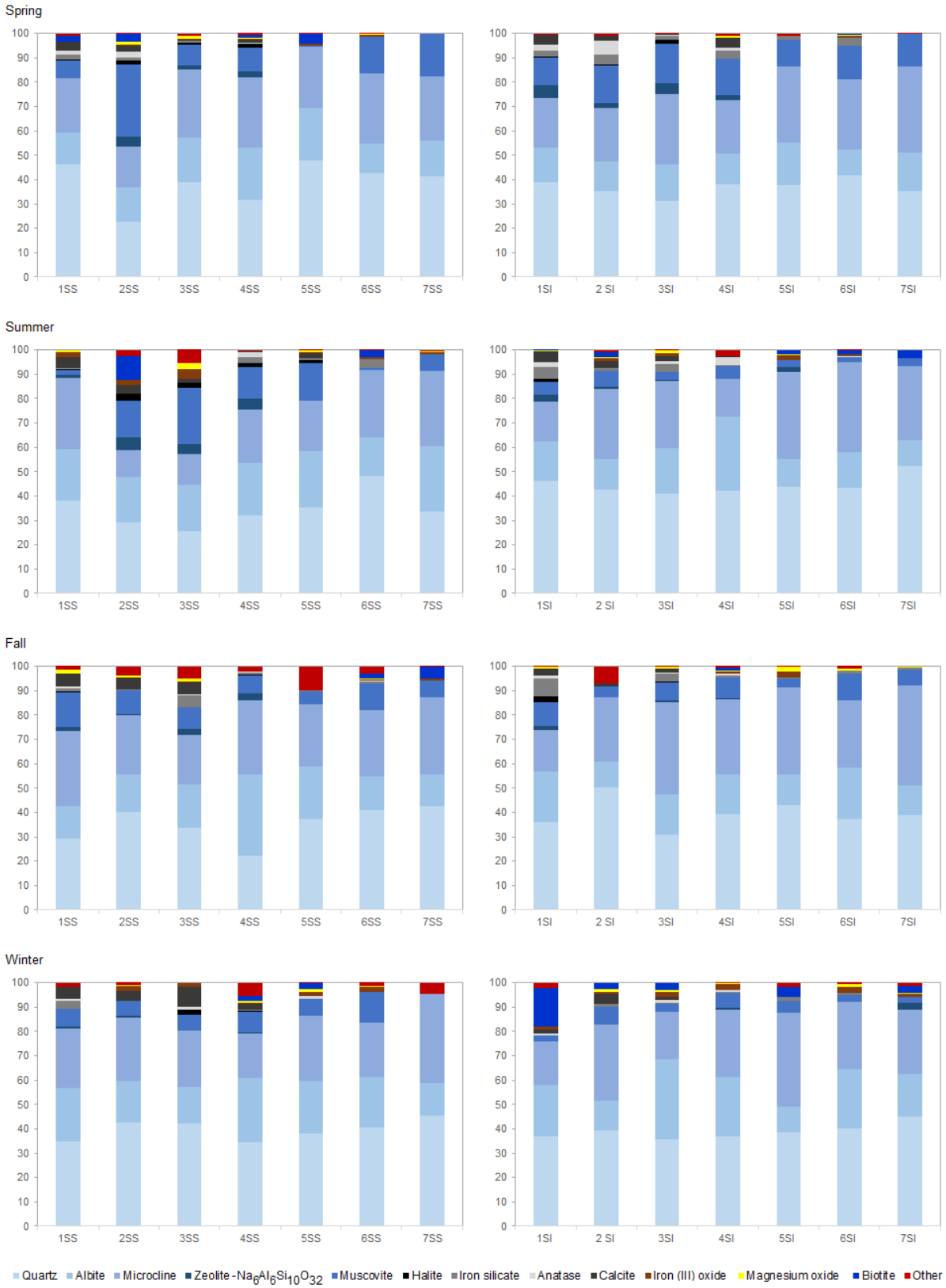

Figure 5.3 Seasonal evolution of the mineral composition of the sediments along the Lima estuary.

Generally, intertidal sediments from the lower estuary presented higher amounts of iron silicate and anatase, being these minerals absent in the uppermost stretch of the estuary. Magnesium oxide and iron (III) oxide showed a scattered behavior, with maximum values during the summer in 3SS, with values of 3.78% and 2.45% for iron (III) oxide, and magnesium oxide, respectively. Based on the mineralogical composition of granite (feldspars, quartz, micas), its amount was calculated in the sediments along the estuary. The subtidal and intertidal sediments recorded the smallest fractions of granite in the 3SS (80.3%) during the summer survey, and in the 1SI (83.4%) in the fall survey. Normally, sediments with a higher percentage of coarser particles had a higher amount of granite, with higher concentrations in the upper estuary being observed (Figure 5.3).

A significant correlation ($p < 0.05$) was found for minerals with the grain size of sediments (Table S5.1), i.e., quartz and microcline correlated with the coarse fraction (gravel), and albite, halite, muscovite, and zeolite with the fine fraction (mud). The distribution of minerals also related with salinity ($p < 0.05$) with anatase, calcite, halite, and zeolite increasing, and quartz and microcline decreasing towards higher salinity areas. Significant correlations ($p < 0.05$) were also found between minerals, e.g., halite, muscovite, and zeolite. Iron silicate ($Fe_{2.89}Si_{1.11}O_{6.07}$), and iron (III) oxide (Fe_2O_3) presented a statistically significant ($p < 0.05$) inverse correlation between them. Despite the differences, mineral composition data did not show a clear seasonal variation in both types of sediments.

5.3.3 Elemental composition

In the elemental composition of the sediments obtained by energy dispersion spectroscopy (Figure 5.4), oxygen (O) and silicon (Si) were the most abundant elements, being O the largest contributor (40–60%). The trend of variation observed by carbon (C) with the amount of mud was monotonically linear, i.e., the amount of C increased as the mud fraction increased. For Si, the trend verified was inversely proportional (Figure S5.3). The granulometry (silt and clay) explained between 61 and 88% (summer and spring, respectively) of the C variation, and between 68–84% (winter and summer, respectively) of the Si variation (Figure S5.3).

The remaining elements did not show a homogeneous trend along the estuary nor between seasons. However, the highest concentrations were observed in the lower and middle estuary, with the exception of potassium (K). Higher concentration values of the latter were observed in subtidal sediments associated with increased mud content, being the highest values found during the spring-summer period. Salinity explained between 72% and 84% of chlorine (Cl) variation (Figure S5.3). However, in subtidal sediments with the higher mud content (2SS, 3SS, 4SS), the Cl concentration was particularly high and did not linearly correlate with the remaining values. The concentration of calcium (Ca), chlorine (Cl) and iodine (I) decreased

along the estuary to values close to zero in the upstream stretch and in all seasons (Figure 5.4). Manganese (Mn) and phosphorus (P) were present in almost vestigial amounts along the estuary.

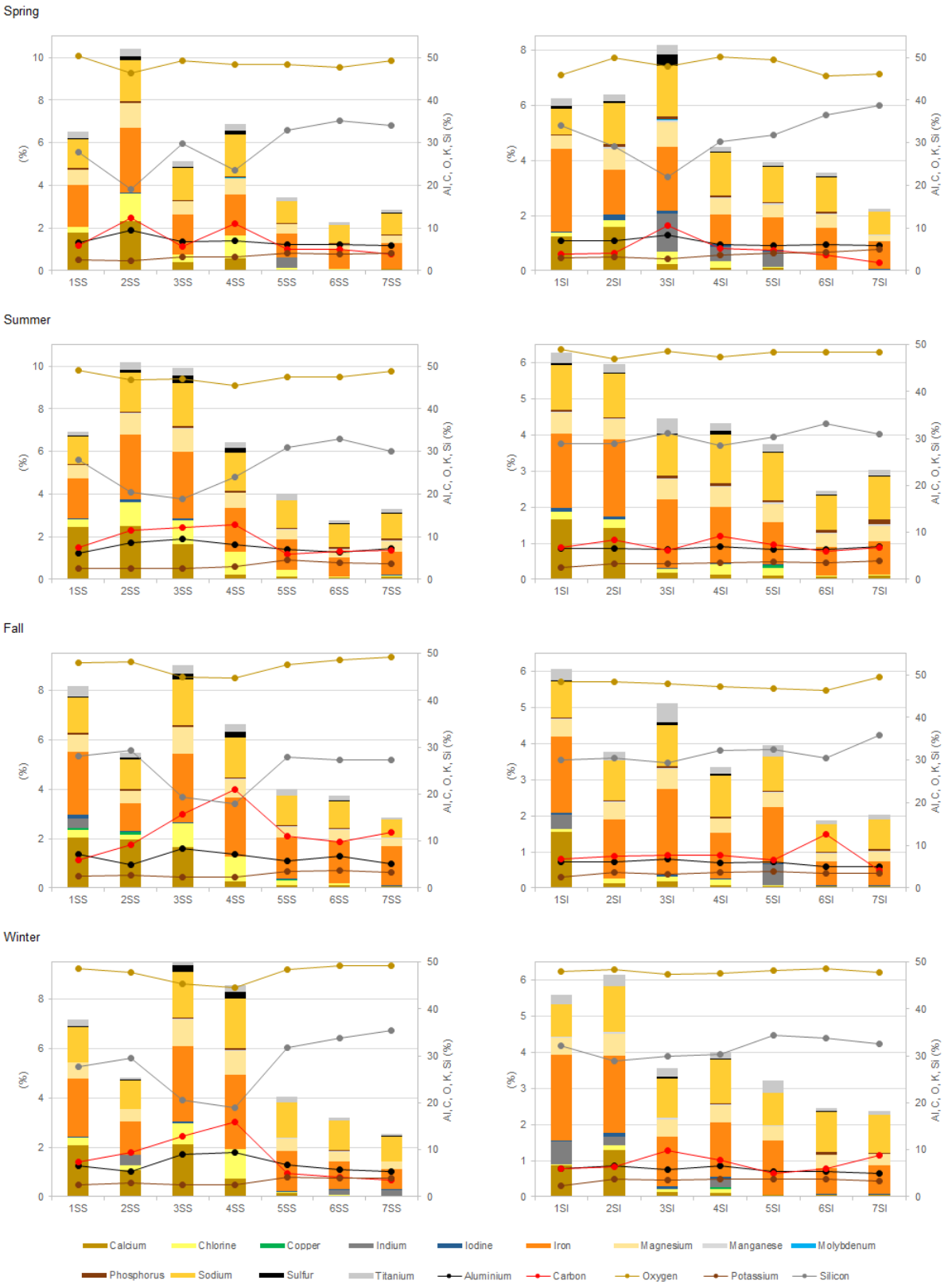

Figure 5.4 Seasonal evolution of the sediments elemental composition along the Lima estuary.

Other elements were observed, such as copper (Cu), indium (In), and molybdenum (Mo), mainly in the lower and middle stretches of the estuary. The values recorded by Cu were very small, with a maximum value of 0.126% (2SS) in the fall. Mn only appeared in the spring survey in the sediments 3SI and 4SS, with values of 0.062% and 0.033%, respectively. In was observed in all seasons except summer, in both types of sediment, and in all areas of the estuary, with values between 0.206% (6SS in the winter), and 1.395% (3SI in the spring).

The obtained data highlighted a significant correlation ($p < 0.05$) for most chemical elements with the proportion of the fine fraction of sediments (Table S5.2). Significant and strong correlations ($p < 0.05$, $R^2 > 0.80$) were also found between chemical elements, e.g., Cl with aluminium (Al), Ca, magnesium (Mg), Si, sodium (Na), and sulfur (S); and Mg with Al, Cl, iron (Fe), Si, and Na (Table S5.2). However, regression analysis showed no significant linear relationships ($p > 0.05$) between Al and Cu, In, Mo, and Mn (Table S5.2). As expected, Al and grain-size covaried in baseline data (Al on grain-size, $R^2 = 0.697$).

When the elemental composition of the sediments obtained by the mineralogical composition (XRD) and by the EDS-SEM technique were compared, it was found that mostly of the results obtained by XRD were inserted in the ranges of maximum and minimum values obtained by EDS-SEM (50–95%), except for titanium (Ti) (32%), although the techniques were not quantitative (Figure S5.4).

5.3.4 Factor analysis

The factor analysis for mineral composition presented five main factors (eigenvalues > 1), explaining 72% of the total variation of the data (Table S5.3). Factor 1 was characterized by high loadings (> 0.612), and contributed with 21% of the total variance, being positive for mud, zeolite, muscovite, and halite, and negative for quartz, i.e., an affinity of the minerals with the finer fraction of the sediments, and quartz-rich minerals (siliciclastic rocks) (Figure 5.5). Factor 2 explained 12% of the total variability with positive loadings for iron (III) oxide (> 0.614) and magnesium oxide (> 0.462), and negative for iron silicate and anatase, reflecting the distribution of crystalline oxides as well as their interrelations with the iron silicate. The mineral hardness differences seem to be reflected in the Factor 3, characterized by positive loadings for magnesium oxide (> 0.700), and negative for biotite, explaining 9.4% of the total variance. Factor 4, explained 19% of the total variability, with positive loadings for salinity, calcite, halite, and anatase, and negative for gravel fraction, and microcline (Table S5.3), reflecting the affinity of minerals with the salinity, and their distribution in the coarse sediments. A total variability of 10% was explained by Factor 5, with positive loading for quartz, and negative for albite, reflecting the distribution relation between the quartz (silicate mineral), and the albite (aluminosilicate mineral). The factor analysis of elemental composition yielded five main

factors (eigenvalues > 1), explaining about 80% of the total variation of the data obtained for the chemical elements (Table S5.4). Factor 1 contributed with 33% of the total variance and was characterized by positive loadings for mud, Al, C, Cl, Mg, Si, Na, S, Fe and P, and negative for O, Si and K. This group showed the elements associated to mud minerals (and OM), with the distribution patterns controlled by the finer fraction of the sediments (Figure 5.5). Factor 2 explained 24.3% of the total variability with positive loadings for salinity, Ca, I, Fe, Mg, Ti, Al, Cl, and Na, and negative for K, reflecting elements related to salinity. The total variation explained by Factor 3 was 9.15%, being characterized by positive loadings for In and Mo, pointing to an anthropogenic origin, since these elements occurred sporadically in the sediments adjacent to the city of Viana do Castelo. The same origin seemed to underlie the Factor 5, characterized by positive charges for Cu and P, since copper was rarely found in the sediments (3 in a total of 56 samples). The remaining 7.23% of the total variability was explained by Factor 4, with positive loadings for Mn and P (Table S5.4).

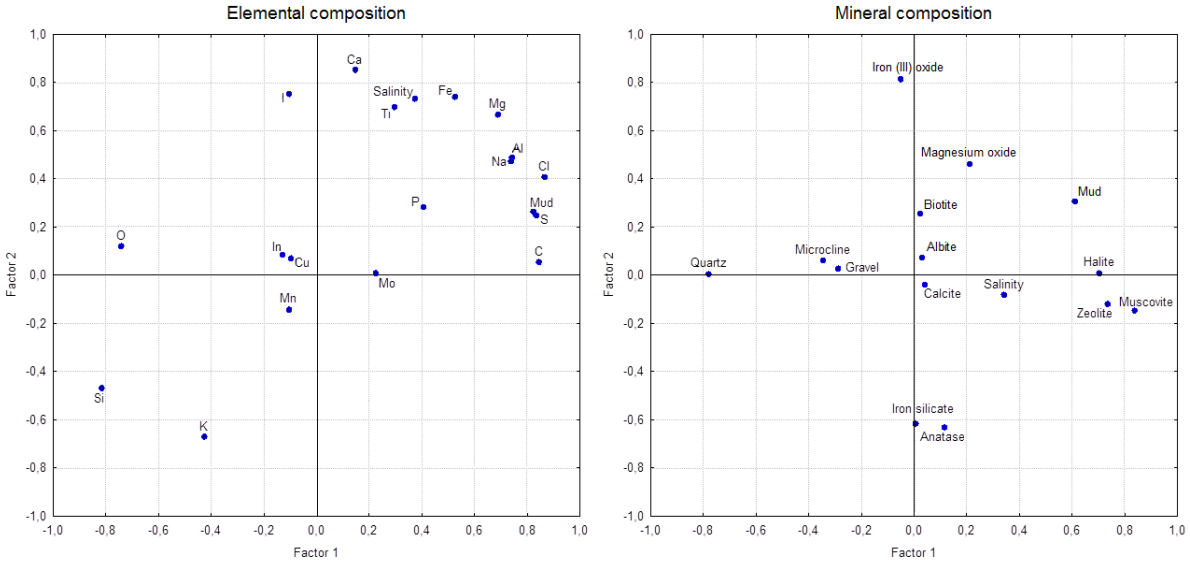

Figure 5.5 Factor loadings plot, Factor 1 vs Factor 2. Rotation Varimax normalized. Extraction: Principal components.

5.4 Discussion

5.4.1 Grain size distribution pattern

The sediments collected in the estuary showed a clear relationship between size-fraction, ORP, and OM. The relationship between the finer grain size, OM content, and negative ORP (environment with reducing conditions) found in sediments (2SS, 3SS and 4SS) could be attributed to the co-sedimentation of particulate organic matter with clay and mineral particles (Ho et al., 2010; Venkatramanan et al., 2013). Coarser size sediments were collected in

upstream locations, similarly to that described for other estuaries (Venkatramanan et al., 2013; Camacho et al., 2014). Since the Lima estuary is a bedrock-controlled estuary, a sediment size gradient was expected due to the energetic textural bipolarity (river and tidal energy), with ebb currents reworking fluvial sediments from the river to the sea, and flood currents introducing marine sediments into the estuary (Camacho et al., 2014). As expected, the Lima estuary recorded a selective sediment deposition, the finer being transported downstream towards the river mouth (2SS, 3SS, and 4SS) by the ebb-dominated tidal flow and current, and the coarser deposited into upstream part of the estuary (L5 to L7). In zones of the estuary dominated by saltmarsh islands and/or located out of the navigation channel, with lower hydrodynamics, differential deposition of finer sediments occurred, as noted by Camacho et al. (2014).

The saltmarsh zones in the Lima estuary are flood-dominated which foment vertical accretion, and reduce the export of finer sediments to the ocean. Since the mud is quite resistant to erosion due to the high resistance to elasticity and viscosity, continuous sedimentation occurs during tides, surpassing the marshes and increasing the muddy banks in the alluvial plain (Camacho et al., 2014). In the saltmarsh zones with higher sandy composition and sparse vegetation (L5), and therefore less effective in dissipating the current energy, the ebb dominated with efficient seaward export of fine sediments. Erosion rather than deposition is promoted, and the grain-size results pointed to a slight increase of the coarser sediments in the lower estuary during the wet season, when large amounts of water transport fluvial sediments to the estuary (Oliveira et al., 2002). However, artificial regulation prevents the occurrence of floods responsible for the washing of coarser sediments, tending the sediments to accumulate by the mouth of the estuary. Indeed, an increase of finer sediments was verified during the wet season, off the navigation channel, within a more protected area in a saltmarsh zone and less affected by the hydraulic regime of the estuary (L4). During the summer, the higher amounts of finer sediments in the lower estuary subtidal areas (L2 and L3), might be related with the low hydrographic conditions verified in dry seasons, which allowed sediment deposition, due to the increase in the particles residence time (Wolanski and Elliott 2016).

5.4.2 Mineral distribution and controlling factors

The most representative minerals were quartz, microcline (k-alkali feldspar), and albite (plagioclase), in line with the surrounding rocks of the river watershed, where granites predominate (Teixeira and Medeiros, 1970; Oliveira et al., 2002). The quartz and the microcline (K feldspar-rich rocks) showed positive correlation with the coarser sediments, and negative with the finer sediments (Table S5.1), being these minerals associated with higher hardness and, therefore, with greater resistance to weathering and erosion (Abdullah et al., 2015). In

addition, microcline (K-alkali feldspar, $KAlSi_3O_8$) was present in higher amounts in the upper estuary, which was supported by the greater K content. The albite appeared normally associated with finer sediments (mud), which may be related to the existence of Na in its composition ($NaAlSi_3O_8$), an element which can be correlated with that sediments type (R^2 = 0.70). Since the subtidal sediments had a higher fine fraction, they also had a greater amount of albite. The correlation pattern presented by the albite with the sediment size was also shown by zeolite ($Na_6Al_6Si_{10}O_{32}$), muscovite ($Al_{13.81}H_{9.52}K_{4.76}O_{57.14}Si1_{4.76}$), and halite (NaCl). No relation was found between the muscovite and salinity, suggesting that its presence in finer sediments resulted from weathering of the upstream granitic rocks (Abdullah et al., 2015), with high fragmentation during transport by the river until its accumulation in the middle and lower estuary. On the other hand, zeolite, halite (NaCl), calcite ($CaCO_3$), and anatase (TiO_2) appeared positively associated with salinity, suggesting that the marine environment may act as source of these minerals to the estuary (Oliveira et al., 2000), observation supported by factorial analysis (Factor 4). The positive correlations shown by muscovite with zeolite and halite appear to be rather the result of the coexistence of these minerals in finer sediments, and not because they had a common source. Factor analysis (Factor 1) reinforces the considerations about the relationship of minerals with the grain fractions of sediments (Pastor-Galán et al., 2013). The silicate minerals associated with the finer fraction may be the result of weathering and erosion of bedrock, while halite may have resulted from the adsorption of chemical elements on the sediment surface, followed by precipitation of NaCl. The iron silicate was more abundant in the lower estuary, where higher concentrations of iron were observed. Iron silicate correlated well with anatase and calcite, minerals related with the salinity, suggesting that the marine environmental can, indeed, feed the estuary with iron silicate. Iron and magnesium oxides presented similar trends, and appeared to coexist in sediments under the same conditions (Martins et al., 2012). On the other hand, biotite ($AlFeH_2KMg_2O_{12}Si_3$) showed no significant correlation with any of the other minerals, which may be due to its low hardness (2.5–3 on the Mohs scale). The latter could result in high fragmentation and great changes in the grain size distribution, leading to transport and deposition differentiated of the sediments, which seems to be corroborated by factorial analysis (Factor 3), that discriminated between biotite and magnesium oxide (hardness 6 on the Mohs scale), as a result of differences in the hardness property of those minerals.

No minerals were found with S, I, P, and Mn, which may be due to the existence of these elements in amorphous materials, or as minor and/or trace elements in crystalline mineralogical structures (White, 2013; Caraballo et al., 2015).

The identified minerals and their abundance seem to support the idea that most of the sediment minerals found in the estuary were the result of the weathering of the upstream granitic rock. The type of granite identified was that of two micas - muscovite and biotite, with predominance

of the first one over the second one, contributing > 80% to the total minerals of the sediments. Despite the differences, mineral composition data did not show a clear seasonal variation in both types of sediment, since the data set for each season did not present a homogeneous trend in the concentration variation, nor differences capable of identifying it.

5.4.3 Major element concentrations and controlling factors

The distribution pattern of the chemical elements recorded by EDS-SEM analysis presented the following order of concentrations: (O) > Si > (C) > Al > K > Fe > Na > Ca > Mg > Cl > Ti > S > P > I > Mn, which is similar to the average crustal granite abundances (Turekian and Wedepohl, 1961). The higher values obtained for Si and O concentrations are in line with expectations. Since the Lima estuary is located in a granitic area as mentioned earlier, it was estimated that sediments would be composed mainly of quartz, a mineral consisting of Si and O. Actually, the values found of 47.8 and 29.3% for the O and Si, respectively, are in line with the amounts recorded for the crust (Dyar et al., 2008).

The strong correlation between the fine grain fraction (mud) and OM, reinforced by the positive correlation with the C concentration, suggests that OM is an important component of this fraction and may coat the surface of the mud particles as referred by Ho et al., (2010). Most of the chemical elements showed a statistically significant correlation ($p < 0.05$) with the amount of mud, with the exception of O, Si, and K. The decrease in the amount of Si and O was observed with the increase of the finer fraction, since they are structural elements of the silicate minerals, e.g., quartz-rich minerals, common in siliciclastic rocks, the sediments inorganic fraction (Pastor-Galán et al., 2013), being the OM a dilution element (Bouchez et al., 2011). The behavioral trend presented by Si and Al with the sediments grain size was inverse, since Al appeared essentially associated to the mud fraction (i.e., aluminosilicates), while the Si was found in greater quantities in coarser sediments, as reported by Cardoso et al. (2008). The affinity between the Si and the coarse fraction seems to suggest that it is composed of the minerals with greater hardness of the granite (quartz) (Guagliardi et al., 2013; Azam and Tripathi 2016). Factor analysis reinforced these results, since Factor 1 showed the same set of elements associated to mud and OM.

The distribution patterns of Al, Ca, C, Cl, Fe, Mg, P, Na, S, and Ti were similar to the presented by the finer grain fraction, with the exception of K. The high concentrations presented by K in coarser sediments can be related to the presence of K feldspar-rich rocks (microcline) in Lima watershed, and their weathering materials (Cardoso et al., 2008; Mil-Homens et al., 2014). The behavior presented by K suggests that it may belong to the structure of minerals with high hardness, as well as the enrichment of the suspended particles with K due to the leaching of agricultural soils. Measured Al and Na values seem to suggest the presence of albite, i.e.,

plagioclase feldspar present in the granites of the rock outcrops of the Lima basin (Mil-Homens et al., 2014) in the finer sediment fraction. While Mg, Ti, and Fe levels can be related to the presence in the composition of minerals with low hardness (e.g., biotite), or to their adsorption in finer particles, due to the larger specific surface and exchange capacity (Cardoso et al., 2008). Additionally, the observed relations between Fe and Al, Mg, Ti, and mud seem to indicate not only their affinity with the fine fraction but also the probable presence of iron oxides/hydroxides (Cardoso et al., 2008). The correlations of Ca, P, and Ti with mud fraction were not too strong (Table S5.2), suggesting that apart from being a constituent of clay minerals and adsorbed on the surface of clay particles, its distributions were also controlled by other factors, such as salinity, and the input of the elements by soil agricultural leaching. Additionally, these elements can be derived from ilmenite ($FeTiO_3$) and apatite ($Ca_5(PO_4)_3F$) deposits. The results suggest the natural origin of the elements due to the presence of Al, a conservative non-reactive element generally not associated with anthropic origin (Mil-Homens et al., 2014), used in geochemical normalization to distinguish between natural concentrations and influenced by anthropogenic inputs (Mali et al., 2015), which can be considered as an indicator of the aluminosilicate fraction of sediments (Tribovillard et al., 2006).

The K and Si appeared to be essentially of terrigenous lithogenic type, while Cl, Ca, I, Mg Na, S, and Ti were related to salinity, and therefore suggesting a marine influence (Cardoso et al., 2008; Valente et al., 2009). The chemical elements can be dissolved in seawater (Ca, Cl, I, Mg, Na, and S), and in marine fragments, which may be of biogenic origin (shells – Ca and Mg; calcite enriched-Mg) (Corredeira et al., 2008; Gredilla et al., 2015), or lithologic (e.g., anatase Ti). The strong correlations between S and OM and salinity, suggests its presence in the OM (Ho et al., 2010), associated with sulphate ions from seawater and marine aerosols (Hopkins et al., 2008). The same considerations can be inferred from the factor analysis (Factor 2). The occurrence of S, I, and P in minute quantities and with a correlation pattern similar to that evidenced by Al seems to suggest that they result from natural sources, being able to be part of silicate and aluminosilicate minerals of sediments of terrigenous and marine origin.

The association of the elements grouped in Factor 1 and Factor 2 seems to suggest the presence of aluminosilicate minerals, such as albite and zeolite, as well as halite. However, the presence of Mn and P in the same group of factorial analysis (Factor 4) may point to the existence, under aerobic conditions, of the removal of the soluble phosphate in the water column by adsorption onto manganese hydroxides coatings (Bojakowska, 2016; Lindeburg, 2017).

The sporadically occurrence of certain elements in sediments of the lower and middle estuary (Cu, In, and Mo) suggests an anthropogenic origin, i.e., chemical inputs from wastewater and activities such as energy usage, agriculture, transport, and industrial activities (Azam and

Tripathi 2016), since they occurred in sediments adjacent to the city of Viana do Castelo, where there are industrial and commercial facilities, as well as leisure and fishing port equipments (Ramos et al., 2010). Those elements in the dissolved form can be adsorbed into suspended solids (Martins et al., 2012), occurring their sedimentation and accumulation in sediments (Koukina et al., 2012).

The distribution of the elements in sediments along the estuary was associated to the hardness of the minerals where they are found, i.e., the minerals with greater hardness suffer less erosion, appearing generally as coarse sediments. The correlation shown by the elements with Si or Al suggests that the main differences of the elements arose as a function of the relative abundance of quartz and mud fraction (Pastor-Galán et al., 2013).

In estuaries, such as the Lima, the grain size distribution pattern and chemical composition of the sediments were controlled by factors, such as lithology, hydrodynamics, and morphology of the river and estuary, riverine and marine inputs, biological activity, paleoclimatic changes, and anthropogenic contamination (Martins et al., 2012). Surficial sediments seem to be mainly siliciclastic, containing a low percentage of bioclastic sediments (Oliveira et al., 2002). Indeed, the Lima sediments are most likely originated from igneous rocks containing quartz, feldspar, and two micas that experienced weathering process from the upstream stretches and settled down within the estuary, but eventually also from the sea at a smaller scale (Abdullah et al., 2015). Actually, the geochemical data presented by the sediments support a major riverine input, showing that the terrigenous component is derived mainly from the weathering and erosion of igneous and metasedimentary source rocks.

5.5 Conclusions

In this study, natural processes, such as weathering and erosion of bedrocks were the main supply sources of minerals in sediments. Among the major elements, more susceptible to rapid variations with lithology, silica, magnesium, potassium, and iron contents were compatible with the geology of the watershed bedrocks.

The natural origin of the elements, (33% terrigenous, 24% marine) seemed to be the major source in the Lima estuary sediments. Among chemical elements, only Cu, In, and Mo are of concern, which occasionally may be associated with adverse contamination. Therefore, identifying the magnitude of natural factors may contribute to the identification of the impact of human activities.

A similar study should be carried out using the fraction of particle size < 0.063 mm, to compare with the results obtained in this study, in order to ascertain to what extent fractions of coarser particle size may dilute the sediment samples, masking the role of anthropogenic factors in an estuarine environment.

5.6 SUPPLEMENTARY INFORMATION

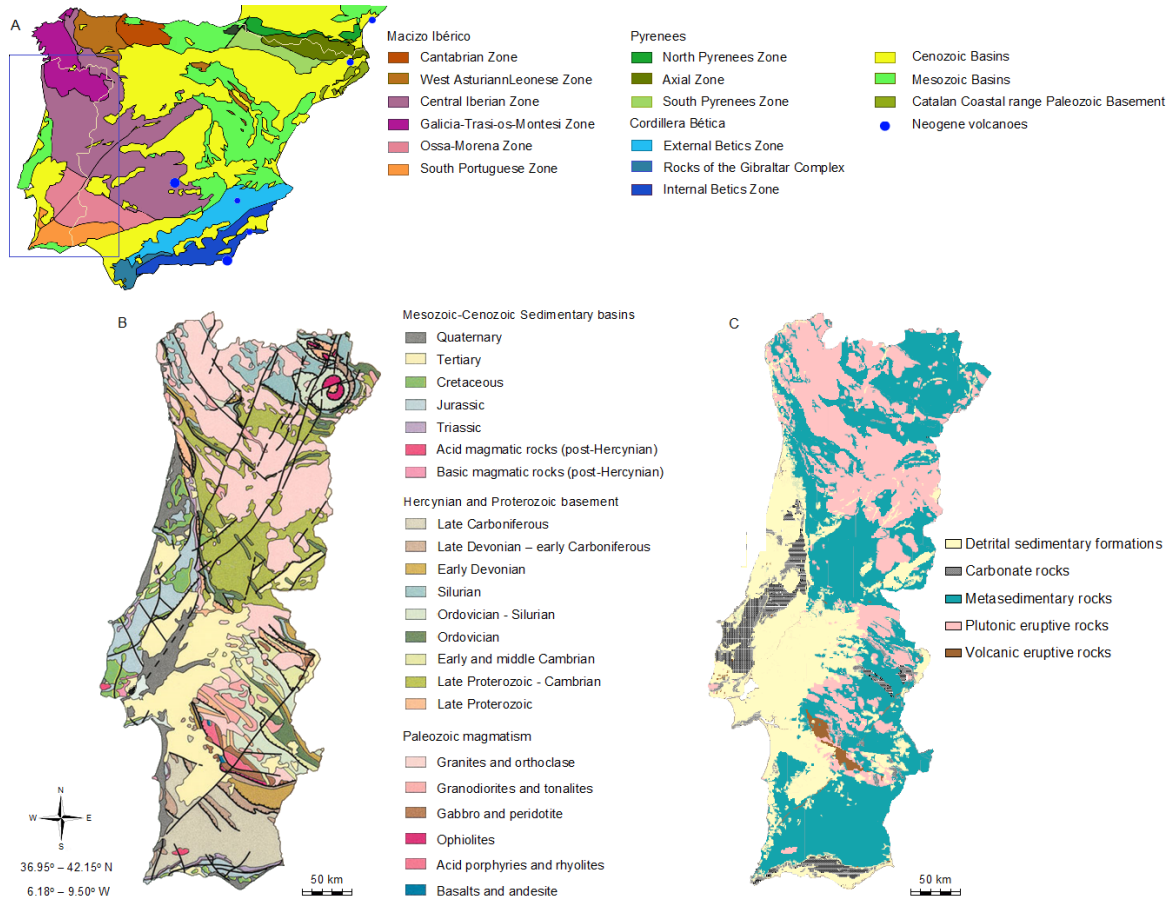

Figure S5.1 Geological information: A and B – Geologic maps; C – Lithological map (Simplified), (adapted from maps of LNEG – Laboratório Nacional de Energia e Geologia, 2017).

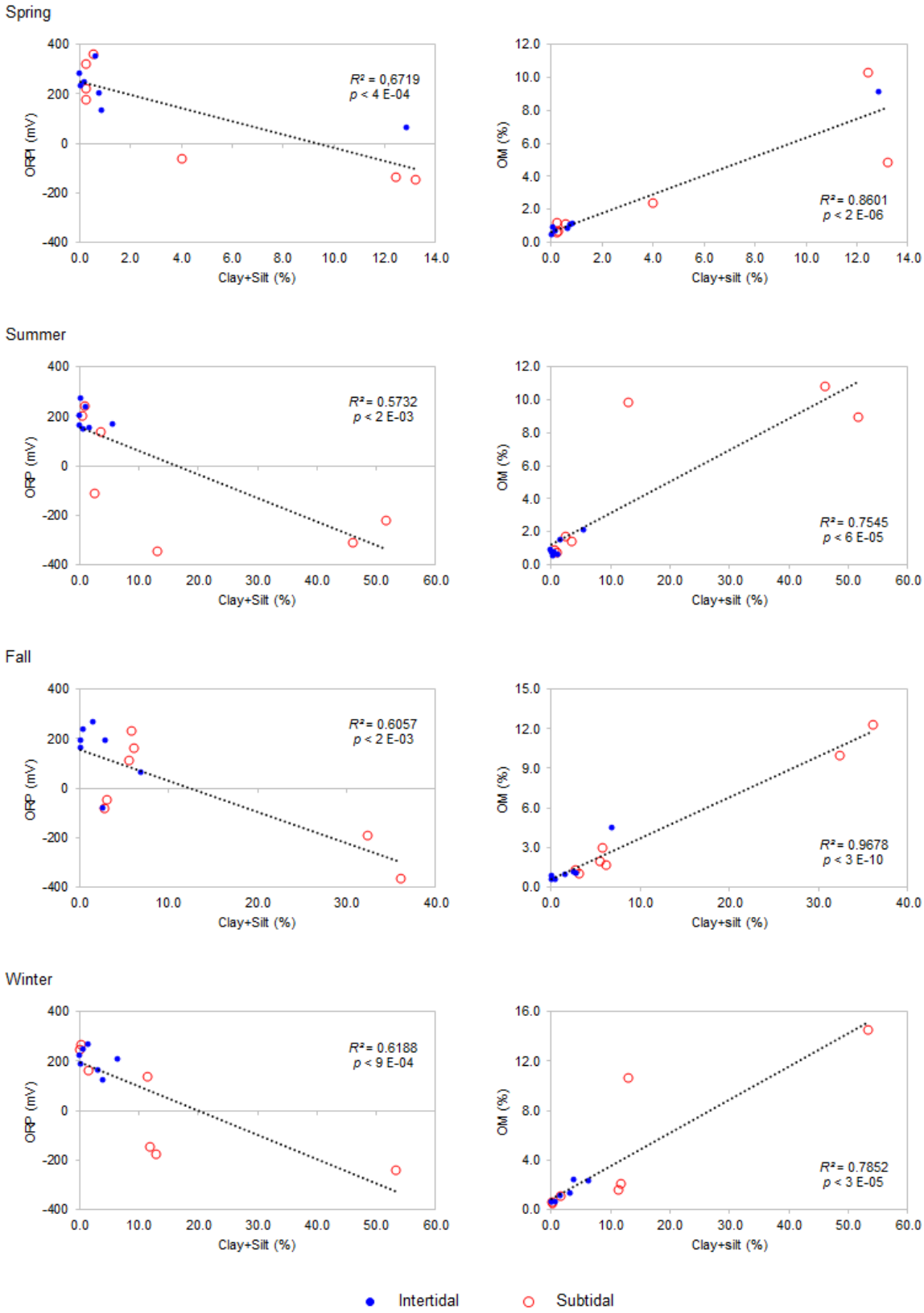

Figure S5.2 Correlation between the amount of silt and clay (mud), organic matter (OM) and oxidation-reduction potential (ORP).

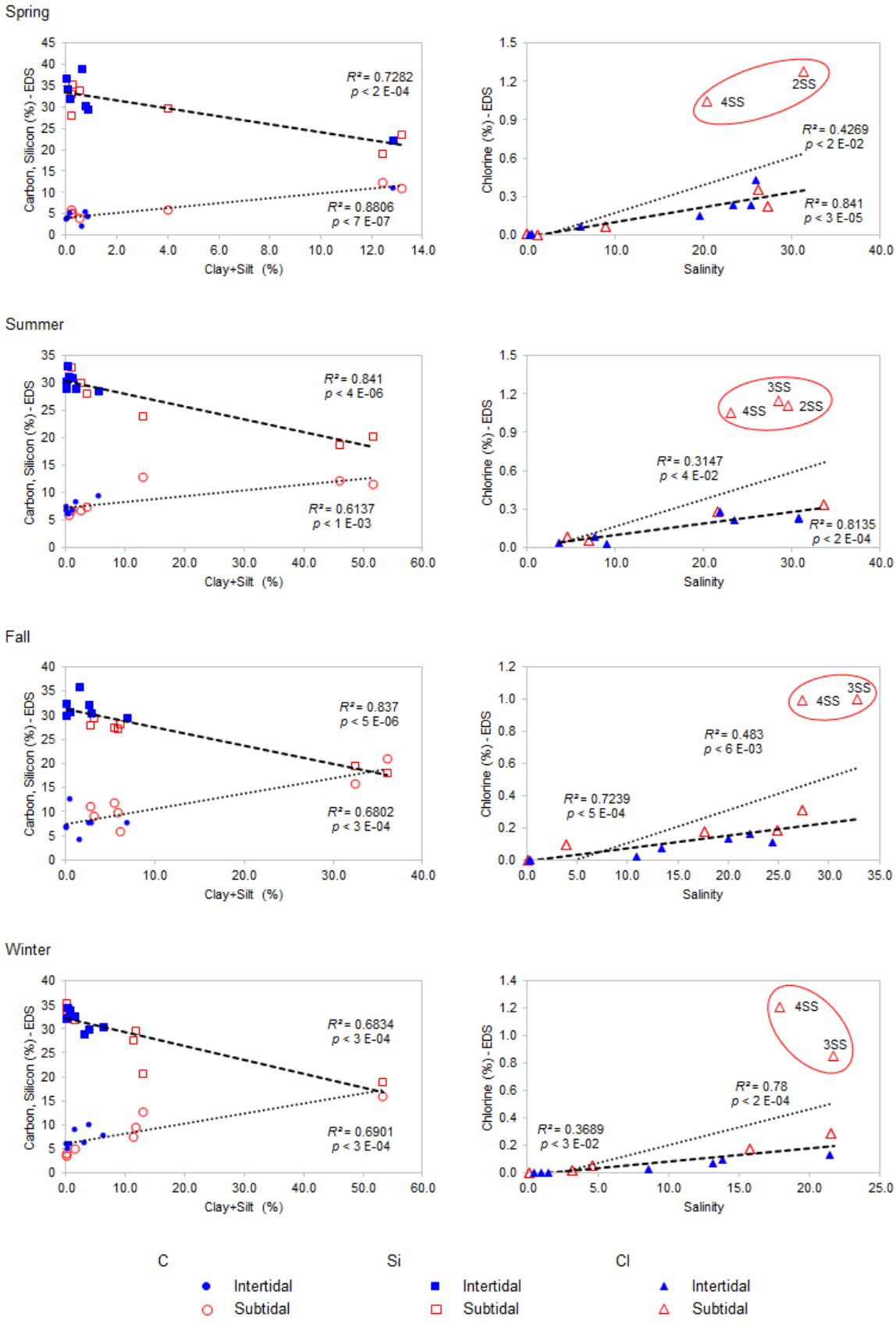

Figure S5.3 Correlation between the amount of silt and clay (mud), carbon and silicon; and chlorine and salinity.

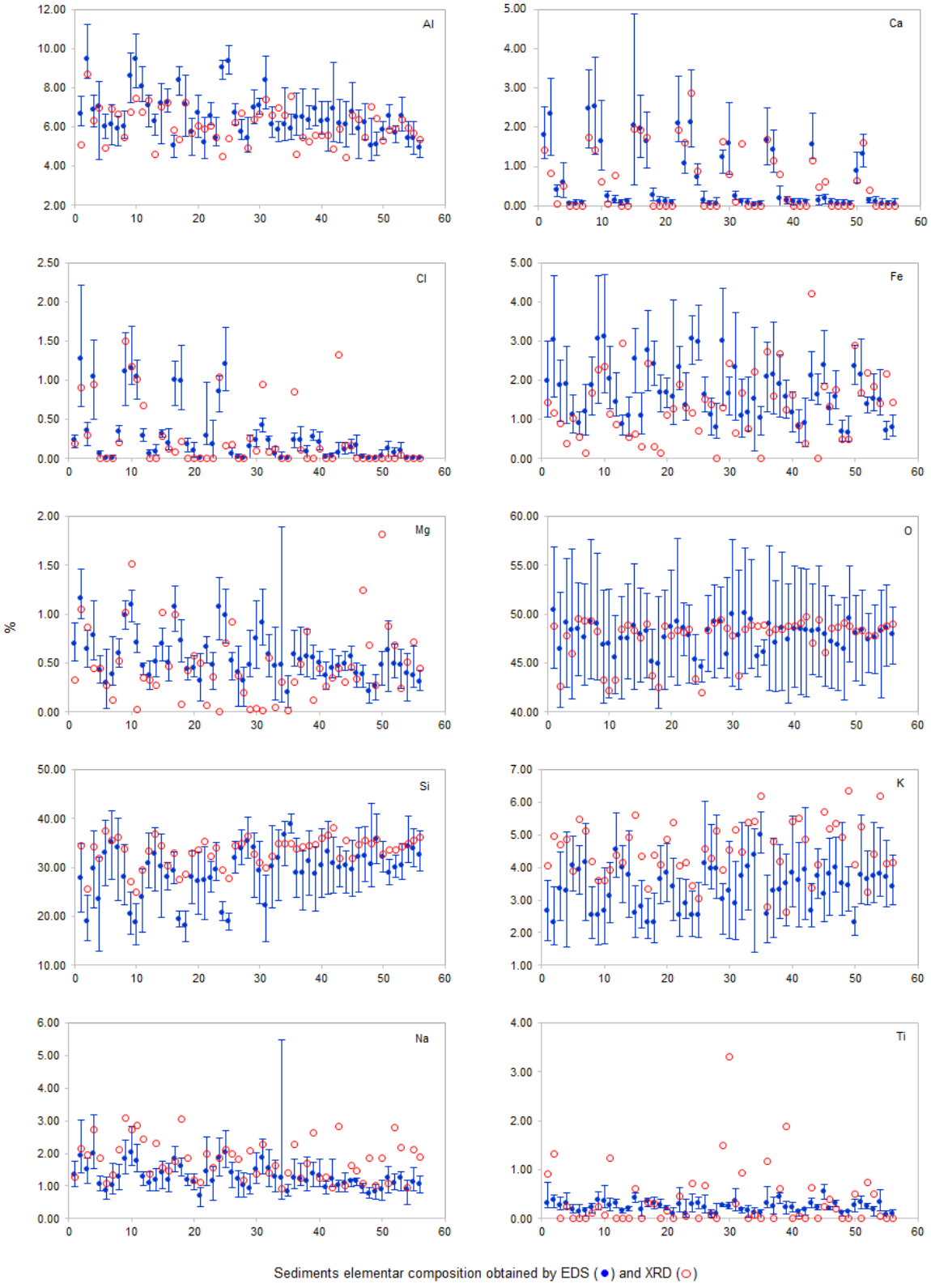

Figure S5.4 Elemental composition of the sediments by Energy Dispersion Spectroscopy-Scanning Eelectron Microscopy (EDS-SEM) and X-ray diffraction (XRD).

Table S5.1 Correlation coefficients obtained for mineral composition determinated by XRD. Only significant correlations are shown (p-value < 0.01 except underlined values with p-value < 0.05).

	Salinity	Mud	Gravel	Quartz	Albite	Microcline	Zeolite	Muscovite	Halite	Iron silicate	Anatase	Calcite	Iron (III) oxide	Magnesium oxide	Biotite
Salinity	1.000														
Mud	0.418	1.000													
Gravel	-0.582	-0.413	1.000												
Quartz	-0.386	-0.570	0.456	1.000											
Albite		0.324	-0.264	-0.399	1.000										
Microcline	-0.437	-0.434	0.422		-0.365	1.000									
Zeolite	0.562	0.490	-0.452	-0.544		-0.413	1.000								
Muscovite		0.313		*-0.611*		-0.384	0.465	1.000							
Halite	0.487	0.491	-0.433	-0.477		-0.521	*0.662*	0.493	1.000						
Iron silicate										1.000					
Anatase	0.362		-0.274			-0.415	0.338			0.425	1.000				
Calcite	*0.616*		-0.533			-0.419			0.350	0.306		1.000			
Iron (III) oxide										-0.377			1.000		
Magnesium oxide				-0.320									0.416	1.000	
Biotite															1.000

Note: **Bold**: very strong correlation (> 0.8); *Italic*: strong correlation (between 0.6 and 0.8).

Table S5.2 Correlation coefficients obtained for elemental analysis performed by EDS-SEM. Only significant correlations are shown (p-value < 0.01 except underlined values with p-value < 0.05).

	Salinity	Mud	Al	Ca	C	Cl	Cu	In	I	Fe	Mg	Mn	Mo	O	P	K	Si	Na	S	Ti
Salinity	1.000																			
Mud	0.418	1.000																		
Al	0.569	*0.697*	1.000																	
Ca	*0.678*	0.365	0.455	1.000																
C	0.410	*0.714*	0.479		1.000															
Cl	*0.629*	**0.827**	**0.836**	0.494	**0.713**	1.000														
Cu							1.000													
In								1.000												
I	0.487		0.296	0.564					1.000											
Fe	*0.665*	*0.635*	*0.779*	*0.673*	0.471	*0.719*			0.410	1.000										
Mg	*0.720*	*0.714*	**0.897**	*0.646*	0.547	**0.877**			0.464	**0.829**	1.000									
Mn				0.271					0.267			1.000								
Mo								0.593					1.000							
O		-0.554	-0.473		*-0.637*	-0.542				-0.449	-0.346			1.000						
P	0.401	0.265	0.553	0.309		0.454			0.264		0.539				1.000					
K	*-0.640*	-0.541	-0.479	-0.748	-0.583	*-0.614*			-0.361	*-0.723*	*-0.683*	0.370			-0.311	1.000				
Si	*-0.671*	*-0.794*	*-0.781*	-0.516	**-0.853**	**-0.889**			-0.311	*-0.740*	**-0.875**			0.443	-0.431	*0.725*	1.000			
Na	*0.660*	*0.703*	**0.847**	0.459	0.530	**0.886**			0.357	*0.654*	**0.922**		0.342	-0.323	0.537	-0.507	**-0.824**	1.000		
S	0.501	*0.713*	*0.770*	0.280	*0.652*	**0.801**				*0.622*	*0.780*		0.512	-0.527	0.442	-0.533	-0.786	*0.790*	1.000	
Ti	*0.613*	0.379	0.597	0.448	0.291	0.492			0.377	*0.766*	*0.642*				0.265	-0.523	-0.553	0.494	0.408	1.000

Note: **Bold**: very strong correlation (> 0.8); *Italic*: strong correlation (between 0.6 and 0.8).

Table S5.3 Factor loadings (Varimax normalized) of mineral variables in Factor Analysis

	Factor 1	Factor 2	Factor 3	Factor 4	Factor 5
Salinity	0.343	-0.083	0.117	**0.745**	-0.039
Mud	**0.612**	0.307	-0.114	0.283	-0.318
Gravel	-0.289	0.028	0.045	**-0.674**	0.287
Quartz	**-0.780**	0.006	-0.196	-0.088	***0.400***
Albite	0.029	0.072	-0.005	0.039	**-0.976**
Microcline	-0.344	0.061	0.239	***-0.594***	0.315
Zeolite	**0.733**	-0.121	-0.063	0.371	0.010
Muscovite	**0.836**	-0.145	0.185	0.001	0.151
Halite	**0.704**	0.010	-0.108	***0.419***	0.030
Iron silicate	0.004	**-0.615**	0.292	0.381	0.081
Anatase	0.116	**-0.631**	0.031	***0.403***	-0.143
Calcite	0.040	-0.038	0.062	**0.860**	0.169
Iron (III) oxide	-0.052	**0.816**	0.066	0.163	-0.132
Magnesium oxide	0.210	***0.463***	**0.700**	0.218	0.013
Biotite	0.024	0.257	**-0.805**	0.104	0.002
Expl.Var	3.098	1.870	1.407	2.898	1.493
% Total variance	20.65	12.47	9.381	19.32	9.96
Cumulative %	20.65	33.12	42.50	61.82	71.78

Note: **Bold**: high to very high loading (> 0.6); **Bold** and *Italic*: moderate loading (between 0.4 and 0.6); Regular: low loading (< 0.4).

Table S5.4 Factor loadings (Varimax normalized) of geochemical variables in Factor Analysis

	Factor 1	Factor 2	Factor 3	Factor 4	Factor 5
Salinity	0.373	**0.732**	0.044	-0.036	0.245
Mud	**0.823**	0.265	-0.047	-0.059	-0.069
Al	**0.742**	***0.490***	0.029	0.235	-0.107
Ca	0.145	**0.852**	-0.139	-0.178	0.205
C	**0.845**	0.055	0.003	-0.189	0.082
Cl	**0.866**	***0.407***	-0.040	-0.002	0.026
Cu	-0.097	0.069	0.014	-0.058	**0.882**
In	-0.130	0.086	**0.888**	0.027	-0.026
I	-0.103	**0.751**	0.161	0.377	0.083
Fe	***0.527***	**0.740**	0.040	-0.153	-0.197
Mg	**0.687**	**0.668**	0.088	0.133	0.027
Mn	-0.105	-0.141	0.135	**0.791**	-0.076
Mo	0.227	0.009	**0.873**	0.099	0.019
O	**-0.742**	0.121	0.136	0.238	0.138
P	***0.405***	0.281	-0.130	***0.478***	***0.426***
K	***-0.428***	**-0.672**	-0.064	0.380	-0.175
Si	**-0.818**	***-0.468***	-0.088	-0.010	-0.068
Na	**0.740**	***0.472***	0.141	0.245	0.088
S	**0.835**	0.247	0.351	0.078	0.023
Ti	0.296	**0.698**	0.092	-0.013	-0.138
Expl.Var	6.599	4.866	1.830	1.446	1.220
% Total variance	32.99	24.33	9.150	7.232	6.099
Cumulative %	32.99	57.32	66.47	73.71	79.81

Note: **Bold**: high to very high loading (> 0.6); **Bold** and *Italic*: moderate loading (between 0.4 and 0.6); Regular: low loading (< 0.4).

CHAPTER 6

Spatial patterns in Sediment and Water Column Nutrients in the mesotidal Lima Estuary (NW Portugal)

Abstract

Materials delivered to the estuary undergo transformation processes before being carried up to the open sea, being important to understand these processes, and to establish to which extent they modify such compounds fluxes as nutrients in transitional waters. At present, environmental coastal studies reveal interest in knowing the direction and magnitude of inorganic nutrients and organic matter, as well as the exchange fluxes between the water column and bottom sediments. These processes, together with the hydrographic conditions, define a fundamental role of these environments, i.e., its function as a sink or source of nutrients and organic matter. Indeed, in estuarine sediments, processes of exchange of organic compounds and nutrients are influenced by the river outflow and tidal cycles, with the sediments acting as a source or sink of nutrients into or out to the water column. Although Lima estuary system is subject to a highly variable seasonal supply of nutrients due to the variable flow of freshwater associated with intense rainfall during the wet seasons (October-April), the results showed that the variability in the nutrient concentrations in pore-water and in sediments with different grain size, was greater than its temporal and spatial variation, suggesting that, for intertidal and subtidal sediments, grain size was an important factor for the dynamics of those quantities. The input of seawater into the estuary was a relevant factor for the spatial differences found in samples from the two estuarine compartments.

Keywords: nutrients; sediments; pore-water; water column; Lima Estuary.

6.1 Introduction

Estuarine and coastal systems are biologically productive areas that play a relevant role in global biogeochemical cycles (Negrin et al., 2011), with spatial and temporal variations in estuarine nutrients extensively studied, because of their importance to estuarine primary producers (Boyle et al., 2004). In some estuarine areas, in addition to the natural seasonal variations of nutrients, it is pertinent to consider anthropogenic nutrient sources (Michel et al. 2000; Boyle et al., 2004), and studies have been carried out to evaluate the effects of anthropogenic eutrophication in estuarine nutrient dynamics and its impacts on macroalgal

blooms, especially in shallow estuaries (Taylor et al., 1995; Boyle et al., 2004). In many estuaries, nutrient supplies are mainly controlled by freshwater inflow from rivers (Mackas and Harrison, 1997; Boyle et al., 2004), depending on the volume and nutrient concentration of the river flow, which varies both seasonally and annually. Seasonal variations in nutrient flux in response to physical and chemical factors variations (e.g., water quality, temperature, sediment condition) have been reported (Sakamaki et al., 2006), as well as the link between watershed inputs and nutrient supplies to estuarine primary producers (McClelland and Valiela, 1998; Boyle et al., 2004).

Estuaries are generally characterized by a close coupling between benthic and pelagic processes, with organic matter being produced by a wide variety of primary producers connected to the sediments (i.e., microphytobenthos, macroalgae, and rooted macrophytes), and to the water column (e.g., phytoplankton)(Marcovecchio et al., 2009). In addition, the occurrence of an efficient water column mixing and frequent re-suspension events ensure the rapid vertical transport of organic and inorganic matter by integrating the pelagic and benthic food chains, moderating the biogeochemical processes function (Xu and Hood, 2006; Marcovecchio et al., 2009). Several physical, chemical, and biological factors affect the nutrient exchange process at the sediment-water interface, i.e., the extent to which nutrients are released or taken up by benthic communities (Feuillet-Girard et al., 1997). The nutrient exchange flux and the vertical concentration profile in the sediment are influenced by the nutrient concentrations variations of the overlying water (Magalhães et al., 2002; Sakamaki et al., 2006), water temperature (Sundbäck et al., 2000), hydrodynamic condition (Oldham and Lavery, 1999; Sakamaki et al., 2006), and sediment condition (Sloth et al., 1995; Sakamaki et al., 2006), as well as biological processes, such as, mineralization of organic nutrients (Yin and Harrison, 2000; Sakamaki et al., 2006), oxygen production and nutrient uptake by benthic microalgae (Asmus et al., 2000; Wilson and Brennan, 2004), nitrification and denitrification (Sundbäck et al., 2000), and various macrofaunal activities, for example, irrigation, excretion, respiration, and physical disturbance of sediment (Webb and Eyre, 2004). Benthic-pelagic fluxes are dependent on nutrient concentrations in the water column (Asmus et al., 2000), being the sediment oxidation state determining the influx or efflux of nutrients (Rysgaard et al., 1996), and the remineralization dependent of the amount of labile organic matter (Sloth et al., 1995; Asmus et al., 2000). Nutrient fluxes at the sediment-water interface can influence or regulate the water column nutrient composition since the sediment can behave as a sink or as a source of inorganic nitrogen, phosphorus, and silica through different biogeochemical processes (Feuillet-Girard et al., 1997).

The surface sediments typically accumulate high loads of organic matter, being regions of intense microbial activity and nutrient cycling, characterized by high concentrations of nitrogen and soluble phosphorus from the remineralization of deposited organic matter and

anthropogenic sources (Dunn et al., 2017). Those sediments become an additional sources of nutrients for surface waters (Kamer et al., 2004; Dunn et al., 2017), with a well established nitrogen and phosphorus release (e.g., Clavero et al., 2000; Grenz et al., 2000; Kamer et al., 2004). Organic matter mineralization in the sediments upper layers releases inorganic nutrients to the pore-water, which can be exchanged with the water column by diffusive and advective transport processes, or adsorbed in organic compounds or clay particles in the sediment (Coelho et al., 2004; Garcia-Robledo et al., 2016), being consumed by microalgae and prokaryotes for assimilation or dissimilation purpose (Garcia-Robledo et al., 2016).

The nutrient exchange through the water-sediment interface that modifies the nutrient reservoirs (pore water, exchangeable/adsorbed and strongly bound) and the water column conditions (Eyre et al., 2010; Dunn et al., 2017), has as key processes, the passive diffusion of solutes, biota-mediated transport (bioirrigation, bioturbation and bioresuspension (Graf and Rosenberg, 1997), and physical disturbances and sediment resuspension (Couceiro et al., 2013; Dunn et al., 2017). The mixing of sediments into the water column due resuspension releases nutrients from the pore-waters and surfaces of the sediment grains (Fanning et al., 1982), depleting the sediment reserves and being able to stimulate the growth of phytoplankton (Fanning et al., 1982), bacteria (Wainright, 1987), and microheterotrophs (Lawrence et al., 2004) in the water column. In the short term, physical disturbance increases the depth of sediments oxygen penetration, allowing faster organic matter mineralization (Forehead et al., 2012). Sediments disturbance and resuspension events may occur under natural circumstances (e.g., tidal currents and wave induced), and as a result of anthropogenic activities such as vessel movement, mooring, and dredging practices (Zhang et al., 2010; Dunn et al., 2017). Anthropogenic activities can lead to negative impacts on water quality, altering suspended sediment and nutrient loadings (Jing et al., 2013), and modifying the fauna biology of bottom sediments (Wulff et al., 1997), and the water column communities (Zhang et al., 2010; Cabrita, 2014; Dunn et al., 2017).

It is accepted that nutrient flux from sediments increases nutrient availability in the water column to primary producers (Kamer et al., 2004), by releasing regenerated nutrients (N and P) from the sediments to the water column in shallow water systems (Asmus et al., 2000; Koho et al., 2008; Human et al., 2015). The role of estuarine sediments as a source of nutrients may be important in systems with nutrient inputs are episodic and availability of nutrients in the water column fluctuates over short time scales (Day et al., 1995), or with strong spatial gradients in water column nutrient availability exist (Nedwell et al., 2002; Kamer el al., 2004).

Most studies are based on processes in subtidal sediments, unlike processes in intertidal sediments (Yin and Harrison, 2000), being the estuarine intertidal flats an important interface between the river discharge and marine waters. Intertidal sediments receive large amounts of sediment-bound nutrients and organic materials from the river, acting as a platform for the

processing of these sediment-bound organics or nutrients that pass through it, therefore they may represent a source or sink of a nutrient into or out of the water column during tidal cycles. The processes involved in nutrient uptake or release from the sediment are complex and depend on the location, depth within the water column, and tidal phases (Yin and Harrison, 2000), being these sediments nutrient-specific, and seasonally dependent (Watson et al., 1993). In estuaries with extensive intertidal flats and mudflats, pore-water exchange occurs between the sediment and the overlying water column only during the high tide, when the tide flats are immersed, with those areas for tidal cycle remaining time exposed to atmosphere (Feuillet-Girard et al., 1997; Marcovecchio et al., 2009). This makes possible to change the redox zone as the air floods the sediments, altering the early diagenetic environment (Marcovecchio et al., 2009). Alternate flooding and exposure of saltmarhes surface by tides are important for remineralization and nutrient cycling, with nutrient and organic matter concentrations in the sediments pore-water that may to vary due to the transformations that the nutrients undergo in the sediment (Negrin et al., 2011). Moreover, the tidal dilution effect may decrease the pore-water concentration of nutrients and organic matter, with tidal currents being the main transportation vehicle of material into or out of saltmarshes (Negrin et al., 2011). An assessment of the spatial and temporal distribution of nutrients is essential to evaluate the cycling of biophilic elements, e.g. nitrogen, phosphorus, and silicon (Magni and Montani, 2006). In estuaries with tidal flats, numerous processes influence nutrient behavior, whether they show a conservative mixing or reflect removal or addition along the estuary (Magni et al., 2002), with the variability related to the interaction between water chemistry, tidal hydrology, and sedimentation processes (Magni and Montani, 2006). The nutrient exchange between the sediment and water interface (benthic-pelagic coupling) in intertidal and subtidal areas of estuaries can play two important and opposing roles (Human et al., 2015), that is, the fluxed regenerated nutrients into the water column are able to provide most of the N and P required for the phytoplankton primary production (Cowan et al., 1996), while bacterial mats remove large amounts of inorganic nutrients from the water column (Human et al., 2015). The primary producers act as a biological control of coastal eutrophication, since nutrient loads are taken by them and removed from the water column. As the removal and production processes are simultaneous, the net direction of the nutrient flux will depend on the dominant process (Magalhães et al., 2002).

The processes in estuarine sediments regulate the flow of nutrients from terrestrial sources to the ocean, and influence the estuarine ecosystems productivity (Yin and Harrison, 2000). In general, 25% of the water column nitrogen used in primary productivity is supplied by sediment nitrogen fluxes (Kemp and Boynton, 1984; Yin and Harrison, 2000), and between 1/4 and 1/2 of the allochthonous carbon inputs plus autochthonous primary productivity are oxidized by sediments (Yin and Harrison, 2000). With increasing human pollution, estuarine sediments

represent a primary repository of anthropogenic chemicals entering the marine environment (Yin and Harrison, 2000).

This study aims to characterize the spatial and temporal variations of nutrient concentrations in the water column, pore-water, and sediments, in response to seasonal variations of water column caused by hydrodynamics and environmental conditions, to investigate the relationship between nutrients of water column, pore-water, and sediments, to verify the relationship between the nutrients behavior of subtidal and intertidal sediments, and to determine the role of the Lima estuary as a sink or source of nutrients. To achieve these goals, the seasonal concentrations of nutrients in the water column, pore-water, and subtidal and intertidal sediments along the estuary were determined, with sediment samples collected on sandy and muddy flats, and surveys always performed during the emersion periods (ebb tide) to simplify the sampling strategy.

6.2 Material and methods

6.2.1 The study area

The Lima temperate estuary, with a geographical coordinates of 41.68º N; 8.84º W, has a semi-diurnal and mesotidal regime (Vale and Dias, 2011), an extension of about 20 km and an average flow of 70 $m^3 s^{-1}$ (Ramos et al., 2006) (Figure 6.1). According to its characteristics, the estuary can be divided into three sections - lower, middle, and upper stretches. The lower estuary located in an area with anthropogenic modifications, such as a jetty and constant dredging, include a shipyard, a commercial seaport, a marina, and a fishing port, is constituted by a narrow and deep navigation channel (9 m) with walled benches (Ramos et al., 2010). The middle estuary corresponds to a saltmarsh area with several sand islands and intertidal channels. The most upstream section of the estuary, the upper estuary, is characterized by a narrow, shallow channel with some intertidal areas and undisturbed banks remaining almost in a natural state (Rebordão and Teixeira, 2009). Throughout its course, there are areas with wastewater discharges that introduce substances transported from urban, industrial, and agricultural areas into the estuary (Almeida et al., 2011).

Figure 6.1 Satelite image of the Lima estuary sampling stations (source: Google Earth). The sampling locations for the water column and subtidal sediments were represented with yellow circles, and for intertidal sediments with red circles.

6.2.2 Sampling

Sampling surveys were carried out on May (spring), July (summer), and November (fall) of 2015, and January (winter) of 2016 on the ebb tide. The collection of samples started 1:30 h before slack water. Samples of sediments were collected from 14 locations (7 subtidal - SS and 7 intertidal - SI) along 12.6 km (Figure 6.1). The water column samples were collected over subtidal sediments. At each sampling station, vertical profiles of salinity, temperature, turbidity, pH, and dissolved oxygen (DO) were obtained with a YSI 6820 CTD multiprobe, calibrated according to the instructions from the manufacturer. The data for the water column presented for the remaining parameters resulted from the analytical determination of the samples collected in the water column with a Van Dorn bottle (surface and bottom water). Pore-water samples were also collected for the subtidal and intertidal sediments by suction. The oxidation-reduction potential (ORP) was measured directly on the wet sediment with a pH meter HI 9023, using an electrode (HI 3130, Hanna Instruments) and a temperature probe (HI 7669/2W). All collected samples were kept refrigerated in an ice chest until processing in the laboratory.

6.2.3 Analytical procedures

For the determination of total suspended solids (TSS) and volatile suspended solids (VSS), the water samples were filtered through pre-combusted glass fiber filters (GF/F Whatman), and dried at 105 °C (TSS), followed by combustion at 550 °C (VSS) (APHA, 2005). The dissolved orthophosphate, ammonium and silicate determinations were performed by the

methods of Koroleff (Grasshoff et al., 1983). The NO_x (nitrate+nitrite) concentration was obtained by the method described by Jones (1984) and adapted by Joye and Chambers (1993). Determination of total dissolved carbon (TDC), dissolved organic carbon (DOC), and total dissolved nitrogen (TDN) was performed by high-temperature catalytic oxidation with a TOC-VCSN analyzer (Shimadzu Instruments). All analyzes were performed in triplicate. The analytical technique used for the chlorophyll *a* determination was molecular absorption spectrophotometry after extraction using 90% acetone (Parsons et al., 1984), and quantification using the SCOR-UNESCO equations (1966).

The sediment samples were dried at 105 ^oC (24 h), and ignited at 500 ^oC (4 h) for the determination of total volatile solids (TVS), a measure of organic matter content (APHA, 2005). The nutrient concentration determinations were performed on dried samples at 40 ° C for 24 hours. The nutrient determination in sediments was performed by the above-mentioned methods, after extraction processes. The NH_4^+ and NO_x were extracted with KCl (2M) (Keeney and Nelson, 1982; Mudrock et al., 1997). The inorganic phosphorus was extracted with HCl for 16 hours with stirring while for the determination of total phosphorus a previous calcination was carried out (Aspila et al., 1976). The biogenic silica extraction method used was the wet chemical alkaline extraction technique with 1% Na_2CO_3 solution and samples sub-sampled at 3, 4 and 5 hours to determine the correction factor of the mineral silicate (Conley and Schelske, 2001; DeMaster, 1981; Mortlock and Froelich, 1989; Sauer et al., 2006). All analyses were performed in triplicate. For the determination of sediment granulometry or grain size estimation, the dry samples were sieved and seven fractions were obtained: silt and clay (< 0.063 mm), very fine sand (0.063–0.125 mm), fine sand (0.125–0.250 mm), medium sand (0.250–0.5 mm), coarse sand (0.5–1 mm), very coarse sand (1–2 mm), and gravel (> 2 mm). Each fraction was weighed and expressed as a percentage of the total weight.

6.2.4 Data analysis

Bi-dimensional contour plots, generated by Surfer 8.01 software (Golden Software Inc.), were used to represent seasonal variations of the measured variables (nutrients) in estuarine compartments. Data were interpolated using the Kriging gridding method (linear variogram model).

STATISTICA 13.0® software package was used to perform the basic statistics. Principal component analysis (PCA) was performed to investigate patterns of similarity between samples based on environmental variables, in data previously log transformed to account for the non-normal distribution of variables and normalized to account for the different units in which variables expressed.

6.3 Results

6.3.1 General water column characteristics

The seasonal water column physical-chemical characteristics are showed in the Table 6.1.

Table 6.1 General characteristics of the water column in the Lima estuary.

Season	Site	Temp.	Sal.	pH	Turb.	DO	Chl *a*	TDC	DOC	TDN	TSS	VSS
Spring	L1	17.96	21.33	7.99	2.45	8.42	-	-	-	-	-	-
	L2	18.30	22.18	8.01	2.40	8.28	1.52	22.46	1.30	0.42	47.40	10.80
	L3	17.95	19.99	7.97	1.90	8.33	1.47	22.53	1.53	0.48	41.00	9.30
	L4	18.06	17.77	7.63	2.75	8.55	0.95	15.87	1.49	0.66	29.50	6.40
	L5	18.55	5.82	6.71	1.05	8.99	1.12	9.52	0.97	0.53	21.90	5.30
	L6	18.08	0.06	6.62	1.00	9.14	0.86	3.71	0.82	0.63	5.70	1.70
	L7	18.40	0.04	6.65	1.85	8.84	1.03	4.10	0.85	1.18	6.20	2.10
Summer	L1	17.22	27.94	7.56	1.80	7.63	4.92	27.65	1.36	0.37	55.50	14.60
	L2	18.25	26.63	7.77	1.35	7.74	4.31	26.15	1.28	0.35	53.60	12.80
	L3	19.21	24.66	7.72	1.90	7.82	4.80	25.23	1.25	0.41	56.40	13.50
	L4	21.01	20.59	7.80	2.80	7.97	7.61	21.18	1.16	0.36	50.80	12.70
	L5	22.55	13.80	7.69	1.10	8.32	13.92	15.75	0.91	0.39	32.00	9.00
	L6	24.25	2.57	7.02	2.60	8.06	16.22	7.25	1.09	0.56	16.00	5.30
	L7	24.69	0.92	6.98	2.90	7.86	9.77	4.90	0.90	0.63	12.80	4.30
Fall	L1	16.86	25.99	8.25	5.70	7.96	1.17	21.07	0.73	0.31	48.20	12.80
	L2	16.66	22.23	8.48	4.25	8.20	1.23	19.58	0.82	0.56	43.10	10.90
	L3	16.80	24.45	8.49	6.95	8.12	1.58	20.09	0.80	0.27	49.70	12.20
	L4	16.62	18.05	8.40	4.35	8.56	1.50	14.50	1.14	0.43	34.60	8.40
	L5	16.18	9.10	8.29	4.35	9.10	1.56	9.76	1.22	0.38	21.00	5.60
	L6	14.89	0.18	8.71	7.50	9.98	1.20	3.77	1.30	0.49	6.10	2.50
	L7	15.03	0.08	8.43	1.40	9.93	1.50	3.45	1.37	0.55	4.50	1.40
Winter	L1	11.52	12.47	8.20	1.25	9.91	0.26	7.86	0.95	0.35	14.20	3.30
	L2	11.00	4.30	8.29	-	10.72	0.10	5.77	0.87	0.49	8.20	2.50
	L3	11.05	2.76	8.19	-	10.82	0.23	5.58	0.88	0.49	7.60	2.10
	L4	11.16	2.32	8.13	-	10.97	0.25	4.37	1.64	0.68	7.80	2.20
	L5	10.87	0.67	8.25	-	11.14	0.16	3.04	0.81	0.48	4.90	1.70
	L6	11.07	0.09	8.47	1.70	11.17	0.05	3.06	0.84	0.65	3.20	1.50
	L7	11.67	0.07	7.90	-	-	0.12	5.85	1.64	1.14	5.00	1.70

Parameters abreviations and units: Temp. – Temperature (^{o}C); Sal. – Salinity; pH – Sørensen scale; Turb. – Turbidity (NTU); DO – dissolved oxygen (mg O_2 L^{-1}); CHL a – chlorophyll *a* (m m^{-3}); TDC – total dissolved carbon (mg L^{-1}); DOC – dissolved organic carbon (mg L^{-1}); TDN – total dissolved nitrogen (mg L^{-1}); TSS – total suspended solids (mg L^{-1}); and VSS – volatile suspended solids(mg L^{-1}).

The salinity decrease upstream the estuary was accompanied by a decrease in TDC, DOC and suspended solids (TSS, VSS) during all seasons. Therefore, the highest values were

recorded at the most downstream stretch, near the estuary mouth (L1) during the summer, with the values of 27.65 mg L^{-1}, 55.50 mg L^{-1} and 14.60 mg L^{-1} for the TDC, TSS and VSS, respectively. Lower values were showed during winter (TDC and TSS) and fall (VSS), at upstream locations. DOC had two distinct behaviors, one during the dry seasons identical to that reported for TDC, and the other with the inverse pattern during the wet seasons, i.e., with increase along the estuary upstream from the mouth of the estuary. However, DOC did not show a clear and consistent behavior, indicating the existence of potential sources (dry seasons), and sinks (wet seasons), along the estuary. The TDN did not show appreciable variations along the estuary, whereas chlorophyll *a* showed the highest values during the summer in the upper estuary, while in the remaining seasons peaked in the lower estuary. Nevertheless, chlorophyll *a* did not show a consistent behavior with salinity. As expected, the decrease in salinity was accompanied by an increase in dissolved oxygen.

6.3.2 Sediments characteristics

Intertidal sediments showed positive values for the oxidation-reduction potential (ORP), while subtidal sediments collected at L2, L3 (lower estuary), and L4 (middle estuary) presented mostly negative values (reduction conditions) in all seasons (Table 6.2). These sediments recorded higher amounts of organic matter (OM), with a maximum in the subtidal sediment collected at L4 (TVS, 14.51% in dry matter), during the winter. These locations also presented the higher occurrence of organic matter within the intertidal sediments, with a maximum value of 9.07% (TVS in dry matter) obtained at the L3. Sediments with higher TVS content also showed higher humidity, 63.38% (L4), and 34.40% (L3), for the subtidal and intertidal sediments, respectively. The pattern of decreasing salinity from the estuary mouth to the upstream river was generally accompanied by pH, however this trend was not very marked.

Table 6.2 General characterization of the sediments in the Lima estuary.

		Sediments: Subtidal (SS)						Sediments: Intertidal (SI)					
Season	Site	Sal.	ORP (mV)	Temp. (ºC)	pH	Hum. (%)	TVS (%)	Sal.	ORP (mV)	Temp. (ºC)	pH	Hum. (%)	TVS (%)
Spring	L1	27.2	220.6	21.0	7.69	21.60	1.17	19.6	230.2	22.6	7.55	22.52	0.89
	L2	31.3	-138.3	17.1	7.70	57.97	10.29	25.3	133.2	20.5	7.00	20.54	1.13
	L3	26.1	-62.9	20.3	7.32	22.36	2.39	25.9	63.2	20.0	6.90	34.40	9.07
	L4	20.3	-144.2	18.5	6.83	39.66	4.89	23.3	203.5	22.1	7.03	17.55	1.01
	L5	8.8	176.2	19.6	7.17	19.51	0.61	6.0	245.2	20.5	6.11	20.49	0.66
	L6	1.2	318.9	17.2	7.48	19.59	0.66	0.5	279.5	21.2	7.34	17.36	0.44
	L7	0.0	359.5	19.4	7.56	23.27	1.09	0.2	352.6	19.1	8.01	20.51	0.80
Summer	L1	33.6	139.6	26.8	7.40	23.61	1.43	30.7	163.0	24.9	7.78	22.59	0.91
	L2	29.6	-221.0	16.8	7.46	53.25	8.94	30.8	152.0	21.7	7.83	21.37	1.52
	L3	28.4	-310.0	16.9	7.47	57.24	10.82	7.7	146.0	22.5	7.72	21.29	0.75
	L4	23.1	-347.0	19.4	7.11	50.86	9.84	21.8	168.0	21.6	6.90	23.14	2.08
	L5	21.6	202.1	23.2	7.45	18.94	0.86	23.4	202.1	22.8	7.75	18.11	0.73
	L6	7.0	240.1	24.9	6.91	16.71	0.72	9.0	269.5	26.5	7.07	14.86	0.55
	L7	4.6	-112.5	25.3	6.86	23.28	1.75	3.6	237.5	26.5	6.98	16.14	0.63
Fall	L1	27.3	162.7	16.8	7.86	23.23	1.69	13.4	189.5	16.4	7.92	26.46	0.82
	L2	24.9	-44.4	16.2	7.85	16.56	1.01	24.4	194.3	16.9	7.86	19.28	1.06
	L3	32.8	-189.7	16.8	7.93	53.57	9.94	20.0	61.8	16.6	7.20	26.68	4.47
	L4	27.3	-363.1	15.5	7.82	54.60	12.29	22.2	-82.1	16.4	7.29	21.77	1.12
	L5	17.6	-83.7	16.0	7.77	21.25	1.35	10.9	160.3	16.1	7.73	18.21	0.56
	L6	3.9	230.1	15.9	6.03	29.07	3.03	0.4	235.4	15.9	7.83	18.20	0.57
	L7	0.2	111.2	15.6	6.53	27.42	1.98	0.3	268.7	16.1	7.41	22.54	0.94
Winter	L1	21.5	136.2	12.3	7.92	20.52	1.62	8.6	222.2	11.8	8.08	17.40	0.64
	L2	15.8	-146.4	12.1	8.00	20.13	2.11	21.4	162.7	12.2	8.02	21.66	1.32
	L3	21.7	-178.6	12.0	7.30	52.78	10.64	13.1	120.2	11.8	8.02	23.74	2.43
	L4	17.9	-241.7	11.8	7.02	63.38	14.51	13.8	206.7	11.7	7.65	23.56	2.29
	L5	4.6	160.7	11.7	7.50	18.20	1.10	0.5	184.8	11.7	7.55	16.36	0.57
	L6	3.2	248.1	12.0	7.07	17.80	0.62	1.5	244.9	12.0	7.33	15.83	0.60
	L7	0.1	265.9	11.9	7.08	14.42	0.45	1.0	268.2	11.8	7.22	19.68	1.06

Parameters information: Sal. – Salinity of the interstitial water; ORP – Oxidation–reduction potential of the sediment; Temp. – Temperature of the sediment; pH – pH of the interstitial water (Sørensen scale); Hum. – Humidity of the sediment; TVS – Total volatile solids in dry matter.

Sediments from the Lima estuary were mainly composed by sand (Figure 6.2). The sediments grain size distribution showed that sediments with higher percentage of small size grain, belonging to lower estuary (2SS and 3SS), and middle estuary (4SS), presented the highest values of organic matter (Table 6.2). Except for the summer, the subtidal sediment with the highest amount of clay and silt (mud) was 4SS (middle estuary), with values varying from 13.2% to 53.4%, for spring and winter, respectively. For the intertidal sediment, the higher

content was found in the 3SS (spring and fall), and 4SS (summer and winter), with values in the range between 5.5% (summer) to 12.9% (spring) (Figure 6.2 and Figure S6.1).

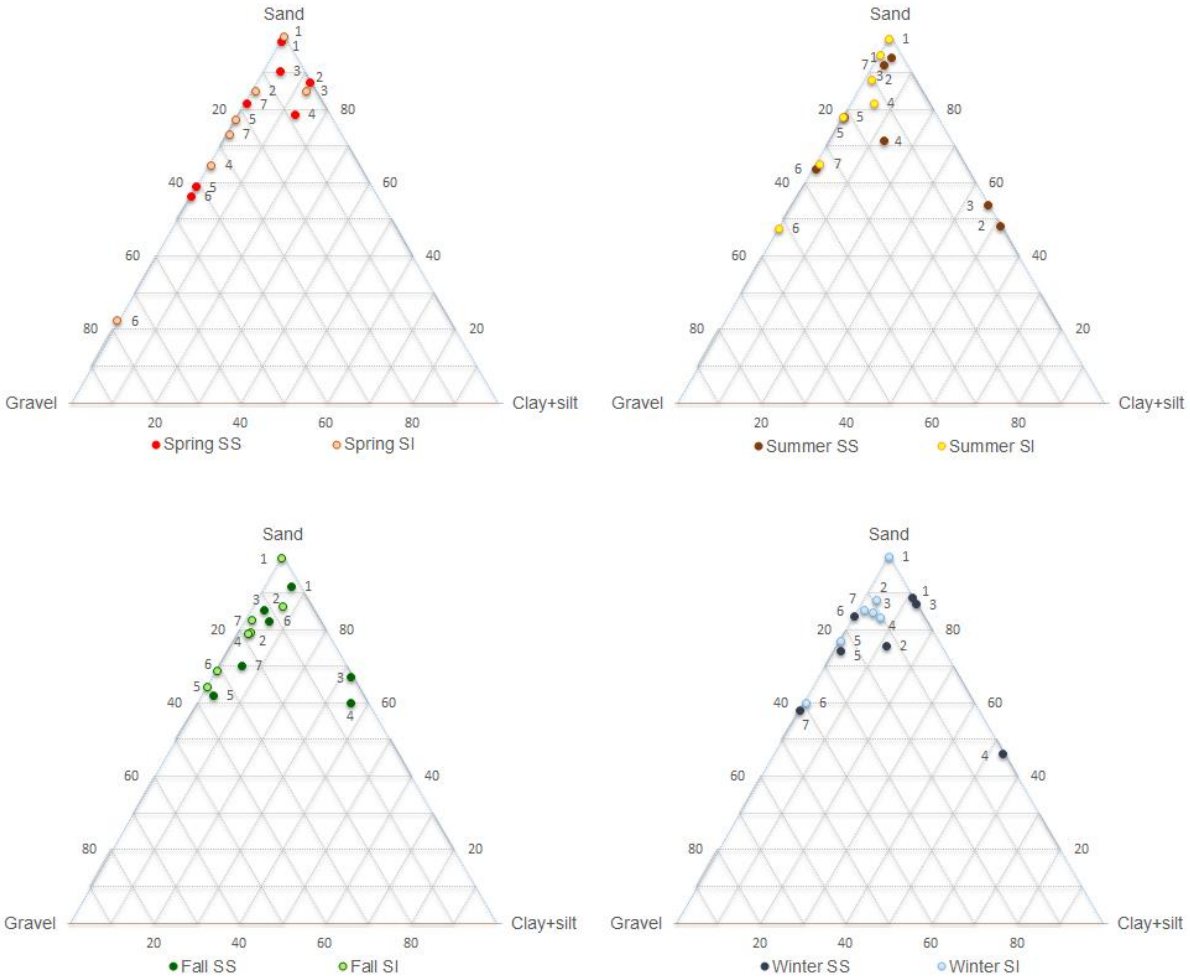

Figure 6.2 Seasonal sediments size distribution in the Lima estuary.

Despite some exceptions, the sediments showed higher amounts of nutrients in the particulate fraction, i.e., most of the inorganic nutrients was associated with the solid fraction (Table 6.3 and Table 6.4). The NO_x concentration for samples collected in the middle estuary during the wet seasons, and in the upper estuary of subtidal sediments during all seasons, and intertidal sediments in wet seasons showed an inverse behavior, that is, the most of the oxidized inorganic nitrogen was dissociated in the interstitial water. The highest amounts of dissociated NO_x (interstitial water) were found in the upper estuary, during the winter, with the smallest amounts associated with sediment with higher mud fraction (Figure 6.2), and higher TVS values (Table 6.2). The intertidal sediments presented lower amounts of total nitrogen in the upper estuary. However, the two types of sediments recorded the highest values in the sediments with the highest percentage of mud and TVS. Conversely, the higher amounts of dissociated NH_4^+ were associated with sediments with higher mud content and higher TVS

values. PO_4^{3-} presented also the highest concentration in the sediments particulate fraction, with the highest concentrations of PO_4^{3-}, as well as of total phosphorus associated with higher values of mud fraction and TSV. The PO_4^{3-} fraction in the total phosphorus was never lower than 45%, ranging from 54.8 to 94.0 in subtidal sediments, and from 45.7 to 95.2 in intertidal sediments. In sediments, silica had always higher concentrations in the particulate fraction, being associated to high values of mud fraction and TVS, as expected. Maximum concentrations of silica were recorded in the upper estuary (dissociated silica), or associated with sediments with high mud fraction and TVS (dissociated and particulate silica).

Table 6.3 Characterization of the subtidal sediments (SS) in the Lima estuary.

Season	Site	NO_x		NH_4^+		PO_4^{3-}		Si		P_{total}	TDC	DOC	TDN
		Part.	Dis.	Part.	Dis.	Part.	Dis.	Part.	Dis.	Part.	Dis.	Dis.	Dis.
Spring	L1	2.23×10^{-2}	22.42	0.301	3.942	7.391	0.551	4.294	36.37	10.25	29.94	2.149	1.122
	L2	6.76×10^{-3}	1.451	5.631	979.4	16.85	5.159	195.5	465.1	26.43	137.3	85.36	15.20
	L3	6.34×10^{-3}	2.799	0.941	159.6	5.600	4.100	16.07	70.94	10.22	53.89	12.68	6.445
	L4	6.59×10^{-3}	2.525	3.100	159.9	11.49	0.290	38.83	106.0	15.02	44.79	27.91	2.850
	L5	4.86×10^{-3}	22.16	1.141	14.12	2.318	0.767	6.281	69.40	3.086	18.93	11.89	0.961
	L6	9.28×10^{-3}	40.37	1.440	6.409	3.924	0.336	8.090	119.2	4.761	5.038	1.727	2.006
	L7	1.03×10^{-2}	59.48	1.795	5.641	3.804	0.521	6.284	126.6	4.619	8.796	2.815	1.627
Summer	L1	6.27×10^{-3}	7.012	1.673	31.98	6.664	0.950	10.46	28.94	7.959	31.27	2.051	1.158
	L2	5.33×10^{-3}	1.635	4.245	60.99	15.50	5.370	129.4	99.98	22.23	35.17	3.662	1.719
	L3	1.52×10^{-3}	2.248	5.367	97.15	17.88	6.694	151.4	105.2	23.28	39.17	3.388	1.996
	L4	9.01×10^{-3}	3.302	6.786	263.6	14.98	2.143	153.8	124.3	23.92	51.46	8.736	4.656
	L5	4.80×10^{-3}	15.88	1.648	9.217	4.936	0.280	8.980	20.38	5.253	21.71	2.001	0.717
	L6	5.47×10^{-3}	29.56	1.967	8.635	3.765	0.554	7.246	67.81	4.430	10.88	1.620	0.773
	L7	5.55×10^{-3}	21.99	3.691	31.55	8.227	0.295	24.18	95.19	11.27	12.02	2.681	0.803
Fall	L1	2.88×10^{-2}	13.55	1.170	18.49	9.976	1.184	6.672	40.67	12.44	27.24	2.265	0.986
	L2	9.77×10^{-3}	5.440	0.996	24.99	3.506	0.872	18.07	55.53	5.698	25.88	1.673	0.814
	L3	1.03×10^{-2}	8.893	4.384	196.3	18.45	0.998	249.9	200.0	26.53	40.19	3.625	3.115
	L4	7.63×10^{-3}	8.985	7.674	506.6	21.04	1.912	210.3	147.1	30.64	75.17	8.246	6.864
	L5	7.00×10^{-3}	14.23	1.915	29.21	6.443	1.017	23.71	57.50	8.269	22.08	2.418	0.811
	L6	5.81×10^{-3}	22.80	3.104	4.610	7.797	0.119	87.79	111.4	9.486	2.961	1.369	0.456
	L7	4.86×10^{-3}	16.25	4.691	14.17	8.481	0.849	78.31	139.3	10.87	7.641	2.888	0.676
Winter	L1	1.99×10^{-2}	20.83	0.860	25.79	8.837	0.920	6.623	53.47	11.62	21.22	1.898	0.828
	L2	4.68×10^{-3}	14.50	1.992	87.30	6.824	3.650	50.31	121.2	8.520	24.66	4.172	1.782
	L3	4.50×10^{-3}	7.805	2.910	237.3	15.90	1.116	176.2	129.4	22.91	59.74	6.300	3.776
	L4	4.09×10^{-3}	26.19	9.709	278.3	21.83	0.392	383.8	117.2	32.70	49.43	6.857	4.299
	L5	5.01×10^{-3}	27.37	1.664	5.573	4.795	0.890	20.12	84.11	6.033	8.470	1.802	0.604
	L6	3.80×10^{-3}	35.90	0.842	1.615	2.773	0.347	6.566	112.6	4.062	4.816	1.294	0.581
	L7	4.59×10^{-3}	65.73	0.876	0.235	2.114	0.392	5.120	122.8	3.287	4.421	1.708	0.915

Units in which the parameters were expressed: particulate nutrients (NO_x, NH_4^+, PO_4^{3-}, Si and P_{total}) – μmol g^{-1} (dry sediment); dissociated nutrients (NO_x, NH_4^+, PO_4^{3-} and Si) – μM; total dissolved carbon (TDC), dissolved organic carbon (DOC), and total dissolved nitrogen (TDN) – mg L^{-1}.

The pore water of intertidal sediments presented lower values of TDC and DOC in the upper estuary. This behavior was followed by the subtidal sediments only with respect to TDC. The higher values of dissolved carbon in the subtidal sediments appeared associated to sediments with high percentage of mud and TVS.

Table 6.4 Characterization of the intertidal sediments (SI) in the Lima estuary.

Season	Site	NO_x		NH_4^+		PO_4^{3-}		Si		P_{total}	TDC	DOC	TDN
		Part.	Dis.	Part.	Dis.	Part.	Dis.	Part.	Dis.	Part.	Dis.	Dis.	Dis.
Spring	L1	3.15×10^{-2}	33.10	0.185	16.75	6.291	0.843	6.925	67.92	7.976	35.86	10.86	5.098
	L2	2.02×10^{-2}	6.357	0.358	5.152	4.447	1.074	11.96	22.78	6.112	29.13	2.338	0.525
	L3	1.54×10^{-2}	1.155	1.131	77.09	10.22	3.884	54.39	96.10	13.74	33.84	7.281	2.071
	L4	1.53×10^{-2}	12.06	1.107	9.509	3.821	1.104	11.58	80.19	4.860	24.47	1.878	0.688
	L5	7.99×10^{-3}	33.26	0.555	4.367	2.902	0.229	8.036	73.12	4.244	11.48	1.671	0.820
	L6	1.57×10^{-2}	59.09	0.347	3.617	3.894	0.152	6.299	119.4	5.778	5.318	1.890	1.019
	L7	2.27×10^{-2}	69.28	0.647	3.878	3.021	0.413	11.02	120.4	4.641	3.943	1.433	1.151
Summer	L1	1.79×10^{-2}	23.57	0.394	5.846	5.190	0.189	0.566	19.76	6.582	30.13	3.888	2.001
	L2	6.61×10^{-3}	7.732	0.593	7.422	5.759	1.534	7.858	17.38	6.050	29.45	1.853	0.813
	L3	6.47×10^{-3}	2.410	0.549	4.187	4.434	5.309	6.220	133.2	7.747	65.04	5.653	0.546
	L4	6.99×10^{-3}	8.518	1.415	5.475	5.076	0.591	33.76	84.81	9.318	15.13	1.807	0.729
	L5	1.29×10^{-2}	31.27	0.655	8.940	2.796	0.143	5.718	8.726	3.641	25.69	2.212	1.156
	L6	1.43×10^{-2}	57.21	0.895	1.866	1.736	0.706	13.68	45.73	2.977	11.49	1.795	1.059
	L7	1.21×10^{-2}	75.87	1.411	1.875	2.887	0.752	8.321	76.45	5.085	10.80	1.791	1.262
Fall	L1	1.07×10^{-2}	36.28	0.693	5.318	4.244	0.880	0.263	33.53	5.912	30.28	10.71	3.047
	L2	9.25×10^{-3}	20.20	0.826	4.351	2.962	1.215	2.941	6.106	5.530	25.89	1.413	0.887
	L3	9.02×10^{-3}	22.18	1.398	22.21	6.204	3.403	11.72	29.82	9.036	24.20	3.290	0.941
	L4	5.03×10^{-3}	18.17	1.412	22.37	3.758	1.108	15.19	103.5	6.480	24.49	1.889	0.694
	L5	6.66×10^{-3}	35.54	0.962	3.908	3.424	0.865	2.955	41.72	5.748	14.36	1.549	0.642
	L6	1.40×10^{-2}	64.17	1.011	3.514	2.064	1.595	5.519	86.50	3.865	8.705	3.028	1.274
	L7	1.02×10^{-2}	65.12	1.294	1.643	2.732	0.849	9.628	103.1	3.495	4.189	1.535	0.974
Winter	L1	1.40×10^{-2}	45.10	0.769	1.823	6.537	0.905	0.958	36.05	9.034	17.80	2.622	1.036
	L2	4.75×10^{-3}	18.54	0.979	4.174	5.084	1.478	7.566	20.42	6.460	26.49	4.246	1.235
	L3	7.30×10^{-3}	8.866	1.198	14.69	5.721	3.243	13.27	45.68	9.413	19.65	2.523	0.611
	L4	4.83×10^{-3}	44.56	1.481	3.133	5.619	0.407	22.57	72.91	8.028	12.33	1.868	0.983
	L5	5.00×10^{-3}	40.41	1.051	2.988	3.351	0.769	6.370	60.54	4.211	6.829	1.606	0.896
	L6	5.62×10^{-3}	62.72	1.130	0.926	2.146	0.573	6.712	92.90	4.694	6.941	0.961	0.892
	L7	5.58×10^{-3}	34.06	1.944	0.727	3.538	0.694	24.88	96.45	5.497	6.613	1.302	0.498

Units in which the parameters were expressed: particulate nutrients (NO_x, NH_4^+, PO_4^{3-}, Si and P_{total}) – μmol g^{-1} (dry sediment); dissociated nutrients (NO_x, NH_4^+, PO_4^{3-} and Si) – μM; total dissolved carbon (TDC), dissolved organic carbon (DOC), and total dissolved nitrogen (TDN) – mg L^{-1}.

6.3.3 Nutrients in each compartment

The water column showed higher values of NO_x and Si in the upper estuary during the winter (Figure 6.3), and during the spring for the Si. Maximum values of 88.83 μM (winter), and 139.7 μM (spring) were recorded at the L7 location for NO_x and Si, respectively. On the other hand, NH_4^+ and PO_4^{3-} showed higher amounts in the lower estuary (maximum values - 3.806 μM and 0.4916 μM, respectively), with the higher concentrations recorded at fall for PO_4^{3-} and dry seasons for NH_4^+.

NO_x concentration in the whole sediment (concentrations of the particulate and dissociated fraction), showed an inverted pattern along estuary relative to the water column, i.e., the highest concentrations were recorded in the lower estuary. Despite this, the maximum value shown by intertidal sediments was at L7 (0.0323 μmoles g^{-1}) of the upper estuary during spring. NO_x did not show a clear seasonal trend pattern, however higher values for intertidal sediments were generally recorded during spring. The behavioral parallelism observed by Si and NO_x in the water column was not verified in the sediments. Throughout the estuary the Si higher concentrations were recorded during the fall for subtidal sediments, and during the spring for intertidal sediments, with higher concentrations generally recorded at L4. The maximum concentrations were recorded at L4 of the middle estuary (140.6 μmoles g^{-1}), and L3 of the lower estuary (35.71 μmoles g^{-1}), for subtidal and intertidal sediments, respectively. NH_4^+ and PO_4^{3-} showed similar patterns, with increased concentrations generally at the locations most downstream of the estuary, this behavior being in line with that observed in the water column. For subtidal sediments the L4 usually presented the highest concentrations for all seasons, wth maximum concentration of 3.761 μmoles g^{-1} and 9.552 μmoles g^{-1}, for NH_4^+ and PO_4^3, respectively, during the fall. Concerning intertidal sediments, NH_4^+ presented the highest concentrations at L4 and L7 (middle and upper estuary), with the absolute maximum at the latter location (1,562 μmoles g^{-1}). PO_4^{3-} showed the maximum concentration of 6,707 μmoles g^{-1} at L3 of the lower estuary, which was usually the location that showed higher values throughout the estuary. For both parameters, winter – when the freshwater flow increases, was the season with the highest recorded concentrations. It was observed that the higher concentrations of nutrients occurred at locations associated with sediments with greater fraction of mud, and the subtidal sediments showed concentrations of nutrients higher than intertidal sediments, with the exception of NO_x.

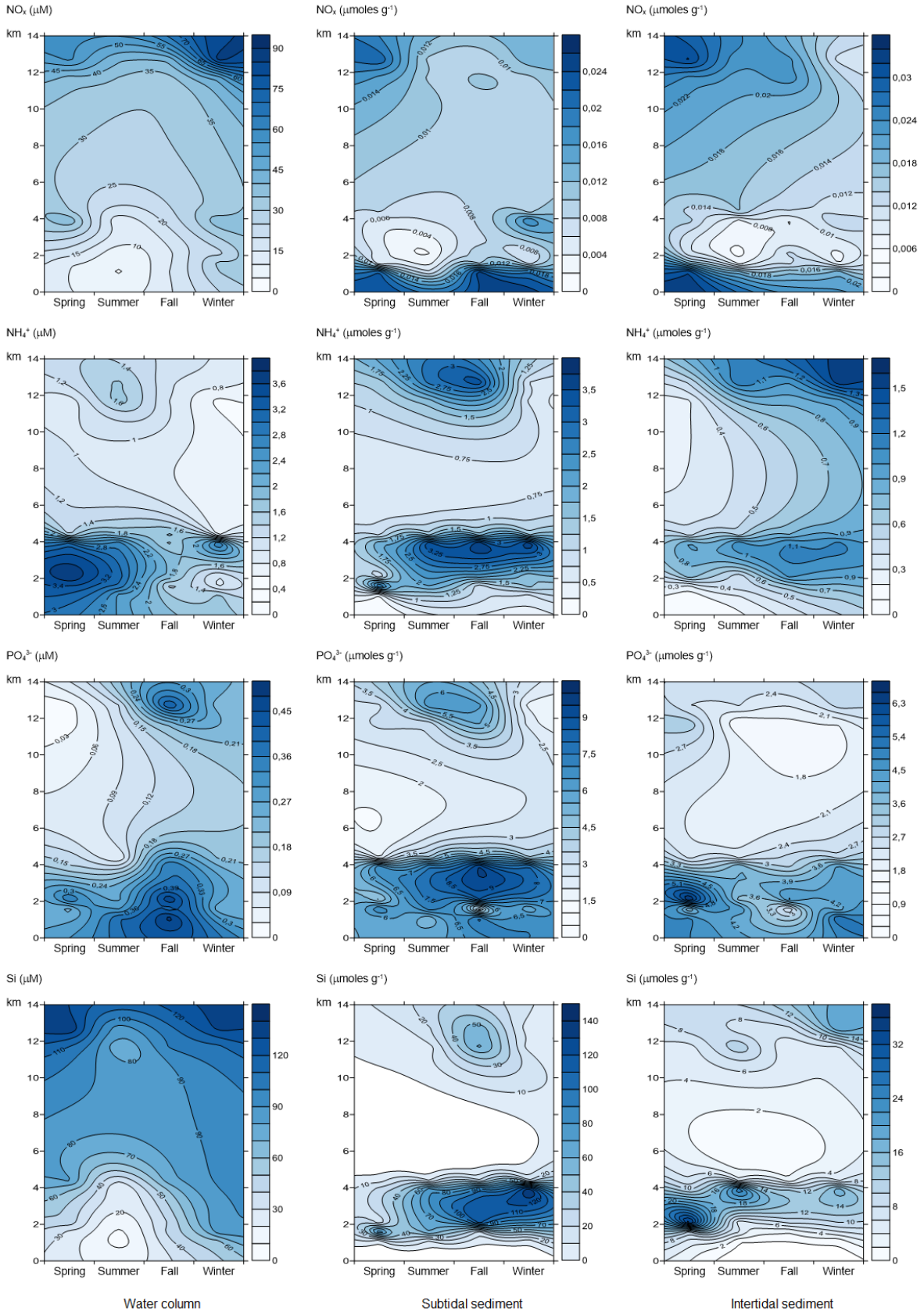

Figure 6.3 Seasonal distribution of nutrients in the water column and subtidal and intertidal sediments, in the Lima estuary.

In general, the spatial trend found for both sediments interstitial water was similar to the water column. For the NO_x, water column concentrations were recorded within the range defined by concentration of the interstitial water of intertidal sediments (higher), and subtidal sediments (lower), whereas for the remaining nutrients the concentration recorded in the water column was always lower than in the interstitial water. The solid fraction and consequently the sediments as a whole, showed an inverted pattern for NO_x, with the highest concentrations in the lower estuary. For the other nutrients, the higher concentrations were found in the solid fraction and, consequently, in the sediments as a whole, with the highest values recorded in the subtidal sediments of the lower and middle estuaries, generally in sediments with a higher amount of a finer fraction. The concentration of nutrients showed statistically significant differences ($p < 0.05$) in the various compartments, except for the NO_x and Si concentration of the water column and interstitial water of the intertidal sediments, and for the phosphate concentration of the interstitial waters of the two types of sediments.

The N:P ratio in the water column (Figure 6.4) showed values always above the Redfield ratio 16:1, with the minimum ratio of 18.9 in the L1 during the summer, suggesting an excess of nitrogen availability and a potential limiting role for phosphate in the estuary water column. The ratio increased along the estuary towards the river upstream from the estuary mouth, with the higher values found in the upper estuary, where the higher concentrations of NO_x, the main source of nitrogen for the estuary column, and the lower concentrations of phosphate were recorded (Figure 6.3). Regarding the Si:N ratio, the values appeared to assign a limiting role to nitrogen. In addition, the values of this index did not present a wide variation range along the estuary (2.08 - 2.20 - 2.30, for the lower, middle and upper estuary, respectively). This evidence may be related to the concentrations parallelism observed by those parameters along the estuary (Figure 6.3). Despite this, the highest values were recorded in the upper estuary and during wet seasons.

In the interstitial (pore) water of the subtidal sediments, only two sediments from the lower estuary during the summer presented a N:P < 16 ratio (11.7 and 14.8 at L2 and L3, respectively), with the middle estuary, showing the higher values and the lower estuary the lower values for this index. The higher values were shown in samples collected in winter and the lower in summer samples. In the Si:N ratio, 36% of the collected samples (10 of 28) showed a potential limiting role of Si. The upper estuary was the one with the highest Si availability, with the wet seasons registering higher values compared to the dry seasons. Interstitial water of the intertidal sediments presented a potential limiting role of 21% of N in the N:P ratio and 32% of Si in the Si:N ratio. The N: P index presented an increased pattern upstream of the estuary (higher values in the upper estuary), while the Si: N index showing an inverse pattern, being the higher values recorded during the dry seasons in both indices.

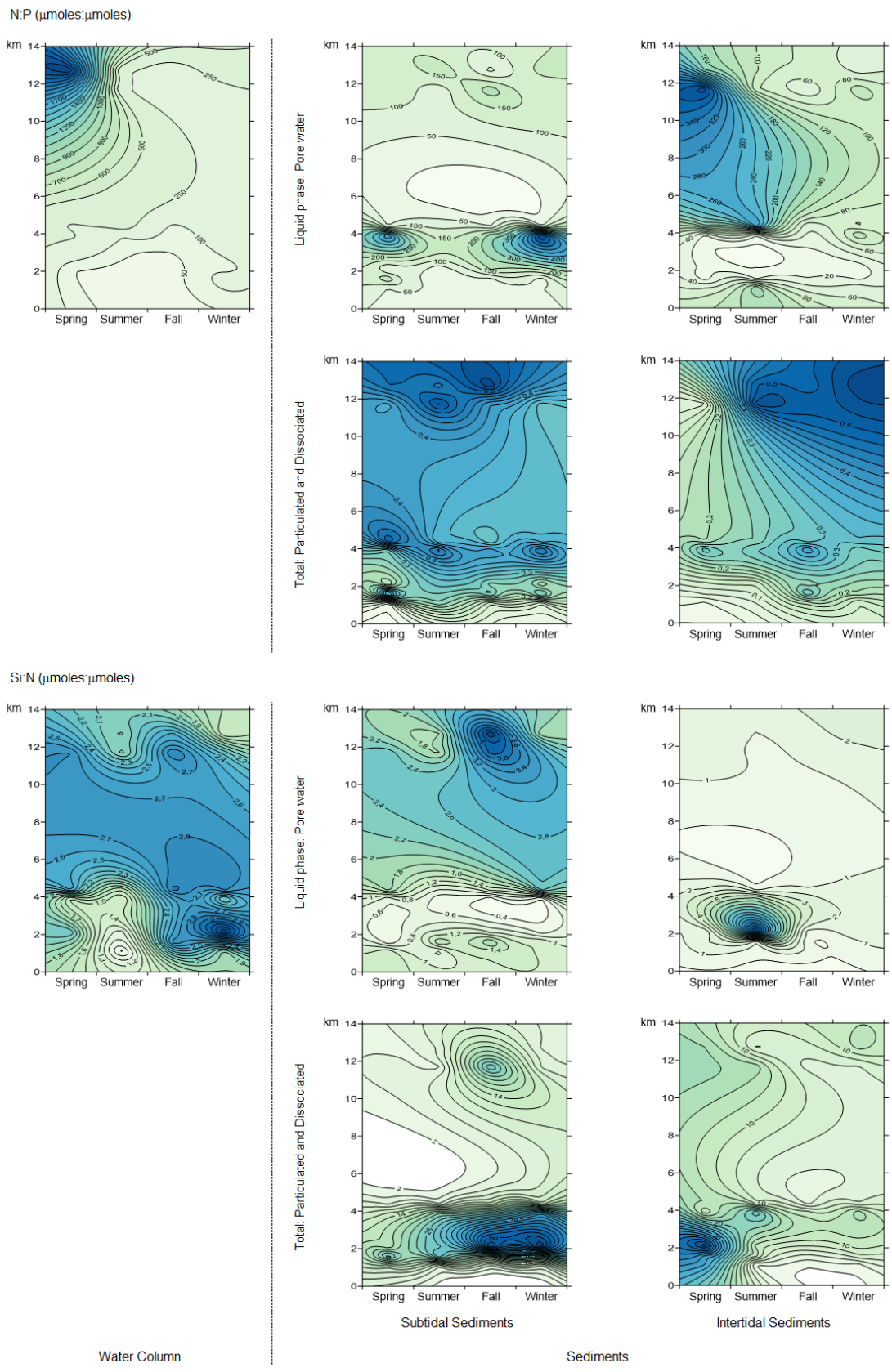

Figure 6.4 Seasonal relationships between Nitrogen and Phosphorus, and Silica and Nitrogen in the water column, pore water of subtidal and intertidal sediments and total subtidal and intertidal sediments, in the Lima estuary.

Subtidal and intertidal sediments showed a similar pattern trend along the estuary for those indices, with the N:P increasing from the lower to upper estuary, and inverse behavior for the Si:N index. The higher values for these indices were recorded in the wet seasons, with the exception of the N:P ratio in the subtidal sediments that did not show a great variation throughout the different seasons. For both types of sediments the N:P ratio always presented values lower than 16, suggesting as in the case of pore water, a potentially limiting role for the nitrogen, being its greater deficiency in the lower estuary, area with greater amount of phosphorus (Figure 6.3). The Si: N index also indicates nitrogen with a potential limiting role (except at location 1 during the fall, with a Si: N ratio of 0.383).

6.3.4 Similarity patterns between samples

For the water column, factorial analysis provided three main factors (eigenvalues > 1) explaining 85.9% (Table 6.5) of the total variation of the data obtained for the samples collected, with the first two factors accounting for 74.9% of the variation total.

Table 6.5 Eigenvectors of correlation matrix and Principal Component Analysis (PCA) factor loadings plot (factors 1 and 2) for the water column.

	Factor 1	Factor 2	Factor 3
Temperature	-0.212	0.434	-0.066
Salinity	-0.328	-0.146	-0.007
pH	-0.007	-0.535	0.007
DO	0.308	-0.237	0.095
NO_x	0.319	0.117	0.108
NH_4^+	-0.280	0.047	0.434
PO_4^{3-}	-0.118	-0.490	-0.021
Si	0.320	0.042	-0.022
CHL *a*	-0.194	0.356	-0.085
TDC	-0.341	-0.062	0.070
DOC	-0.050	-0.040	0.814
TDN	0.238	0.239	0.331
TSS	-0.349	-0.016	-0.002
VSS	-0.349	-0.005	0.041
Expl.Var	7.864	2.798	1.358
% Total variance	56.17	19.99	9.697
Cumulative %	56.17	76.15	85.85

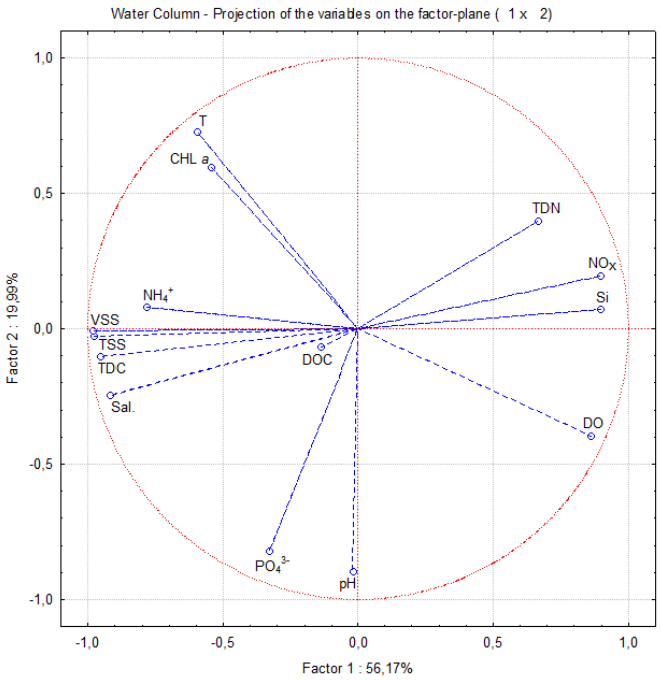

The variables that contributed most to PC1 were DO, NO_x, and silica (positively), and salinity, TDC, and suspended solids (negatively), suggesting a dominant influence of salinity, i.e., the pattern seems to reflect variables with a distribution associated with salinity. For PC2,

temperature and chlorophyll *a* contributed most positively, while PO_4^{3-} and pH contributed negatively, suggesting variables with distribution profile related to temperature and pH. PC3 was highly positively participated by NH_4^+, DOC and TDN.

The projection of samples in the space defined by the first two main components (Figure 6.5), seemed to indicate differences between the seasons mainly between the dry and wet. Along the PC1 axis, samples collected during winter (except at L1), were projected to the same side of the positive contribution of NO_x, Si, and DO, and the samples collected in the lower estuary during the remaining seasons to the opposite side, quadrant associated with positive salinity contributions. This is in agreement with the highest contribution of salinity to the lower estuary, and lower to the upper estuary (Table 6.1). In relation to PC2, the samples collected during dry seasons in the upper and middle estuaries were spread on the positive side of the axis, being associated with positive contributions of temperature and chlorophyll *a*, whereas some wet seasons samples were scatered at the negative side.

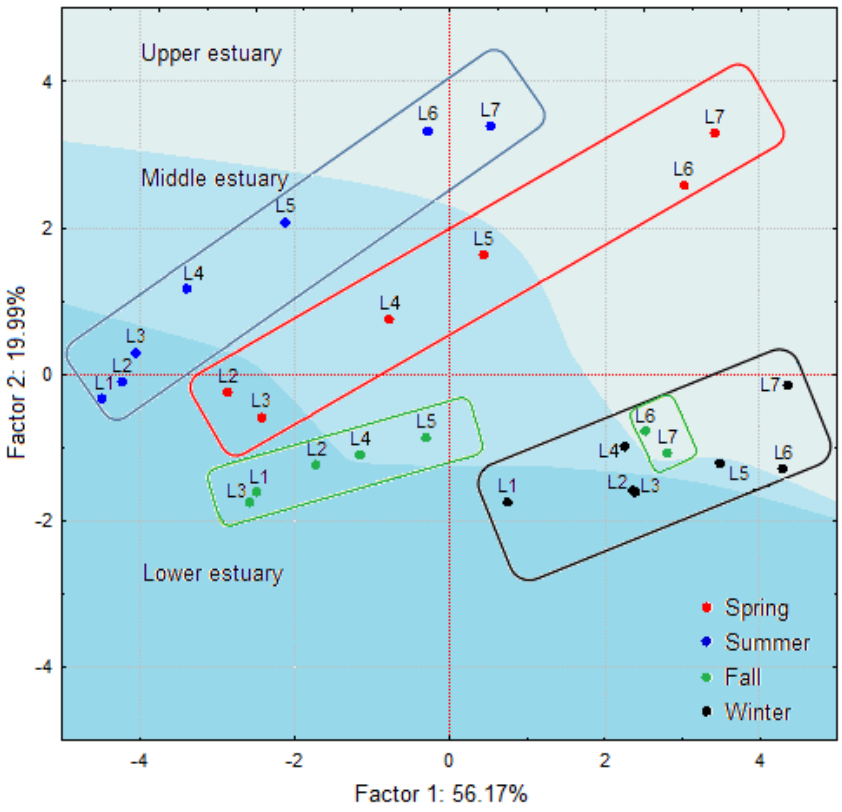

Figure 6.5 Projection of samples in the space defined by the first 2 principal components for the water column (samples labelling variable: season).

Sediment factorial analysis provided three main factors (eigenvalues > 1), explaining 78.7% of the characteristic variation showed by sediments (Table 6.6). Factor 1 contributed with 53.3% of the total variance, and was characterized by positive charges for NH_4^+, PO_4^{3-}, Si, humidity, TVS, and mud, and negative for the redox potential. This seems to reflect variables with a

concentration distribution influenced by grain size of the sediments. Factor 2, accounting for 15.1% of total variability, presented positive loadings for salinity and pH, and negative for NH_4^+ and gravel, suggesting parameters with a salinity-related estuarine distribution. Temperature and salinity contributed negatively and pH positively to factor 3.

Table 6.6 Eigenvectors of correlation matrix and Principal Component Analysis (PCA) factor loadings plot (factors 1 and 2) for sediments.

	Factor 1	Factor 2	Factor 3
Temperature	-0.071	0.056	-0.816
Salinity	0206	0.424	-0.368
pH	-0.019	0.529	0.420
ORP	-0.341	0.027	0.000
NO_x	-0.212	0.210	0.085
NH_4^+	0.300	-0.367	0.087
PO_4^{3-}	0.340	0.190	-0.033
Si	0.335	0.291	-0.013
Humidity	0.367	0.037	-0.019
TVS	0.381	0.007	-0.003
> 2.000 mm	-0.233	-0.485	-0.010
< 0.063 mm	0.372	-0.016	0.082
Expl.Var	6.398	1.807	1.241
% Total variance	53.31	15.05	10.34
Cumulative %	53.31	68.37	78.71

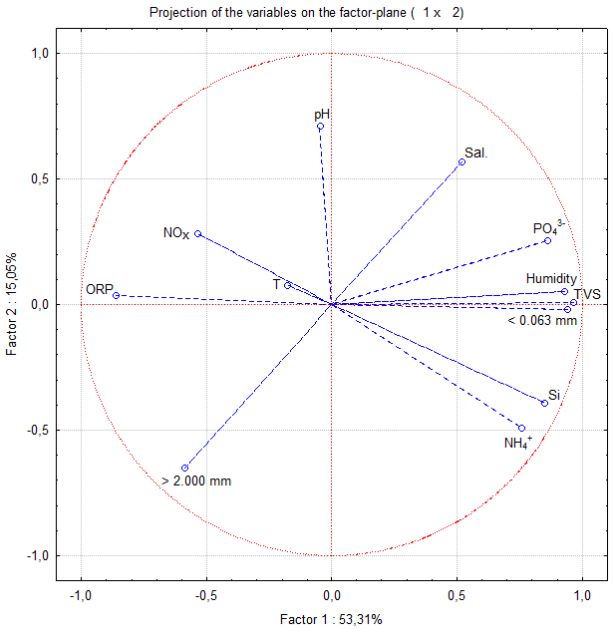

The sediment samples collected during the different seasons did not present, apparently, great differences, being projected mostly along the xx axis (Figure 6.6). Nevertheless, the projection of samples in the space defined by the first two main components, discriminated differences between samples of subtidal and intertidal sediments, as well as between samples collected in different estuarine areas. The samples of the subtidal sediments were projected along the PC1 axis, on the same side of the positive contribution of NH_4^+, PO_4^{3-}, Si, humidity, TVS, and mud, being the samples of intertidal sediments located on the opposite side, a quadrant associated with positive contributions of redox potential. The samples collected at the lower and middle stretches were spread along the PC1 axis, with the subtidal sediment samples projected on the positive quadrant, and the intertidal sediment samples on the negative side. Most samples of both sediment types collected in the upper estuary were projected along the negative side of PC1. In relation to PC2, the samples from the lower estuary were projected on the positive side of the axis, being associated with the positive contribution of pH and salinity (higher pH values), and the upper estuary samples in the opposite quadrant (lower salinity and pH values; and higher content of NH_4^+ and coarser sediments).

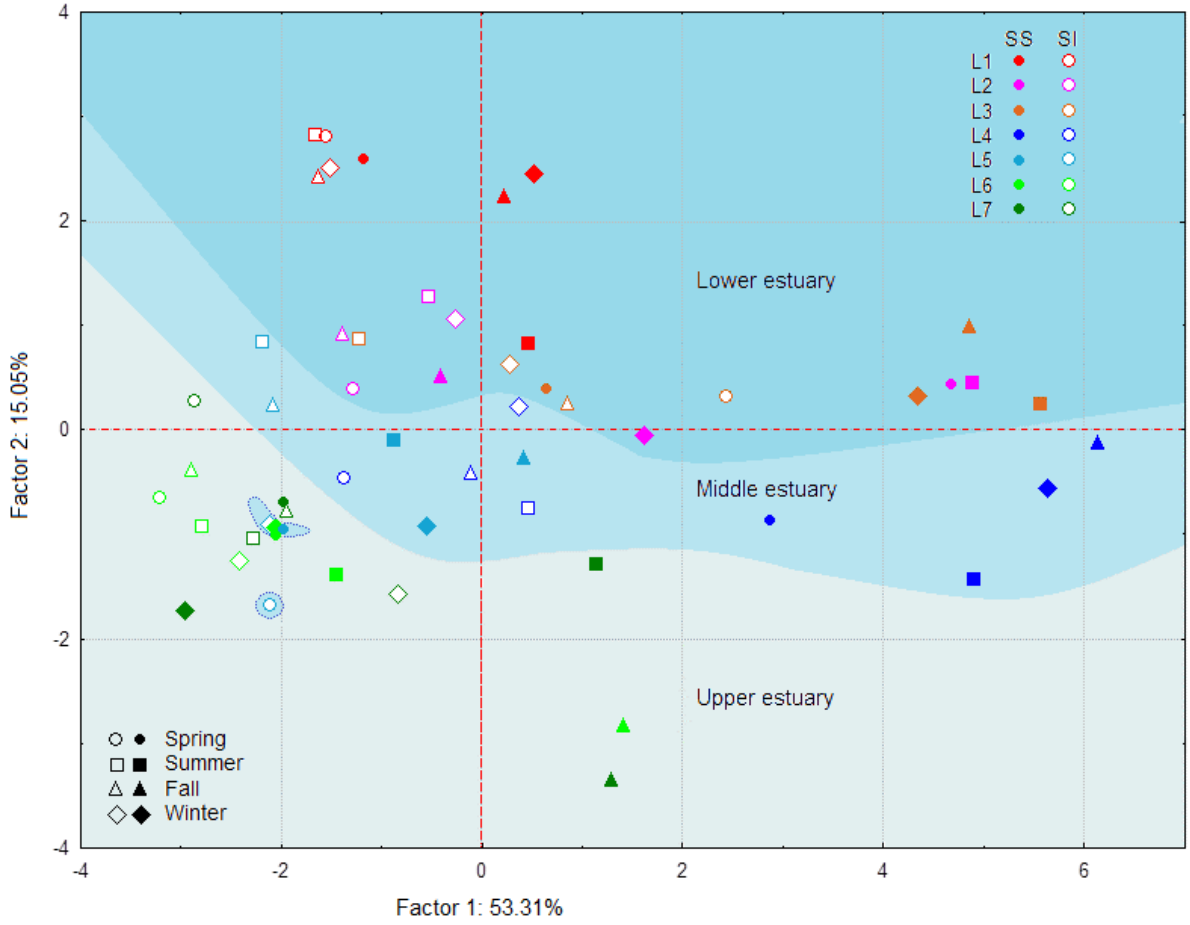

Figure 6.6 Projection of samples in the space defined by the first 2 principal components (samples labelling variable: seasons and location).

6.4 Discussion

6.4.1 General water column characteristics

The seasonal salinity variations observed (Table 6.1) in the lower estuary were in agreement with freshwater dominance during high winter flows (dam discharges and rainfall), and with those reported in other estuaries, such as the Guadiana estuary (Garel et al., 2009; Camacho et al., 2014). Like most estuaries, the Lima estuary is a dynamic system, being dependent on river inflow variability (Morais et al., 2009), associated to seasonal changes that dominate water circulation (Vieira and Bordalo, 2000). Salinity and water temperature revealed a marked seasonal variation typical of temperate estuaries (Gonçalves et al., 2015). There was an increase in dissolved oxygen and a decrease in concentrations of TDC, DOC, SST, and VSS, during winter when the river flow increased (Table 6.1). The higher DO values were found at lower temperatures (wet seasons) in agreement with Garel and Ferreira (2011) data, in the

upper estuary. Therefore, during winter, when the contribution of river water is higher, low salinities, high dissolved oxygen values, and low temperatures are characteristic in the temperate Lima estuary; and during summer, when insolation and evaporation are the most important factors, salinity increases, dissolved oxygen decreases and temperature increases (Camacho et al., 2014). The higher values of TDC, DOC, TSS, and VSS in the higher salinity range during the dry seasons (Table 6.1), suggest a source related to seawater, in line with the behavior reported by Ramos et al. (2017) for this estuary. The estuarine TSS concentration depend on the transport of sediments from the river and the locally derived suspended sediments associated with the resuspension of sediments from the estuary bed (Azevedo et al., 2008), and its relationship with salinity may be also influenced by winds and floods. The predominance of suspended solids in the lower/middle estuary can be interpreted as a result of the water circulation (Oliveira et al., 2017), during tidal cycles with mixing of fluvial sediments and marine sediments in the lower estuarine channel and/or as the result of saltmarsh particles (Caetano et al., 2016), located in the middle estuary. The pH recorded higher values downstream river, since sea water has a slightly alkaline nature (Fatema et al., 2015).

Chlorophyll *a* showed higher concentration during summer, as reported also by Alvarez et al. (2012), and Azevedo et al. (2008). The increased values can be explained by the higher temperatures (Winder and Cloern, 2010; Buchan et al., 2014), higher light availability (Winder and Cloern, 2010; Barrio et al., 2014; Buchan et al., 2014; Lu and Gan, 2015), and hydrodynamic conditions favoring the existence of stratification/stabilization of the water column and longer residence times of water (Lu and Gan, 2015). Chlorophyll *a* concentration tended to decrease with salinity, suggesting that river functioned as a source in the Lima estuary (Azevedo et al., 2008). The occurrence of concentration peaks along the estuary can be attributed to conditions that increase growth rates or decrease loss rates. The upper part of the estuary, surrounded by intensive agriculture (irrigated maize), seemed to behave as a source of chlorophyll *a*, suggesting association with higher nitrogen content in the water column (Desmit et al., 2015), and lower concentration of total suspended solids.

6.4.2 Sediments characteristics

Sediments with a higher amount of fine grain as those found in 2SS, 3SS and 4SS, tend to present higher amounts of organic matter (Mil-Homens et al., 2014), due to its higher surface area (Venkatramanan et al., 2013; Fields et al., 2014), and negative redox potential (environment with reducing conditions). The organic matter increase with the decrease in the grain size (Gredilla et al., 2015) could be attributed to co-sedimentation of particulate organic matter with clay and mineral particles (Ho et al., 2010; Venkatramanan et al., 2013). Coarser sediments were collected in upstream river locations, as reported for other estuaries

(Venkatramanan et al., 2013; Camacho et al., 2014). The Lima estuary is a bedrock-controlled estuary, therefore a sediment size gradient was expected due to the energetic textural bipolarity (river and tidal energy), with ebb currents reworking fluvial sediment from the river to the sea, and flood currents introducing marine sediment, into the estuary (Camacho et al., 2014). In the lower estuarine channel, during tidal cycles, fluvial and marine sediments were mixed, with active sedimentation on the lateral banks, being more pronounced in shallower areas, with lower velocity currents, (Magalhães e Dias, 1992; Camacho et al., 2014; Wolanski and Elliott, 2016), such as locations 2SS, 3SS, and 3SI. The saltmarsh zone in the middle estuary showed finer sediments (4SS), transported in suspension by the river. During the flood, the finer sediments were deposited in the marsh area with reduced hydrodynamism and tidal currents, being wind waves attenuated by vegetation (Wolanski and Elliott, 2016). Therefore, those flood-dominated areas promote vertical accretion, and reduce the export of finer sediments to the ocean. Due to its high resistance to elasticity and viscosity, the mud is resistant to erosion, sedimentation occurs continuously during tides, surpassing the marshes and increasing the muddy banks in the alluvial plain. In the saltmarsh areas with greater sandy composition, the ebb dominated with the efficient seaward sediments export, being the vegetation sparse or absent (5SS), and less effective in dissipating the current energy. In those cases, the coarse granulometry and the exposure to tidal currents promote erosion rather than deposition (Camacho et al., 2014). In the Lima estuary, a selective deposition of sediments is apparent, where the finer were transported downstream to the estuary mouth (2SS, 3SS, and 4SS) by the ebb-dominated tidal flow and current, being the coarser sediments deposited into the upstream part of the estuary (5SS to 7SS and 5SI to 7SI). In the estuarine areas dominated by saltmarsh islands and/or located out of the navigation channel (2SS, 3SS and 4SS), with lower hydrodynamics, differential deposition of fine sediments occured.

The granulometry showed the dominance of coarse and medium sand size sediments (Figure 6.2), with a slight increase in the fraction of coarser sediments (> 2.000 mm) in the lower estuary during wet seasons, for both sediment types, and also in spring for intertidal sediments. During the wet period of the year, large water flows transport fluvial sediments to the estuary (Oliveira et al., 2002), with dominant hydrodynamic conditions not favoring sediment deposition and accretion in saltmarsh stretches. However, artificial regulation controls the occurrence of floods responsible for washing coarser sediments, so these sediments tend to accumulate within the estuary mouth. An increase of finer sediments (Figure 6.2 and Figure S6.1) was recorded in the estuary during winter and fall at L4, outside the navigation channel, in a saltmarsh area more protected, and less affected by the hydraulic regime of the estuary. Locations 2 and 3 (lower estuary) showed the higher amounts of finer fraction for the subtidal sediments in the summer period, which might be related to the low hydrographic conditions

with increase of the residence time of the particles in the dry season, allowing the deposition of sediments (Wolanski and Elliott, 2016).

6.4.3 Nutrients and carbon in each compartment

The behavior presented by TDC may also be related to the degradation of organic matter by the sediments of the intertidal areas of the estuary (Pereira et al., 2007), and the transfer to the water column of the dissolved inorganic carbon (larger fraction of the TDC) stored in the sediments of saltmarshes and in their water pores by tidal pumping (Oliveira et al., 2017). The assumption appears supported by the higher TDC concentration values shown by the pore water of both sediments types when compared to the water column. However, the spatial and temporal trend of these compartments was maintained (Table 6.1, 6.3 and 6.4). Although interstitial water showed an increase of DOC and TDN downstream, the water column did not exhibit a clear and homogeneous spatial trend during the seasons, indicating potential sources and sinks along the estuary, with the concentration affected by the processes *in situ* and depending on the biological absorption and regeneration, and also the equilibrium between the water column and the sediments. The similar spatial trend shown by the finer fraction (mud), TVS, TDC and DOC, suggests that carbon is an important component of this fraction, and may coat the surface of the mud particles as reported by Ho et al. (2010).

In the water column, NO_x and silica had an inverse relationship with salinity, as reported also by Azevedo et al. (2008), and Cloern et al. (2017), and higher concentrations during the wet seasons. Their concentration increased along the upstream estuary (Figure 6.6), with higher values in the upper freshwater estuary (Figure 6.3), probably due to agricultural activities and soil leaching (Tréguer and De La Rocha, 2013; Caetano et al., 2016), i.e., with the chemical weathering of silicate from the land, as the main process of supplying dissolved and particulate silicate to river (Domingues et al., 2005). Concomitantly, freshwater was the main supplier of nitrogen to the estuary as reported elsewhere (e.g., Hitchcock and Mitrovic, 2015; Liu and Chan, 2016). Ammonium and phosphate did not show a clear trend with salinity, although higher values were recorded in samples collected in the lower and middle estuaries, suggesting potential sources and sinks along the estuary (Figure 6.3), with concentrations strongly affected by *in situ* processes (Cloern et al., 2017), despite the effects of external and physical variables, such as river flow, rainfall, and salinity (Magni and Montani, 2000).

The higher concentration of nutrients recorded in sediments, followed by interstitial water, and lower in the water column (except for NO_x), apparently suggests a direction of nutrient flow from the water column to the sediments, and the latter acting as traps. The explanation could be the diffusion of the overlying water nutrients in the sediments, and subsequent storage or removal in the sediments (Cowan and Boynton, 1996; Cowan et al., 1996). In addition, higher

values of NO_x and NH_4^+ recorded in interstitial water relative to the water column may be the result of organic matter mineralization in the overlaying water and DIN release from the sediments (remineralization) (Testa et al., 2013). For the increase of NO_x in pore water of the intertidal sediments, the aerobic oxidation of ammonia (nitrification) may also have contributed (Testa et al., 2013). The increased values of ammonia concentration in the subtidal sediments in relation to the intertidal sediments and their relationships with the sediments finer fraction, as well as the inverse trend showed by the NO_x, seems to suggest the stimulation of ammonia production from the pore water NO_x, proportionally to the time of immersion of the sediments (Marcovecchio et al., 2009). The results seem to indicate that the lack of oxygen due to sediment immersion caused changes in the redox environment (most reducing environments) of sediments, and affected the extent of nitrification and/or nitrate reduction reactions (Marcovecchio et al., 2009). In general, sediments with negative redox potential (environment with reducing conditions) showed the highest concentrations of ammonium ion (nitrogen reduced specie). Marcovecchio et al. (2009) recorded that nitrate and nitrite in the porewater markedly decreased during immersion. This could not be explained only by molecular diffusion toward the water column, since the external forces caused by tidal currents and waves can account for the mixing of pore water with overlying water. In this sense, De Jonge and Van Beusekom (1995) speculated that the surface layer is more permeable as a result of hydrodynamic reworking. The cyclic process of sediments emersion and immersion (intertidal sediments) can mediate belowground transport of nutrients and organic matter and, therefore, with the advective transport of solutes playing an important role in the distribution of nutrients within salt marsh creek banks (Howes and Goehringer, 1994). The sediments oxygen penetration may increase during emersion with changes in the redox environment, affecting the rates and pathways of nutrients flow related to, e.g., aerobic nitrifiers and anaerobic denitrifiers (Marcovecchio et al., 2009).

The results seem to indicate the diffusion of phosphates and silica from the overlying water into the sediments, with the nutrients trapped in the sediment particles, adsorbed on the surface organic matter (Testa et al., 2013), and showing the highest concentrations in the sediments with the higher finer fraction, due to its specific surface larger (Cardoso et al. 2008; Junakova et al., 2013). Since more than 90% of the phosphorus transported by rivers to estuaries and coastal waters has been reported to be associated with suspended solids (Jordan et al., 2008), it is expected that an important fraction in the estuaries is particle-bound phosphorus, i.e., associated with sediments (Li et al., 2017), which is in line with the results of this study. As a result, the phosphorus concentrations within estuaries are controlled to some extent, by interaction with sediment or suspended material. The coincident location of the higher concentrations of phosphates in the water column and sediments (sediments with higher finer fraction and lower ORP), may be due to their sediment release, since phosphate

fluxes are affected by O_2 and the ORP of sediments, with phosphate release from sediments during periods of hypoxia/anoxia (Mortazavi et al., 2012).

The surface estuarine sediments normally accumulate high loads of organic matter, being regions of intense microbial activity and nutrient cycling, and frequently characterized by high concentrations of nitrogen, phosphorus, and soluble silica, resulting from the remineralization of deposited organic matter (Nixon, 1981; Dunn et al., 2017).

Organic matter mineralization in surface sediments, particularly in shallow environments, releases inorganic nutrients in the interstitial water, which can be exchanged with the water column (Kamer et al., 2004) by diffusive and advective transport processes, becoming additional sources of nutrients (Garcia-Robledo et al., 2016; Dunn et al., 2017), for primary producers use (Mortazavi et al., 2012); or adsorbed onto organic compounds or clay particles in sediments (Coelho et al., 2004), being consumed by sedimentary microalgae and prokaryotes for the purpose of assimilation or dissimilation (Garcia-Robledo et al., 2016). Despite the differences, nutrients composition data of both sediments type did not show a clear seasonal variation.

Redfield molar ratios can be analysed as indicators of potential limitation in processes occurring in the estuary in terms of temporal and spatial scales (Gameiro et al., 2007). The water column recorded N: P > 16, which expresses a potential phosphorus deficiency, with higher values in the upper estuary. Similar results were found for the Douro river estuary, as reported by Azevedo et al. (2008). The increased upstream values of nitrogen may result from the nitrate transported by river water (nitrate, dominant form of DIN) (Gameiro et al., 2004). The excess of N relative to P in freshwater entering the estuary of Lima is probably indicative of human activities in the watershed (Medeiros et al., 2012). As suggested by Caetano et al. (2016), the lack of large industrial complexes and the proportion of cultivated land in the Lima basin, seems to associate the excess of N to agriculture. The similar trend presented by pore water of the most sediments may be due to the diffusion of nitrogen from the water column and sediments (high amounts of NH_4^+ within the middle estuary in the finer sediments). On the other hand, the N: P < 16 ratio, which expresses a nitrogen deficiency potential, was recorded in all sediments, being the higher values in the upper estuary. A possible explanation is the existence of a large amount of phosphorus adsorbed in the sediments, that is, the diffusion of the phosphorus from the water column to the sediments, being adsorbed, trapped, and stored there (Testa et al., 2013), and thus, the sediments functioning as a phosphorous sink in the estuary.

Regarding the Si: N ratio in the water column, the values seemed to attribute a limiting role to the nitrogen, with values not showing a large variation along the estuary. The similarity of the ratio values may have resulted from the common origin of those nutrients. Due to agricultural activities and soil leaching, upstream river water functioned as a source of nitrogen and silica

(Caetano et al., 2016), that is, the chemical weathering of silicates on land as the main process of supply of silicate dissolved and particulate to the river (Domingues et al., 2005; Hitchcock and Mitrovic, 2015; Liu and Chan, 2016), and the fertilization of agricultural soils followed by leaching as the main supplier of nitrogen to the river. In the sediments pore water, the values presented by the Si: N ratio did not assign the potential limiting role always to the same nutrient. In the pore water of the subtidal sediments, the higher values of the Si: N ratio were found in the upper estuary during the wet seasons, probably due to the direct relationship between the amount of silica in the estuary and the soils leaching (Tréguer and De La Rocha, 2013), more effective during the wet seasons. The lower values of the ratio in the lower estuary may be due to the adsorption of silicon in the sediments with the higher amount of the finer fraction (Cardoso et al., 2008). The pore water of intertidal sediments presented higher values of the ratio in the lower estuary and in the dry seasons, which may be related to the resuspension of finer sediments and silica release, since these sediments are subject to the immersion and emersion cycle, caused by the tidal cycle. The sediments indicated a potential nitrogen deficiency, with higher values recorded where the finer fraction dominated, probably because the silica adsorption in these sediments is more efficient due to its greater surface area (Cardoso et al., 2008).

6.4.4 Similarity patterns between samples

The water column factorial analysis results (FA) pointed out the factors that may have contributed most meaningfully to the control of the dynamic processes in the Lima estuarine system (Table 6.5). Positive contributions given by DO, NO_x, and silica, and negative by suspended solids (TSS and VSS), TDC, and salinity, show spatial and temporal differences along Factor 1 (Figure 6.5), suggesting that freshwater inputs from the river and the tidal action were the main factors responsible for the differences between the samples in the estuary Discharges from the Lima River seem to have been the driving force of most of the dynamic processes associated with the nutrients (NO_x and silica) that occurred in the estuary as observed in other temperate estuaries (e.g., Azevedo et al., 2008; Hofmeister et al., 2017). Suspended solids and TDC concentrations, and its distribution in the estuary seem to result of the predominant action of the tide cycles (Oliveira et al., 2017). It seems clear that the temporal differences emerged along the FA 2, with concentration of chlorophyll *a* associated to the temperature, i.e., higher concentrations of chlorophyll *a* during the dry seasons, as noted previously (Azevedo et al., 2010), contrary to the observed for the concentrations of phosphate. The relationship between the parameters showed by FA 3 seems to indicate *in situ* processes, involving the release of ammonium and dissolved organic carbon, which can be attributed to mechanisms such as microbial remineralization, sediment reworking, etc., as

suggested by Marcovecchio et al. (2009). To determine the patterns of temporal and spatial similarity between samples, the first two factors were represented in two dimensions (Figure 6.5). Samples from seasons were plotted in different quadrants of the PCA , reflecting changes in the variables concentrations, suggesting as an explanation the seasonal variations of the hydrodynamic conditions (Lima river flow and tidal cycles), and climatic conditions (rainfall and temperature). The high Lima river flow enhanced by precipitation seems to have a higher positive impact on the wet period of the year (PC1), while temperature and the tidal cycle appear to influence more dry seasons (PC2). Differences between the dry and wet seasons were greater than between seasons within each group (wet and dry seasons). Samples of different estuarine areas (upper, middle, and lower stretches) were plotted in different areas of the PCA, suggesting differences among them, although the differentiation for the middle estuarine samples was not so evident. Most samples from the upper estuary were associated with lower salinity and higher concentration of nitrates and silica, i.e. associated with river freshwater and soil leaching (Tréguer and De La Rocha, 2013; Hitchcock and Mitrovic, 2015). The upper estuary samples collected in the dry seasons were associated with higher temperatures and higher amounts of chlorophyll *a*, as also reported for the Douro estuary by Azevedo et al. (2010). An inverse pattern was presented in most samples from the lower estuary, since they were related with higher salinity, suggesting an association with the input of seawater into the estuary. The observed differences between the samples seem to be related to Lima flow and temperature, which vary seasonally (Gonçalves et al., 2015), as well as to the introduction and extension of coastal waters in the estuary during the tidal cycle (Camacho et al., 2014), since in highly variable systems such as estuarine, photonic and mixing conditions can vary from hour to hour (Azevedo et al., 2010). These physical factors are precursors of the biogeochemical processes in the estuary (Cloern et al., 2017), being related to the variables that contribute most to the existence of differences between the samples.

For the factor analysis of the sediments samples, Factor 1 represented the set of nutrients associated with mud and organic matter, with distribution patterns controlled by the finer fraction of the sediments, and the ORP related to the sediments oxygen content. The association between fine-grained fraction (mud) and organic matter (TVS) suggests that organic matter was an important component of this fraction, and may coat the mud particles surface as reported by Ho et al. (2010). The higher distribution patterns of some nutrients with organic matter and the finer fraction of the sediments, imply that these nutrients can be related to mud that sorb them directly (Junakova et al., 2013), or related to organic matter which coats the mud surface (Ho et al., 2010). The nutrients association with sediments can be increased by processes such as direct adsorption by fine-grained inorganic particles of clay, adsorption of organic substances which may be associated with inorganic particles and direct precipitation

as new solid phases (Uwah et al., 2013). On the other hand, Factor 2 reflected the group of constituents related to salinity and, therefore, its distribution was controlled by freshwater inputs of the river, and by the tidal action. Sediment samples were plotted in different quadrants of the PCA, reflecting changes in the variables concentrations, and suggesting as an explanation the spatial variations of the grain size distribution of sediments and hydrodynamic conditions (Lima river flow and tidal cycles). The samples projection showed differences between samples of subtidal and intertidal sediments, as well as between samples collected in different estuary areas. Sediment grain size seems to be the property responsible for most of the variability between the subtidal and intertidal sediment samples, with most of the subtidal sediments assciated with the mud as opposed to the intertidal sediments. Regarding the differences showed by the samples collected in different estuarine areas, besides the sediment grain size, salinity also seems to be an important factor to consider. The sediment samples from the lower estuary were projected on the positive side of the PC2 axis, associated with higher salinities, and the other estuarine samples in the PC2 negative quadrants. The factors responsible for the differences between the samples from the different estuarine areas seem to be the tidal action with the introduction of salt water in the estuary (higher salinity in the lower estuary), and the freshwater input from the river (lower salinity in the upper estuary). In estuaries, such as the Lima, the pattern of substances distribution in the sediments were controlled by factors such as lithology, hydrodynamics, and morphology of the river and estuary, riverine and marine inputs, biological activity, and anthropogenic contamination (Martins et al., 2012).

6.5 Conclusions

In the Lima estuary, the main factors responsible for the observed differences among the samples were the freshwater inputs from the river and the tidal action. The samples collected at different seasons showed differences, indicating as possible cause the seasonal variations of hydrodynamic and climatic conditions. The high flow of the Lima river increased by precipitation, appears to have a greater positive impact during the wet period of the year, while temperature and tidal cycle seem more important during the dry period. Despite this, the results seem to indicate the existence of *in situ* processes, involving the various compartments of the estuary, that is, water column, pore water, and sediments. The concentration of nutrients decreased from sediments to the interstitial water, and then to the water column, suggesting a direction of nutrient flow from the water column to the sediments, i.e., the diffusion of the overlying water nutrients in the sediments, and subsequent storage or removal in the sediments. The Lima estuary presented a sediment grain size gradient due to energetic textural bipolarity (river and tidal energy), with the ebb currents reworking river sediments to

the sea, and flood currents introducing marine sediments into the estuary. The study appears to indicate a selective sediment deposition, the finer fraction transported downstream to the estuary mouth by the ebb-dominated tidal flow, and the coarser fraction deposited into the upstream part of the estuary, being the sediment grain size the property that appears to be responsible for most of the variability between the sediment samples. Nutrient fluxes at the sediment-water interface can influence or regulate the water column nutrient composition since the sediment can behave as a sink or as a source of inorganic nitrogen, phosphorus, and silica through different biogeochemical processes.

6.6 SUPPLEMENTARY INFORMATION

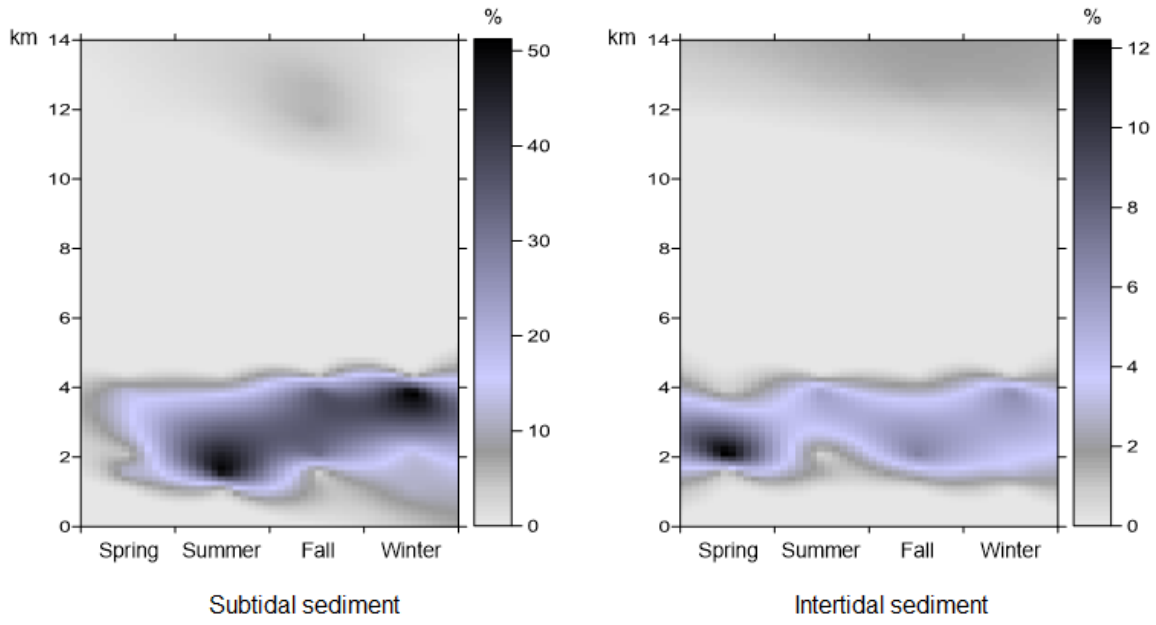

Figure S6.1 Seasonal distribution of the mud in sediments (fraction of particle size < 0.063 mm) in the Lima estuary.

CHAPTER 7

Sediment-water nutrient fluxes in intertidal and subtidal sediments from Lima estuary (NW Portugal)

Abstract

In an estuary, nutrients are subject to transformation before being delivered to costal waters. Therefore, it is important to understand the turnover processes, and to what extent they modify the nutrient fluxes. These processes, together with the hydrographic conditions, define the fundamental role of estuarine environments as a sink or source of nutrients that ultimately will end up in the oceans. Benthic fluxes of dissolved inorganic nitrogen (NO_x and NH_4^+), and phosphorus (PO_4^{3-}) were measured in sediments from Lima River estuary (NW Portugal). A laboratory microcosm was developed to study the nutrients dynamics with intact sediment cores incubated under continuous water flow. Sediment cores were collected at eight locations along the salinity gradient during summer and winter. The experiments were conducted with intertidal and subtidal sediments, and sediment–water fluxes of inorganic nutrients were measured. The overall decreasing pattern presented by PO_4^{3-}, NH_4^+, and NO_x concentrations in the overlying water seemed to indicate its diffusion in the sediments and subsequent storage and/or removal by physicochemical and biochemical processes. The negative fluxes were more accentuated in winter with no significant differences ($p > 0.05$) noted between intertidal and subtidal sediments. The Lima estuary water did not present enrichment of nitrogen and phosphorus, acting as a sink for inorganic nutrients, and thus appearing to limit the transport of N and P from land to sea.

Keywords: inorganic nutrient fluxes; intertidal and subtidal sediments; Lima Estuary.

7.1 Introduction

Estuaries are dynamic ecosystems being at the land–sea interface and characterized by high rates of primary production that support economically important food nets. Primary production is controlled by the supply of one or more nutrients (nitrogen, phosphorous, and silica), that are supplied to estuaries from rivers, groundwater discharge, atmospheric deposition, tidal exchange with marine systems, or regeneration during organic matter decomposition (Paerl, 2002; Mortazavi et al., 2012). Human interactions with the environment – e.g., alterations to nutrient regimes - change the ecosystem functioning. Crucial processes for ecosystem

functioning, such as nutrient cycling, occur mostly in the sediment (Alsterberg et al., 2012; Fields et al., 2014), that can act both as source of nutrients to the water column and/or promote their retention and removal. The biogeochemical cycling of elements is influenced by competing and interacting physical and biological factors, resulting in significant spatial and temporal variations (Dunn et al., 2013).

Eutrophication is presently considered the most damaging problem in estuaries (Mortazavi et al., 2012). This phenomenon has been mainly attributed to increased nutrient concentration in surface waters (Bernard et al., 2014), as a result of increased anthropogenic inputs. The recycling and regeneration of nutrients, obtained from the combination of benthic and pelagic processes, contributes to the ecosystem recovery from eutrophication (Pinckney et al., 2001). In shallow estuaries, the mineralization of phytodetritus in the sediments regenerates nutrients, releasing N and P compounds into water column that can be used by primary producers (Koho et al., 2008). In sediments under oxic conditions, nitrifying microorganisms can oxidize ammonium (NH_4^+) to nitrite (NO_2^-), and thereafter to nitrate (NO_3^-) which is released into the water column, while in anaerobic conditions, the NO_3^- can be reduced to nitrogen gas (N_2) by heterotrophic bacteria through denitrification process. Denitrification is important because it is often the main nitrogen sink, removing the eventual excess of bioavailable nitrogen, and therefore, potentially reducing the nitrogen impact of eutrophication. Denitrification is affected by the availability of organic matter and nitrate, temperature, and the abundance and activity of denitrifying microbes (Knowles, 1982). In systems with abundance in OM, NO_3^-, and with an active microbial community, temperature exerts a strong control over denitrification rates (Seitzinger, 1988). Denitrification rates are usually higher in summer than in winter (LaMontagne et al., 2002), this is especially valid for temperate estuaries (Ferguson and Eyre, 2007). Other processes can co-occur, such as anaerobic ammonium oxidation (anammox), and dissimilatory nitrate reduction, and influenciate the ultimate fate of nitrogen (Mortazavi et al., 2012). Fluxes of phosphate (PO_4^{3-}) are also affected by O_2 and sediments potencial redox, being PO_4^{3-} released from the sediments during hypoxia/anoxia periods. Particle-bound phosphorus is expected to be a major fraction of phosphorus in estuaries, since more than 90% of phosphorus transported by rivers to estuaries and coastal waters has been reported to be associated with suspended solids (Li et al., 2017). As a result, phosphorus concentrations within estuaries is controlled to some extent by the interaction with sediment or suspended material.

The study and quantification of the sediment-water interface and microbial/biochemical processes in sediments are difficult *in situ*. A possibility to study the processes and water-sediment fluxes is using intact sediment cores in controlled laboratory experiments. These experiments - laboratory microcosms with intact sediments have been successfully used to study nutrient dynamics (Andersen and Jensen, 1992; Binnerub et al., 1992; Liikanen et al.,

2002). The knowledge of the spatial and temporal variability of the benthic nitrogen and phosphorus cycling, can be use to obtain and scale rates, to achieve reliable estimates for the whole system being crucial for understanding of estuarine productivity (Dunn et al., 2013).
The aim of this study was to estimate sediment-water fluxes of inorganic nitrogen and phosphorus, using laboratory microcosms, in subtidal and intertidal sediments in the Lima estuary in winter and summer seasons.

7.2 Material and methods

7.2.1 The study area

The Lima River crosses the north of Portugal and meets the Atlantic Ocean by the city of Viana do Castelo, draining an area of approximately 2,450 km^2 (1,143 km^2 in Portugal). The estuary (Figure 7.1) is a relatively wide but shallow basin with extensive mudflats that inundate during reflux, having an extension of about 24 km, and an average freshwater influx of 70 m^3 s^{-1} (Ramos et al., 2006).

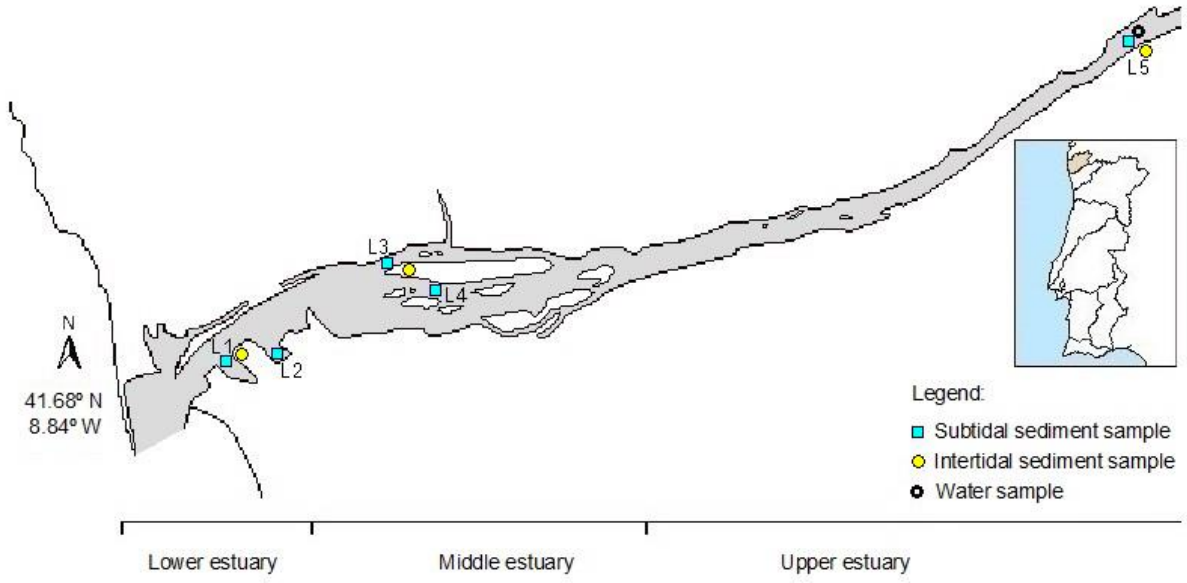

Figure 7.1 Map of the Lima estuary and sediment sample stations.

The lower estuary is a deep (9 m) and narrow navigation channel, modified by industrial and comercial instalations, and leisure and fishing harbour equipments (Ramos et al., 2010). Along the middle estuary there are sand islands, wetlands with typical marsh vegetation and intertidal channels, while the upper estuary consists of a narrow and shallow channel (Rebordão and Teixeira, 2009). The estuary has an impact of urban, industrial, and agricultural areas in the region that introduce nutrients and other substances into the estuary (Almeida et al., 2011).

7.2.2 Sampling

Sampling surveys were carried out on February (winter) and July (summer) of 2016, during the ebb tide. Samples of sediments were collected from 8 locations (5 subtidal - SS and 3 intertidal - SI) along 12.6 km (Figure 7.1). During each survey, four sediment cores were collected at each site. Triplicate sediment cores to be used in the incubation experiments for the determination of sediment-water fluxes of inorganic nitrogen (NO_x, NH_4^+ and PO_4^{3-}), and one for sediment characterization. Cores of 5–10 cm of undisturbed sediment were taken in plexiglass tubes (diameter 3.5 cm), which were capped and sealed at the bottom with a rubber bung, for transportation to the laboratory. The incubation water was collected at the most upstream sediment sampling site (L5), using 6 L plastic container.

At each sampling site, water column salinity, pH, turbidity, dissolved oxygen, and temperature were measured with a YSI 6920 CTD multiprobe, calibrated according to the instructions from the manufacturer. Sediment redox potencial was measured *in situ* with a pHmeter HI 9023, using the electrode HI 3130 (Hanna Instruments), and a temperature probe (HI 7669/2W).

All collected samples were kept refrigerated in an ice chest until processing in the laboratory.

7.2.3 Laboratory nutrient flux assays

The incubation water consisted of filtered estuarine water (0.2 µm), with added nutrients (50 µmol NO_3^- L^{-1}, 10 µmol NH_4^+ L^{-1} and 5 µmol PO_4^{3-} L^{-1}). Seawater solution was added to match the salinity gradient normally found along the estuary: lower estuary sediments (L1, L2) - salinity 30; site L3 sediments - salinity 20; site L4 sediments - salinity 10; site L5 sediments - no addition. The concentrated artificial seawater was prepared according the MBL formulae (Cavanaugh, 1975). Nutrients were added to avoid nutrient limitation during incubation time.

The cores were placed in a water bath, and maintained at 20 ^oC. One hundred mL of incubation water was added to each sediment core. A peristaltic pump was fitted to each core to facilitate water circulation (2.7 mL min^{-1}), and resuspension of core sediments was avoided, being the cores equilibrated for 10 minutes period prior to samples collection (Figure 7.2). At intervals of 0, 3, 6, 9, 12 and 24 h, 3 mL aliquots of the inflow water from each microcosm were taken for analysis of dissolved NO_x (NO_3^- + NO_2^-), NH_4^+, and PO_4^{3-}. After collecting the last water sample from the microcosms (24h), the peristaltic pump was turned off, the microcosms emptied, and sediment collected for NH_4^+, NO_x, and PO_4^{3-} analysis. Then, the four sediment cores (initial and microcosms) from each site are mixed for organic matter (OM), and grain size determinations.

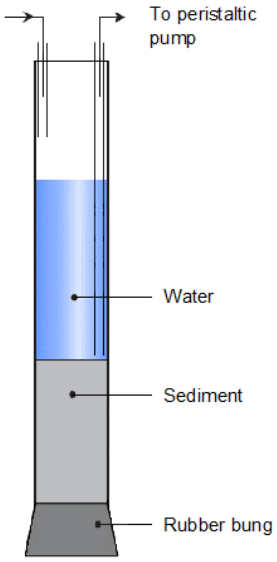

Figure 7.2 Experimental microcosm design.

7.2.4 Analytical procedures

In water samples the ammonium (NH_4^+) was analysed by the Koroleff method (Grasshoff et al., 1983), and nitrate plus nitrite (NO_3^- + NO_2^- or NO_x), by the method described by Jones (1984), and adapted by Joye and Chambers (1993). For the determination of phosphates (PO_4^{3-}) in the estuarine water, the Koroleff method was used (Grasshoff et al., 1983).
After the experiments, sediments were dried at 40 ºC. The determination of the the NH_4^+, NO_x and PO_4^{3-} concentrations in sediments was performed by the above-mentioned methods, after extraction with KCl (2M) for the nitrogen species and with HCl (1 M) for the inorganic phosphorus (Keeney and Nelson, 1982; Mudrock et al., 1997). In the total phosphorus determination before the extraction, the sample was previously calcined at 550ºC for 2h (Mudrock et al., 1997). For the determination of organic matter content, combined sediment samples were dried at 105 ºC (24 h), and then ignited at 500 ºC (4 h), (APHA, 2005). All analyses were performed in triplicate. The sediment grain size was estimated by sieving the samples, obtaining seven fractions: silt and clay (< 0.063 mm), very fine sand (0.063–0.125 mm), fine sand (0.125–0.250 mm), medium sand (0.250–0.5 mm), coarse sand (0.5–1 mm), very coarse sand (1–2 mm), and gravel (> 2 mm). Each fraction was weighed and expressed as a percentage of the total weight.

7.2.5 Data analysis

Nutrient fluxes were calculated by linear regression of the concentration data as a function of incubation time, core water volume, and surface area. Temporal and spatial differences were examined using analysis of variance (one-way ANOVA) followed by a post hoc Tukey honestly

significant difference (HSD) multi-comparison test. ANOVA was performed using the software Tibco Statistica 13.3. Before statistical analysis was carried out, environmental data were tested for normality and homogeneity of the variances. The significance level used for all tests was 0.05.

7.3 Results

7.3.1 Water column characterization

The temperature, salinity, pH, turbidity and dissolved oxygen profiles were carried out for the water column at the sites where the subtidal sediments were sampled (Figure 7.3).

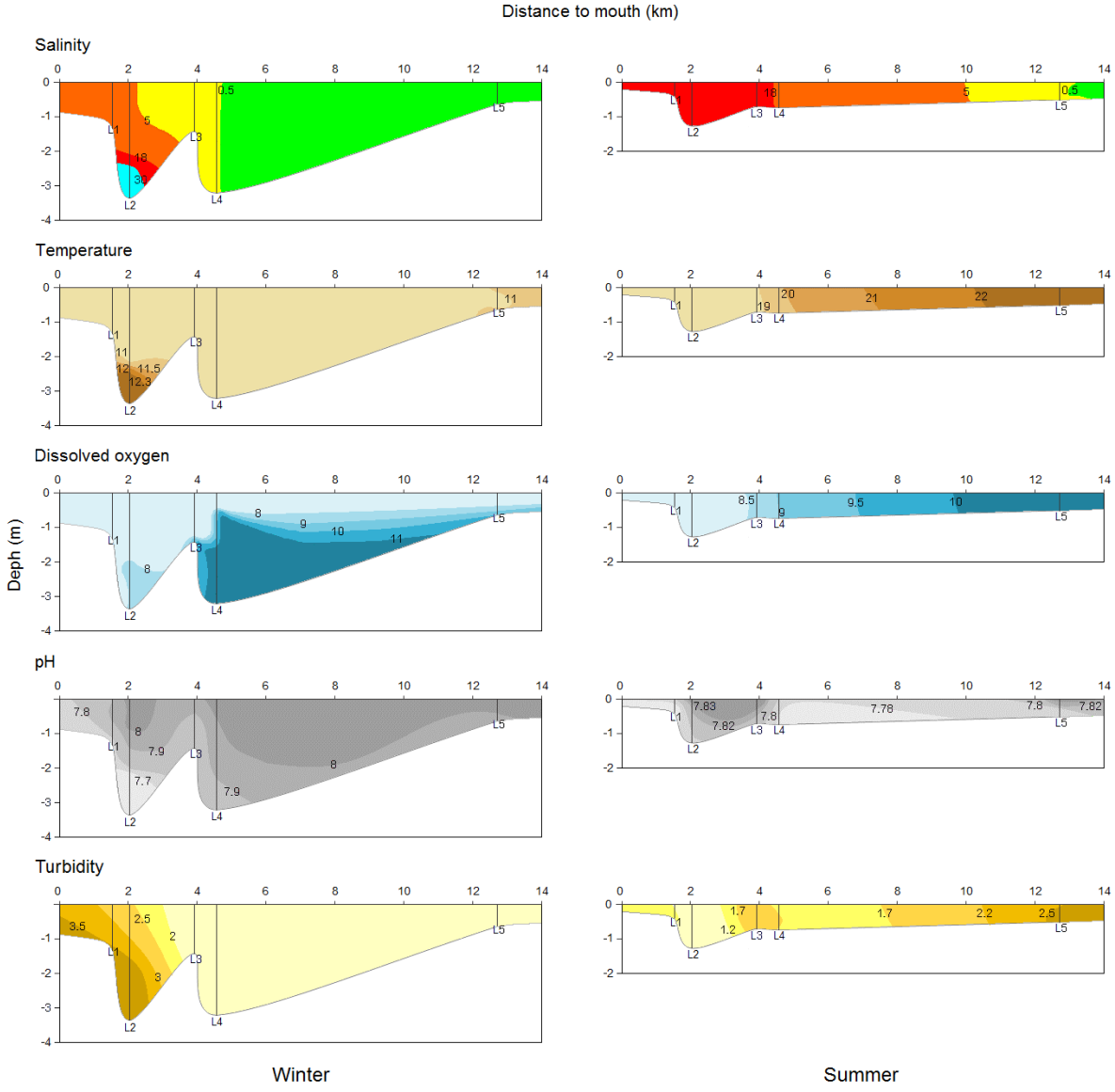

Figure 7.3 Spatial distribution of salinity, temperature, dissolved oxygen, pH, and turbidity in the Lima estuary during the winter and summer surveys.

The DO and pH values did not show large variations between sampling locations and surveys (8.14–11.25 mg O_2/L, and 7.68–8.11, respectively). The values presented by salinity and temperature were higher in the summer survey, as expected. At each sampling location, the increase in salinity with depth was inversely followed by temperature. In the winter survey, turbidity was higher towards the mouth, while during the summer survey it was higher upstream.

Lower salinities and higher oxygen levels were registered in winter, as a result of increased freshwater inflow (dam discharges and rainfall). Inorganic nutrients in the uppermost site of the estuary were higher during winter (Table 7.1). Maximum dissolved inorganic nitrogen (DIN = NH_4^+ + NO_x) concentration in winter/wet season, with the dissolved inorganic phosphorus presenting similar behavior. The NO_x amount was the main contributor to the DIN concentrations, with 98.7 and 91.9 % in the winter and summer, respectively.

Table 7.1 Inorganic nutrient present in estuarine water used for incubation experiments.

Season	NH_4^+ (μM)	NO_x (μM)	PO_4^{3-} (μM)	N:P
Winter	1.09	80.7	0.211	388
Summer	2.62	29.5	0.128	251

7.3.2 Sediments characterization

Sediments from the Lima estuary were mainly composed by sand (Figure 7.4), especially intertidal sediments that presented low spatial and temporal variability of grain size. The sediments with higher amounts of clay and silt were 2SS (30.9% and 11.4% in summer and winter, respectivelly), and 3SS (54.0% and 18.5% in summer and winter, respectively). The percentage of finer particles was lower than 4% for the remaining sediments. Accordingly, subtidal sediments collected from sites L2 and L3 presented the high organic matter content, and negative redox potential (reducing conditions) (Table 7.2). Coarser sediments were present in the upper estuary.

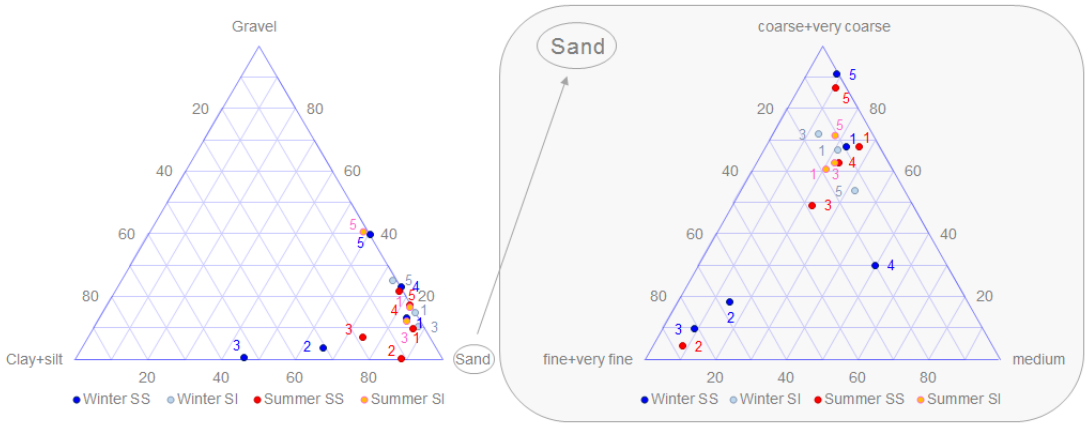

Figure 7.4 Sediments size distribution in the Lima estuary.

The 3SS sample presented the highest values for NH_4^+ (68.3 μg N-NH_4^+ g^{-1} dry sediment, summer), PO_4^{3-} (661.3 μg P-PO_4^{3-} g^{-1} dry sediment, winter), and organic matter (14.26% dry sediment, winter). Levels of NO_x in the sediments were always modest, with the highest value obtained for the L5SI sample (0.814 μg N-NO_x g^{-1} dry sediment, winter). Total phosphorus showed a percentage of dissolved inorganic phosphorus higher than 60% (except for the L3SS sample, winter).

Table 7.2 Sediments characterization from each of the sampling sites in the Lima estuary.

Location	Season	ORP [1] (mV)	Temperature (ºC)	Organic matter (%) [2]	N-NH_4^+ (μg g^{-1}) [2]	N-NO_x (μg g^{-1}) [2]	P-PO_4^{3-} (μg g^{-1}) [2]	Total P (μg g^{-1}) [2]
L1SS	Winter	55	10.5	0.77	12.3	0.149	79.7	83.4
	Summer	98	21.7	1.02	19.2	0.103	89.6	140.3
L1SI	Winter	108	10.6	0.74	11.4	0.090	82.9	132.9
	Summer	222	21.5	0.82	10.7	0.057	93.9	132.1
L2SS	Winter	-166	12.8	8.89	25.0	0.447	451.5	669.2
	Summer	-307	18.8	10.61	43.2	0.226	566.9	828.7
L3SS	Winter	-41	10.9	14.26	67.3	0.386	661.3	1,057
	Summer	-208	20.9	5.90	68.3	0.243	412.4	1,960
L3SI	Winter	99	10.9	0.80	13.9	0.382	96.0	120.6
	Summer	207	24.6	1.66	27.2	0.376	152.5	202.7
L4SS	Winter	86	10.6	0.96	9.62	0.248	114.7	127.4
	Summer	24	21.5	1.03	20.2	0.077	167.9	172.8
L5SS	Winter	195	11.1	0.58	11.7	0.230	84.6	87.2
	Summer	292	23.7	0.88	34.2	0.115	85.4	141.6
L5SI	Winter	193	11.0	0.82	13.3	0.814	81.6	117.8
	Summer	268	26.1	1.14	29.8	0.110	137.2	140.5

[1] ORP: Oxidation-reduction potential; [2] Dry sediment.

7.3.3 Subtidal sediment fluxes

Levels of ammonium and oxidized nitrogen, and inorganic dissolved phosphate were measured in the incubation water in time 0 after the core equilibration time. The oxidized nitrogen concentration decreased throughout that period time in all microcosms (14–56%). The ammonium ion increased in 2SS and 3SS cores (up to three fold), in agreement with the respective sediment characteristics. In general, the phosphate ion amount decreased, suggesting the adsorption and desorption of phosphate ions by sediments.

During the experiment, the amount of NO_x tended to decrease for all subtidal sediments, with the exception of the microcosms with 4SS sediment collected in the summer survey (Figure 7.5). The NO_x concentration did not appear to be the limiting factor in the microcosm reactions, since the minimum value reached in all microcosms was 2.25 mmol m^{-2}. The NH_4^+ decreased in all microcosms in the winter survey. In some experiments, NH_4^+ was totally consumed within 24h (sediments: 4SS - 12h, and 5SS - 9h), suggesting that even with the enrichment, the concentration of ammonium ions was a limiting factor to the existing processes in the microcosms. The NH_4^+ levels for the summer survey varied depending on the sediments of the microcosms, decreased for the microcosms with 1SS and 5SS sediments, increased for the 2SS and 4SS sediments, and showed almost no variation for the 3SS sediments. Only the microcosms with 2SS and 4SS sediments presented a concentration increase throughout the experiment (always positive fluxes). Generally, in the period of 0–3h, for both surveys, an increase of concentration occurred (positive fluxes). Phosphate ion decreased in concentration in all microcosms.

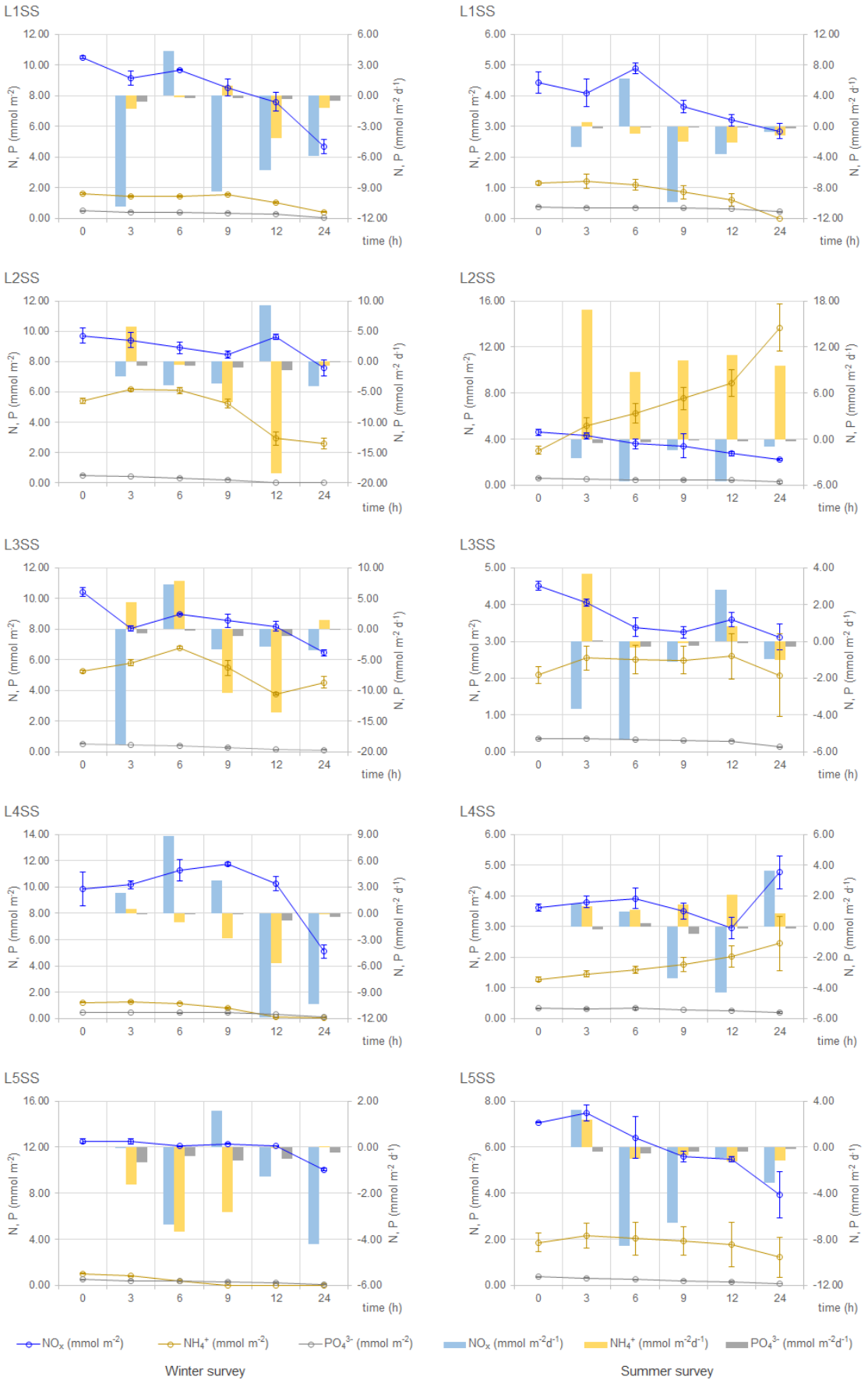

Figure 7.5 Subtidal sediments fluxes in the Lima estuary.

7.3.4 Intertidal sediments fluxes

The oxidized nitrogen concentration also decreased during core equilibration time in intertidal sediment microcosms (3–44%). The ammonium ion increased in incubation water (10–60%), with the exception of sample 3SI during summer survey. The phosphate ion amount decreased in the water in all cores. The water concentrations of PO_4^{3-}, NO_x, and NH_4^+ decreased in the microcosms of intertidal sediments, with the exception of the NO_x in 5SI microcosms during the summer survey (Figure 7.6). The concentration variation over time varied with survey and sediment, occurring even accumulation periods (positive fluxes). The evolution of concentration and fluxes obtained for nitrogen species (NO_x and NH_4^+) throughout the experiment were similar for the microcosms with sediments belonging to the lower and middle estuay (1SI and 3SI), during both surveys. NH_4^+ was always consumed before 24h, except for 5SI microcosms in summer survey.

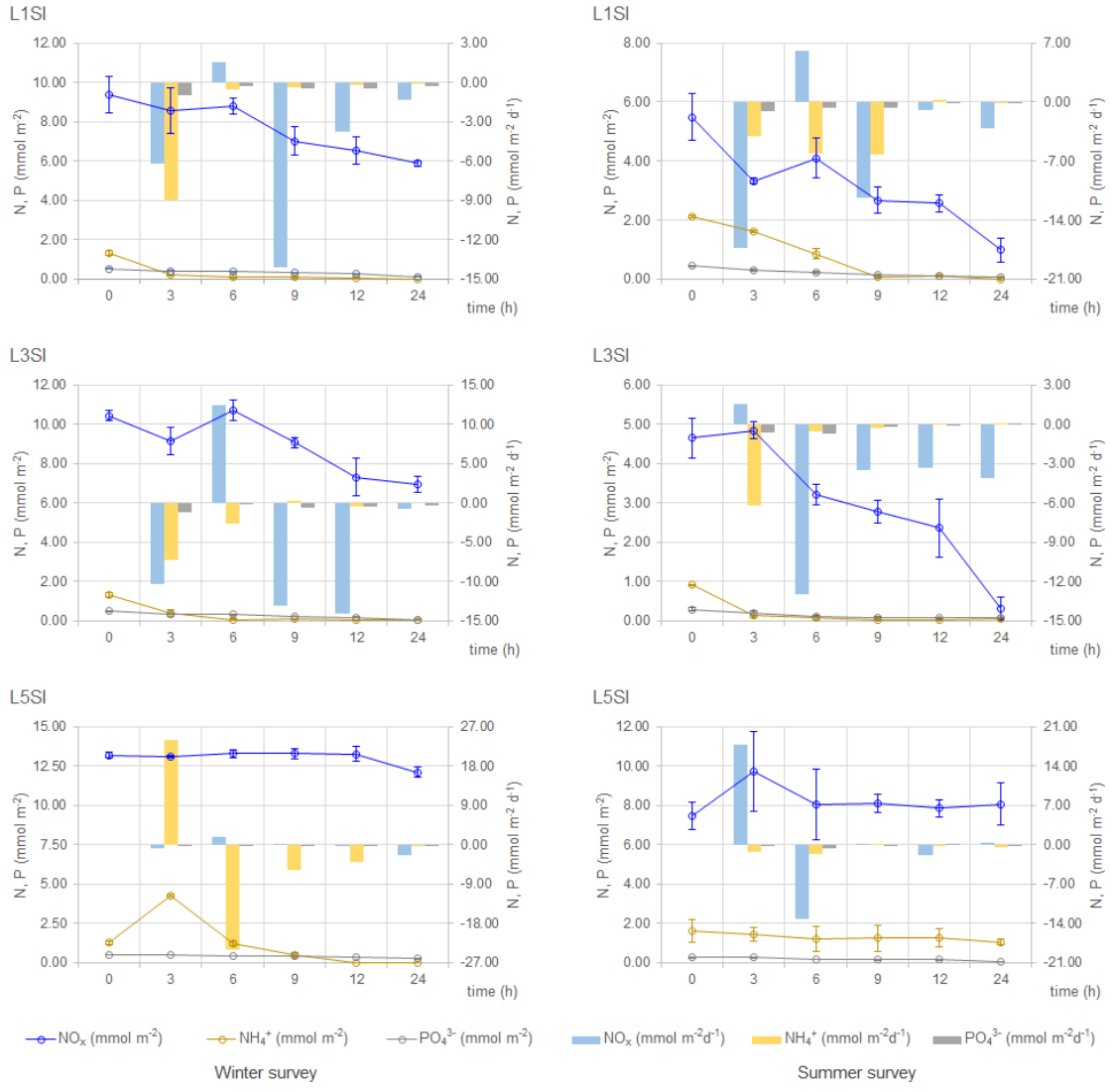

Figure 7.6 Intertidal sediments fluxes in the Lima estuary.

7.3.5 Net nutrients fluxes

The dynamics of inorganic nutrient cycling in the Lima estuary was assessed using core incubations. The nutrient fluxes are presented in Table 7.3. Sediments acted as sinks of inorganic nitrogen and phosphorus during most of the incubations. Ammonium fluxes varied between -218 and 421 μmol m^{-2} h^{-1}, while NO_x fluxes varied between -357 and 64 μmol m^{-2} h^{-1}. Only subtidal sediments from L4 acted as sources of inorganic nitrogen, but only during the summer. Phosphate fluxes always presented negative values, and varied from -39 to -7 μmol m^{-2} h^{-1}. Inorganic nutrient fluxes were significantly higher (higher consumption rates) during winter ($p < 0.05$).

Table 7.3 Fluxes of dissolved inorganic nitrogen and phosphorus (μmol m^{-2} h^{-1}, mean ± SE) in winter and summer surveys in the Lima estuary.

Location	Season	NH_4^+	NO_x	PO_4^{3-}
L1SS	Winter	-50 ± 3	-237 ± 23	-17.5 ± 0.5
	Summer	-57 ± 4	-92 ± 23	-7 ± 1
L1SI	Winter	-179 ± 24	-185 ± 3	-16.3 ± 0.5
	Summer	-218 ± 15	-170 ± 40	-27 ± 2
L2SS	Winter	-185 ± 15	-121 ± 12	-39 ± 3
	Summer	421 ± 96	-100 ± 14	-18 ± 3
L3SS	Winter	-64 ± 13	-158 ± 6	-33 ± 1
	Summer	-7 ± 39*	-49 ± 15	-10.3 ± 0.3
L3SI	Winter	-186 ± 15	-202 ± 3	-26 ± 3
	Summer	-151 ± 5	-245 ± 56	-21 ± 4
L4SS	Winter	-131 ± 8	-357 ± 39	-16 ± 1
	Summer	12 ± 3	64 ± 19	-7 ± 2
L5SS	Winter	-117 ± 5	-103 ± 10	-21 ± 5
	Summer	-89 ± 26	-155 ± 18	-21 ± 2
L5SI	Winter	-106 ± 13	-37 ± 15	-11 ± 2
	Summer	-20 ± 20*	15 ± 66*	-15 ± 4

* Statistical significance of the regressions > 0.05.

To assess the role of the estuary as a sink or source of nitrogen and phosphorus, a rough estimate of potential net fluxes of DIN and DIP were calculated from the incubation results, the volume, and the surface area from the different sections of the estuary. The NH_4^+, NO_x and PO_4^{3-} sediment/water fluxes are presented in the Table 7.4. The calculations confirmed that the Lima estuary acted as a sink for all species (NH_4^+, NO_x and PO_4^{3-}) in all its stretches.

Removal rates were in the order of 131 ton y^{-1}, 208 ton y^{-1}, and 55 ton y^{-1} for $N\text{-}NH_4^+$, $N\text{-}NO_x$, and $P\text{-}PO_4^{3-}$, respectively.

Table 7.4: Net nutrient fluxes in Lima estuary.

Location[1]	Sediment	Month	$N\text{-}NH_4^+$ (ton y^{-1})	$N\text{-}NO_x$ (ton y^{-1})	$P\text{-}PO_4^{3-}$ (ton y^{-1})
Lower	L1SS+L1SI+L2SS	Winter	-9.60	-38.8	-6.54
		Summer	-9.07	-15.2	-2.79
Middle	L3SS+L3SI+L4SS	Winter	-27.9	-65.3	-8.67
		Summer	-4.94	-3.04	-4.18
Upper	L5SS+L5SI	Winter	-43.5	-36.4	-16.7
		Summer	-36.2	-49.2	-16.1
Estuary			-131	-208	-55.0

[1] Areas (m^2) – Sediment (A(winter, m^2); A(summer, m^2)):

Lower estuary: L1SS (2551699; 2424114); L1SI (115494; 121269); L2SS (40063; 38060);

Middle estuary: L3SS (277708; 263822); L3SI (563690; 676428); L4SS (2537382; 2029905);

Upper estuary: L5SS (5531489; 5254915); L5SI (606359; 727631)

7.4 Discussion

7.4.1 Water column characteristics

Lower salinities and higher oxygen concentrations were registered in winter, as a result of increased river flow (dam discharges and rainfall). Higher salinity and lower oxygen were observed in the summer, due the factors such as insolation and evaporation (Camacho et al., 2014). The high values of DO (> 8 mg O_2 L^{-1}) recorded in the water column suggested that aerobic processes (e.g. nitrification) were not limited by the lack of oxygen (Figure 7.3). The amount of suspended matter (measured by turbidity) was always reduced (except at L3 in the winter survey), thereby facilitating the light penetration required for the metabolism of the primary producers (Cloern et al., 2014). The estuarine water presented maximum concentration for the dissolved inorganic nitrogen (DIN = NH_4^+ + NO_x), and inorganic phosphorus in the winter wet season, coinciding with reduced salinity, and by higher external inputs of stormwater (Mortazavi et al., 2012; Dunn et al., 2013). The NO_x amount was the main contributor to the DIN concentrations (98.7 and 91.9 % in the winter and summer surveys, respectively), as reported also by Li et al. (2017) and Dunn et al. (2013). As the estuarine water to be used in the incubations presented low nutrients concentrations, especially ammonium and phosphate ions (Table 7.1), nutrients were added to prevent them from becoming limited during incubation time.

7.4.2 Sediments characterization

In the collected sediments, a relation was found between the granulometry, the redox potential and the organic matter (Table 7.2, Figure 7.4). Sediments with finer grain size (2SS and 3SS) presented higher amounts of organic matter, due to the higher surface area (Fields, 2014), and negative redox potential (environment with reducing conditions), also showing the highest concentrations of ammonium ion (nitrogen reduced species) in both surveys (winter and summer). The increase of organic matter with the decrease in the grain size is attributed to co-sedimentation of particulate organic matter with clay and mineral particles (Venkatramanan et al., 2010). Sediments of larger grain size were collected in the upper estuary, both subtidal and intertidal sediments (5SS and 5SI). In estuarine systems, selective deposition of the sediments occur with finer particles being transported downstream to the estuary mouth (2SS and 3SS) by the ebb-dominated tidal flow and current, and the coarser deposited into upper estuary (5SS and 5SI) (Venkatramanan et al., 2013). In areas dominated by saltmarsh islands and/or located out of the navigation channel (2SS and 3SS), with lower hydrodynamics, differential deposition of fine sediments occurs (Camacho et al., 2014). The grain size, in general, showed the dominance of coarser to medium sand size sediments. The presented data point to an increase in the proportion of finer sediments in the estuary during winter, especially in L2 and L3, being the localization of these sites outside the navigation channel, inside more protected areas, and less affected by the hydraulic regime of the estuary. Sediments with higher organic matter content presented higher amounts of NH_4^+ and PO_4^{3-}. NH_4^+, and PO_4^{3-}, probably originated from organic matter diagenesis (Dunn et al., 2013; Testa et al., 2013). Moreover, PO_4^{3-} can also be sorbed onto particles, and deposited to sediments (Testa et al., 2013; Watson et al., 2018). The phosphorus results indicate that the inorganic fraction was the most important phosphorus speciation representing 60–98% of the total phosphorus, which is in agreement with previous reports (Liu et al., 2004; Watson et al., 2018).

7.4.3 Sediment-water fluxes

During the stabilization period of the microcosms, nutrients were promptly diffused between water and sediment. The NO_x concentration decreased in the aqueous layer of the microcosm, being swiftly consumed or diffuse into sediments and afterwards storaged or removed (Cowan and Boynton, 1996). Conversely, the NH_4^+ presented positive fluxes to the overlying water, appearing to indicate the release from the sediments, by adsorption and resuspension of that compound. During the incubations, different patterns for the NH_4^+ and NO_x fluxes were observed. For the diverse sediments collected in the two seasons, the most commonly found pattern for NH_4^+ and NO_x concentrations, was a global decrease during the incubation time, i.e., negative fluxes were obtained. The removal of the dissolved inorganic nitrogen (DIN) can

occur due to the assimilation of NO_3^- and NH_4^+ by the primary producers in the overlying water (Kaiser et al., 2015), and to the diffusion of the DIN into the sedimentary layer (Stief, 2013; Testa et al., 2013). The assimilation process did not appear to be the most preponderant process, with exception of the 2SS and 3SS sediments from the winter survey, since the DIN concentration decrease was similar or even higher in the dark period (12–24h) (Kaiser et al., 2015). Temporary increases in NO_x and NH_4^+ might be the result of organic matter mineralization in the overlaying water and/or DIN release from the sediments (remineralization) (Testa et al., 2013). The aerobic oxidation of ammonia (nitrification) may also have contributed for the increase of NO_x (Testa et al., 2013). Several factors could contribute to the different concentration fluctuations observed during the 24h incubations, such as the simultaneous occurrence of N transformation processes. The decrease of NH_4^+ with simultaneous increase of NO_x, suggested the presence of the nitrification process. The loss of NH_4^+ in the same magnitude order of the NO_x gain seems to support the nitrification as main process (winter: 2SS 9–12h; summer: 3SS 0–3h). In some microcosms, the lack of NH_4^+ due to its total consumption may have limited some biochemical reactions, such as nitrification (winter: 4SS, 3SI). The prevalence of denitrification would consume NO_x, provided there is availability of organic carbon (Knowles, 1982). In the microcosms, this process appears to predominate after the first few incubation hours (winter: 1SS 6–24h, 1SI 6–24h, 3SI 6–24h, 4SS 9–24h; summer: 1SS 6–24h, 3SI 3–24h, 5SS 3–24h). 2SS microcosm was the only one that presented a continuous increase of the ammonium ion in the incubation water during the 24h. Together with the simultaneous consumption of NO_x, and the sediment characteristics (negative redox), this could suggest the presence of dissimilatory nitrate reduction to ammonium in this sediment (Buresh and Patrick, 1981).

The decrease pattern showed by PO_4^{3-} seems to indicate its diffusion from the overlying water into the sediments, being trapped in the sediment particles, and adsorbed on the organic matter surface (Testa et al., 2013), and/or biological assimilation (Correll, 1999). Periods with PO_4^{3-} concentration increase in the overlying water (3SS and 4SS, middle estuary), can result from its production by the organic matter diagenesis (Dunn et al., 2013; Testa et al., 2013), and release by desorption (Mortazavi et al., 2012; Watson et al., 2018). The higher PO_4^{3-} concentrations at time 0 for the winter survey may be related to the salinity increase when the saline incubation waters were added to the microcosms. The addition of saline water may have induced a rapid desorption of phosphorus during the stabilization time, the ions compete with the phosphorus for the adsorption sites, inducing its desorption, which is a purely abiotic process (Deborde et al., 2007).

7.4.4 Estuarine net fluxes

The Lima estuary water did not present enrichment of nitrogen and phosphorus, not functioning as a source of nutrients to the sea. Indeed, sediments acted as a sink for inorganic nutrients. The water column showed potential negative fluxes for all studied species (NH_4^+, NO_x, and PO_4^{3-}) in the different estuarine stretches for both surveys, in agreement to that reported by Welsh et al. (2000) for the nitrogen species. Net uptake of inorganic nitrogen and phosphorus was not influenced by changes in the salinity of overlying water, since no significant differences were found comparing fluxes measured in the three estuarine sections.

In these productive areas, the sediments receive high concentrations of organic matter due to shallow water depths and river inputs, with the sedimentary organic particles acting as a phosphorus sink (Andrieux-Loyer et al., 2008). Water residence time can exert strong control on the nutrients ratio of export to loading, i.e., if estuarine communities have sufficient time to process nitrogen, their export downstream sea will be decreased through burial or denitrification (Nixon et al., 1996). Denitrification would be the main pathway for nitrogen loss from estuaries with longer residence times (Stief, 2013).

7.5 Conclusions

Sediments with finer grain size presented higher amounts of organic matter and negative redox potential, in addition to higher concentrations of NH_4^+ and PO_4^{3-}. Selective deposition of the sediments occurred with finer particles being transported downstream to the estuary mouth by the ebb-dominated tidal flow and current, and the coarser particles deposited in the upper estuary. Nonetheless, coarser to medium sand size sediments were dominant throughout the estuary. Sediments microcosms showed negative fluxes for all studied species (PO_4^{3-}, NH_4^+, and NO_x) along the estuary in both surveys. In general, the global variation of nutrient concentrations suggests the diffusion of PO_4^{3-}, NH_4^+ and NO_x from the overlying water into the sediments, and the simultaneous occurrence of physical-chemical and biochemical transformation processes. The estuary of Lima did not present enrichment of nitrogen and phosphorus in any of its stretches, or in any of the studied seasons, neither functioned as a source of nutrients to the sea, functioning as a sink for inorganic nutrients.

CHAPTER 8

Final considerations and future research

8.1 Final considerations

Estuaries are among the most productive and dynamic aquatic ecosystems, where the coupling of physics, biogeochemistry, and ecology occurs at various spatial scales. On the other hand, due to dense human populations along the coastal zone, estuaries and nearshore coastal waters are ecosystems most vulnerable to anthropogenic impacts, resulting in increased riverine nutrient fluxes to coastal areas.

The Lima estuarine ecosystem comprises important and sensitive areas that preserve important biodiversity and has also been identified as a nursery area for several commercially important marine species. Changes in water circulation and quality that affect estuarine communities and production depend on the characteristics of ecosystems, so understanding their functioning and the ability to predict the responses to changes in control factors, is important for estuarine management.

The present study began with a spatial and temporal characterization of the key environmental variables, and the relationship between them, during different seasons and tidal conditions, and a box model based on the hydrodynamics of the estuary was developed to evaluate the behavior of phyto and bacterioplankton within the estuary.

Lima river inflow was the driving force of most of the dynamic processes associated with nutrients (nitrates and silica), and the tidal cycles action associated with suspended solids and total dissolved carbon. Higher values of nitrate and silica were observed during the ebb tides of wet seasons in maximum river flows, and chlorophyll *a* and bacteria during the dry seasons, with lower river flow and higher availability of light and temperature. Some parameters had a behavior indicative of *in situ* processes (ammonium and phosphate, chlorophyll *a* and bacteria), despite the strong effect of external and physical variables.

Tidal dynamics played a crucial role in regulating the short-term variability of the water physical-chemical characteristics, with the distribution patterns and dispersion varying significantly on a time-scale of hours due to ebb advection of freshwater and flood intrusion of saltwater. The differences between the samples were closely connected to the hydrodynamic variations between the neap-spring cycles and ebb-flood cycles, with the tidal phase being the main driving factor of the parameters behavior, i.e., the mixing of water from different sources

promoted by tidal advection, and dilution by diffusion processes, as factors to explain the results variance.

Concentration gradients structure showed variations with temperature, river flow, and tidal action, with spatial and temporal patterns of the estuarine ecosystem strongly linked to the hydrodynamic and climate setting, with estuarine properties showing greater temporal (seasons, tides) variability than spatial variability. The physical precursor factors of the biogeochemical processes in the estuary were associated to the most relevant variables for the differences between the samples.

The box model results showed that phytoplankton tended to burst within the oligohaline zone, and was generally higher at spring tide, while higher bacterioplankton counts were found in the mesohaline stretch, in the middle estuary, an area with saltmarsh islands, and also in the upper estuary, during the coldest period of the year. Chlorophyll *a* showed net loss in salinities above 18, and freshwater appeared to be the main source for bacteria during neap tides; whereas coastal waters took over this role during the summer spring tide and also for the fall neap tide. Bacterial growth was higher during the warmest months of the year, with faster generation times in the lower reaches, increasing toward the upper estuary, being the highest at the summer spring tide. In the water column stratified part, similar tide-independent trends were found for chlorophyll *a* and bacterial fluxes, with net growth in the upper boxes and consumption beneath the halocline. In the non-stratified upper estuary, other controls emerged for phyto and bacterioplankton, as nitrogen and carbon inputs, respectively. The results show that while tidal hydrodynamics influenced plankton variability, production and consumption rates resulted from the interaction of additional factors, i.e., estuarine geomorphological characteristics and nutrient inputs.

Within the estuary, fluxes occurred between the water column and the sediments that depended on the degree of benthic-pelagic coupling. The benthic boundary layer, which includes the water column bottom layer and the sediment upper layer, directly influenced by the overlying water, is an integral part of the benthic zone, and has a great influence on the biological activity. The nutrient cycling rates within the water column (pelagic zone) and its fluxes through the sediment-water interface have been linked to the benthic hydrodynamics, sediment type and water transparency. In sediments, a multiplicity of physical, chemical, and biological processes co-existed.

The mineral distribution in the sediments upper layer resulted from the combined effect of river and coastal inputs, and may present seasonal patterns due to forcing, e.g. floods, storms, waves, and tides. Indeed, the Lima estuary granulometry showed the dominance of coarser to medium sand size sediments. The estuary subtidal sediments were usually anoxic in the

middle estuary, presenting larger amounts of mud than intertidal sediments. Oxygen, silicon, carbon, aluminum, and potassium were the most abundant elements, with the silicon and carbon amounts related to the sediments mud content. The sediments mineralogical composition reflected the watershed lithology, with the most representative minerals being quartz, microcline (k-alkaline feldspar), and albite (plagioclase), in agreement with the results obtained in the elementary characterization. No clear seasonal variation was found for the elemental and mineralogical composition of the sediments. Natural processes such as weathering and bedrocks erosion were the main sources of mineral supply in the sediments. Among the chemical elements, only Cu, In, and Mo are of concern, which may occasionally be associated with adverse contamination. Therefore, identifying the impact of natural factors can contribute to the identification of the impact of human activities. Factorial analysis explained 80% of the elemental origin, being 33% related to terrestrial origin, 24% to marine sediments, and 15% to anthrogenic inputs.

The exchange processes of compounds carried out in estuarine sediments were influenced by river flow and tidal cycles, with sediments acting as a source or sink of nutrients into or out of the water column. The results seem to indicate the existence of *in situ* processes, involving the various compartments of the estuary, i.e., water column, interstitial water, and sediments. The nutrients concentration decreased from the sediments to the water column, suggesting the nutrient flux from the water column to the sediments, i.e., the diffusion of the overlying water nutrients onto the sediments, and subsequent storage or removal in the sediments. The estuary presented a sediment grain size gradient due to energetic textural bipolarity (river and tidal energy), with the ebb currents reworking river sediments to the sea, and flood currents introducing marine sediments into the estuary. The result was a selective sediment deposition, with the finer fraction transported downstream to the estuary mouth by the ebb-dominated tidal flow, and the coarser fraction deposited in the upstream part of the estuary, with the sediment size appearing to be the property responsible for most of the variability among sediment samples. Despite the great seasonal variation of the water column estuarine nutrients, due to the variable freshwater inflow, the results showed that in the sediments the variability of the nutrients concentration was strongly linked to the granulometry. Therefore, the grain size was probably a key factor for the dynamics of organic matter and nutrients.

Nutrient fluxes at the sediment-water interface influenced or regulated the water column nutrient composition, since sediments behaved as a sink or as a source of inorganic nitrogen, phosphorus, and silica through different biogeochemical processes. Microcosm experiments yielded a connection between the granulometry, the redox potential, and the organic matter, with finer grain size sediments, presenting higher amounts of organic matter and negative redox potential, besides the higher concentrations of NH_4^+ and PO_4^{3-}. The water column

showed potential negative fluxes for all studied species (PO_4^{3-}, NH_4^+, and NO_x), along the estuary. The sediments presented similar behavior for the nitrogen species and the opposite for the phosphorus, except for the inorganic phosphorus during the summer survey in the middle estuary section, an estuarine stretch with high primary production activity. The global variation showed by nutrients concentration suggests the diffusion of PO_4^{3-}, NH_4^+, and NO_x from the overlying water into the sediments, and subsequent storage or removal by physicochemical and biochemical transformation processes. The Lima estuary did not present nitrogen and phosphorus enrichment in any of its stretches or seasons, neither functioned as a source of nutrients to the sea, but rather as a sink of inorganic nutrients.

A good understanding of how the environmental conditions within estuarine systems influence biological responses to nutrients is essential for the development of a coherent estuarine management strategy, as well as understanding the nutrient sources and processes involved in the transformation, cycling, and retention of nutrients within the estuary. The data from this study can serve as an important baseline for other studies concerned with the management of the estuarine natural environment, and its ecosystems and fishing grounds, flood protection, tourism, and maintenance of navigation channel issues, and its connections with existent structures.

8.2 Future research

Understanding the role of nutrients and knowledge their dynamics in the diverse estuarine compartments is critical to assess the ecosystems health. Throughout this thesis, information gaps have been identified that need to be studied and filled in to allow a more effective contribution towards the management of the estuary. To collate these gaps, it is suggested for future investigation:

- Research to understand the spatial and temporal structure of the salt wedge resulting from tidal dynamics (flood and ebb tides, and neap and spring tides), coupled with the influence of different river flow regimes (seasonality), to evaluate the response of the estuarine system to the variations in river discharge and geomorphological, imposed by human activity;
- Sediment characterization should also be performed for the grain size fraction < 0.063 mm, and the results compared with those obtained in this study, to determine to what extent the larger particle size fractions dilute the concentration of the minor elements, masking the role of anthropogenic factors in an estuarine environment;

- Studies of the physical-biochemical processes between the sediment and the water column, based on nutrient fluxes to evaluate the nutrient dynamics. Physical-biogeochemical controls in the benthic pelagic coupling of nutrient fluxes can be performed using laboratory microcosms and *in situ* cores. The cores should also be analyzed for additional indicators of nutrient enrichment, harmful algae proliferation, and changes in ecosystems;
- Research on nutrient dynamics applying the developed box model with improvements. Due to the estuarine complexity and the simplicity of the developed model, new variables must be introduced in the model so that the study of nutrient dynamics in the estuary is more comprehensive and better describes the reality;
- Identification and quantification of additional continuous and discrete sources of substances and maximum concentrations of discharged substances, as well as their consequences for water quality, to enable the identification of sensitive areas, thus applying the concept of prevention.

In future research suggested here, the results would be better achieved by long-term monitoring at intervals short enough to adequately assess short-term fluctuations and long-term variability.

REFERENCES

Abdullah, N.A., Abdullah, L.I., Shazili, N.A.M, Sokiman, S., 2015. Clay Minerals on Recent Surface Estuarine Sediments from Selected Rivers of Terengganu, Malaysia. Journal of Earth Sciences. 1 (1), 8–16.

Adams, J.B., Bate, G.C., O'Callaghan, M., 1999. Primary Producers. In: Allanson, B.R., Baird, D. (Eds.), Estuaries of South Africa. Cambridge University Press, Cambridge, UK. pp. 91–117.

Akomeah, E., Lindenschmidt, K.E., 2017. Seasonal Variation in Sediment Oxygen Demand in a Northern Chained River-Lake System. Water. 9, 254.

Allanson, B.R., Read, G.H.L., 1995. Further comment on the response of Eastern Cape Province estuaries to variable freshwater inflows. Southern African Journal of Aquatic Sciences. 21, 56–70.

Allanson, B.R., Winter, P.E.D., 1999. Chemistry. In: Allanson, B.R., Baird, D. (Eds.), Estuaries of South Africa. Cambridge University Press, Cambridge, UK. pp. 53–90.

Almeida, C.M.R., Mucha, A.P., Vasconcelos, M.T., 2011. Role of different salt marsh plants on metal retention in an urban estuary (Lima estuary, NW Portugal). Estuarine, Coastal and Shelf Science. 91, 243–249.

Alsterberg, C., Sundba, K., Hulth, S., 2012. Functioning of a Shallow-Water Sediment System during Experimental Warming and Nutrient Enrichment. PLOS ONE. 7 (12), 1–10: e51503.

Alvarez, I., Lorenzo, M.N., deCastro, M., 2012. Analysis of chlorophyll a concentration along the Galician coast: seasonal variability and trends. Journal of Marine Science. 69 (5), 728–738.

Alves, M.I.C., 2004. A sedimentação fluvial cenozoica na região do entre-Douro-e-Minho (NW de Portugal). In: Geomorfologia do Noroeste da Península Ibérica 2002. GEDES – Gabinete de Estudos de Desenvolvimento e Ordenamento do Território, Porto. pp. 93–115.

Amorim, E., Ramos, S., Elliott, M., Bordalo, A.A., 2016. Immigration and early life stages recruitment of the European flounder (*Platichthys flesus*) to an estuarine nursery: The influence of environmental factors. Journal of Sea Research. 107, 56–66.

Anaya-Gregorio, A., Armstrong-Altrin, J.S., Machain-Castillo, M.L., Montiel-García, P.C., Ramos-Vázquez, M.A., 2018.Textural and geochemical characteristics of late Pleistocene to Holocene fine-grained deep-sea sediment cores (GM6 and GM7), recovered from southwestern Gulf of Mexico. Journal of Palaeogeography. 7 (3), 253–271.

Andersen, F.Ø., Jensen, H.S., 1992. Regeneration of inorganic phosphorus and nitrogen from decomposition of seston in a freshwater sediment. Hydrobiologia. 228, 71–81.

Anderson, O.R., 2016. The role of heterotrophic microbial communities in estuarine C budgets and the biogeochemical C Cycle with implications for global warming: research opportunities and challenges. Journal of Eukaryotic Microbiology. 63, 394–409.

Andrieux-Loyer, F., Philippon, X., Bally, G., Kérouel, R., Youenou, A., Le Grand, J., 2008. Phosphorus dynamics and bioavailability in sediments of the Penzé Estuary (NW France): in relation to annual P-fluxes and occurrences of *Alexandrium Minutum*. Biogeochemistry. 88 (3), 213–231.

APA, 2016. Plano de Gestão da Região Hidrográfica do Minho e Lima (RH1), Plano de Gestão da Região Hidrográfica 2016/2021. Agência Portuguesa do Ambiente.

APHA, WWA, WEF, 1992. Standard Methods for the Examination of Water and Wastewater. 18th ed. American Public Health Association, Washington, DC.

APHA, WWA, WEF, 2005. Standard Methods for the Examination of Water and Wastewater. 21th ed. American Public Health Association, Washington, DC.

ARH Norte - Administração da Região Hidrográfica do Norte, Agência Portuguesa do Ambiente (APA), 2012. Plano de Gestão da Região Hidrográfica do Minho e Lima RH1 - Relatório Técnico. Comissão Europeia, Porto.

Armendáriz, M., López-Guijarro, R., Quesada, C., Pin, C., Bellido, F., 2008. Genesis and evolution of a syn-orogenic basin in transpression: Insights from petrography, geochemistry and Sm–Nd systematics in the Variscan Pedroches basin (Mississippian, SW Iberia). Tectonophysics. 461, 395–413.

Asmus, R.M, Sprung, M., Asmus, H., 2000. Nutrient fluxes in intertidal communities of a South European lagoon (Ria Formosa) – similarities and differences with a northern Wadden Sea bay (Sylt-Rømø Bay). Hydrobiologia. 436, 217–235.

Aspila, K. I., Agemian, H., Chau, A.S. Y., 1976. A semi-automated method for the examination of inorganic, organic and total phosphate in sediments. Analyst. 101, 187.

Aston, S.R., 1978. Estuarine chemistry. In: Riley, J.P., Chester, R. (Ed.), Chemical Oceanography. 2nd edition. Academic Press, London, UK. pp. 362–440.

Attermeyer, K., Tittel, J., Allgaier, M., Frindte, K., Wurzbacher, C., Hilt, S., Kamjunke, N., Kamjunke, H., 2015. Effects of light and autochthonous carbon additions on microbial turnover of allochthonous organic carbon and community composition. Microbial Ecology. 69, 361–371.

Azam, M.M., Tripathi, J.K., 2016. Recent Contributions in the Field of Sediment Geochemistry. Proceedings of the Indian National Science Academy - Spl Issue. 82 (3), 805–815.

Azevedo, I., Ramos, S., Mucha, A.P., Bordalo, A.A., 2013. Applicability of ecological assessment tools for management decision-making: a case study from the Lima estuary (NW Portugal). Ocean & Coastal Management. 72, 54–63.

Azevedo, I.C., Duarte, P., Bordalo, A.A., 2010. Temporal and spatial variability of phytoplankton photosynthetic characteristics in a Southern European estuary (Douro, Portugal). Marine Ecology Progress Series. 412, 29–44.

Azevedo, I.C., Duarte, P.M., Bordalo, A.A., 2006. Pelagic metabolism of the Douro estuary (Portugal) - Factors controlling primary production. Estuarine, Coastal and Shelf Science. 69, 133–146.

Azevedo, I.C., Duarte, P.M., Bordalo, A.A., 2008. Understanding spatial and temporal dynamics of key environmental characteristics in a mesotidal Atlantic estuary (Douro, NW Portugal). Estuarine, Coastal and Shelf Science. 76, 620–633.

Azhikodan, G., Yokoyama K., 2016. Spatio-temporal variability of phytoplankton (Chlorophyll-a) in relation to salinity, suspended sediment concentration, and light ntensity in a macrotidal estuary. Continental Shelf Research. 126, 15–26.

Bacelar-Nicolau, P., Nicolau, L.B., Marques, J.C., Morgado, F., Pastorinho, R., Azeiteiro, U.M., 2003. Bacterioplankton dynamics in the Mondego estuary (Portugal). Acta Oecologica. 24, S67–S75.

Baird, D., Winter, P.E.D., 1989. Annual flux budgets of suspended particulate material in a shallow, well mixed estuary. Proceedings of the International symposium on ‘Estuarine Water Quality Management’. Reinbek, West Germany.

Baird, D., Winter, P.E.D., 1992. Flux of inorganic nutrients and particulate carbon between a Spartina maritime salt marsh and the Swartkops estuary, eastern Cape. Southern African Journal of Aquatic Sciences. 18, 64–73.

Barbier, E.B., Hacker, S.D., Kennedy, C., Koch, E.W., Stier, A.C., Silliman, B.R., 2011. The value of estuarine and coastal ecosystem services. Ecological Monographs. 81, 169–193.

Barrio, P., Ganju, N.K., Aretxabaleta, A.L., Hayn, M., García, A., Howarth, R.W., 2014. Modeling future scenarios of light attenuation and potential seagrass success in a eutrophic estuary. Estuarine, Coastal and Shelf Science. 149, 13–23.

Basset, A., Barbone, E., Elliott, M., Li, B.-L., Jorgensen, S.E., Lucena-Moya, P., Pardo, I., Mouillot, D., 2013. A unifying approach to understanding transitional waters: Fundamental

properties emerging from ecotone ecosystems. Estuarine, Coastal and Shelf Science. 132, 5–16.

Bate, G.C., Whitfield, A.K., Adams, J.B., Huizinga, P., Wooldridge, T.H., 2002. The importance of the River Estuary Interface zone in estuaries. Water SA. 28, 271–279.

Beaumont, N.J., Austen, M.C., Atkins, J.P., Burdon, D., Degraer, S., Dentinho, T.P., Derous, S., Holm, P., Horton, T., van Ierland, E., Marboe, A.H., Starkey, D.J., Townsend, M., Zarzycki, T., 2007. Identification, definition and quantification of goods and services provided by marine biodiversity: Implications for the ecosystem approach. Marine Pollution Bulletin. 54, 253–265.

Bernard, R.J., Mortazavi, B., Wang, L., Ortmann, A.C., Macintyre, H., Burnett, W.C., 2014. Benthic nutrient fluxes and limited denitrification in a sub-tropical groundwater-influenced coastal lagoon. Marine Ecology Progress Series. 504, 13–26.

Binnerup, S.J., Jensen, H.S., Revsbech, N.P., Jensen, M.H., Sørensen, J., 1992. Denitrification, dissimilatory reduction of nitrate to ammonium, and nitrification in a bioturbated estuarine sediment as measured with 15N and microsensor techniques. Applied and Environmental Microbiology. 58, 303–313

Bojakowska, I., 2016. Phosphorus in lake sediments of Poland – Results of monitoring research. Limnological Review. 16 (1), 15–25.

Boonphakdee, T., Fujiwara, T., 2008. Temporal Variability of Nutrient Budgets in a Tropical River Estuary: the Bangpakong River Estuary, Thailand. EnviromentAsia. 1, 7–21.

Bordalo, A.A., 2003. Microbiological water quality in urban coastal beaches: the influence of water dynamics and optimization of the sampling strategy. Water Research. 37, 3233–3241.

Bordalo, A.A., Vieira, M.E.C., 2005. Spatial variability of phytoplankton, bacteria and viruses in the mesotidal salt wedge Douro Estuary (Portugal). Estuarine, Coastal and Shelf Science. 63, 143–154.

Bouchez, J., Gaillardet, J., France-Lanord, C., Maurice, L., Dutra-Maia, P., 2011. Grain size control of river suspended sediment geochemistry: Clues from Amazon River depth profiles. Geochemistry and Geophysics Geosystems. 12 (3), 1–24.

Boyle, K.A., kamer, K., Fang, P., 2004. Spatial and Temporal Patterns in Sediment and Water Column Nutrients in a Eutrophic Southern California Estuary. Estuaries. 27 (3), 378–388.

Brils, K., 2008. Sediment monitoring and the European Water Framework Directive. Annali dell'Istituto superiore di sanità. 44 (3), 218–223.

Bruesewitz, D.A., Gardner, W.S., Mooney, R.F., Pollard, L., Buskey, E.J., 2013.Estuarine ecosystem function response to flood and drought in a shallow, semiarid estuary: Nitrogen cycling and ecosystem metabolism. Limnology and Oceanography. 58, 2293–2309.

Buchan, A., LeCleir, G.R., Gulvik, C.A., González, J.M., 2014. Master recyclers: features and functions of bacteria associated with phytoplankton blooms. Nature Reviews Microbiology. 12, 686–698.

Bukaveckas, P.A., Barry, L.E., Beckwith, M.J., David, V., Lederer, B., 2011. Factors determining the location of the chlorophyll maximum and the fate of algal production within the tidal freshwater James River. Estuaries and Coasts. 34, 569–582.

Bunse, C., Bertos-Fortis, M., Sassenhagen, I., Sildever, S., Sjöqvist, S., Godhe, A, Gross, S., Kremp, A., Lips, I., Lundholm, N., Rengefors, K., Sefbom, J., Pinhassi, J., Legrand1, C., 2016. Spatio-temporal interdependence of bacteria and phytoplankton during a Baltic Sea Spring Bloom. Frontiers Microbiology. 7, 517.

Buresh, R.J., Patrick Jr, W.H., 1981. Nitrate reduction to ammonium and organic nitrogen in an estuarine sediment. Soil Biology and Biochemistry. 13 (4), 279–283.

Burone, L., Muniz, P., Pires-Vanin, A.M., Rodrigues, M., 2003. Spatial distribution of organic matter in the surface sediments of Ubatuba Bay (Southeastern – Brazil). Anais da Academia Brasileira de Ciências. 75, (1), 77–90

Buzzelli, C., Wan, Y., Doering, P.H., Boyer, J.N., 2013. Seasonal dissolved inorganic nitrogen and phosphorus budgets for two sub-tropical estuaries in south Florida, USA. Biogeosciences. 10, 6721–6736.

Cabeçadas, G., Nogueira, M., Brogueira, M.J., 1999. Nutrient dynamics and productivity in three European estuaries. Marine Pollution Bulletin. 38 (12), 1092–1096.

Cabrita, M.T., 2014. Phytoplankton community indicators of changes associated with dredging in the Tagus estuary (Portugal). Environmental Pollution. 191, 17–24.

Cabrita, M.T., Catarino, F., Vale, C., 1999. The effect of tidal range on the flushing of ammonium from intertidal sediments of the Tagus estuary, Portugal. Oceanologica Acta. 22, 291–302.

Caetano, M., Raimundo, J., Nogueira, M., Santos, M., Mil-Homens, M., Prego, R., Vale, C., 2016. Defining benchmark values for nutrients under the Water Framework Directive: Application in twelve Portuguese estuaries. Marine Chemistry. 185, 27–37.

Calbet, A., Landry, M.R., 2004. Phytoplankton growth, microzooplankton grazing, and carbon cycling in marine systems. Limnology and Oceanography. 49, 51–57.

Camacho, S., Moura, D., Connor, S., Boski, T., Gomes, A., 2014. Geochemical characteristics of sediments along the margins of an atlantic-mediterranean estuary (the Guadiana, Southeast Portugal): spatial and seasonal variations. Revista de Gestão Costeira Integrada/Journal of Integrated Coastal Zone Management. 14 (1), 129–148.

Campbell, B., Kirchman, D.L., 2013. Bacterial diversity, community structure and potential growth rates along an estuarine salinity gradient. International Society for Microbial Ecology. 7, 210–220.

Canfield, D.E., Kristensen, E., Thamdrup, B., 2005. The silicon cycle. In: Canfield, D.E., Kristensen, E., Thamdrup, B. (Eds.), Aquatic geomicrobiology: advances in marine biology, vol 48. Academic Press, London, UK. pp. 441–463.

Caraballo, M.A., Michel, F.M., Hochella Jr, M.F., 2015. The rapid expansion of environmental mineralogy in unconventional ways: Beyond the accepted definition of a mineral, the latest technology, and using nature as our guide. American Mineralogist. 100 (1), 14–25.

Carbone, M.E., Spetter, C.V., Marcovecchio, J.E., 2016. Seasonal and spatial variability of macronutrients and Chlorophyll a basead on GIS in the South American estuary (Bahía Blanca, Argentina). Environmental Earth Sciences. 75 (736), 1–13.

Carbonnel, V., Vanderborght, J.P., Chou, L., 2013. Silica Mass-Balance and Retention in the Riverine and Estuarine Scheldt Tidal System (Belgium/The Netherlands). Aquatic Geochemistry. 19, 501–516.

Cardoso, R., Araújo, M.F., Freitas, M.C., Fatela, F., 2008. Geochemical characterisation of sediments from marginal environments of Lima Estuary (NW Portugal). Revista Electrónica de Ciências da Terra. Geosciences On-line Journal. GEOTIC – Sociedade Geológica de Portugal. 5 (6), 1–11.

Carvalhido, RP., Pereira, D.I., Cunha, P.P., Buylaert, J.P., Murray, A.S., 2014. Characterization and dating of coasta.l deposits of NW Portugal (Minho e Neiva area): a record of climate, eustasy and crustal uplift during the Quaternary. Quaternary International. 328–329, 94–106.

Cavanaugh, G.M., 1975. Formulae and methods VI of Marine Biological Laboratory Chemical Room. Marine Biological Laboratory, Woods Hole, Massachusetts, USA.

Cermeño, P., Maranon, E., Pérez, V., Serret, P., Ferna´ndez, E., Castro, C., 2006. Phytoplankton size structure and primary production in a highly dynamic coastal ecosystem (Ría de Vigo, NW-Spain): seasonal and shorttime scale variability. Estuarine, Coastal and Shelf Science. 67, 251–266.

CGP – Carta Geológica de Portugal - escala 1/1 000 000, 2010. DGEG - Direcção-Geral de Energia e Geologia.

Chaudhuri, K., Manna, S., Sarma, K.S., Naskar, P., Bhattacharyya, S., Bhattacharyya, M., 2012. Physicochemical and biological factors controlling water column metabolism in Sundarbans estuary, India. Aquatic Biosystems. 8 (26), 1–16.

Clark, G.F., Kelaher, B.P., Dafforn, K.A., Coleman, M.A., Knott, N.A., Marzinelli, E.M., Johnston, E.L., 2015. What does impacted look like? High diversity and abundance of epibiota in modified estuaries. Environmental Pollution. 196, 12–20.

Clavero, V., Izquierdo, J.J., Fernandez, J.A., Niell, F.X. 2000. Seasonal fluxes of phosphate and ammonium across the sediment-water interface in a shallow small estuary (Palmones River, southern Spain). Marine Ecology Progress Series. 198, 51–60.

Cloern, J. E., Jassby, A.D., Schraga, T.S., Nejad, E., Martin, C., 2017. Ecosystem variability along the estuarine salinity gradient: Examples from long-term study of San Francisco Bay. Limnology and Oceanography. 62, S272–S291.

Cloern, J., 1991. Tidal stirring and phytoplankton bloom dynamics in an estuary. Journal of Marine Research. 49, 203–221.

Cloern, J.E., Foster, S.Q., Kleckner, A.E., 2014. Phytoplankton primary production in the world's estuarine-coastal ecosystems. Biogeosciences. 11, 2477–2501.

Coelho, J.P., Flindt, M.R., Jensen, H.S., Lillebø, A.I., Pardal, M.A., 2004. Phosphorus speciation and availability in intertidal sediments of a temperate estuary: relation to eutrophication and annul P-fluxes. Estuarine, Coastal and Shelf Science. 61, 583–590.

Conley, D.J., 2000, Biogeochemical nutrient cycles and nutrient management strategies. Hydrobiologia. 419, 87–96.

Conley, D.J., Schelske, C.L., 2001. Biogenic silica. In: Smol, J. P., Birks, H. J. B., Last, W. M. (Eds.), Tracking Environmental Change Using Lake Sediments. Volume 3: Terrestrial, Algal, and Siliceous Indicators. Kluwer Academic Publishers, Dordrecht, Netherlands. pp. 281–293.

Cooper, J.A.G., 2001. Geomorphological variability among the microtidal estuaries from the wave -dominated South African coast. Geomorphology. 40, 99–122.

Corbett, D.R., 2010. Resuspension and estuarine nutrient cycling: insights from the Neuse River Estuary. Biogeosciences. 7, 3289–3300.

Corredeira, C., Araújo, M.F., Jouanneau, J.M., 2008. Copper, zinc and lead impact in SW Iberian shelf sediments: An assessment of recent historical changes in Guadiana river basin. Geochemical Journal. 42, 319–329.

Correll, D.J., 1999. Phosphorus: A Rate Limiting Nutrient in Surface Waters. Poultry Science. 78, 674–682.

Costa-Dias, S., Sousa, R., Antunes, C., 2010. Ecological quality assessment of the lower Lima Estuary. Marine Pollution Bulletin. 61, 234–239.

Couceiro, F., Fones, G.R., Thompson, C.E.L., Statham, P.J., Sivyer, D.B., Parker, R., Kelly-Gerreyn, B.A., Amos, C.L., 2013. Impact of resuspension of cohesive sediments at the Oyster Grounds (North Sea) on nutrient exchange across the sediment–water interface. Biogeochemistry. 1331, 37–52.

Cowan, J.L.W., Boynton, W.R., 1996. Sediment-water oxygen and nutrient exchanges along the longitudinal axis of Chesapeake Bay: seasonal patterns, controlling factors and ecological significance. Estuaries. 19 (3), 562–580.

Cowan, J.L.W., Pennock, J.R., Boynton, W.R., 1996. Seasonal and interannual patterns of sediment-water nutrient and oxygen flux in Mobile Bay, Alabama (USA): regulating factors and ecological significance. Marine Ecology Progress Series. 141, 229–245.

Cravo. A., Cardeira, S., Pereira, C., Rosa, M., Alcântara, P., Madureira, M., Rita, F., Luis, J., Jacob, J., 2014. Exchanges of nutrients and chlorophyll a through two inlets of Ria Formosa, South of Portugal, during coastal upwelling events. Journal of Sea Research. 93, 63–74.

Cravo. A., Madureira, M., Felícia, H., Rita, F., Bebianno., M.J., 2006. Impact of outflow from the Guadiana River on the distribution of suspended particulate matter and nutrients in the adjacent coastal zone. Estuarine, Coastal and Shelf Science. 70, 63–75.

Crump, B.C., Hopkinson, C.S., Sogin, M.L., Hobbie, J.E., 2004. Microbial biogeography along an estuarine salinity gradient: combined influences of bacterial growth and residence time. Applied and Environmental Microbiology. 70 (3), 1494–1505.

Dame, R.F., Chrzanowski, T.H., Bildstein, K., Kjerfe, B., McKellar, H., Nelson, D., Spurrier, J.D., Stancyk, S., Stevenson, H., Vernberg, F.J., Zingmark, R.G., 1986. The outwelling hypothesis and North Inlet, South Carolina. Marine Ecology Progress Series. 72, 153–166.

Das, S., Giri, S. Dasa, I., Chanda, A., Ghosha, A., Mukhopadhyay, A., Akhandb, A., Choudhury, S.B., Dadhwald, V.K., Maity, S., Kumar, T.S., Lotliker, A.A., Mitra, D., Hazra, D., 2017. Nutrient dynamics of northern Bay of Bengal (nBoB)—Emphasizing the role of tides. Regional Studies in Marine Science. 10, 116–134.

Davies, O. A., Ugwumba, O. A., 2013. Tidal Influence on Nutrients Status and Phytoplankton Population of Okpoka Creek, Upper Bonny Estuary, Nigeria. Journal of Marine Biology. 2013 (Article ID 684739), 1–16.

Day Jr., J.W., Hall, C. A., Kemp, W. M., Yanez-Arancibia, A., 1989. Estuarine Ecology. 2nd edition. John Wiley & Sons, New York. pp. 558.

Day Jr., J.W., Yáñez-Arancibia, A., Kemp, W.M., Crump, B.C., 2013. Introduction to Estuarine Ecology. In: Day Jr., J.W., Kemp, W.M., Yáñez-Arancibia, A., Crump, B.C. (Eds.), Estuarine Ecology. 2nd edition. John Wiley & Sons, Inc., New Jersey, USA. pp.1–18.

Day, J.W. Jr., Pont, D., Hensel, P.F., Ibanez, C., 1995. Impacts of sea-level rise on deltas in the Gulf of Mexico and the Mediterranean: the importance of pulsing events to sustainability. Estuaries. 18, 636–647.

De Jonge, V.N., Elliott, M., 2001. Eutrophication. In: Steele, J., Thorpe, S., Turekian, K. (Ed.), Encyclopedia of Ocean Sciences. Academic Press, London, UK. pp. 852–870.

De Jonge, V.N., Van Beusekom, J.E.E., 1995. Wind- and tide-induced resuspension of sediment and microphytobenthos from tidal flats in the Ems estuary. Limnology and Oceanography. 40, 766–778.

Deborde, J., Anschutz, P., Chaillou, G., Etcheber, H., Commarieu, M.V., Lecroart, P., Abril, G., 2007. The dynamics of phosphorus in turbid estuarine systems: Example of the Gironde estuary (France). Limnology and Oceanography. 52(2), 862–872.

DeBusk, W.F., 1999. Document SL170. Soil and Water Science Department, Florida Cooperative Extension Service, Institute of Food and Agricultural Sciences, University of Florida, USA.

DeMaster, D.J., 1981. The supply and accumulation of silica in the marine environment. Geochimica et Cosmochemica Acta. 45, 1715–1732.

Derry, L.A., Kurtz, A.C., Ziegler, K., Chadwick, O.A., 2005. Biological control of terrestrial silica cycling and export fluxes to watersheds. Nature. 433, 728–731.

Desmit, X., Ruddick, K., Lacroix, G., 2015. Salinity predicts the distribution of chlorophyll *a* spring peak in the southern North Sea continental waters. Journal of Sea Research. 103, 59–74.

Dionne, J.C., 1963. Towards a more adequate definition of the St. Lawrence estuary. Zeitschrift für Geomorphologie. 7, 36–44.

Domingues, R.B., Barbosa, A., Galvão, H., 2005. Nutrients, light and phytoplankton succession in a temperate estuary (the Guadiana, south-western Iberia). Estuarine, Coastal and Shelf Science. 64, 249–260.

Downing, J.A., 1997. Marine nitrogen: Phosphorus stoichiometry and the global N:P cycle. Biogeochemistry. 37, 237–252.

Ducklow, H.W., Schultz, G., Raymond, P., Bauer, J., Shiah, F.K., 1999. Bacterial dynamics in large and small estuaries. In: Bell C. R., Brylinsky, M., Johnson-Green, P. (Eds.), Microbial Ecology of Estuaries. Atlantic Canada Society for Microbial Ecology. Halifax, Canada. pp. 105–111.

Dunn, R. J.K., Waltham, N.J., Teasdale, P.R., Robertson, D., Welsh, D.T., 2017. Short-Term Nitrogen and Phosphorus Release during the Disturbance of Surface Sediments: A Case Study in an Urbanised Estuarine System (Gold Coast Broadwater, Australia). Journal of Marine Science and Engineering. 5 (16) 1–13.

Dunn, R.J.K., Robertson, D., Teasdale. P.R., Waltham, N.J., Welsh, D.T., 2013. Benthic metabolism and nitrogen dynamics in an urbanised tidal creek: Domination of DNRA over denitrification as a nitrate reduction pathway. Estuarine, Coastal and Shelf Science. 131, 271–281.

Dyar, M.D., Gunter, M.E., Tasa, D., 2008. Mineralogy and Optical Mineralogy. Mineralogical Society of America, Chantilly, Virginia, USA.

Dyer, K.R., 1997. Estuaries. A Physical Introduction. 2nd edition. John Wiley & Sons, Chichester, UK. ISBN 978-0-471-97471-0.

Edgar, G.J., Barrett, N.S., Graddon, D.J., Last, P.R., 2000. The conservation significance of estuaries: a classification of Tasmanian estuaries using ecological, physical and demographic attributes as a case study. Biological Conservation. 92, 383–397.

EEC, 1975. Council Directive of 16 June 1975 Concerning the Quality Required of Surface Water Intended for the Abstraction of Drinking Water in the Member States (75/440/EEC). Official Journal of the European Community. L194, 26–31 (25-07-1975).

Elliott, M., McLusky, D.S., 2002. The need for definitions in understanding estuaries. Estuarine, Coastal and Shelf Science. 55, 815–827.

Elliott, M., Whitfield, A.K., 2011. Challenging paradigms in estuarine ecology and management. Estuarine, Coastal and Shelf Science. 94, 306–314.

EU, 2000. Directive 2000/60/EC of the European Parliament and of the Council of 23 October 2000 establishing a framework for community action in the field of water policy. Official Journal of the European Union. L327, 1–72.

Eyre, B., Twigg C., 1997. Nutrient behaviour during post-flood recovery of the Richmond River Estuary northern NSW, Australia. Estuarine, Coastal and Shelf Science. 44, 311–326.

Eyre, B.D., Ferguson, A.J.P., Webb, A., Maher, D., Oakes, J.M., 2010. Denitrification, N-fixation and nitrogen and phosphorus fluxes in different benthic habitats and their contribution

to the nitrogen and phsphorus budgets of a shallow oligotrophic sub-tropical coastal system (southern Moreton Bay, Australia). Biogeochemistry. 102, 111–133.

Falcão, A.P., Mazzolari, A., Gonçalves, A.B., Araújo, M.A.V.C., Trigo-Teixeira, A., 2013. Influence of elevation modelling on hydrodynamic simulations of a tidally-dominated estuary. Journal of Hydrology. 497, 152–164.

Fanning, K.A., Carder, K.L., Betzer, P.R., 1982. Sediment resuspension by coastal waters: a potential mechanism for nutrient re-cycling on the ocean's margins. Deep-Sea Research. 29, 953–965.

Fatema, K., Omar, W. M.W., Isa, M. M., 2015. Effects of Tidal Events on the Water Quality in the Merbok Estuary, Kedah, Malaysia. Journal of Environmental Science and Natural Resources. 8(2), 15–19.

Ferguson, A.J.P, Eyre, B.D., 2007. Seasonal discrepancies in denitrification measured by isotope pairing and N_2: Ar techniques. Marine Ecology Progress Series. 350, 19−27.

Feuillet-Girard, M., Gouleau, D., Blanchard, G., Joassard, L., 1997. Nutrient fluxes on an intertidal mudflat in Marennes-Oléron Bay, and influence of the emersion period. Aquatic Living Resources. 10, 49–58

Fields, L., Nixon, S.W., Oviatt, C., Fulweiler, R.W., 2014. Benthic metabolism and nutrient regeneration in hydrographically different regions on the inner continental shelf of Southern New England. Estuarine, Coastal and Shelf Science. 148, 14–26.

Fisher, T.R., Harding Jr, L.W., Stanley, D.W., Ward, L.G., 1988. Phytoplankton, nutrients, and turbidity in the Chesapeake, Delaware, and Hudson estuaries. Estuarine, Coastal and Shelf Science. 27 (1), 61–93.

Flynn, A.McG., 2008. Organic Matter and Nutrient Cycling in a Coastal Plain Estuary: Carbon, Nitrogen, and Phosphorus Distributions, Budgets, and Fluxes. Journal of Coastal Research. 55, 76–94.

Folk, R.L., 1954. The distinction between grain size and mineral composition in sedimentary-rock nomenclature. The Journal of geology. 62 (4), 344–359.

Forehead, H., Thomson, P., Kendrick, G.A., 2012. Shifts in composition of microbial communities of subtidal sandy sediments maximise retention of nutrients. FEMS Microbiology Ecology. 83, 279–298.

Fulweiler, R., Nixon, S.W., Buckley, B., 2010. Spatial and temporal variability in benthic oxygen demand and nutrient regeneration in an anthropogenically impacted New England estuary. Estuaries and Coasts. 33, 1377–1390.

Gameiro, C., Brotas, V., 2010. Patterns of Phytoplankton Variability in the Tagus Estuary (Portugal). Estuaries and Coasts. 33, 311–323.

Gameiro, C., Cartaxana, P., Brotas, V., 2007. Environmental drivers of phytoplankton distribution and composition in Tagus Estuary, Portugal. Estuarine, Coastal and Shelf Science. 75, 21–34.

Gameiro, C., Cartaxana, P., Cabrita, M.T., Brotas, V., 2004. Variability in chlorophyll and phytoplankton composition in an estuarine system. Hydrobiologia. 525, 113–124.

Gao, L., Li, D.J., Ding, P.X., 2009. Quasi-simultaneous observation of currents, salinity and nutrients in the Changjiang (Yangtze River) plume on the tidal timescale. Journal of Marine Systems. 75, 265–279.

Garcia-Robledo, E., Bohorquez, J., Corzo, A., Jimenez-Arias, J.L., Papaspyrou, S., 2016. Dynamics of Inorganic Nutrients in Intertidal Sediments: Porewater, Exchangeable, and Intracellular Pools. Frontiers in Microbiology. 7 (761), 1–14.

Garel, E., Ferreira Ó., 2011. Monitoring estuaries using non-permanent stations: practical aspects and data examples. Ocean Dynamics. 61 (7), 891–902.

Garel, E., Pinto, L., Santos, A., Ferreira, Ó., 2009. Tidal and river discharge forcing upon water and sediment circulation at a rockbound estuary (Guadiana estuary, Portugal). Estuarine, Coastal and Shelf Science. 84 (2), 269–281.

Gonçalves, D.A., Marques, S.C., Primo, A.L., Martinho, F., Bordalo, M., Pardal, M.A., 2015. Mesozooplankton biomass and copepod estimated production in a temperate estuary (Mondego estuary): effects of processes operating at different timescales. Zoological Studies. 54:57, 1–12.

Graf, G., Rosenberg, R., 1997. Biodeposition and bioresuspension: A review. Journal of Marine Systems. 11, 269–278.

Grange, N., Allanson, B.R., 1995. The influence of freshwater inflow on the nature, amount and distribution of seston in estuaries of the Eastern cape, South Africa. Estuarine, Coastal and Shelf Science. 40, 403–420.

Grasshoff, K., Ehrhardt, M., Kremling, K. (Eds.), 1983. Methods of Seawater Analysis. 2nd edition. Verlag Chemie. Weinheim, Germany.

Gredilla, A., Stoichev, T., Vallejuelo, S.F.-O., Rodriguez-Iruretagoiena, A., Morais, P., Arana, G., Diego, A., Madariaga, J.M., 2015. Spatial distribution of some trace and major elements in sediments of the Cávado estuary (Esposende, Portugal). Marine Pollution Bulletin. 99 (1–2), 305–311.

Grenz, C., Cloern, J.E., Hager, S.W. and Cole B.E. 2000. Dynamics of nutrient cycling and related benthic nutrient and oxygen fluxes during a spring phytoplankton bloom in South San Francisco Bay (USA). Marine Ecology Progress Series. 197, 67–80.

Guagliardi, I., Apollaro, C., Scarciglia, F., De Rosa, R., 2013, Influence of particle-size on geochemical distribution of stream sediments in the Lese river catchment, southern Italy. Biotechnology, Agronomy, Society and Environment. 17(1), 43–55.

Hatzenpichler, R., 2012. Diversity, physiology and niche differentiation of ammonia-oxidizing archaea. Applied and Environmental Microbiology. 78, 7501–7510.

Herbert, R.A., 1999. Nitrogen cycling in coastal marine ecosystems. FEMS Microbiology Reviews. 23, 563–590.

Herlemann, D.P.R., Lundin, D., Andersson, A.F., Labrenz, M., Jürgens, K., 2016. Phylogenetic signals of salinity and season in bacterial community composition across the salinity gradient of the Baltic Sea. Frontiers Microbiology. 7, Article 1883, 1–13.

Hernández-Hinojosa, V., Montiel-García, P.C., Armstrong-Altrin, J.S., Nagarajan, R., Kasper-Zubillaga, J.J., 2018. Textural and geochemical characteristics of beach sands along the western Gulf of Mexico, Mexico. Carpathian Journal of Earth and Environmental Sciences. 13 (1), 161–174.

Herschy, R.W., 1995. Streamflow Measurement. 2nd edition. E & FN Spon. London, UK. pp. 5–13.

Hitchcock, J.N., Mitrovic, S.M., 2015. Highs and lows: The effect of differently sized freshwater inflows on estuarine carbon, nitrogen, phosphorus, bacteria and chlorophyll *a* dynamics. Estuarine, Coastal and Shelf Science. 156, 71–82.

Ho, H.H., Swennen, R., Van Damme, A., 2010. Distribution and contamination status of heavy metals in estuarune sediments near Cua Ong Harbor, Ha Long Bay, Vietnam. Geologica Belgica. 13 (1–2), 37–47.

Hobbie, J.E., 1988. A comparison of the ecology of planktonic bacteria in fresh and salt water. Limnology and Oceanography. 33, 750–764.

Hoch, M.P., Kirchman, D.L., 1993. Seasonal and inter-annual variability in bacterial production and biomass in a temperate estuary. Marine Ecology Progress Series. 98, 83–295.

Hofmeister, R., Flöser, G., Schartau, M., 2017. Estuary-type circulation as a factor sustaining horizontal nutrient gradients in freshwater-influenced coastal systems. Geo-Marine Letters. 37, 179–192.

Hopkins, R.J., Desyaterik, Y., Tivanski, A.V., Zaveri, R.A., Berkowitz, C.M., Tyliszczak, T., Gilles, M.K., Laskin, A., 2008. Chemical speciation of sulfur in marine cloud droplets and particles: Analysis of individual particles from the marine boundary layer over the California current. Journal of Geophysical Research. 113 (D04209), 1–15.

Howes, B.L., Goehringer, D.D., 1994. Porewater drainage and dissolved organic carbon and nutrient losses through the intertidal creekbanks of a New England salt marsh. Marine Ecology Progress Series. 114, 289–301.

Hulot, F.D., Morin, P.J., Loreau, M., 2001. Interactions between algae and the microbial loop in experimental microcosms. Oikos. 95, 231–238.

Human, L.D.R., Snow, G.C., Adams, J.B., Bate, G.C., 2015. The benthic regeneration of N and P in the Great Brak estuary, South Africa. Water SA. 41 (5), 594–605.

Inácio, M., Pereira, V., Pinto, M., 2008. The Soil Geochemical Atlas of Portugal: Overview and applications. Journal of Geochemical Exploration. 98, 22–33.

INAG - Instituto da Água, 2009. Questões significativas da gestão da água – Região hidrográfica do Minho e Lima. http://dqa.inag.pt/dqa2002/port/p_dispos/QSigaPP/ Questoes_ Minho_Lima_30_01_2009.pdf (accessed 01.04.2017).

IPMA - Instituto Português do Mar e da Atmosfera. Clima, Boletins climatológicos. http://www.hidrografico.pt/previsao-mares.php (accessed 30.09.2017).

Iriarte, A., Villate, F., Uriarte, I., Alberdi, L., Intxausti, L., 2015. Dissolved oxygen in a temperate estuary: the influence of hydro-climatic factors and eutrophication at seasonal and inter-annual time scales. Estuaries and Coasts. 38 (3), 1000–1015

Ji, Zhen-Gang, 2017. Hydrodynamics and Water Quality – Modeling Rivers, Lakes and Estuaries. 2nd edition. Wiley, USA.

Jickells, T.D., Andrews, J.E., Parkes, D.J., 2016. Direct and Indirect Effects of Estuarine Reclamation on Nutrient and Metal Fluxes in the Global Coastal Zone. Aquatic Geochemistry. 22 (4), 337–348.

Jickells, T.D., Andrewsa, J.E., Parkes, D.J., Suratman, S., Aziz, A.A., Hee, Y.Y., 2014. Nutrient transport through estuaries: The importance of the estuarine geography. Estuarine, Coastal and Shelf Science. 150, 215–229.

Jing, L.D., Wu, C.X., Liu, J.T., Wang, H.G., Ao, H.Y., 2013. The effects of dredging on nitrogen balance in sediment-water microcosms and implications to dredging projects. Ecological Engineering. 52, 167–174.

Jones, M. N., 1984. Nitrate reduction by shaking with cadmium: alternative to cadmium columns. Water Research. 18, 643–646.

Jordan, T.E., Cornwell, J.C., Boynton, W.R., Anderson, J.T., 2008. Changes in phosphorus biogeochemistry along an estuarine salinity gradient: The iron conveyer belt. Limnology and Oceanography. 53(1), 172–184.

Jordan, T.E., Correll, D.L., Miklas, J., Weller, D.E., 1991. Nutrients and chlorophyll at the interface of a watershed and an estuary. Limnology and Oceanography. 36, 251–267.

Joye, S. B., Chambers, R. M., 1993. Nitrogen exchange between microvegetated intertidal sediments and the overlying water column. Estuarine Research Federation Annual Meeting. Hilton Head, Sc., Published Abstract. 58.

Joye, S.B., Paerl, H.W., 1993. Nitrogen fixation and denitrification in the intertidal and subtidal environments of Tomales Bay, California. In: Oremland, R. S. (Ed.), Biogeochemistry of global change: Radiative trace gases. Blackwell Scientific, New York. pp. 635–653.

Junakova, N., Balintova, M., Petrilakova, A., 2013. Study of particle granularity impact on nutrient concentration. Chemical Engineering Transactions. 32, 2169–2166.

Kaiser, D., Kowalski, N., Böttche, M.E., Yan, B., Unge, D., 2015. Benthic Nutrient Fluxes from Mangrove Sediments of an Anthropogenically Impacted Estuary in Southern China. Journal of Marine Science and Engineering. 3, 466–491.

Kamer, K., Fong, P., Kennison, R.L., Schiff, K., 2004. The relative importance of sediment and water column supplies of nutrients to the growth and tissue nutrient content of the green macroalga Enteromorpha intestinalis along an estuarine resource gradient. Aquatic Ecology. 38, 45–56.

Kappenberg, J., Berendt, M., Ohle, N., Riethmüller, R., Schuster, D., Strotmann, T., 2016. Seasonal, Spring-Neap and Tidal Variation of Hydrodynamics and Water Constituents in the Mouth of the Elbe Estuary, Germany. Ocean Science Discussions. https://doi.org/10.5194/os-2016-7.

Kara, E., Shade, A., 2009. Temporal Dynamics of South End Tidal Creek (Sapelo Island, Georgia) Bacterial Communities. Applied and Environmental Microbiology. 75, 1058–1064.

Keeney, D. R., Nelson, D. W., 1982. Nitrogen-inorganic forms, in Methods of soil Analysis – Part 2 – Chemical and Microbiological Properties, Page, A. L., Miller, R. H. and Keeney, D. R., Eds., 2nd edition. Agronomy Series No. 9. American Society of Agronomy, Inc. and Soil Science of America, Inc., Madison, Wisconsin, USA. pp. 643–698.

Kemp, W.M., Boynton, W.R., 1984. Spatial and temporal coupling of nutrient inputs to estuarine primary production: the role of particulate transport and decomposition. Bulletin of Marine Science. 35, 522–535.

Kemp, W.M., Boynton, W.R., Adolf, J.E., Boesch, D.F., Boicourt, W.C., Brush, G., Cornwell, J.C., Fisher, T.R., Glibert, P.M., Hagy, J.D., Harding, L.W., Houde, E.D., Kimmel, D.G., Miller, W.D., Newell, R.I.E., Roman, M.R., Smith, E.M., Stevenson, J.C., 2005. Eutrophication in Chesapeake Bay: Historical trends and ecological interactions. Marine Ecology Progress Series. 303, 1–29.

Ketchum, B.H., 1969. Eutrophication in estuaries. Eutrofication-causes, consequences, correctives. Proceedings of the Symposium of the National Academy of Sciences. pp. 197–209.

Kimmerer, W.J., 2002. Effects of freshwater flow on abundance of estuarine organisms: physical effects or trophic linkages? Marine Ecology Progress Series. 243, 39–55.

Knowles, R., 1982. Denitrification. Microbiological reviews. 46 (1), 43−70.

Koho, K.A., Langezaal, A.M., van Lith, Y.A., Duijnstee, I.A.P., van der Zwaan, G.J., 2008. The influence of a simulated diatom bloom on deep-sea benthic foraminifera and the activity of bacteria: a mesocosm study. Deep-Sea Research I. 55 (5), 696–719.

Koukina, S., Vetrov, A., Belyaev, N., 2012. Ecological Research of Arctic Restricted Exchange Environments (Kandalaksha Bay, White Sea, Russian Arctic). In: Ali M (Ed.), Diversity of Ecosystems. InTech Europe, Rijeka, pp. 199–220.

Lalli, C.M., Parsons, T.R., 2006. Biological Oceanography an Introduction. 2nd edition. Elsevier Butterworth-Heinemann, China.

Lam-Hoai, T., Guiral, D., and Rougier, C. 2006. Seasonal change of community structure and size spectra of zooplankton in the Kaw River estuary (French Guiana). Estuarine, Coastal and Shelf Science. 68, 47–61.

LaMontagne, M., Astorga, V., Giblin, A., Valiela, I., 2002. Denitrification and the stoichiometry of nutrient regeneration in Waquoit Bay, Massachusetts. Estuaries. 25, 272−281.

Lawrence, D., Dagg, M.J., Liu, H.B., Cummings, S.R., Ortner, P.B., Kelble, C., 2004. Wind events and benthic-pelagic coupling in a shallow subtropical bay in Florida. Marine Ecology Progress Series. 266, 1–13.

Lebreton, B. Pollack, P., Blomberg, B., Palmer, T., Adams, L., Guillou, G., Montagna, P., 2016. Origin, composition and quality of suspended particulate organic matter in relation to

freshwater inflow in a South Texas estuary. Estuarine, Coastal and Shelf Science. 170, 70–82.

Li, R., Xu, J., Li, X., Shi, Z., Harrison, P.J., 2017. Spatiotemporal Variability in Phosphorus Species in the Pearl River Estuary: Influence of the River Discharge. Scientific Reports. 7, Article 13649, 1–13.

Libes, S., 2009. Introduction to Marine Biogeochemistry. 2nd edition. Elsevier Inc., New York, USA. ISBN 978-0-12-088530-5.

Liikanen, A., Tanskanen, H., Murtoniemi, T., Martikainen, P.J., 2002. A laboratory microcosm for simultaneous gas and nutrient flux measurements in sediments. Boreal Environmental Research. 7, 151–160.

Lindeboom, H., 2002. The coastal zone: an ecosystem under pressure, in: Field, J.G., Hempel, G., Summerhayes, C. (Eds.), Oceans 2020: Science, Trends, and the Challenge of Sustainability. Island Press, Washington DC, USA. pp. 49–84.

Lindeburg, M.R., 2017. Environmental Engineering – Water Quality. In: FE Civil Review. PPI, Professional Publications, Inc., USA.

Little, S., Spencer, K.L., Schuttelaars, H.M., Millward, G.E., Elliott, M., 2017. Unbounded boundaries and shifting baselines: Estuaries and coastal seas in a rapidly changing world. Estuarine, Coastal and Shelf Science. 198, 311–319.

Liu, S.M., Zhanga, J., Li, D.J., 2004, Phosphorus cycling in sediments of the Bohai and Yellow Seas. Estuarine, Coastal and Shelf Science. 59, 209–218.

Liu, W.C., Chan, W.T., 2016. Assessment of climate change impacts on water quality in a tidal estuarine system using a three-dimensional model. Water. 8 (2), 60.

LNEG - Laboratório Nacional de Energia e Geologia, I.P., geoPortal. http://geoportal.lneg.pt/index.php (accessed 27.03.2017).

Lu, Z., Gan, J., 2015. Controls of seasonal variability of phytoplankton blooms in the Pearl River Estuary. Deep-Sea Research II. 117, 86–96.

Lyngsgaard, M.M., Markager. S., Richardson, K., Møller, E.F., Jakobsen, H.H., 2017. How Well Does Chlorophyll Explain the Seasonal Variation in Phytoplankton Activity? Estuaries and Coasts. https://link.springer.com/article/10.1007/s12237-017-0215-4.

Mackas, D.L., Harrison, P.J., 1997. Nitrogenous nutrient sources and sinks in the Juan de Fuca Strait/Strait of Georgia/Puget Sound estuarine system: Assessing the potential for eutrophication. Estuarine, Coastal and Shelf Science. 44, 1–21.

Magalhães, C., Teixeira, C., Teixeira, R., Machado, A., Azevedo, I., Bordalo, A.A., 2008. Dissolved organic carbon and nitrogen dynamics in the Douro River estuary, Portugal. Ciencias Marinas. 34, 271–282.

Magalhães, C.M., Bordalo, A.A., Wiebe, W.J., 2002. Temporal and spatial patterns of intertidal sedimentewater nutrient and oxygen fluxes in the Douro River estuary, Portugal. Marine Ecology Progress Series. 233, 55–71.

Magalhães, F., Dias, J. M. A., 1992. Depósitos sedimentares da plataforma continental a norte de Espinho. Gaia. 5, 6–17.

Magni, P., Montani, S., 2000. Water chemistry variability in the lower intertidal zone of an estuary in the Seto Inland Sea, Japan: seasonal patterns of nutrients and particulate compounds. Hydrobiologia 432, 9–23.

Magni, P., Montani, S., 2006. Seasonal patterns of pore-water nutrients, benthic chlorophyll *a* and sedimentary AVS in a macrobenthos-rich tidal flat. Hydrobiologia. 571, 297–311.

Magni, P., Montani, S., Tada, K., 2002. Semidiurnal dinamycs of salinity, nutrients and suspended particulated matter in an estuary in the Seto inland sea, Japan, during a spring tide cycle. Journal of Oceanography. 58, 389–402.

Malham, S.K., Rajko-Nenow, P., Howlett, E., Tuson, K.E., Perkins, T.L., Pallett, D.W., Wang, H., Jago, C.F., Jones, D.L., McDonald, J.E., 2014. The interaction of human microbial pathogens, particulate material and nutrients in estuarine environments and their impacts on recreational and shellfish waters. Environmental Science: Process & Impacts. 16, 2145–2155.

Mali, M., Dell'Anna, M.M., Mastrorilli, P., Damiani, L., Ungaro, N., Belviso, C., Fiore, S., 2015. Are conventional statistical techniques exhaustive for defining metal background concentrations in harbour sediments? A case study: The Coastal Area of Bari (Southeast Italy). Chemosphere. 138, 708–717.

Mallin, M.A., Paerl, H.W., Rudek, J., Bates, P.W., 1993. Regulation of estuarine primary production by watershed rainfall and river flow. Marine Ecology Progress Series. 93, 199–203.

Mallin, M.A., Williams, K.E., Esham, E.C., Lowe, R.P., 2000. Effect of human development on bacteriological water quality in coastal watersheds Ecological Applications. 10, 1047–1056.

Marathe, R.B., 2012, XRD and SEM Analysis of Tapti River Sediment: A Case Study. Archives of Applied Science Research. 4 (1), 78–84.

Marcovecchio, J., Spettera, C., Bottéa, S., Delucchia, F., Ariasa, A., Severinia, M.F., Negrina, V., Popovichd, C., Freije, R.H., 2009. Tidal time-scale variation of inorganic nutrients and

organic matter in Bahía Blanca mesotidal estuary, Argentina. Chemistry and Ecology. 25 (6), 453–465.

Martinez, E., Antoine, D., D'Ortenzio, F., Montégut, C.B., 2011. Phytoplankton spring and fall blooms in the North Atlantic in the 1980s and 2000s. Journal of Geophysical Research. 116, C11029, 1–11.

Martin-Jézéquel, V., Hildebrand, M., Brzezinski, M.A., 2000. Silicon metabolism in diatoms: implications for growth. Journal of Phycology. 36, 821–840.

Martins, R., Azevedo, M.R., Mamede, R., Sousa, B., Freitas, R., Rocha, F., Quintino, V., Rodrigues, A.M., 2012. Sedimentary and geochemical characterization and provenance of the Portuguese continental shelf soft-bottom sediments. Journal of Marine Systems. 91, 41–52.

Martins. A.A., Cabral, J., Cunha, P.P., Stokes, M., Borges, J., Caldeira, B., Martins, A.C., 2017. Tectonic and lithological controls on fluvial landscape development in central-eastern Portugal: Insights from long profile tributary stream analyses. Geomorphology. 276, 144–163.

Martinussen, I., Thingstad, T.F., 1987. Utilization of N, P and organic C by heterotrophic bacteria. II. Comparison of experiments and a mathematical model. Marine Ecology Progress Series. 37, 285–293.

Maznah, W.O.W., Rahmah, S., Lim, C.C., Lee, W.P., Fatema, K., Isa, M.M., 2016. Effects of tidal events on the composition and distribution of phytoplankton in Merbok river estuary Kedah, Malaysia. Tropical Ecology. 57 (2), 213–229.

McClelland, J., Valiela, I., 1998. Linking nitrogen in estuarine producers to land-derived sources. Limnology and Oceanography. 43, 577–585.

McLusky, D.S., Elliott, M., 2004. The estuarine ecosystem: ecology, threats and management. 3rd edition. Oxford University Press, UK. ISBN 0-19-852508-7.

Medeiros, J., Chaves, M., Silva, G., Azeda, C., Costa, J., Marques, J., Costa, M., Chainho, P., 2012. Benthic condition in low salinity areas of the Mira estuary (Portugal): Lessons learnt from freshwater and marine assessment tools. Ecological Indicators. 19, 79–88.

Menéndez, M.C., Dutto, S., Piccolo, M.C., Hoffmeyer, M.S., 2012. The role of the seasonal and semi-diurnal tidal cycle on mesozooplankton variability in a shallow mixed estuary (Bahía Blanca, Argentina). ICES Journal of Marine Science. 69 (3), 389–398.

Michel, P., Boutier, B., Chiffoleau, J.F., 2000. Net fluxes of dissolved arsenic, cadmium, copper, zinc, nitrogen and phosphorus from the Gironde Estuary (France): Seasonal variations and trends. Estuarine, Coastal and Shelf Science. 51, 451–462.

Mil-Homens, M., Vale, C., Raimundo, J., Pereira, P., Brito, P., Caetano, M., 2014. Major factors influencing the elemental composition of surface estuarine sediments: The case of 15 estuaries in Portugal. Marine Pollution Bulletin. 84, 135–146.

Monsen, N.E., Cloern, J.E., Lucas, L.V., Monismith, S.G., 2002. A comment on the use of flushing time, residence time, and age as transport time scales. Limnology and Oceanography. 47, 1545–1553.

Montani, S., Magni, P., Shimamoto, M., Abe, N., Okutani, K., 1998. The Effect of a Tidal Cycle on the Dynamics of Nutrients in a Tidal Estuary in the Seto Inland Sea, Japan. Journal of Oceanography. 54, 65–76.

Morais, P., Chícharo, M.A., Chícharo L., 2009. Changes in a temperate estuary during the filling of the biggest European dam. Science of the Total Environment. 407 (7), 2245–2259.

Morris, A.W., 1985. Estuarine Chemistry and general survey strategy. In: Head, P.C. (Ed.), Practical Estuarine Chemistry, Cambridge University Press, Cambridge, UK. pp. 1–60.

Morse, J.L., Megonigal, J.P., Walbridge, M.R., 2004. Sediment nutrient accumulation and nutrient availability in two tidal freshwater marshes along the Mattaponi River, Virginia, USA. Biogeochemistry. 69, 175–206.

Mortazavi, B., Riggs, A.A., Caffrey, J.M., Genet, H., Phipps, S.W., 2012. The Contribution of Benthic Nutrient Regeneration to Primary Production in a Shallow Eutrophic Estuary, Weeks Bay, Alabama. Estuaries and Coasts. 35, 862–877.

Mortlock, R.A., Froelich, P.N., 1989. A simple method for the rapid determination of biogenic opal in pelagic marine sediments. Deep-sea research. Part A, Oceanographic research papers. 36 (9), 1415–1426.

Mudrock, A., Azcue, J. M., Mudrock, P., 1997. Determination of nutrients in aquatic sediments. In: Manual of Physico-Chemical Analysis of Aquatic Sediments, CRC/Lewis Publishers, Boca Raton, Florida, USA. ISBN 1-56670-155-4. pp. 175–228.

Munro, P.M., Gauthier, M.J., Breittmayer, V.A., Bonjiovanni, J., 1989. Influence of osmoregulation processes on starvation survival of *Escherichia coli* in seawater. Applied and Environmental Microbiology. 55, 2017–2024.

Nedwell, D.B., Sage, A.S., Underwood, G.J.C., 2002. Rapid assessment of macroalgal cover on intertidal sediments in a nitrified estuary. Science of the Total Environment. 285, 97–105.

Négrel, P., Merly, C., Gourcy, L., Cerdan, O., Petelet-Giraud, E., Kralik, M., Klaver, G., Wirdum, G., Vegter. J., 2014. Soil–Sediment–River Connections: Catchment Processes Delivering Pressures to River Catchments. In: Brils, J., Brack, W., Müller-Grabherr, D., Négrel, P.,

Vermaat, J.E. (Eds.), Risk-informed management of European river basins. Springer-Verlag, Berlin Heidelberg.

Negrin, V.L., Spetter, C.V., Asteasuain, R.O., Perillo, G.M.E., Marcovecchio, K.E., 2011. Influence of flooding and vegetation on carbon, nitrogen, and phosphorus dynamics in the pore water of a *Spartina alterniflora* salt marsh. Journal of Environmental Sciences. 23(2) 212–221.

Nixon, S.W., 1981. Remineralization and nutrient cycling in coastal marine ecosystems. In: Neilson, B.J., Cronin, L.E. (Eds.), Estuaries and nutrients, Humana Press: New York, USA. pp. 111–138.

Nixon, S.W., 2003. Replacing the Nile: Are anthropogenic nutrients providing the fertility once brought to the Mediterranean by a great river? Ambio. 32, 30–9.

Nixon, S.W., Ammerman, J.W., Atkinson, L.P., Berounsky, V.M., Billen, G., Boicourt, W.C., Boynton, W.R., Church, T.M., Ditoro, D.M., Elmgren, R., Garber, J.H., Giblin, A.E., Jahnke, R.A., Owens, N.J.P., Pilson, M.E.Q., Seitzinger, S.P., 1996. The fate of nitrogen and phosphorus at the land-sea margin of the north Atlantic Ocean. Biogeochemistry. 35, 141–180.

NRC (National Research Council), 2000. Clean Coastal Waters: Understanding and Reducing the Effects of Nutrient Pollution. National Academy Press, Washington DC, USA.

Odum, E.P., 1959. Fundamentals of ecology. 2nd edition. Philadelphia: Saunders.

Ogilvie, B., Nedwell, D.B., Harrison, R.M., Robinson, A., and Sage, A., 1997. High nitrate, muddy estuaries as nitrogen sinks: the nitrogen budget of the River Colne estuary (United Kingdom). Marine Ecology Progress Series. 150,217–228.

Oldham, C.E., Lavery, P.S., 1999. Porewater nutrient fluxes in a shallow fetch-limited estuary. Marine Ecology Progress Series.183, 39–47.

Oliveira, A., Rocha, F., Rodrigues, A., Dias, J.A., 2000. The fine sediments as dynamic sedimentary tracers (NW Iberian margin). In: Book of Abstract 3º Simpósio sobre a Margem Continental Ibérica Atlântica/3rd Symposium on the Iberian Atlantic Margin. Universidade do Algarve, Faro. 399–400.

Oliveira, A., Rocha, F., Rodrigues, A., Jouanneau, J., Dias, A., Weber, O., Gomes, C., 2002. Clay minerals from the sedimentary cover from the Northwest Iberian shelf. Progress in Oceanography. 52, 233–247.

Oliveira, A.P., Cabeçadas, G., Mateus, M.D., 2017. Inorganic carbon distribution and CO_2 fluxes in a large European estuary (Tagus, Portugal). Scientific Reports. 7, Article 7376, 1–14.

Paerl, H.W., 2002. Connecting atmospheric deposition to coastal eutrophication. Environmental Science & Technology. 36, 323–326.

Paerl, H.W., 2006. Assessing and managing nutrient-enhanced eutrophication in estuarine and coastal waters: Interactive effects of human and climatic perturbations. Ecological Engineering. 26 40–54.

Paerl, H.W., Justic, D., 2011, Primary Producers: Phytoplankton Ecology and Trophic Dynamics in Coastal Waters. In: Wolanski, E, McLusky, D.S. (Eds.), Treatise on Estuarine and Coastal Science, Vol 6. Waltham: Academic Press. pp. 23–42.

Page, H. M., Petty, R. L., Meade, D. E., 1995. Influence of watershed runoff on nutrient dynamics in a southern California salt marsh. Estuarine, Coastal and Shelf Science. 41, 163–180.

Painchaud, J., Lefaivre, D., Therriault, J.C., 1996. Bacterial Dynamics in the upper St. Lawrence estuary. Limnology and Oceanography. 41, 1610–1618.

Parsons, C.T., Rezanezhad, F., O'Connell, D.W., Van Cappellen, F., 2017. Sediment phosphorus speciation and mobility under dynamic redox conditions. Biogeosciences. 14, 3585–3602.

Parsons, T.R., Maita, Y., Lalli, C.M., 1984. A Manual of Chemical and Biological Methods for Seawater Analysis. Pergamon Press, Oxford, UK. ISBN 0-08-030288-2.

Pastor-Galán, D., Gutiérrez-Alonso, G., Fernández-Suárez, J., Murphy, J.B., Nieto, F., 2013. Tectonic evolution of NWIberia during the Paleozoic inferred from the geochemical record of detrital rocks in the Cantabrian Zone. Lithos. 182–183, 211–228.

Paytan, A., McLaughlin, K., 2007. The Oceanic Phosphorus Cycle. Chemical reviews. 107, 563−576.

Pereira, P., Caçador, I., Vale, C., Caetano, M., Costa, A. L., 2007. Decomposition of belowground marshes (Tagus litter and metal dynamics in salt Estuary, Portugal). Science of the Total Environment. 380, 93–101.

Pereira-Filho, J., Schettini, C.A.F., Rorig, L., Siegle, E., 2001. Intratidal variation and net transport of dissolved inorganic nutrients, POC and chlorophyll a in the Camboriu River estuary, Brazil. Estuarine, Coastal and Shelf Science. 53, 249–257.

Perillo, G.M.E., 1995. Geomorphology and Sedimentology of Estuaries. Elsevier, Amsterdam, Netherlands.

Pinckney, J.L., Paerl, H.W. Tester, P., Richardson, T.L., 2001. The Role of Nutrient Loading and Eutrophication in Estuarine Ecology. Environmental Health Perspectives. 109, 699–703.

Porter, K.G., Feig, Y.S., 1980. The use of DAPI for identifying and counting aquatic microflora. Limnology and Oceanography. 41, 1610–1618.

Potter, I.C., Chuwen, B.M., Hoeksema, S.D., Elliott, M., 2010. The concept of an estuary: A definition that incorporates systems which can become closed to the ocean and hypersaline. Estuarine, Coastal and Shelf Science. 87, 497–500.

Prandle, D., 2009. Estuaries: Dynamics, Mixing. Sedimentation and Morphology. Cambridge University Press. New York, USA. ISBN-13 978-0-511-48101-7.

Pritchard, D.W., 1967. What is an estuary: a physical viewpoint, in: Lauff, G.H. (Ed.), Estuaries. American Association for the Advancement of Science, Washington DC, USA. pp. 3–5.

Pritchard, D.W., 1969. Dispersion and flushing of pollutants in estuaries. Journal of the Hydraulics Division. 95, 115–124.

Purkhold, U., Pommerening-Roser, A., Juretschko, S., Schmid, M.C., Koops, H.-P., Wagner, M., 2000. Phylogeny of all recognized species of ammonia oxidizers based on comparative 16S rRNA and amoA sequence analysis: implications for molecular diversity surveys. Applied and Environmental Microbiology. 66, 5368–5382.

Ragueneau, O., Conley, D.J., Leynaert, A., Ni Longphuirt, S., Slomp, C.P., 2006. Role of diatoms in silicon cycling and coastal marine food webs. In: Ittekot, V., Unger, D., Humborg, C., TacAn, N. (Eds.), The silicon cycle: human perturbations and impacts on aquatic systems. SCOPE 66. Island Press, Washington, USA. pp. 163–195.

Ragueneau, O., Tréguer, P., Leynaert, A., Anderson, R.F., Brzezinski, M.A., DeMaster, D.J., Dugdale, R.C., Dymond, J., Fischer, G., Francois, R., Heinze, C., Maier-Reimer, E., Martin-Jézéquel, V., Nelson, D.M., Quéguiner, B., 2000. A review of the Si cycle in the modern ocean: recent progress and missing gaps in the application of biogenic opal as a paleoproductivity proxy. Global and Planetary Change. 26, 317–365.

Rahaman, S.M.B., Biswas, S.K., Rahaman, M.S., Ghosh, A.K., Sarder, L., Siraj, S.M.S., Islam, S.S., 2014. Seasonal nutrient distribution in the Rupsha-Passur tidal river system of the Sundarbans mangrove forest, Bangladesh. Ecological Processes. 3 (18), 1–11.

Raimonet, M., Andrieux-Loyer, F., Ragueneau, O., Michaud, E., Kerouel, R., Philippon, X., Nonent, M., Mémery, L., 2013. Strong gradient of benthic biogeochemical processes along a macrotidal temperate estuary: focus on P and Si cycles. Biogeochemistry. 115 (1–3), 399-417.

Ramos, S., Cowen, R.K., Paris, C., Ré, P., Bordalo, A.A., 2006. Environmental forcing and larval fish assemblage dynamics in the Lima River estuary (northwest Portugal). Journal of Plankton Research. 28 (3), 275–286.

Ramos, S., Paris, C.B., Angélico, M.M., 2017. Larval fish dispersal along an estuarine–ocean gradient. Canadian Journal of Fisheries and Aquatic Sciences. 74 (9), 1462–1473.

Ramos, S., Ré, P., Bordalo, A.A., 2010. Recruitment of flatfish species to an estuarine nursery habitat (Lima estuary, NW Iberian Peninsula). Journal of Sea Research. 64, 473–486.

Ramos-Vázquez, M.A., Armstrong-Altrin, J.S., Machain-Castillo, M.L., Gío-Argáez. F.R., 2018. Foraminiferal assemblages, ^{14}C ages, and compositional variations in two sediment cores in the western Gulf of Mexico. Journal of South American Earth Sciences. 88, 480–496.

Rebordão, I., Teixeira, A.T., 2009. Tidal propagation in the Lima estuary. Journal of Coastal Research. 56, 1400–1404.

Regnier, P., Arndt, S., Goossens, N., Volta, C., Laruelle, G.G., Lauerwald, R., Hartmann, J., 2013. Modelling Estuarine Biogeochemical Dynamics: From the Local to the Global Scale. Aquatic Geochemistry. 19, 591–626.

Renshun, Z., 1992. Suspended sediment transport processes on tidal mud flat in Jiangsu Province, China. Estuarine, Coastal and Shelf Science. 35, 225–233.

Robarts, R.D., Zohary, T., Waiserl, M.J., Yacobi, Y.Z., 1996. Bacterial abundance, biomass, and production in relation to phytoplankton biomass in the Levantine Basin of the southeastern Mediterranean Sea. Marine Ecology Progress Series. 137, 273–281.

Roberts, D.A., 2012. Causes and ecological effects of resuspended contaminated sediments (RCS) in marine environments. Environment international. 40, 230–243.

Robins, P.E., Skov, M.W., Lewis, M.J., Giménez, L., Davies, A.G., Malham, S.K., Neill, S.P., McDonald, J.E., Whitton, T.A., Jackson, S.E., Jago, C.F., 2016. Impact of climate change on UK estuaries: A review of past trends and potential projections. Estuarine, Coastal and Shelf Science. 169, 119–135.

Robson, B.J., Bukaveckas, P.A., Hamilton, D.P., 2008. Modelling and mass balance assessments of nutrient retention in a seasonally-flowing estuary (Swan River Estuary, Western Australia). Estuarine, Coastal and Shelf Science. 76, 282–292.

Roegner, G., 1998. Hydrodynamic control of the supply of suspended chlorophyll a to infaunal estuarine bivalves. Estuarine, Coastal and Shelf Science. 47, 369–384.

Russi, D., ten Brink, P., Farmer, A., Badura, T., Coates, D., Förster, J., Kumar, R., Davidson, N., 2013. The economics of ecosystems and biodiversity for water and wetlands. IEEP, London and Brussels.

Rysgaard, S., Risgaard-Petersen, N., Sloth, N.P., 1996. Nitrification, denitrification and nitrate ammonification in sediments of two coastal lagoons in Southern France. Hydrobiologia. 329, 133–141.

Sabater, S., 2009. Diatoms. In: Likens GE (Ed.), Encyclopedia of Inland waters, vol 1. Elsevier, Oxford, UK. pp. 149–156.

Sakamaki, T., Nishimura, O., Sudo, R., 2006. Tidal time-scale variation in nutrient flux across the sediment–water interface of an estuarine tidal flat. Estuarine, Coastal and Shelf Science. 67 (4), 653–663.

Saraiva, S., Pina, E.P., Martins, E.F., Santos, E.M., 2007. Modelling the influence of nutrient loads on Portuguese estuaries. Hydrobiologia. 587, 5–18.

Sauer, D., Saccone, L., Conley, D. J., Herrmann, L., Sommer, M., 2006. Review of methodologies for extracting plant-available and amorphous Si from soils and aquatic sediments. Biogeochemistry. 80, 89–108.

SCOR-UNESCO, 1966. Determination of photosynthtic pigments in sea water. In: UNESCO (Ed.), Unesco Monographs on Oceanographic Methodology. UNESCO Press, Paris, France. 1, 10–69.

Seitzinger, S.P., 1988. Denitrification in freshwater and coastal marine ecosystems: ecological and geochemical significance. Limnology and Oceanography. 33, 702−724.

Seitzinger, S.P., 1990. Denitrification in Aquatic Sediments. In: Revsbech, N. P. & Sorensen, J (Eds.), Denitrification in Soil and Sediment. Plenum Press, New York. pp. 301–322.

Selje, N., Simon, M., 2003. Composition and dynamics of particle-associated and free-living bacterial communities in the Weser estuary, Germany. Aquatic Microbial Ecology. 30, 221–237.

Serpetti, N., Witte, U.F.M., Heath, M.R., 2016. Statistical Modeling of Variability in Sediment-Water Nutrient and Oxygen Fluxes. Frontiers in Earth Science. 4, Article 65, 1–17.

Sloth, N.P., Blackburn, H., Hansen, L.S., Risgaard-Petersen, N., Lomstein, B.A., 1995. Nitrogen cycling in sediments with different organic loading. Marine Ecology Progress Series. 116, 163–170.

Smith, V.H., 1998. Cultural eutrophication of inland, estuarine, and coastal waters In: Pace, M.L., Groffman, P.M. (Eds.), Successes, limitations, and frontiers in ecosystem science. Springer, New York, pp. 7–49.

Smith, V.H., Tilman, G.D., Nekola, J.C., 1999. Eutrophication: impacts of excess nutrient inputs on freshwater, marine, and terrestrial ecosystems. Environmental Pollution. 100,179–196.

SNIRH - Sistema Nacional de Informação de Recursos Hídricos. Dados de base. http://snirh.apambiente.pt/snirh/_dadosbase/site/janela_verdados.php?sites=1627743428&pars=212296818&tmin=01/10/2013&tmax=30/04/2015 (accessed 30.09.2017).

Solá, A. R., Chichorro, M., Pereira, M. F., Medina, J., Linnemann, U., Hofmann, M., Silva, J. B., 2011. Idades U-Pb dos zircões detríticos do grupo das Beiras – Implicações para a evolução do SW da Ibéria durante o neoproterozóico. In: Livro de Actas do VIII Congresso Ibérico de Geoquímica - XVII Semana de Geoquímica. Instituto Politécnico de Castelo Branco, Castelo Branco, 1–7.

Stief, P, 2013. Stimulation of microbial nitrogen cycling in aquatic ecosystems by benthic macrofauna: mechanisms and environmental implications. Biogeosciences. 10, 7829–7846.

Sundararajan, M., Natesan, U., 2010. Geochemistry of Elements in Core Sediments Near Point Claimere, the Southeast Coast of India. International Journal of Environmental Research. 4 (3), 379–394.

Sundbäck, K., Miles, A., Goransson, E., 2000. Nitrogen fluxes, denitrification and the role of microphytobenthos in microtidal shallow-water sediments: an annual study. Marine Ecology Progress Series. 200, 59–76.

Tapia-Fernandez, H.J., Armstrong-Altrin, J.S., Selvaraj, K., 2017. Geochemistry and U-Pb geochronology of detrital zircons in the Brujas beach sands, Campeche, Southwestern Gulf of Mexico, Mexico. Journal of South American Earth Sciences. 76, 346–361.

Taylor, D., Nixon, S.W., Granger, S.L., Buckley, B.A., 1995. Nutrient limitation and the eutrophication of coastal lagoons. Marine Ecology Progress Series. 127, 235–244.

Taylor, D.I., Allanson, B.R., 1995. Organic fluxes between a high marsh and estuary, and the inapplicability of the outwelling hypothesis. Marine Ecology Progress Series. 120, 263–270.

Teixeira, C., Medeiros, A., 1970. Carta Geológica de Portugal 1/50000 - Folha 05-A – Viana do Castelo. Serviços Geológicos de Portugal, Lisboa.

Testa, J.M., Brady, D.C., Di Toro, D.M., Boynton, W.R., Cornwell, J.C., Kempa, W.M., 2013. Sediment flux modeling: Simulating nitrogen, phosphorus, and silica cycles. Estuarine, Coastal and Shelf Science. 131, 245–263.

Testa, J.M., Kemp W.M., 2008. Variability of biogeochemical processes and physical transport in a partially stratified estuary: a box-modelling analysis. Marine Ecology Progress Series. 356, 63–79.

Tett, P., Hydes, D., Sanders, R., 2003. Influence of nutrient biogeochemistry on the ecology of northwest European shelf seas. In: Black, K.D., Shimmield, G.B. (Eds.), Biogeochemistry of Marine systems. Blackwell Publishing Ltd. pp. 293–363.

Tréguer, P., Nelson, D.M., Van Bennekom, A.J., DeMaster, D.J., Leynaert, A., Quéguiner, B., 1995. The silica balance in the world ocean: a reestimate. Science. 268, 375–379.

Tréguer, P., Pondaven, P., 2000. Silica control of carbon dioxide. Nature. 406, 358–359.

Tréguer, P.J., De La Rocha, C.L., 2013. The World ocean silica cycle. Annual Review of Marine Science. 5, 477–501

Tribovillard, N., Algeo, T.J., Lyons, T., Riboulleau, A., 2006. Trace metals as paleoredox and paleoproductivity proxies: An update. Chemical Geology. 232, 12–32.

Turekian, K.K., Wedepohl, K.H., 1961. Distribution of the elements in some major units of the earth's crust. Geological Society of American Bulletin. 72, 175–192.

Uncles, R.J., Stephens, J.A., 1996. Salt intrusion in the Tweed Estuary. Estuarine, Coastal and Shelf Science. 43 (3), 271–293.

Uwah, I.E., Dan, S.F., Etiuma; R.A., Umoh, U.E., 2013. Evaluation of Status of Heavy Metals Pollution of Sediments in Qua-Iboe River Estuary and Associated Creeks, South-Eastern Nigeria. Environment and Pollution. 2 (4), 110–122.

Valdes-Weaver, L.M., Piehler M.F., Pinckney J,L., Howe K.E., Rossignol K., Paerl H.W., 2006. Long-term temporal and spatial trends in phytoplankton biomass and class-level taxonomic composition in the hydrologically variable Neuse-Pamlico estuarine continuum, North Carolina U. S. A. Limnology and Oceanography. 51(3), 1410–1420.

Vale, L. M., Dias, J. M., 2011. The effect of tidal regime and river flow on the hydrodynamics and salinity structure of the Lima Estuary: Use of a numerical model to assist on estuary classification. Journal of Coastal Research. SI 64, 1604–1608.

Valente, T., Fatela, F., Moreno, J., Moreno, F., Guise, L., Patinha, C., 2009. A comparative study of the influence of geochemical parameters on the distribution of Foraminiferal assemblages in two distinctive tidal marshes. Journal of Coastal Research. SI 56, 1439–1443.

Vallières, C., Retamal. L., Ramlal, P., Osburn, C.L., Vincent, W.F., 2008. Bacterial production and microbial food web structure in a large arctic river and the coastal Arctic Ocean. Journal of Marine Systems. 74, 756–773.

Van Alstyne, K.L., Nelson, T.A., Ridgway, R.L., 2015. Environmental chemistry and chemical ecology of ‘‘green tide’’ seaweed blooms. Integrative and Comparative Biology. 55 (3), 518–532.

Van Luijn, F., Boers, P.C.M., Lijklema, L., Sweats, J.P.R.A., 1999. Nitrogen fluxes and processes in sandy and muddy sediments from shallow eutrophic lake. Water Research. 33, 33–42.

Venice System, 1958. Symposium on the classification of brackish waters, Venice April 8–14, 1958. Archivio di Oceanografia e Limnologia. 11 (Suppl), 1–248.

Venkatramanan, S., Ramkumar, T., Anithamary, I., 2010. Textural characteristics and organic matter distribution patterns in Tirumalairajanar river Estuary, Tamilnadu, East Coast of India. International Journal of Geomatics and Geosciences. 1, (3), 552–562.

Venkatramanan, S., Ramkumar, T., Anithamary, I., 2013. Distribution of grain size, clay mineralogy and organic matter of surface sediments from Tirumalairajanar Estuary, Tamilnadu, east coast of India. Arabian Journal of Geosciences. 6, (5), 1371–1380.

Vieira, M., Bordalo, A.A., 2000. The Douro estuary (Portugal): a mesotidal salt wedge. Oceanologica Acta. 23, 585–594.

Vinita, J., Lallu, K.R., Revichandran, C., Muraleedharan, K.R., Jineesh, V.K., Shivaprasad, A., 2015. Residual fluxes of water and nutrient transport through the main inlet of a tropical estuary, Cochin estuary, West Coast, India. Environmental Monitoring and Assessment. 187, Article 675, 1–13.

Viveen, W., Schoorl, J. M., Veldkamp, A., van Balend R.T, Vidal-Romanib, J.R., 2013. Fluvial terraces of the northwest Iberian lower Minõ River. Journal of Maps. 9 (4), 513–522.

Vogel, R.M., 2011. Hydromorphology. Journal of Water Resources Planning and Management. 137, 147–149.

Vollenweider, R.A., 1992. Coastal marine eutrophication: principles and control. In: Vollenweider, R.A., Marchetti, R., Vivian, R. (Eds.), Marine coastal eutrophication. Science of the Total Environmental, Supplement Elsevier, Amsterdam, Netherlands. pp.1–20.

Wainright, S.C., 1987. Stimulation of heterotrophic microplankton production by resuspended marine sediments. Science. 238, 1710–1712.

Wan, Y., Qiu, C., Doering, P., Ashton, M., Sun, D., Coley, T., 2013. Modeling residence time with a three-dimensional hydrodynamic model: Linkage with chlorophyll a in a subtropical estuary. Ecological Modelling. 268, 93–102.

Watson, P.G., Frickers, P.E., Howland, R.J.M., 1993. Benthic fluxes of nutrients and some trace metals in the Tamar estuary, SW England. Netherlands Journal of Aquatic Ecology. 2, 135–146.

Watson, S.J., Cade-Menun, B. J., Needoba, J.A., Peterson1, T.D., 2018. Phosphorus Forms in Sediments of a River-Dominated Estuary. Frontiers in Marine Science. 5, Article 302, 1–11.

Webb, A.P., Eyre, B.D., 2004. The effect of natural populations of the burrowing and grazing soldier crab (Mictyris longicarpus) on sediment irrigation, benthic metabolism and nitrogen fluxes. Journal of Experimental Marine Biology and Ecology. 309, 1–19.

Welsh, D.T., Bartoli, M., Nizzoli, D., Castaldelli, G., Riou, S.A., Viaroli, P., 2000. Denitrification, nitrogen fixation, community primary productivity and inorganic-N and oxygen fluxes in an intertidal *Zostera noltii* meadow. Marine Ecology Progress Series. 208, 65–77.

Wepener, V., 2007. Carbon, nitrogen and phosphorus fluxes in four sub-tropical estuaries of northern KwaZulu-Natal: Case studies in the application of a mass balance approach. Water SA. 33 (2), 203–214.

White, W.M., 2013.Trace Elements in Igneous Processes. In: Geochemistry. 1st edition. Wiley-Blackwell, Oxford, pp 259–313.

Whitfield, A.K., 1992. A Characterization of Southern African Estuarine Systems. South African Journal of Aquatic Science. 18, 89–103.

Wilson, J.G., Brennan, M.T., 2004. Spatial and temporal variability in modeled nutrient fluxes from the unpolluted Shannon estuary, Ireland, and the implication for microphytobenthic productivity. Estuarine, Coastal and Shelf Science. 60, 193–201.

Winder, M., Cloern, J.E., 2010. The annual cycles of phytoplankton biomass. Philosophical Transactions of the Royal Society B. 365, 3215–3226.

Wolanski, E., 2007. Estuarine Ecohydrology. 1st edition. Elsevier. Amsterdam, Netherlands. ISBN 978-0-444-53066-0.

Wolanski, E., Andutta, F., Delhez, E., 2012. Estuarine hydrology, In: Bengtsson, L., Herschy. R.W., Fairbridge, R.W. (Ed.), Encyclopedia of Lakes and Reservoirs. Springer-Verlag, Netherlands. pp. 238–8249.

Wolanski, E., Elliott, M., 2016. Estuarine Ecohydrology - an Introduction. 2nd edition. Elsevier, Amsterdam. ISBN 978-0-444-63398-9.

Wollast, R., 1974. The silica problem. In: Goldberg, E.D. (Ed.), The sea, vol 5. Wiley, New York, USA. pp. 359–392.

Wulff, A., Sundbaeck, K., Nilsson, C., Carlson, L., Jönsson, B., 1997. Effect of sediment load on the microbenthic community of a shallow-water sandy sediment. Estuaries. 20, 547–558.

Xia, X., Guo, W., Liu, H., 2015. Dynamics of the bacterial and archaeal communities in the Northern South China Sea revealed by 454 pyrosequencing of the 16S rRNA gene. Deep-Sea Research II. 117, 97–107.

Xu, J., Hood, R.R., 2006. Modelling biogeochemical cycles in Chesapeake Bay with a coupled physical-biological model. Estuarine, Coastal and Shelf Science. 69, 19–46.

Yin, K., Harrison, P. J., 2000. Influences of flood and ebb tides on nutrient fluxes and chlorophyll on an intertidal flat. Marine Ecology Progress Series. 196, 75–85.

Yin, K., Harrison, P. J., Pond, S., Beamish, R. J., 1995. Entrainment of nitrate in the Fraser river estuary and its biological implications. III. Effects of winds. Estuarine, Coastal and Shelf Science. 40, 545–558.

Zehr, J. P., Kudela R. M., 2011. Nitrogen cycle of the open ocean: from genes to ecosystems. Annual Review of Marine Science. 3,197–225.

Zhang, S., Zhou, Q., Xu, D., Lin, J., Cheng, S., Wu, Z., 2010. Effects of sediment dredging on water quality and zooplankton community structure in a shallow of eutrophic lake. Journal of Environmental Sciences. 22, 218–224.